
**UNIVERSITY OF PISA**

**BIOS** - Research Doctorate School in **BIO**molecular **S**ciences

**Ph.D.** *in* **BIOMATERIALS** - *XX Cycle*

# *Environmentally Compatible Polymeric Blends and Composites Based on Oxo-Biodegradable Polyethylene*

**Sílvia Maria Martelli**

Supervisor: Prof./Dr. Emo Chiellini

Tutor: Dr. Elizabeth Grillo Fernandes

Department of Chemistry and Industrial Chemistry

*To my parents, my husband, and*
*To the most precious inspiration of my life:*
*Natália Manoela with great love.*

# ACKNOWLEDGEMENTS

While I was working on this Thesis in the last three years, I often imagined the moment I would get to this part: when the manuscript would be written, the final stress would be gone, when I finally would have a free weekend with my husband, my daughter and my little dog. I knew I would look back at this period of my life with pleasure, “saudade” and gratitude. Finally, this moment has come. The examiners will evaluate the results of this work, but I can certainly say that the process had been pleasant. So I am glad to complete it by remembering many wonderful people who have contributed to it in various ways.

My firsts thanks goes to God, for its constant presence in my life, for guiding my choices and for the comfort in the difficult moments.

Sincere thanks to my supervisor, Prof. Emo Chiellini, who gave me the opportunity to achieve this important objective. I also gratefully appreciated the help that Prof. Galli, Prof. Solaro, and Dr. D’Antone have given me in the moments of need.

I also thank the reading committee members who kindly agreed to read my manuscript and to participate in this discussion.

Special thanks to Maria Viola, Michela Bianchi and Maria Caccamo. Persons that help me in all situations!

Very special thanks to my tutor Dr. Elizabeth Grillo Fernandes (Beth); she had been so generous with her time. Her contribution to this Thesis is immeasurable. When I was starting my PhD I had an objective in my mind. Beth helped me to go far beyond my modest limits. For all the teachings, friendship, trust and patience I am truly grateful.

To Sabrina my genuine thanks; she has always been close to me.

I would also like to thank several people from the DCCI and BIOLAB for all the time we spent together in these years, for share the good times and for the help that they gave me in the moments I needed. Great colleagues like Elisa (and Luca), Matteo (and Luisa), Sara, Ahmed, Federica, Cristiano, Luca Lotti, Veska!, Marcella, Antonella, Sangram, Mamoni, Marianna, Serena, Mahesh, Chiara, Andrea, Arianna, Patrizia, Lorenzo, Marina and all the others that are too long to list... I will remember you when returning home!

Finally, I am greatly indebted to my family. Deciding to do this PhD was not simple for me because I had to leave home for a long period of time. My family encouraged me in all moments providing emotional support without which I certainly would not be able to accomplish this work. A huge thanks to my parents, Vitório and Anair, to my brothers, Eriberto (and Geneci), Wilson (and Shirley), Sérgio (and Cinthya) and Iracy (and Joel) and to all my nephews and nieces. Finally, a truthful thanks to my husband Laerte, for allowing me the time and space to follow my dreams and ideas, for its love, support, advices and faith, for being father and mother in the lasts weeks, for everything…

# INDEX

# LIST OF ABBREVIATIONS

| | |
|---|---|
| AM: | Aquatic Medium |
| AN: | Aniline |
| ANOVA: | Analysis of Variance |
| CCD: | Central Composite Design |
| COD: | Chemical Oxygen Demand |
| $CO_i$: | Carbonyl Index |
| $C_S$: | Amount of carbon in the sample |
| CS: | Corn-Starch |
| C22: | Docosane |
| C16: | Hexadecane |
| DEX: | Statistical Design Experiment |
| DMTA: | Dynamic Mechanical Thermal Analysis |
| DO: | Dissolved Oxygen |
| DS: | Inoculum derived from activate sludge, sewage effluents, surface water, soil or a mixture of them |
| DSC: | Differential Scanning Calorimetry |
| Dt: | Mineralization |
| DTGA: | Derivative Thermogravimetric Analysis |
| E: | Elastic Modulus |
| E': | Storage Modulus |
| E'': | Loss Modulus |
| Ea: | Activation Energy |
| EAA: | Poly(ethylene-*co*-acrylic acid) |
| EC: | European Community |
| EEA: | European Environmental Agency |
| EDP: | Environmentally Degradable Plastics |
| EDS: | Energy Dispersive X-ray Microanalysis Spectroscopy |
| EGMA: | Poly(ethylene-*co*-glycidyl methacrylate) |
| EMAC: | Poly(ethylene-*co*-methyl acrylate) |
| EPI: | Environmental Technologies Inc. |
| EU: | European Union |

| | |
|---|---|
| EVA: | Poly(ethylene-*co*-vinyl acetate) |
| EVOH: | Ethylene-vinyl alcohol copolymer |
| FDA: | Food and Drug Administration |
| GL: | Glucose |
| FTIR: | Fourier Transform Infrared Spectroscopy |
| GMA: | Glycidyl Methacrylate |
| HDPE: | High-density polyethylene |
| Hm: | Melting Enthalpy |
| HPLC: | High Pressure Liquid Chromatography |
| ID: | Molecular Weight Distribution |
| IMSM: | Inoculum Mineral Salt Medium |
| IMSM16: | Inoculum Mineral Salt Medium Containing Hexadecane |
| IMSM22: | Inoculum Mineral Salt Medium Containing Docosane |
| IRU: | Inoculum |
| k: | Rate Constant |
| KE: | Acetone Extractable Fraction |
| LDPE: | Low-density polyethylene |
| LLDPE: | Linear low-density polyethylene |
| MA: | Methyl Acrylate |
| MBAS: | Methylene Blue Active Substances |
| MFI: | Melt Flow Index |
| Mn: | Number-Average Molecular Weight |
| MO: | Microorganism |
| MSM: | Mineral Salt Medium |
| MW: | Weight-Average Molecular Weight |
| NA: | Ammonia Nitrogen |
| PAS-FTIR: | Photoacoustic Fourier Transform Infrared Spectroscopy |
| PE: | Polyethylene |
| PER: | Perlite |
| PET: | Poly(ethylene terephthalate) |
| PHA: | Poly(hydroxyalkanoates) |
| PHB: | Poly(3-hydroxybutyrate) |
| PHBV: | Poly(3-hydroxybutyrate-*co*-valerate) |
| PP: | Polypropylene |

PS: Pristine Sample

PT: Total phosphate

PVC: Polyvinyl chloride

PVdC: Poly(vinylidene chloride)

PWC: Pure Whatman Cellulose Filter Paper

Re: Residue

$ROO_i$: Hydroperoxide Index

SB: Strain at Break

SBi: Soil Burial

$SB_P$: Strain at Break in the Parallel Direction of Blow

$SB_T$: Strain at Break in the Transverse Direction of Blow

SBo: Sodium Benzoate

SBS: Styrene-butadiene copolymer

SEC: Size Exclusion Chromatography

SEM: Scanning Electron Microscopy

Sm: Melting Entropy

SS: Sodium Stearate

ST: Tensile Stress at Break

$ST_P$: Strain at Stress in the Parallel Direction of Blow

$ST_T$: Strain at Stress in the Transverse Direction of Blow

Tan δ: Damping Factor

TAS: Thermally Aged Sample

$T_c$: Crystallization Temperature

$T_{cc}$: Cold Crystallization Temperature

$T_d$: Decomposition Temperature

TDPA®: Totally Degradable Plastics Additives

$T_g$: Glass Transition Temperature

TGA: Thermogravimetric Analysis

$ThCO_2$: Theoretical Amount of $CO_2$

TIT: Titrymetry

TNI: Total Nitrogen Input

$T_m$: Melting Temperature

TOC: Total Organic Carbon

$T_p$: Peak Degradation Temperature

| | |
|---|---|
| TPS: | Thermoplastic Corn-starch |
| T6: | TDPA® DCP562 |
| T7: | TDPA® DCP571 |
| US: | United States |
| UV: | Ultraviolet |
| VA: | Vinyl Acetate |
| $V_F$: | Flask Volume |
| $V_S$: | Flask Containing MSM |
| WAXS: | Wide Angle x-ray Scattering |
| WG: | Weight Gain |
| $W_S$: | Total Sample Amount |
| WSP: | Soil:Perlite (2:1) |
| $X_c$: | Crystallinity Degree |
| YM: | Young Modulus |
| $YM_P$: | Young Modulus in the Parallel Direction of Blow |
| $YM_T$: | Young Modulus in the Transverse Direction of Blow |

## LIST OF TABLES

## LIST OF FIGURES

## ABSTRACT

The study of this thesis was focused on materials based on polyethylene (PE), which remains as the largest polymer used in the field of packaging. This polymer is not biodegradable and its waste represents a serious problem to the environment. A proposal of eco-compatible PE based materials will be presented. This is bound to the enhancement of the polyethylene oxo-biodegradability through the blending with biodegradable polymers of biosynthetic origin, [poly(hydroxybutyrate) (PHB) or starch] and commercial prodegradant additives.

This work was structured in three chapters. In the first chapter, the compatibilization between PE and PHB was studied. For this purpose, a screening statistical design experiment (DEX) was preformed, in order to assist in the selection of the better compatibilizer and materials proportions. The variables selected were three copolymers, containing both PE and polar segments, and their amount in the blend, which was constrained at the limits of 10 wt-% and 40 wt-% depending on the compatibilizer. These compatibilizers were poly(ethylene-*co*-vinyl acetate) (EVA), poly(ethylene-*co*-glycidyl methacrylate) (EGMA) and poly(ethylene-*co*-methyl acrylate (EMAC). The films were characterized by means of thermal analysis (TGA and DSC), scanning electron microscopy (SEM), wide angle x-ray scattering (WAXS), Photoacoustic Fourier Transform Infrared Spectroscopy (PAS-FTIR), dynamic mechanical thermal analysis (DMTA) and tensile tests (Instron). EGMA was chosen as the compatibilizer to formulate a new series of materials. This compatibilizer promoted the better adhesion between PE and PHB than the others two tested copolymers did. The best formulation was found for PE matrix with 10 wt-% of EGMA (68E22B10G).

In the second chapter, PE-PHB-EGMA blends were formulated in presence or not of prodegradant additives (Totally Degradable Plastics Additives - TDPA®) DCP562 (T6) and DCP571 (T7). The formulation strategy followed a central composite design (CCD) where the independent variables were the amount of the biodegradable polymer PHB and of the prodegradant additives T6 and T7. Films were characterized by means of

SEM, TGA, DSC, FTIR and Instron. This family of materials was submitted to a thermal aging experiment at three temperatures (45, 55 and 65 °C). Gravimetry, FTIR, SEC, TGA, DSC and Instron were carried out to characterize the thermal aged samples. The prodegradants were effective in promoting PE oxidation. Thermal aged PE-PHB-EGMA-TDPA blends samples showed significant changes on weight gain and carbonyl index ($CO_i$) measured in FTIR spectra. By means of $CO_i$ were evaluated the activation energy (Ea) of thermal degradation applying the Arrhenius equation. Blends containing PHB presented lower values of activation energy (54 kJ/mol for 2B3T6) compared to the equivalent blend without PHB (81 kJ/mol for 3T6). Samples from thermal aging were biodegraded in both aquatic media and soil burial. The biodegradation of the blends in both ambient showed low mineralization. For example, the maximum mineralization of 2B3T6t (85.5PE-9.5EGMA-2PHB-3T6) sample was *ca*. 4 % after 140 days in soil burial, probably as a consequence of the large extent of crosslinking occurred during the thermal aging, which in this case increased up to 76 %.

The last chapter of this thesis comprises two series of experiment concerning PE-Starch composites. In the first one, the compatibilization of compression moulded PE-Starch materials was studied. In the second part, selected composites of compatibilized PE-Starch were prepared by melt blow extrusion. Two different types of starches and two compatibilizers were defined as variables: thermoplastic corn-starch (TPS) and natural corn starch (CS) as fillers and EVA and EGMA as compatibilizers. The results obtained showed that: i) PE-TPS films resulted in very distinct phase separation even when higher amounts of EVA and EGMA were used; ii) In the PE-CS films the compatibilizer EGMA at 20 wt-% provided a good dispersion of starch granules. In addition, blends containing CS produced films more homogeneous than that with TPS. The best compatibilized formulation was used to prepare by melt blow extrusion PE-CS based composites and PE-Biopar blends containing or not T6 and T7 prodegradants, whose films were mechanically tested. The mechanical properties of PE family of materials containing CS and Biopar presented similar values for Young modulus (100-200 MPa). However, films with Biopar presented higher values of tensile strain (*ca*. 200 %) than films with CS (*ca*. 100%).

# 1. INTRODUCTION

It is projected a growth of about fifty percent in the global population over the next fifty years. This will put a significant pressure on the environment issue. In accordance with studies of European Environmental Agency (EEA)[1] the population of the developing countries will achieve levels of material wealth similar to today's levels in industrialised countries. Naturally, world consumption of resources would increase by a factor ranging from two to five and a huge growing volume of municipal and industrial wastes will have to be handled.

Waste consists of a mix of very different materials. Each material has its own characteristics, environmental impact, recycle and re-use options. The inevitable waste resulting from plastic goods and packaging are found all over the world. Plastics are relatively cheap, durable and versatile materials. However, when is transformed in waste it constitutes a sizeable percentage of the litter. Besides, many of the plastics are also non-biodegradable or are difficult to re-use and/or recycle, which may represent risks to human health and to the environment.

Figure 1.1 gives a panoramic view of the most frequently polymers used in the packaging market. Polyolefin family is of great importance in this market with more than 60% of the total plastic weight. In this context, packaging represents one of the most important topics in the waste management. For example, it represents roughly one-third of municipal waste in the industrialized countries as United States[2]. Naturally, this representation depends of several factors as for example country, culture and so on. Any way, polyolefin is a material family that justifies any activity in innovation[3].

In 2007, the global consumer packaging market was estimated to be around US $410 billion with a growth projection of about 5% per annum that can arrive over US $470 billion in 2010. The more representative markets are North of America and Europe that absorb 29% and 33 % of this market, respectively. Food and beverage packaging are the two largest segments, accounting for more than two-thirds of the total[4].

In relation to the production of de most common polyolefin, it can be said that at the present both polyethylene (PE) and polypropylene (PP) dominate the demand for global thermoplastics, which represent over 60% of all commodity resins consumed on an annual basis. This means that they represent a large portion of the global thermoplastic business and consequently waste. Figure 1.2 shows the relationship between demand and capacity with a projection up to 2009 that anticipate a production of about 90 million of tons for PE[5, 6].

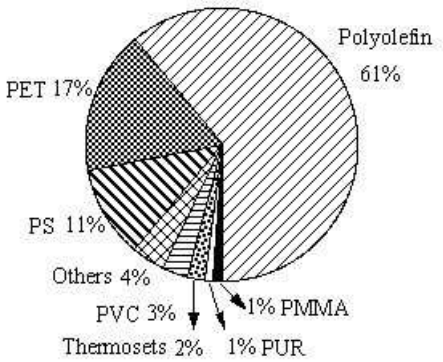


**Figure 1.1.** Plastic shares in the packaging market.

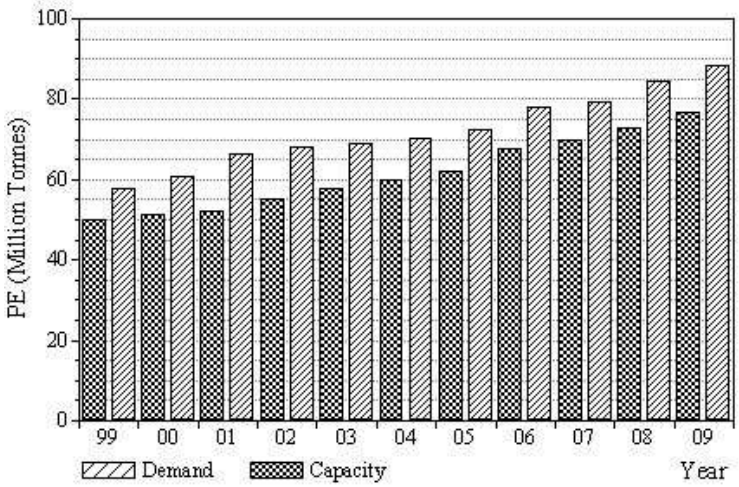


**Figure 1.2.** Relationship between demand and capacity of PE.

PE is the plastic most well known to the consumer and is used in greater volume worldwide than any other plastic. Future annual demand growth for PE plastics in Western Europe is predicted to be about 6% (Fig. 1.2), with the major application continuing to be packaging. This versatile polymer is used in a variety of areas from packaging to agriculture, building to electronics as illustrated in Figure 1.3. Packaging is the major application for PE. The second most important one is wholesale.

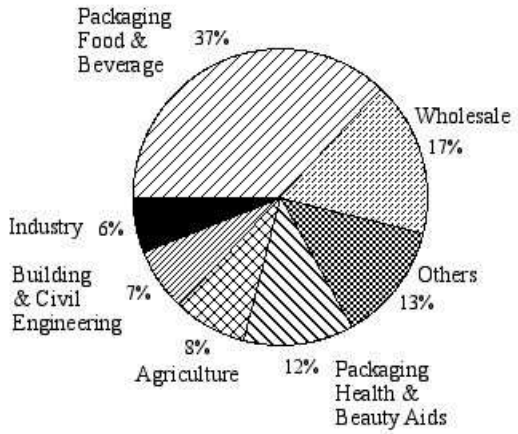


**Figure 1.3.** Demand as a function of consumption purpose of PE.

The continuous growth of polymer materials for food packaging applications in conjunction with their recalcitrance toward degradation and their visibility in the environment when discarded have stimulated further research in the field of food packaging. It has been estimated that 2% of all plastics eventually reach the environment, thus contributing considerably to a currently acute ecological problem[7].

## 1.1. Waste disposal issues and legislative background

The greatest environmental pressure for the packaging chain comes from legislation. According to the European Environmental Agency[1], packaging waste is the major and growing waste stream. Its amounts have

increased in most European countries despite the agreed objective of waste prevention. The projections show that packaging waste amounts will arrive at 77 million tonnes in 2008.

A well-known example at European level is the EC Directive on Packaging and Packaging Wastes. This directive stipulate that "*packaging* shall mean all products made of any materials of any nature to be used for the containment, protection, handling, delivery and presentation of goods, from raw materials to processed goods, from the producer to the user or the consumer. *Non-returnable* items used for the same purposes shall also be considered to constitute packaging"[8]. "*Packaging waste* shall mean any packaging material covered by the definition of waste in Directive 75/442/EEC, excluding production residues" and "*waste* means any substance or object which the holder disposes of or is required to dispose of pursuant to the provisions of national law in force"[9].

Packaging Directive revision (2004/12/EC) was published in February 2004. It sets new recovery and recycling targets as a percentage of all packaging waste (Tab. 1.1) that need to be accomplished up to 31 December 2008. Besides, this revision modified packaging definition presented in the Directive 94/62/EC by inclusion of new criteria. For example, "items shall be considered to be packaging if they fulfil the abovementioned definition without prejudice to other functions which the packaging might also perform, unless the item is an integral part of a product and it is necessary to contain, support or preserve that product throughout its lifetime and all elements are intended to be used, consumed or disposed of together"[10].

These normative aims to harmonise the management of packaging waste in the EU and tackle the impact that packaging and packaging waste have on the environment. Although the primary objective is to increase the recovery and recycling of packaging waste in a consistent way in all Member States of the EU (so as to avoid barriers to trade), priority is also given to reducing the amount of packaging used and the reuse of packaging.

However, recycling has often ecological, economical, technical, or hygienic limits. Ecological limits arise when the environmental disturbances resulting from recycling are higher than without recycling. This is the

function of local conditions and infrastructure. Economic limits appear when recovery is more expensive than the disposal of packages and are a theme of much debate. The re-processing operation itself uses oil-based energy; almost one third of the energy used in the manufacture of PE is invested in the processing operation[11].

There is a wide moral opposition against economical reasons winning over ecology. Besides, it is very difficult to express in money terms the environmental disturbances arising from landfill, such as visual disturbance and the loss of amenity. Nevertheless, when reprocessing energy is added to the energy expended in transportation and cleaning the waste and in the additives used to provide a good product, the ecological benefits of recycling is frequently lost.

**Table 1.1.** Recovery and Recycling Targets to be attained up to 31 December 2008.

| Targets | wt-% |
|---|---|
| Recover or incinerate with energy recovery | > 60 |
| Recycle in general | 55-80 |
| Glass recycled | > 60 |
| Paper and board recycled | > 60 |
| Metals recycled | > 50 |
| Plastics recycled | > 22.5 |
| Wood recycled | > 15 |

The more obvious obstacles are the technical limits of recycling. They are the subjects of concern at plastics recycling, because of the ageing of material at recycling. Unlike glass and metals, which can be recycled to products with properties essentially similar to the primary materials, recycled plastics do never have the same quality as the virgin material. Mechanical recycling of individual polymers results in the reformation of similar but generally downgraded products. Each time polymers are reprocessed there is a loss in physical and mechanical properties due to peroxidation[11].

There are also the hygienic limits, once plastics are often soiled by food and other biological substances, making physical recycling of these materials impractical[12]. Moreover, health hazard reasons to avoid using these recycled materials for packaging food. Besides, materials recycling of household waste plastic is particularly difficult when they are contaminated with biological residues or, as is usually the case, when they are a mixture of different kinds of plastics.

Another solution for litter is the burning, but this is no longer and ecologically acceptable way of disposing of consumer wastes. Incineration with energy recovery is an ecologically acceptable way of utilising carbon-based polymer wastes due to their high calorific value. The calorific value of PE is similar to that of fuel oil (Table 1.2) and the thermal energy produced by incineration of PE is of the same order as that used in its manufacture. However, there is a widespread distrust of incineration by the public due to the possibility of toxic emissions from some polymers. An alternative to direct incineration is to convert polymer wastes by pyrolysis or by hydrogenation to low molecular weight hydrocarbons for use either as portable fuels or as polymer feed stocks. This is a highly specialised operation, which is not appropriate for municipal waste disposal[11].

**Table 1.2.** Calorific values of plastics compared with conventional fuels[11].

| Fuel | Calorific value (MJ/kg) | Fuel | Calorific value (MJ/kg) |
|---|---|---|---|
| Methane | 53 | Polyethylene | 43 |
| Gasoline | 46 | Mixed plastics | 30-40 |
| Fuel oil | 43 | Municipal solid waste | 10 |
| Coal | 30 | | |

The U.S. Environmental Protection Agency and Community of European Norms recommend composting as one of the most promising

methods of waste management[13]. Since biodegradable polymers are suitable for composting, there is an increasing interest in polymers that can be biologically recycled to biomass and this type of polymers may be based either on renewable resources or on petrochemicals. This biological recycling should be considered as an alternative to the more traditional recycling procedures and this has stimulated researches around the world to modify existing polymers or to synthesise new polymers that can be returned to the biological cycle after use[12, 13].

Taking into account all these routes for waste reduction, it seems inevitable then that environmental biodegradable polymers will have an increasing role in the management of waste and litter in the future.

## 1.2. Use of polyethylene in packaging

### 1.2.1. *The importance of polyethylene in packaging*

Polyethylene, the first commodity plastic used on packaging, came into general use in the 1950s. Polyethylene (PE) is a family of polymers including for example the following: low-density polyethylene (LDPE), linear low-density polyethylene (LLDPE) and high-density polyethylene (HDPE). These PE differ principally in their density, which is related with their degree of crystallinity. Consequently, this property will influence their melting point ranges. Some typical properties values ranges for PEs are illustrated in Table 1.3[14].

**Table 1.3.** Typical PEs properties.[a)]

| Type of PE | Density ($g/cm^3$) | Crystallinity (%) | $T_m$ (°C) | MW (KDa) |
|---|---|---|---|---|
| LDPE | 0.915-0.940 | 45-55 | 105-115 | 10-50 |
| LLDPE | 0.915-0.926 | 30-45 | 112-124 | 50-200 |
| HDPE | 0.940-0.970 | 70-90 | 120-130 | up to 250 |

[a)] $T_m$ is melting temperature; MW is average molecular weight.

The dominance of PEs on packaging products is principally due to its low cost. Some other advantages with their disadvantages are described in Table 1.4. The range of packaging forms for which PE is used extends from simple plastic film bags to combinations with other plastics or materials, such as paperboard and aluminium, to provide sealable packaging ensuring that the quality of the packaged foodstuff is effectively maintained.

**Table 1.4.** Advantages and disadvantages of polyethylenes.

| Advantages | Disadvantages |
|---|---|
| Very low cost | Susceptible to environmental stress cracking |
| Excellent chemical resistance | Low strength, stiffness and maximum service temperature |
| Very good processability | High gas permeability, particularly carbon dioxide |
| High impact strength at low temperature | Poor UV resistance |
| Excellent electrical insulating properties | Highly flammable |
| Very low water absorption | High-frequency welding and joining impossible |
| FDA compliant | |

Although PE plastics were first produced over 50 years ago, manufacturing and processing developments continue to improve its properties, performance, and packaging applications[14]. One well-known example is concerned with the oxidation stability of PE. Olefin polymers are prone to oxidative degradation, particularly at the elevated temperatures used in their processing. The reaction of PE oxidation results in the formation of long-chain branches and cross-linking. Therefore, the formulations of all commercial PE plastics contain antioxidants[15, 16]. Besides, other additives must be incorporated in order to maintain and provide the desired physical

properties and to ensure the efficient processing and handling of the finished products[17].

Additives such as colorants, whitening agents, slip additives, and antistatic agents are often conveniently incorporated into the basic polymer before processing into the final product (films, containers, etc.) by means of master batches. Master batches are concentrates of the additive(s) dispersed in the same or similar polymer types.

Both HDPE and LDPE plastics are used to produce a wide variety of caps and covers for bottles and containers. The use as films for container labels is also growing. To make PE films, the particular properties of slip (friction) and blocking (film layers sticking together) must be enhanced for effective and efficient handling during manufacture and processing into the finished packaging. Enhancement of these properties is achieved by the addition of slip agents and suitable fine particulate fillers to the polymer. Typical slip agents are the fatty acid amides oleamide and erucamide, which "bloom" (exudates) to the film surface after manufacture. Titanium dioxide and calcium carbonate are typically used to produce white plastics. The inclusion of calcium carbonate in the polymer also improves the properties of hardness, stiffness, and printability as well as permeability to oxygen and to water vapour. Shrinkage and elongation are reduced[14].

To improve adhesive properties of PE its structure was modified forming a class of polymer called ionomer. This new family of material is a polyolefinic copolymer containing a small amount of ionic comonomer, which contain sulphonic or carboxylic acid groups neutralized with a metal cation. Aggregation of these metal salt groups induces heterogeneity with a length scale of a few nanometers. The best-known (and commercially most important) ionomer are derived from ethylene-methacrylic acid copolymers, by neutralizing some or all of the methacrylic acid units with a metal cation (*e.g.*, $Na^+$ or $Zn^{2+}$). Materials in this category are marketed by DuPont under the trade-mark Surlyn®. This polymer can be used in packaging seals, films, cosmetic goods and personal care sports, recreation foam sheet and encapsulants[18].

In multi-layers films PE is combined with a variety of polymer types, such as polyethylene terephthalate (PET), polypropylene (PP), poly(vinylidene chloride) (PVdC), and ethylene-vinyl alcohol copolymer (EVOH). The polymer used in each layer is selected to provide a required properties and performance characteristics. When good oxygen barrier property is essential, an aluminium foil layer is incorporated. Such flexible packaging is used for coffee, where the structure also acts as gas barrier in reverse, ensuring that the coffee aromas are retained. In special multi-layer packaging materials, PE is combined with paperboard and aluminium by extrusion coating. A typical example is the container for packaging long-life fruit juices and milk (Tetra Pak)[19]. The PE allows the container to be easily heat-sealed and also provides water barrier. The paperboard provides rigidity, and the aluminium acts as oxygen barrier, which ensures that the safety and quality of the packaged product are maintained during its shelf life. For foodstuffs with a short shelf life, it is not used the aluminium layer. Paperboard coated on both surfaces with PE is extensively used for boxed containers for milk products, take-away high-moisture and fatty foods, and for disposable beverage cups. Polyethylene-coated paperboard is widely used as external cartons for many foods, over a wide temperature range (frozen to ambient). Such cartons are easily heat sealed in food packaging line processes by spot contact heating.

Polyethylene-coated aluminium foil is extensively used as lidding material for pots and other containers. The PE coating that melts under heat and bonds the aluminium to the substructure provides the sealability of these foils[20].

Many of the PE films and containers used to package are printed to provide product identification, information on use, and decoration. Because PE has low surface energy, surface treatments are necessary to enable printing inks to achieve adequate adhesion. Corona discharge, flame, and ozone treatments are commonly used to increase the surface energy by imparting a degree of oxidation to the PE surface.

### 1.2.2. *Disposal of polyethylene*

In the 1970s, all the technical advantages, which made hydrocarbon polymers so useful in the past (as biologically inert and resistant to peroxidation) become disadvantages. This was a consequence of the discarded polymer-based products at the end of their useful life, particularly when they appeared as litter in the environment. As the concentration of the PE used in packaging sectors such as in the manufacturing of shopping bags, bottles and containers is very large, the amount of problems relating the final disposal in landfills increases. Hence, the degradation and disposal options, or possibly the biodegradation of the used PE represent a very important subject from the point of view of both economic and environmental aspects.

As aforementioned, in an attempt to reduce the visible environmental pollution caused by post-consumer plastic materials, the members of EU States brought together to find a solution to plastic pollution. One of the objectives is the reduction of the waste through the recovery and recycling of these materials. However, recycling presents a great number of limitations. The most important is related to the technological problems, once this type of material often are disposed with organic products such as food, making recycling hard and sometimes impossible. Moreover, the costs of collecting, cleaning and sorting all these post-consumer plastics are high and the market for mechanically recycled plastics is limited, partly for this reason. Proper incineration of waste plastics would enable the recovery of most of the energy stored in them (polyolefins are excellent fuels) but modern incinerators are expensive.

Considering the aspects above, one possible solution for the problem of the PE disposal can be the partial or total replacement of PE for the named "Environmentally Degradable Plastics" (EDP). EDP can be considered to include a wide group of natural and synthetic polymeric materials or blends of both, that undergo chemical change under the influence of environmental factors[21]. The chemical changes must be followed by complete microbial assimilation of degradation products resulting in carbon dioxide and water[22]. The process of EDP degradation comprises two phases, disintegration and

mineralization. During the firs phase, disintegration is associated with the deterioration in physical properties, such as discoloration, embrittlement and fragmentation. In the second phase is assumed that a complete conversion of plastic fragments, after being broken down to low molecular weights should occurs[23].

## 1.3. Environmentally degradable plastics (EDP)

### 1.3.1. *General considerations*

The worldwide consumption of biodegradable polymers has increased from 14 million kg in 1996 to 68 million kg in 2001. Mainly markets for biodegradable polymers include packaging materials as shopping bags and food containers, hygiene products, consumer goods as fast-food tableware and toys, containers and agricultural materials as mulch films[12].

Several definitions are useful in understanding the complexity of the topic of biodegradable polymers. These begin with the concept of plastic waste following with that of natural polymers, degradable, biodegradable, hydrolytically degradable, and oxidatively degradable materials.

Natural polymers are by definition those biosynthesized by various routes in the biosphere. Proteins, polysaccharides, nucleic acids, lipids, natural rubber, and lignin, among others, are all biodegradable polymers. Moreover, the rate of the biodegradation may vary from hours to years depending on the nature of the functional group and degree of complexity of the macromolecule[24].

Degradation is a process where the deterioration in the polymer properties takes place due to different factors like light, heat, shear, *etc*[25]. As a consequence, the resulting smaller fragments do not contribute effectively to the mechanical properties and the material becomes brittle. Besides, the life of the material becomes limited[26]. The degradation of polymers may proceed by one or more mechanisms, including biodegradation, chemical degradation, photo and thermal oxidation, *etc*., depending on the polymer environment and desired application[27].

Environmentally biodegradable polymers are designed to degrade upon disposal by the action of living organisms[12]. Biodegradation is defined as the conversion of a material to $CO_2$, $H_2O$ and traces of inorganic chemicals under aerobic conditions or to $CH_4$, $CO_2$ and inorganic chemicals under anaerobic conditions by the action of Microorganisms (MO). So, biodegradation in aerobic (Eq. 1.1) and anaerobic (Eq. 1.2) environments may be described by the following chemical equations taking into account a hydrocarbon polymer[28]:

$$\text{Polymer} + \text{MO} + O_2 \rightarrow CO_2 + H_2O + \text{biomass} + \text{residue} \qquad \text{(Eq. 1.1)}$$

$$\text{Polymer} + \text{MO} \rightarrow CH_4 + CO_2 + H_2O + \text{biomass} + \text{residue} \qquad \text{(Eq. 1.2)}$$

Biomass represents an important part of the organic carbon cycle, which has been assimilated by microorganisms.

It should be pointed out that though fragmentability of the polymer and loss of elongation (95 % is defined as the embrittlement point) should constitute inherent characteristics of degradable polymers, several additional features are required if the polymers are to be acceptable from the ecological point of view: (i) a predetermined service time (induction time) during which no properties change whatever; (ii) the end of induction period should be followed by an accelerated fragmentation stage; (iii) a final, total and innocuous assimilation of the fragmentary products by the ecosystem[29].

At the present time, there are three main classes of biodegradable polymers. In the first one, it is found the synthetic polymers. These polymers contain groups susceptible to hydrolysis attack by microbes such as polyesters, polyanhydrides, polyamides, polycarbonates, polyurethanes, polyureas and polyacetals[29, 30]. The second class of materials is composed of bacterial polymers as poly(3-hydroxybutyrate) (PHB) and poly(3-hydroxybutyrate-*co*-valerate) (PHBV)[31]. Finally, it is considered the polymeric blends and bio-based composites as the third series of materials that are readily consumed by microorganisms. A classic example is the blends of PE with starch[30, 32, 33].

In this introduction, special attention will be given to the third class of EDP. In particular, it will be reviewed the literature related to materials based on oxo-biodegradable polyolefins, their preparation, its blends with natural polymers, the thermo and/or biodegradation mechanisms, the main applications, advantages and inconvenient of this family of materials.

### 1.3.2. *Oxo-degradable polyolefins*

There are two mainly applications for oxo-degradable polymers. The first is where biodegradability is part of the function of the product as for example in the biomedical or agriculture fields, and the second application is when degradability is desired at the end of the use of the product, as for packaging. An essential feature for both applications is a variable and controllable induction time to the beginning of peroxidation, which is the rate-controlling step in the overall biodegradation process[25, 34]. Carbon-chain polymers vary remarkably in their ability to resist peroxidation. The following sequence shows some common commercial hydrocarbon polymers in order of decreasing oxidative stability: Polyvinyl chloride (PVC) > Polyethylene (PE) > Polypropylene (PP)[35].

What is needed, is a way of controlling the time during which the polyolefin retains its normal, useful properties as well as a way of having it undergo subsequent oxo-biodegradation at a much higher than normal rate that is commensurate with the application and with the disposal environment[35]. The key to this control requirement is a sound understanding of the peroxidation mechanisms and kinetics[36]. In the environmental degradation of oxo-degradable polymers, the total degradation will be a synergistic effect of several agents[37]. The main degradant agents are UV-radiation, heat and oxidizing agents leaving to a brittle material with a higher susceptibility to biodegradation[22, 38]. The final end products of the total mineralization will be carbon dioxide and water. Before that stage is reached, many low molecular weight degradation products will be evolved, which in turn can increase or decrease the degradation[38].

It is accepted that polyolefins are bioinert[38], which means that they are highly resistant to assimilation by microorganisms such as fungi and bacteria. This is expected, since the surfaces of materials and articles made from polyolefins are hydrophobic, which inhibit the growth of microflora on them. Besides, there are common mechanisms of biodegradation that involve bio-assimilation from the ‘‘ends’’ of substrate molecules. Since commercial polyolefins have relatively high molar mass values, there are very few ends of molecules accessible on or near the surfaces of materials made from these resins. Different approaches to render synthetic plastics degradable have been considered. It is generally found that photo and thermal-oxidation increases the biodegradation of polymers[21]. Photo and thermal-oxidation increase the amount of low molecular weight material by breaking bonds, increasing the surface area, through embrittlement and increasing the hydrophilicity by the introduction of carbonyl groups and all these effects promote biodegradation[39]. Although the family of polyolefins is considered to be not eco-friendly, it has been observed that its oxidation products are biodegradable[35, 40]. Such products have molar mass values that are significantly reduced, and they incorporate polar, oxygen-containing groups such as acid, alcohol and ketone. This is the basis for the term oxo-biodegradable polyolefins. This concept is used to distinguish polymers that biodegrade by a hydrolysis mechanism from those that are inert to hydrolysis but undergo oxidation. Oxo-biodegradation then denotes a two-stage process involving, in sequence, oxidative degradation, which is normally abiotic in the first instance, followed by the biodegradation of the oxidation products[35].

Oxo-degradable polymers can be produced by the addition of sensitizer additives that will promote the formation of free radicals in the presence of heat. Hence, peroxides will be generated and auto-oxidation will be consequently enhanced[41]. Oxo-degradable polymers can also be prepared by changing the polymer structure by introducing chromophores[41]. In this class of materials, the carbonyl groups can be introduced, for example, through the copolymerization of PE with a small amount of monomer such as carbon monoxide producing a degradable copolymer. Jones *et al*.[42] has formulated a

copolymer of vinyl ketones and styrene or ethylene where the ketone groups are part of the main polymer chain. These materials were shown to biodegrade and the degradation was monitored using respirometry.

Albertsson and Karlsson present different means of modifying otherwise relatively inert polymers (in particular PE) in order to obtain environmentally degradable polymers[39]. They concluded that the incorporation of transition metal complexes facilitates the photo-oxidation of inert LDPE, and that was also possible to induce early photo-oxidation by polymerization of ethylene with carbon monoxide or by the addition of other ketonic groups to PE. LDPE samples containing (1) iron dimethyldithiocarbamate, (2) iron dimethyldithiocarbamate and (3) 0.8% carbon black and iron dimethyldithiocarbamate and nickel dibutyldithiocarbamate were aging in a weatherometer where the temperature increased during ageing, achieving a mean value of about 50°C. The dithiocarbamates are effective processing stabilizers and heat stabilizers for polyolefins. Their photo-antioxidant activity depends on the metal ion, where iron and manganese complexes are the least stables. These metal complexes show a well-characterized induction period, which increases with their concentration in the polymer. The sulphur ligand iron complexes combine a high level of antioxidant activity during processing, storage and in the early stages of exposure to light. After this initiation, a very fast photo-oxidation occurs[39].

Polyolefins with enhanced degradability have been available commercially for more than three decades and have been successful used in agricultural products for most of this time. They can be obtained through the mixture of inert polymers with others from renewable resources as starch.

Starch is the lowest priced and most abundant worldwide commodity, it is the major form in which carbohydrates are stored by plants in the form of granules (mainly from potatoes, corn, and rice). Among other features, it is inexpensive and annually renewable. Starch granules vary from plant to plant but are in general composed of a linear polymer, amylase (in most cases up about 20 wt-% of the granule), and a branched polymer, amylopectin[43]. It is produced in most countries and is available at low cost in all countries. In

Europe, it is industrially produced with a volume of almost 7 million tones/year. Nearly 50 % of the starch produced is already used for non-food applications and about 30 % of the starch production is industrially precipitated from aqueous solutions because of its very good film-forming properties[44]. Animals, plants and microorganisms are able to utilize starch as a source of energy. Microorganisms produce various starch hydrolyzing enzymes such as amylase and their wide distribution assures the biodegradation of starch in nature[39].

The first attempts to increase degradation of hydrocarbon chain polymers as PE, regards to the incorporation of natural polymers, in particular starch and transition metal pro-oxidants. Microorganisms initially attack this biopolymer leaving a brittle material with a greater surface/volume ratio. Hence, the sunlight, heat, oxygen, *etc*. promote auto-oxidation of the chemically unstable pro-oxidant, generating free radicals, which attack the molecular structure of the PE. With time, the molecular weight will have decreased so much that biodegradation of the PE can take place These materials are useful in applications such as mulching films[27, 39]. However, this type of blends usually leads a phase separation and reduction in mechanical properties due to the lack of compatibility between hydrophilic biopolymer and generally hydrophobic thermoplastic[26].

The idea of using starch inside synthetic polymer matrix was proposed by Griffin[45]. His study was based on introducing starch in its natural form into the synthetic matrix at amounts lower than 10 % while keeping the granular structure intact. In this case, starch is only a filler susceptible to enzymatic degradation but unable to affect the mechanical properties of the final material (20-30 MPa tensile strength and 700-900 % elongation at break point for a 90:10 PE:starch blend). The original concept has been improved also by the addition of unsaturated polymer, a thermal stabilizer and together with the formulation containing starch, a transition metal salt. The starch and other additives are mixed in a master batch (MB), which can be included in polymers in different concentrations. However, blends of LDPE with high amounts of starch exhibits poor mechanical properties owing to their inherent differences in polarity that results in immiscible blends[46]. The main areas of

research concentrate on determining compatibility or coupling agents and repeatable processing parameters[30]. Different ways has been proposed to incorporate functionalized PE in LDPE-starch blends[47-49]. In these studies, either dry granular starch or starch plasticized with water and glycerol have been used. Nevertheless, poor water resistance is a major limitation in their use. An alternative approach is to bring about some compatibility in starch and synthetic polymer by blending starch with polymers containing polar functional groups that can interact with starch improving the adhesion and hence the mechanical properties of these biodegradable blends.

Another method of producing compatible thermoplastic blends is *via* reactive blending, which relies on the *in situ* formation of copolymers or interacting polymers. This differs from other compatibilization routes where the addition of a separate compatibilizer is required. In reactive blending, the blend components themselves are either chosen or modified so that reaction occurs during melt blending, which improves the compatibility and interfacial adhesion of the two immiscible polymers. The small amount of graft or block copolymers formed during the blending process, due to reaction between the two components, is generally enough to stabilize the morphology and improve the properties of the blends.

Sailaja *et al.*[46] studied blends consisting of LDPE and esterified starches, starch acetate (Stac) and starch phthalate (Stph). Starch esters were melted with LDPE using LDPE-*co*-glycidyl methacrylate copolymer as compatibilizer. The results indicate that, in general, LDPE-Stph blends perform better than LDPE-Stac blends. Esterified starch has better mechanical properties than unmodified starch when incorporated in LDPE. The tensile strength and modulus are close to that of pure LDPE for LDPE-Stph blends while the impact strength values are 80 % of that of pure LDPE for 20-40 % Stph loading. The elongation at break values were in the range of 60-70 % of that of pure LDPE for LDPE-Stph blends.

Jeziorska *et al.*[50] reported results of starch-based blends (5 - 30 wt-%) with LDPE and poly(ethylene-*co*-acrylic acid) (EAA). During the reactive blending of LDPE/EAA blend with starch, the carboxylic groups in EAA can react with the hydroxyls of the starch to form hydrogen bonds. Results

showed that the tensile strength of the blends remained practically unchanged when the starch content increased from 5 to 30 wt-%. Besides, all blends containing starch supported the microbes growth, which was faster for the blends with oxidized potato starch than corresponding samples with corn starch. Moreover, the bigger amount of starch in the samples the higher the rate of microbes growth.

Of all the modifying approaches to render starch and PE more compatible, the more efficient is when the compatibilizer is introduced into the blends[51]. When the starch compatibilized synthetic polymer is placed in a biologically active environment, the microbes show considerable amount of surface growth. The surface growth may not result in the degradation of the body of the polymer if the starch is confined to the surface. For complete degradation of the starch to be notice, the starch fraction should exceed the percolation threshold, so that a number of significant pathways for microbial invasion/enzymatic diffusion are generated[52].

At 1974, a commercial product was released, which the Coloroll Company offered as shopping bags in Europe. Griffin has since then made improvements in the technology and the auto-oxidant, which earlier was food oil, was then replaced by other polymer blends. In these formulations, the auto-oxidation has a more clearly defined induction period after which the molecular weight decreases as does also the physical strength, and the biological breakdown is then said to begin[53]. In the 1990s, Griffin discloses a degradable polymer composition wherein an antioxidant and pro-oxidant are combined whereby as the antioxidant is stated to be depleted with time. After total depletion of the antioxidant a residual concentration of pro-oxidant remains and is stated to provide a sharp loss in the physical strength of the degradable polymer composition. The applications discloses use of a stable polymer such as low-density polyethylene, linear low density polyethylene, high density polyethylene, polypropylene, or polystyrene, together with a less stable unsaturated elastomer type compound made from the polymerization of 1:4 dienes, or the copolymerization of such 1:4 dienes with ethenoid comonomers, such as styrene-butadiene elastomer or natural rubber. The invention embodies less stable substances capable of auto-

oxidation because such substances are more readily initiated by the oxidation process by virtue of their unsaturation. Once the auto-oxidation process is initiated, the process is said to involve more resistant saturated substances such as polyolefins[54, 55].

In another study, Albertsson *et al.*[33] assessed LDPE containing different amounts of corn-starch without further additives and corn-starch in a pro-oxidant formulation (MB) (10 %, 15 % and 20 % by weight) after irradiation for periods of up to 500 h. The carbonyl and hydroperoxide indexes of samples containing 20 % MB after 500 h irradiation were about 3 times the values obtained in pure LDPE and in LDPE-starch blends. Besides, during the irradiation, the tensile strength decreased to almost the same extent for all three materials. In this study, a material susceptible to photolysis was obtained by the addition of corn-starch and a master batch containing LLDPE, styrene-butadiene copolymer (SBS) and manganese stearate. Incorporating only starch into LDPE did not significantly change the susceptibility of the material to photolysis. LDPE-MB was degraded by an initial photo-oxidation (auto-oxidation) and a subsequent attack by microorganisms (biodegradation).

Suominen in his patents describe that a biologically degradable film was prepared consisting of a synthetic polymer and a biologically degradable polymer. The biologically degradable polymer was divided into small particles in an aqueous suspension by means of enzymes that split and release small molecules from the surface of the biopolymer particles. After achieving desired particle size, an emulsion was formed with vegetable oil and the particles coated with enzyme protein become coated with vegetable oil, which at the same time interrupts the degradation of the biopolymer particles by the enzyme. The coated particles with the oil were separated from the suspension to remove small molecules after which the particles were re-dried and then pulverized. The final film was prepared in a film extruder in which the biopolymer was mixed with the synthetic polymer and possibly other additives that are generally used in forming polymer films[56, 57].

Another attempt to improve PE biodegradability could be through its blending with poly(hydroxybutyrate) (PHB). PHB is a member of a family of

natural biodegradable polyesters[58], the poly(hydroxyalkanoates) (PHA). It is produced directly from renewable resources by fermenting a sugar feedstock (glucose is currently being used)[59] with several naturally occurring microorganisms as carbon and energy reserves and can be accumulated to high levels in bacteria, approximately 95% of their dry weight, which can grow in a wide variety of natural environments. PHB can be rapidly hydrolyzed to the monomer by extra cellular depolymerase enzymes secreted by a wide variety of bacteria and fungi that can utilize this compound after it is liberated by the death and lyses of bacteria in which it is stored[60, 61].

Since its discovery in the 1920s, by Maurice Lemoigne[60], PHB has been extensive studied[62]. PHB is produced commercially by Monsanto and finds applications in different packaging materials, such as thin films and paper coatings. Besides, it is degradable in several environments, including marine water, soil, sewage sludge and compost[58, 63-65]. PHB has a high melting point, around 180°C and forms highly crystalline solids which crystallize slowly[66-68] and form large spherulitic structures that impart poor mechanical properties in moulded plastics and films, although, addition of nucleating agents and suitable post-treatment after extrusion or casting can lead to much improved properties[60]. A consequence of this high melting point is that PHB is also susceptible to thermal degradation during melt processing[69, 70] by ester pyrolysis of the aliphatic secondary esters of the repeating units. The pure homopolymer PHB, produced in large quantities, is a brittle material (elongation at break $\Upsilon$ = 10%, impact strength 3 kJ/mm$^2$) with a large elastic modulus (E =1.7 GPa) and high fracture stress ($\sigma$ = 35 MPa)[59]. Studies of how melt processing influences PHB have shown that the molecular weight is significantly affected by high temperatures and shear forces[61, 69, 71, 72].

The brittleness of PHB is attributed to: (1) the secondary crystallization of the amorphous phase during storage time at room temperature leading to rapid decrease of elongation at break. As a result of secondary crystallization in the amorphous region, density, crystallinity, stress and modulus increase while the material becomes brittle and hard with much lower elongation at break; (2) the glass transition temperature ($T_g$) being close to room

temperature; (3) the low nucleation density, which results in the development of large spherulites exhibiting inter spherulitic cracks[59].

Oxo-degradable PE-PHB blends could be a good solution to improve PE degradability resulting in a new material for use in the production of eco-compatible packaging. However, PE and PHB are not compatible due to significant differences in their polarity, so as in the case of starch, to reach a product with good processability and mechanical properties a compatibilizer needs to be used. The literature for this type of blend is very modest, mainly regarding blends of PE-PHB without prodegradants[73, 74] remaining a field still to be explored.

### 1.3.3. *Degradation after the useful life-time*

Since degradation is not desirable during the lifetime of a material, the induction period is a crucial property in that it ensures that the material has a certain shelf life. The lifetime of a polymer is dependent not only on the intrinsic characteristics of the material but also on the surroundings (heat, light, pollutants *etc*.)[75].

Even before its use, soon after polymerization, polyolefins are subjected to several processing steps involving extrusions. These processing cycles, which employ temperature and shear cause chemical reactions inside the polymeric matrix. Degradation can be initiated by oxygen, shear, heat, catalyst residues or any combination of these factors[76]. Besides, a variety of environmental factors may affect the polymer: oxygen, temperature, sunlight, water, stress, living organisms and pollutants. The combination of these factors can be cumulative, synergistic or antagonistic[39].

Oxidation can be defined as the reaction of a polymer with oxygen at temperatures where thermal degradation is negligible. This distinguishes it from pyrolysis, the thermal decomposition of the polymer in the absence of oxygen, and from combustion, the reaction between oxygen and the volatile products of thermal decomposition of the polymer[77]. Model compound studies suggest that most polymers should not oxidise significantly at temperatures of normal use. In fact, oxidation is a major technological

problem and few polymers can be used without stabilisation. The reason is the presence of impurities and structural defects in polymers, especially after processing. Oxidation is typically a very slow reaction between a solid, possibly semi-crystalline, polymer and a gas. Oxidative degradation differs from thermal degradation in several important ways: (i) it is slow – reactions over weeks or years; (ii) the production of volatiles may be almost negligible; (iii) diffusion of oxygen into the polymer is required; (iv) polymer is usually solid, and restricted mobility gives complex kinetics; (v) it is possible to stabilize polymers against oxidation, using additives.

It was showed that the release of small molecules from the polymer chains during thermal aging change the morphology during the degradation. It is generally known that the amorphous part of a polymer is more easily degradable, in particular this is the case for hydrolysable polymers. This gives a gradual increase in the crystallinity of the remaining polymer because of the rearrangement of the chains[24].

The thermal oxidation of polyolefins includes initiation, propagation, chain branching and termination steps. Under oxygen deficient conditions not all alkyl radicals ($R^{\bullet}$) can be transformed to $ROO^{\bullet}$[76] (Scheme 1.1).

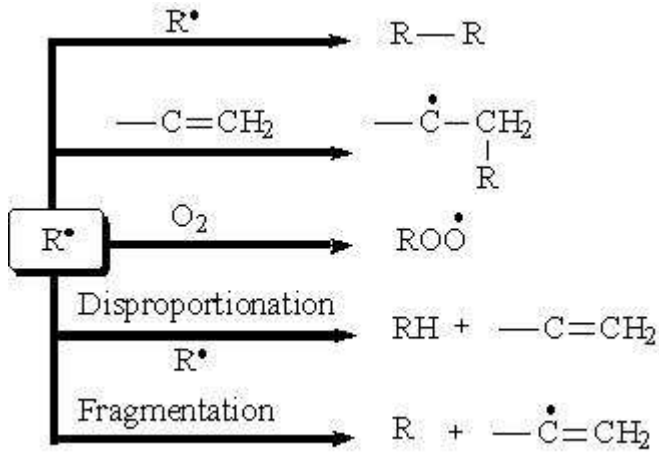


**Scheme 1.1.** Thermal oxidation of polyolefins starting from $R^{\bullet}$.

As shown in the Scheme 1.1, the carbon radical $R^{\bullet}$ reacts with oxygen to form the $ROO^{\bullet}$ radical. The recombination of two radicals $R^{\bullet}$ is a

termination reaction leading to an increase in the molecular weight of the polymer. Another termination reaction is the disproportionation of two $R^{\bullet}$ radicals. The addition of a $R^{\bullet}$ radical to a $-C=C-$ bond is energetically favoured by the formation of a σ-bond at the expense of a π-bond. This reaction leads to chain branching or cross-linking and is related to an increase in the molecular weight of the polymer. The inverse of the addition reaction to a $-C=C-$ bond would be the fragmentation of the $R^{\bullet}$ radical.

In the thermal oxidation of polymers, the first oxygen radical formed is the peroxy radical $ROO^{\bullet}$. After that, occurs the $H^{\bullet}$ radical abstraction from the polymer backbone, which lead to the formation of hydroperoxide ROOH and the carbon radical $R^{\bullet}$. The life-time of the hydroperoxide ROOH must be considered to be very short under processing conditions and it will decompose immediately to form the alkoxy radical $RO^{\bullet}$ and the hydroxyl radical $^{\bullet}OH$. Both species will react by abstraction of a $H^{\bullet}$ radical from the polymer backbone. The carbon radical $R^{\bullet}$ reacts with oxygen to form the $ROO^{\bullet}$ radical. With unactivated olefins, $ROO^{\bullet}$ radicals react mainly by abstraction of a $H^{\bullet}$ radical at the allylic position. The reaction of a peroxy radical $ROO^{\bullet}$ with the carbon radical $R^{\bullet}$ causes the formation of ROOR. This species will split into two alkoxy radicals $RO^{\bullet}$ at the processing temperatures. The reaction of two peroxy radicals $ROO^{\bullet}$ is a termination reaction, leading to non-radical products in the case of primary and secondary species[76].

Hydroperoxide is unstable to both heat and UV light, and its destruction will lead to the formation of several types of oxygen-containing products. One of the few differences between peroxidation initiated by heat and by light is that ketone products are stable to heat but not to UV light. In either case, one is dealing with a branching chain reaction sequence in which the reaction of the hydroperoxide group is the rate-determining step in peroxidation leading to molar mass reduction[35].

Because of its extremely high reactivity, the alkoxy radical $RO^{\bullet}$ reacts by the abstraction of an $H^{\bullet}$ radical from the polymer backbone or by β-scission. The β-splitting of alkoxy radicals into molecules with carbonyl groups (ketones and aldehydes, which are subsequently oxidised to form

carboxylic acids) and carbon radicals R• leads to a decrease in the molecular weight of the polymer (Scheme 1.2). The reactions of RO• with other radicals as R• and RO• are insignificant[76].

In the case of oxo-degradable polymers, it is common to use light and/or heat to initiate free radical chain reactions in polymerization and oxidation processes. There are two examples of this process: (i) molecules whose excited states behave as radical initiating species (carbonyl compounds) and (ii) molecules which dissociate to free radicals (peroxides and transition metal ion salts). Using these processes, it is possible to control the oxidative breakdown of polymers.

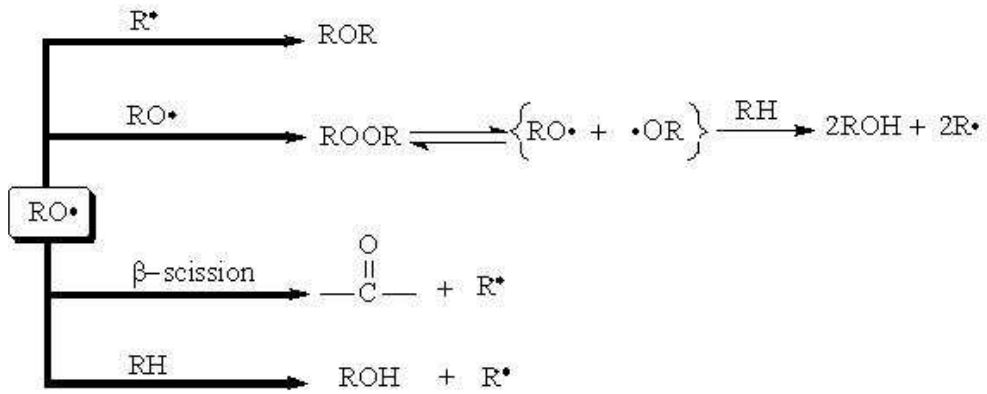


**Scheme 1.2.** Thermal oxidation of polyolefins starting with RO•.

Abiotic peroxidation of the polyolefins gives rise to some vicinal hydroperoxides and this process is particularly favoured in the poly-α-olefins, such as polypropylene due to the susceptibility of the tertiary carbon atom to hydrogen abstraction via a hydrogen-bonded intermediate. A major proportion of the peroxidic products are hydrogen-bonded vicinal hydroperoxides that break down to small biodegradable molecules[35] such as carboxylic acids, alcohols and ketones as well as longer chain oxygen-modified breakdown products, which oxo-biodegrade more slowly[25].

The decomposition of the vicinal hydroperoxides is also facilitated by internal hydrogen bonding and the low molar mass products of this self-induced degradation are small biodegradable molecules such as acetic and formic acids. In the case of the polyolefins, random chain scission is initially

the dominant process. However, some low molar mass oxidation products are formed via vicinal hydroperoxides even in PE. The alkoxyl radicals formed by decomposition of the hydroperoxides contain weak carbon-carbon bonds in the α positions to the hydroperoxide groups, which lead to the formation of low molecular weight aldehydes and alcohols that rapidly oxidise further to carboxylic acids[25].

Hydroperoxides are important intermediate products in the oxidation scheme and their decomposition rate greatly affects the overall oxidation rate of the polymer matrix. Two examples of reactions of metal catalysts with hydroperoxides[32] are showed in Equations 1.3 and 1.4.

$$ROOH + Me^{n+} \rightarrow RO^{\bullet} + Me^{(n+1)+} + OH^{-} \quad \text{(Eq. 1.3)}$$

$$ROOH + Me^{(n+1)+} \rightarrow ROO^{\bullet} + Me^{n+} + H^{+} \quad \text{(Eq. 1.4)}$$

Although biodegradable plastics are required to disintegrate rapidly followed by biodegradation at the end of their use life, it is equally important that their mechanical properties remain essentially unchanged during use. The rate of peroxidation of hydrocarbons, including polyolefins, depends on two primary parameters. The first is the rate of the free radical chain reaction of the polymer with oxygen, which is in turn governed by the rate of reaction of peroxyl radicals with polymers. The second is the presence of initiators that lead to the formation of radicals, of which the most important are the hydroperoxides (ROOH) that are the products of the chain reaction (Eq. 1.5).

$$RH + ROO^{\bullet} \rightarrow R^{\bullet} + ROOH \quad \text{(Eq. 1.5)}$$

The gel content or insoluble fraction (Scheme 1.3) is formed in polyethylene by cross-linking and it is one of the products of PE thermal aging. The thermo-oxidative and thermo-mechanical oxidation can influence polymer molecular weight in two different ways either increasing by cross-linking or decreasing by chain scission and both of these events lead to changes in polymer properties. Cross-linking via an oxidation reaction is due

to the recombination of alkyl radicals $R^{\bullet}$ with each other, with $RO^{\bullet}$ or $ROO^{\bullet}$ radicals like is shown in Scheme 1.3[76, 78, 79].

The natural polymers are biodegraded by a range of catabolic metabolisms catalyzed by series of enzymes. This catabolism produces both energy and building blocks for the biosynthesis of new materials. The ultimate degradation products of biopolymers are carbon dioxide, water, and to some extent ammonia. But, it is very important to remember that only a very few amount of the biopolymers ends up as carbon dioxide and water. Series of other called natural metabolites accumulate and are used again and again in nature[24].

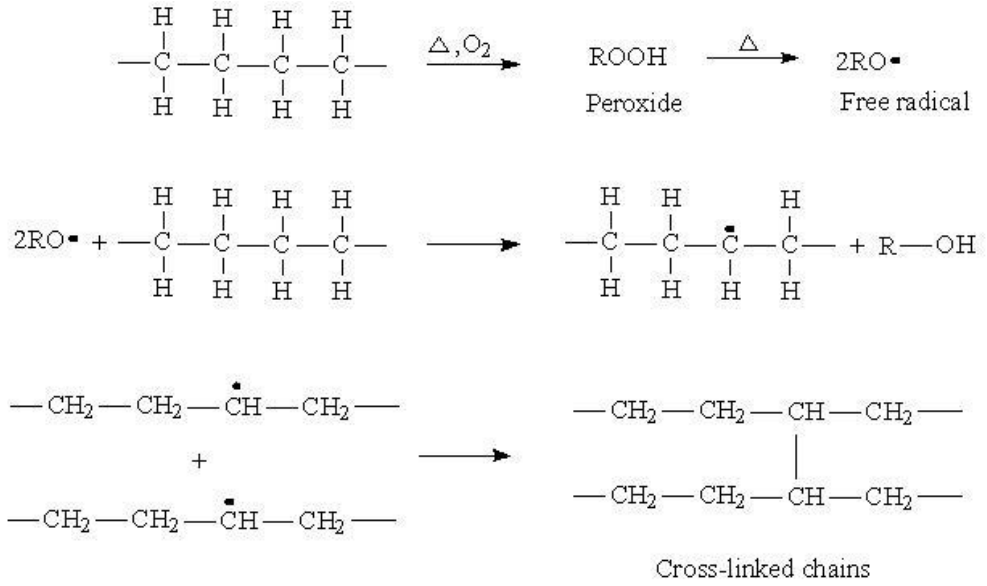


**Scheme 1.3.** General mechanism of polyethylene cross-linking

Biodegradation of oxidable polymers is generally slower than biodegradation of hydrolysable ones. Even polyethylene, which is rather inert to direct biodegradation, has been shown to biodegrade after initial photo-oxidation. Many inert polymers are, however, more susceptible also to biodegradation if modifications are done. Low molecular weight compounds present in polymers render the polymer more susceptible to biodegradation because they become inherently more accessible to chemical reactions. An

oxidized polymer is more brittle and hydrophilic than a non-oxidize polymer, which also usually gives a material with increased biodegradability[24].

As aforementioned, a very used way to increase the biodegradability of LDPE is the introduction of a natural polymer in the inert matrix. For this purpose, the most commonly used natural polymer is starch. However, the use of starch alone in polyethylene, requires rather large amounts in order to really create an increase in the biodegradation rate[24]. Certainly, the filler that is biodegradable always gives a matrix that is more easily accessible to abiotic degradation.

Albertsson and co-workers[34] studying the degradation of LDPE films containing biodegradable starch filler and a pro-oxidant formulations in aqueous media inoculated with bacteria or fungi demonstrated the greater susceptibility to degradation of the LDPE matrix of the samples containing the pro-oxidant and starch than of samples containing only starch or of pure LDPE samples. In its investigations, authors found that the mechanisms responsible for initiating degradation of the LDPE matrix were hydroperoxyde-catalyzed auto-oxidation of the pro-oxidant in synergistic combination with biodegradation of the starch particles.

The biodegradation mechanism of polyethylene showed that initial oxidation is followed by the removal of two-carbon fragments from the chain. This mechanism is confirmed by analysis of carbonyl group formation in the PE surface, which decreases with time in biotic environments[25]. Thus, microorganisms assimilate the degradation products of PE at the same time as the polymer chains gradually biodegrade[24].

## OBJECTIVES

Currently, it can be said that the energy-environmental crisis represents the challenge of an era. Demographic growth creates enormous pressure on environmental resource bases and ecosystem due to its “unsustainable” character. One of the problems contributing to this is that of waste disposal. Their amount naturally is rising constantly, not only due to the increasing of the world population but additionally due to its features: urbanization increasing; rising standards of living and consequent changing patterns of social behaviour and habits (higher consumption); and changes in waste composition patterns (more consumer product packaging). These social changes and the waste generation are independent of the status of the countries: industrialized or in developing. Besides, the mode of waste disposal still predominantly remains through land filling, a conventional and unhygienic method. Alternative modes like composting and other scientific approaches are scarcely used. Consequently, land and water are polluted and degraded besides the fact of being a health hazard. Polyolefins are the largest family of polymer used in packaging applications arriving up to 61 % of total material used in packaging market. Among polyolefins, polyethylene presents a constant increasing demand. Although this polymer is characterized by an excellent cost-benefit ratio, it represents a big problem for the environment. An attempt to overcome this drawback, different approaches has been used to improve the PE degradability. One of them is based on the addition of biodegradable polymers obtained from renewable resources.

The aim of this work is to improve polyethylene oxo-biodegradability through the blending of PE with prodegradants and biodegradable polymers of biosynthetic origin (PHB and starch). To achieve this, two aspects need to be faced up to resolve both the incompatibility of PE with the biodegradable, polar, polymers and to find the ideal proportion of components. Accordingly, a screening study about PE-PHB compatibilization was carried out. Good miscibility between the components of a blend is a very important parameter affecting directly its performance as for example its mechanical and thermal

properties. At the present, little information regarding to the compatibility between PE and PHB was found. Some studies report the compatibility of PHB and EVA containing high VA fraction. Other authors studied the compatibility of PE and starch using EGMA. PE and PHB are polymers with distinct polarities, so a third component, normally a copolymer, which contain in its chain both polar and non-polar comonomer units are needed in order to promote their compatibilization. It is supposed that the amount of PHB, type and amount of compatibilizer are variables that will influence morphological and bulk properties of PE-PHB blends. To promote the compatibility between PE and PHB, it was employed three copolymers containing PE segment and the other segment was from a comonomer compatible with PHB. The formulation of PE-PHB based blends followed a systematic screening statistical design experiment (DEX). Compatibilizers were chosen from available commercial polymers and for economic reasons their proportion limits in the formulations were fixed at a maximum of 15 wt-%. To verify the effect of the copolymers as compatibilizers, films were prepared by compression moulding and characterized in relation to their morphology, thermal and mechanical properties.

The second topic of the thesis corresponds to the study of the oxo-biodegradation of the PE-PHB based blends. In literature there is little about PE-PHB but nothing including a prodegradant. The formulation strategy will follow a factorial design at two levels ($2^3$) with a central point where the independent variables are the amounts of the biodegradable polymer PHB and of prodegradant additives T6 and T7. PE-PHB based materials will be processed to obtain thin films. These films will be characterized in terms of morphology and thermal and mechanical properties. To evaluate their characteristics of oxo-biodegradability, their thermal degradation in a static oven at 45 °C, 55 °C and 65 °C will be performed and periodically analysed by means of FTIR to determine both carbonyl and hydroperoxide index. Data from this analysis will be used for determination of activation energy of thermo-oxidation. Samples aged at 55 °C will be characterized by thermal and mechanical analysis. In addition, the amount of crosslinking formed during thermo-oxidation will be evaluated by means of extraction.

Biodegradation experiments in aquatic media and soil burial will be performed on pristine and thermal aged samples at 55 °C.

PE starch blends and composites are not a new subject, commercial products containing PE and starch have being available since the 1970s mainly in the form of shopping bags. However, it will be studied PE-Starch based materials containing prodegradants in the third chapter. To mix PE and starch with a good homogeneity of the dispersed phase it is required a good compatibilizer. So, this chapter will focalize in the first part the compatibilization of PE-Starch and in the second one formulate this type of material with the addition of prodegradant. Two PE copolymers, EVA and EGMA are selected compatibilizers for PE-Starch and PE-thermoplastic (TPS) materials. A screening experiment consisting of a factorial design $2^2$ combined or not with a mixture design will be used to define formulations. The space of mixture design was constrained at 30 wt-% for starches and at 20 wt-% for compatibilizers. PE-based materials will be prepared in an internal mixer and the films by compression moulding. The second study of PE-Starch-Prodegradant materials will follow the same design experiment of the previous study. However their components will be mixed in a extruder and the films obtained by blow moulding. These materials will be submitted to thermal aging.

# 2. EXPERIMENTAL

The experimental chapter provides the chemicals and polymers used in the formulation of the three families of materials based on polyethylene (PE) and details of their physico-chemical and oxo-biodegradation characterization. The commercial products were used as received if not otherwise stated. Material formulations methodology followed a statistical design experiment (DEX). DEX approach is addressed to the formulation optimization with a higher number of variables and a minimal number of experiments. This is possible by means of factorial, or mixture experiment, for example. In this type of DEX the effects of several variables are investigated simultaneously over some pre-assigned range that is covered by the levels of variables. To perform the analysis of variance (ANOVA) the experiment treatments need to be replicated. However, if the number of trials is considered large, it can be used only a single replication as in the case of central composite design where only the central treatment will be replicated. Details of DEX performed in the present thesis will be described in the sections corresponding each family of material.

## 2.1. Reagents and Solvents

Potassium hydroxide pellets, technical grade (KOH) [1310-58-3]; hydrochloric acid volumetric standard, 0.1N in water, analytical grade (HCL) [7647-01-0]; barium chloride, technical grade ($BaCl_2$) [10326-27-9]; acetone HPLC grade (CH3COCH3) [67-64-1]; and chloroform HPLC grade ($CHCl_3$) [67-66-3] were purchased from Carlo Erba Chemical Co., Italy. Xylenes isomers plus ethyl benzene, 98.5%, ACS reagent ($C_6H_4(CH_3)_2$) [1330-20-7], phenolphthalein, ACS reagent ($C_{20}H_{14}O_4$) [77-09-8], were supplied by Sigma-Aldrich Chemical Co., Germany.

### 2.1.1. *Materials used in biodegradation experiments*

Soil burial experiments employed "humus" from Pine and Quercia trees in Marina di Pisa woods (Italy) and perlite (a heat expanded naturally occurring siliceous rock with d = 80-120 $g \cdot cm^{-3}$ and granulometry = 1-3 mm) in order to provide aeration and moisture retention during tests.

Aquatic biodegradation experiment was performed using an inoculum originally taken from the "Morto" river, which receives domestic sewage water from the north quarter of Pisa (Italy). Table 2.1 shows the mean values of some physico-chemical characteristics and microorganisms of the river water sampled before reaching the sea (inside San Rossore park).

**Table 2.1.** Characteristics of river "Morto" at 26 September 2003.[a)][80]

| Property | Units | Range Values |
|---|---|---|
| pH | — | 7.3 – 7.9 |
| DO | % saturation | 0 – 280 |
| COD | (mg/L) | 20 – 120 |
| NA | (mg/L) | 1.0 – 7.5 |
| Chloride | (mg/L) | 3332 |
| Sulphate | (mg/L) | 120 – 600 |
| PT | (mg/L) | 0.5 – 2.0 |
| MBAS | (mg/L) | < 0.05 |
| TNI | (mg/L) | < 0.5 – 0.10 |
| Total coliforms | /100 mL | $10^4 – 10^7$ |
| Fecal coliforms | /100 mL | $10^4 – 10^7$ |

[a)] D.O.: Dissolved Oxygen; COD: Chemical Oxygen Demand; NA: Ammonia nitrogen; PT: Total phosphate; MBAS: Methylene Blue Active Substances; TNI: Total nitrogen input.

The following high purity chemicals were used in the aquatic biodegradation study: magnesium nitrate hexahydrate $Mg(NO_3)_2.6H_2O$ [13446-18-9], purchased from Aldrich Chemical Co., Germany. Hexadecane

($C_{16}H_{34}$) [544-76-3], potassium dihydrogenphosphate ($KH_2PO_4$) [7778-77-0], docosane ($C_{22}H_{46}$) [629-97-0], potassium hydrogenphosphate ($K_2HPO_4$) [7758-11-4], calcium chloride dihydrate ($CaCl_2.2H_2O$) [10035-04-8], sodium hydrogenphosphate ($Na_2HPO_4$) [7558-79-4], ammonium chloride ($NH_4Cl$) [12125-02-9], magnesium sulphate heptahydrate ($MgSO_4.7H_2O$) [10034-99-8] and iron (III) chloride hexahydrate ($FeCl_3.6H_2O$) [10025-77-1] were supplied by Carlo Erba Chemical Co., Italy.

## 2.2. Additives

Totally Degradable Plastics Additives (TDPA®) DCP562 (T6), melt flow index (MFI) [at 125 °C/2.16 kg] = 23 - 28 g·10 $min^{-1}$ and DCP571 (T7), MFI [at 125 °C/2.16 kg] = 25 - 30 g·10 $min^{-1}$ (is a proprietary masterbatch containing prodegradants, mainly of cobalt and manganese stearate, stabilizers and fillers in PE resin matrix) were kindly supplied by EPI Environmental Technologies Inc. ("EPI"), Canada.

## 2.3. Polymers

Riblene® FF33 a linear low density polyethylene (LLDPE that will be simplified to PE) [9002-88-4] pellet with a MFI [at 190 °C/2.16 kg] = 7.93 g·10 $min^{-1}$ and density (d) = 0.92 g·$cm^{-3}$ at 23 °C was kindly supplied by Polimeri Europa, Italy. Biocyle poly(hydroxybutyrate) (PHB) [26063-00-3] pellet with average molecular weight (Mw) = 425 kDa and polydispersity (Mw/Mn) = 2.51 was kindly supplied by PHB Industrial S.A., Brazil. ELVAX® 3185 a poly(ethylene-*co*-vinyl acetate) (EVA) [24937-78-8] with 33 wt% vinyl acetate, MFI [at 190 °C/2.16 kg] = 43 g·10 $min^{-1}$; d = 0.96 g·$cm^{-3}$, and melting point ($T_m$) 61 °C was supplied by DuPont. Lotader AX 8840 a poly(ethylene-*co*-glycidyl methacrylate) (EGMA) [26061-90-5] with 8 wt-% of glycidyl methacrylate and d = 0.94 g·$cm^{-3}$ at 23 °C was supplied by Arkema, Italy. Poly(ethylene-*co*-methyl acrylate (EMAC) [25103-74-6] with 20 wt% of methyl acrylate, d of 0.942 g.$cm^{-3}$ and MFI [at 190 °C/2.16 kg] = 6 g·10 $min^{-1}$ was kindly supplied by Eastman, EUA. Corn starch (CS)

from Cerestar-Cargill Company was supplied by Novamont, Italy. Termoplastic corn starch (TPS) and Biopar® FG ML 1007 (BTPS) (a bio-plastic resin consisting mainly of thermoplastic starch (TPS), biodegradable synthetic co-polyesters and additives), MFI [at 190 °C/2.16 kg] = 14.5, d = 1.26-1.28 $g \cdot cm^{-3}$, were kindly supplied by Biop Biopolymer Technologies, Germany. In Scheme 2.1 are represented the chemical structure of polymers PE, PHB, and EVA, EGMA and EMAC.

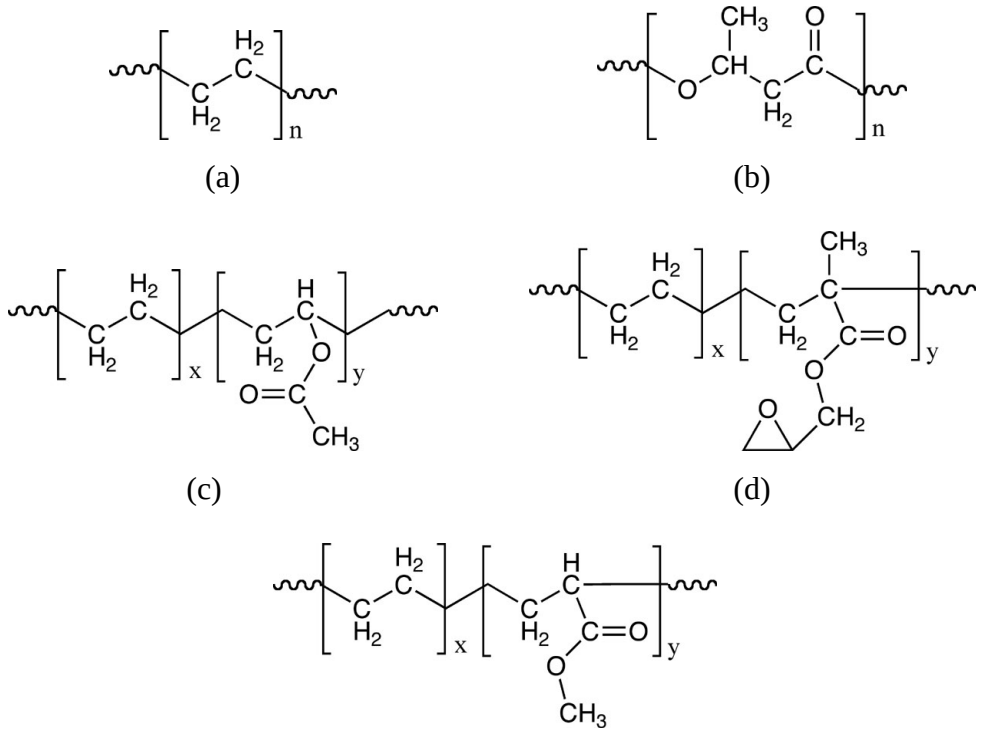


**Scheme 2.1.** Structure of polymers PE (a), PHB (b), EVA (c), EGMA (d) and EMAC (e).

## 2.4. Formulation and Processing

Three families of materials based on PE were formulated and processed with different strategies and will be detailed in the following sub-sections.

### 2.4.1. *PE-PHB Blends*

PE-PHB blends consist of two polymers of different polarity and, consequently, they are not compatible. To study these blends compatibilization, three copolymers containing PE segments and a polar polymer segment were selected. These compatibilizers are EVA, EGMA and EMAC. The variables to be evaluated are the amount of each component of polymer blend matrix and type and amount of compatibilizer. Considering that the levels of each component of mixture are dependent of the levels of the other ones, a DEX called "mixture experiment" was employed to obtain the formulations. The condition of this type of experiment is that the sum of the proportions by weight of all components is 100 wt-%. The design space for formulations of the PE-PHB-compatibilizer blends is a triangle as shown in the Figure 2.1. This space was constrained for the variable amount of compatibilizers EVA and EGMA at 10 wt-% and for EMAC at 40 wt-%. Blends compositions and samples identification codes are presented in Tables 2.2 – 2.4. All formulations were prepared randomly and replicated.

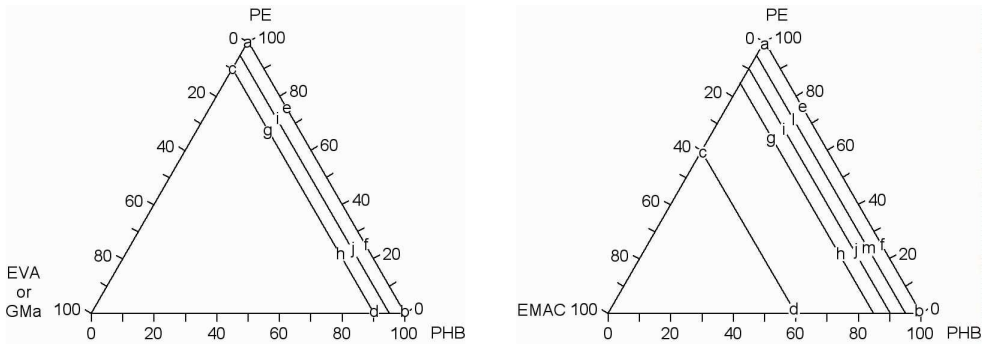


(a) (b)

**Figure 2.1.** Space of the components in the mixture for (a) PE-PHB-EVA (or EGMA) and (b) PE-PHB-EMAC blends.

All formulation components were initially mixed physically (Tab. 2.2-2.4) and then dried at 60 °C for 48 h in a laboratory oven with air circulation before melt processing, since the presence of humidity promotes the

hydrolysis of polyesters like PHB. Following, dried formulations were melting processed in a torque rheometer W 50 EHT with roller blade connected to a Plastograph Can-Bus Brabender. Mixing conditions for all PE-PHB based blends were temperature at 180 °C, and velocity at 60 rpm by 7 minutes.

**Table 2.2.** Composition and sample identification codes of PE-PHB-EVA blends.

| Trial | Code[a)] | PE (wt-%) | PHB (wt-%) | EVA (wt-%) |
|---|---|---|---|---|
| a | PE | 100.0 | — | — |
| b | PHB | — | 100.0 | — |
| c | 90E10V | 90.0 | — | 10 |
| d | 90B10V | — | 90.0 | 10 |
| e | 75E25B | 75.0 | 25.0 | — |
| f | 25E75B | 25.0 | 75.0 | — |
| g | 68E22B10V | 67.5 | 22.5 | 10 |
| h | 22E68B10V | 22.5 | 67.5 | 10 |
| i | 71E24B5V | 71.2 | 23.8 | 5 |
| j | 24E71B5V | 23.8 | 71.2 | 5 |

[a)] E = PE; B = PHB; V = EVA.

About 8 g of blend were compression moulded in a laboratory mould press Collin (model P 200E) with a water-cooling system to obtain films of around 300-500 µm. Moulding conditions were heating up to 180°C and leaving isothermically for 5 min at 9 MPa (90 bar) in a teflonated mould. Subsequently, it was cooled to ambient temperature by about 8 min maintaining the same pressure of isotherm step.

**Table 2.3.** Composition and sample identification codes of PE-PHB-EGMA blends.

| Trial | Code[a)] | PE (wt-%) | PHB (wt-%) | EGMA (wt-%) |
|---|---|---|---|---|
| a | PE | 100.0 | — | — |
| b | PHB | — | 100.0 | — |
| c | 90E10G | 90.0 | — | 10 |
| d | 90B10G | — | 90.0 | 10 |
| e | 75E25B | 75.0 | 25.0 | — |
| f | 25E75B | 25.0 | 75.0 | — |
| g | 68E22B10G | 67.5 | 22.5 | 10 |
| h | 22E68B10G | 22.5 | 67.5 | 10 |
| i | 71E24B5G | 71.2 | 23.8 | 5 |
| j | 24E71B5G | 23.8 | 71.2 | 5 |

[a)] E = PE; B = PHB; G = EGMA.

**Table 2.4.** Composition and sample identification codes of PE-PHB-EMAC blends.

| Trial | Code[a)] | PE (wt-%) | PHB (wt-%) | EMAC (wt-%) |
|---|---|---|---|---|
| a | PE | 100 | — | — |
| b | PHB | — | 100 | — |
| c | 60E40EM | 60 | — | 40 |
| d | 60B40EM | — | 60 | 40 |
| e | 75E25B | 75 | 25 | — |
| f | 25E75B | 25 | 75 | — |
| g | 64E21B15EM | 63.8 | 21.2 | 15 |
| h | 21E64B15EM | 21.2 | 63.8 | 15 |
| i | 68E22B10EM | 67.5 | 22.5 | 10 |
| j | 22E68B10EM | 22.5 | 67.5 | 10 |
| l | 71E24B5EM | 71.2 | 23.8 | 5 |
| m | 24E71B5EM | 23.8 | 71.2 | 5 |

[a)] E = PE; B = PHB; EM = EMAC

### 2.4.2. *PE-PHB-EGMA blends formulated with prodegradant*

The best compatibilization found for PE-PHB blends was with EGMA and was selected to formulate a new series of materials. Initially, it was prepared the blend containing 90 wt-% of PE and 10 wt-% of EGMA as the basic matrix for all the other formulations which was called PEL. Formulation strategy followed a central composite design (CCD) where the independent variables were amounts of the biodegradable polymer PHB and of prodegradant additives T6 and T7. This DEX is a factorial at two levels ($2^3$) with a central level as described in the Table 2.5. Sample identification codes with the corresponding experimental trials are shown in the Table 2.6. The sequence of blend preparation was random to avoid systematic error and only the central point was replicated three times.

All formulation components were previously dried at 50 °C for 24 h in a vacuum oven. Blends were obtained in a twin-screw (diameter of 25 mm; length 18 x D) co-rotating extruder from Collin GmbH Teach Line, a bench type compounder ZK 25 T with water-bath WB 850 T and pelletizer CSG 171 T. Pellets were fed in the extruder at speed of 4.7 rpm with temperature zones fixed at 180°C, 180°C, 180°C and 150°C and screw speed of 15 rpm. PE-PHB based blends preparation followed two stage. Firstly, it was blended PE matrix and EGMA compatibilizer to obtain pellets of PEL material at composition mentioned above. The second stage was the blending of the formulations presented in the Table 2.6. The resultant pellets blends were stored under vacuum and in a freezer to prevent possible oxo-degradation of them due to the presence of prodegradant.

**Table 2.5.** Central composite design for PE-PHB blends formulated with prodegradant.

| Component | Low (–) | Central (0) | High (+) |
|---|---|---|---|
| PHB (wt-%) | 0 | 1.0 | 2.0 |
| T6 (wt-%) | 0 | 1.5 | 3.0 |
| T7 (wt-%) | 0 | 1.5 | 3.0 |

To obtain thin films (about 50-80μm), pellets of the blends were blow extruded in a SHOUMAN machine (model SH-F16) with L/D ratio of 25/1 and head diameter of 40 mm. Screw zones temperatures were adjusted to 170°C, 160°C and 155°C and speed of extrusion was 30 rpm. The obtained films were stored under vacuum and in a freezer prior to characterization.

**Table 2.6.** Composition and sample identification codes of PE-PHB based blends.[a)]

| | | PHB | | T6 | | T7 | | PEL |
|---|---|---|---|---|---|---|---|---|
| Trial | Code | level | wt-% | level | wt-% | level | wt-% | wt-% |
| 1 | PEL | — | 0 | — | 0 | — | 0 | 100 |
| a | 2B | + | 2 | — | 0 | — | 0 | 98 |
| b | 3T6 | — | 0 | + | 3 | — | 0 | 97 |
| c | 2B3T6 | + | 2 | + | 3 | — | 0 | 95 |
| ab | 3T7 | — | 0 | — | 0 | + | 3 | 97 |
| ac | 2B3T7 | + | 2 | — | 0 | + | 3 | 95 |
| bc | 3T63T7 | — | 0 | + | 3 | + | 3 | 94 |
| abc | 2B3T63T7 | + | 2 | + | 3 | + | 3 | 92 |
| 0 | BT6T7[b)] | 0 | 1 | 0 | 1.5 | 0 | 1.5 | 96 |

[a)] PEL: 90 wt-% PE/10 wt-% EGMA; (–), (0) and (+) mean low, central and high level variables, respectively; (1) is the low level of each factor; a, b and c, are the main effects; ab, ac and bc, are two factors interaction; and abc, are three factors interaction. [b)] Replicated three times.

### 2.4.3. *PE-TPS and PE-CS composites compatibilization*

A screening experiment consisting of a factorial $2^2$ design combined or not with a mixture design was performed to formulate PE based blends containing starches (Fig. 2.2). The dependent variables in the factorial design were type of starch and of compatibilizer as described in Table 2.7. The starches selected were thermoplastic (TPS) and corn-starch (CS) and the compatibilizers were EVA and EGMA. The space of mixture design was constrained at 30 wt-% for starches and at 20 wt-% for compatibilizers.

Composition and sample identification codes of blends are presented in Tables 2.8-2.9.

PE-starch blending were carried out in two steps in a torque rheometer W 50 EHT (with roller blade) connected to a Plastograph Can-Bus Brabender at 150 °C and 50 rpm by 6 minutes. Before each melt processing, blend components were mixed physically. The first step was the preparation of masterbatchs containing a compatibilizer and a starch. These masterbatchs correspond to the four combinations of the factorial variables (Tab. 2.7): EVA-TPS, EGMA-TPS (MVT and MGT, respectively) and EVA-CS, EGMA-CS (MVCS and MGCS, respectively). It was supposed that a better starch dispersion could be obtained in the incompatible PE matrix if initially were blended with the more compatible compatibilizer. The subsequent step was the blending of the masterbatch with PE to obtain the compositions presented in Tables 2.8-2.9.

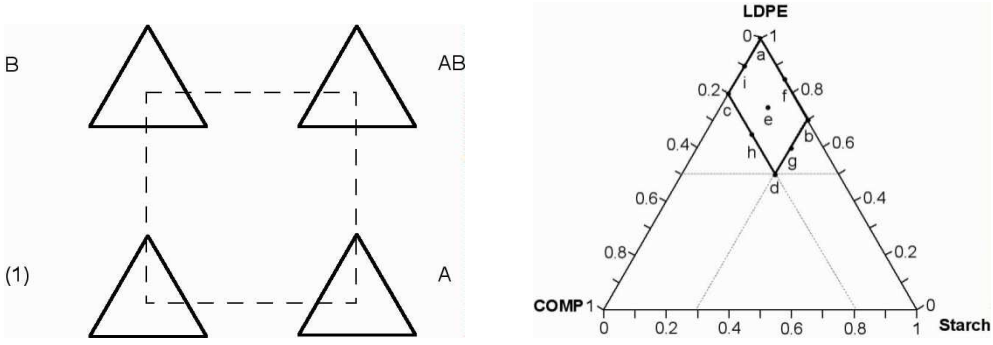


(a) (b)

**Figure 2.2.** Factorial $2^2$ with mixture experiment at each level (a) and Space of the mixture experiment (b).

**Table 2.7.** Factorial $2^2$ design.[a)]

| Component | Low (–) | High (+) |
|---|---|---|
| Starch | TPS | CS |
| Compatibilizer | EVA | EGMA |

[a)] TPS and CS are thermoplastic and corn starches, respectively; EVA and EGMA are poly(ethylene-*co*-vinyl acetate) and poly(ethylene-*co*-glycidyl methacrylate), respectively.

**Table 2.8.** Composition and sample identification codes of PE-TPS blends.

| Trial | Code[a)] | PE wt-% | TPS wt-% | EGMA wt-% | Code | PE wt-% | TPS wt-% | EVA wt-% |
|---|---|---|---|---|---|---|---|---|
| | MGT | — | 60 | 40 | MVT | — | 60 | 40 |
| a | PE | 100 | — | — | — | — | — | — |
| b | 7E3T | 70 | 30 | — | — | — | — | — |
| c | 8E2G | 80 | — | 20 | 8E2V | 80 | — | 20 |
| d | 5E2G3T | 50 | 30 | 20 | 5E2V3T | 50 | 30 | 20 |
| e | 75E1G15T | 75 | 15 | 10 | 75E1V15T | 75 | 15 | 10 |
| f | 85E15T | 85 | 15 | — | — | — | — | — |
| g | 6E1G3T | 60 | 30 | 10 | 6E1V3T | 60 | 30 | 10 |
| h | 65E2G15T | 65 | 15 | 20 | 65E2V15T | 65 | 15 | 20 |
| i | 9E1G | 90 | — | 10 | 9E1V | 90 | — | 10 |

[a)] E = PE; T = TPS; G = EGMA; V = EVA.

**Table 2.9.** Composition and sample identification codes of PE-CS blends.

| Trial | Code[a)] | PE wt-% | CS wt-% | EGMA wt-% | Code | PE wt-% | CS wt-% | EVA wt-% |
|---|---|---|---|---|---|---|---|---|
| | MGCS | — | 60 | 40 | MVCS | — | 60 | 40 |
| b | 7E3C | 70 | 30 | — | — | — | — | — |
| d | 5E2G3C | 50 | 30 | 20 | 5E2V3C | 50 | 30 | 20 |
| e | 75E1G15C | 75 | 15 | 10 | 75E1V15C | 75 | 15 | 10 |
| f | 85E15C | 85 | 15 | — | — | — | — | — |
| g | 6E1G3C | 60 | 30 | 10 | 6E1V3C | 60 | 30 | 10 |
| h | 65E2G15C | 65 | 15 | 20 | 65E2V15C | 65 | 15 | 20 |

[a)] E = PE; C = CS; G = EGMA; V = EVA.

Blend films were obtained in a laboratory compression press - model Collin P 200E - with water-cooling system. Compression moulding were performed by heating to 150 °C for 7 min following a cooling for 7 min both under a pressure of 90 bar ($9x10^6$ Pa). Using teflonated moulds, it was weight *ca.* 8 g of polymer blend to obtain films of about 400-600 µm.

### 2.4.4. *PE-CS and PE-BTPS composites with prodegradant*

Polyethylene-corn starch (PE-CS) and polyethylene-Biopar (PE-BTPS) blends containing prodegradant T6 (Tab. 2.10) were obtained in a twin-screw (diameter of 25 mm; length 18 x D) co-rotating extruder from Collin GmbH Teach Line, a bench type compounder ZK 25 T with water-bath WB 850 T and pelletizer CSG 171 T. Pellets feed in the extruder was at 5.0 rpm. Extrusion was performed at temperature zones of 150°C, 150°C, 150°C and 130°C and screw speed of 15 rpm. To avoid systematic errors, trials of the experimental design (equivalent to the previous section 2.4.3) were carried out randomly.

**Table 2.10.** Composition and sample identification codes of PE-corn starch and PE-Biopar extruded blends.

| Trial | Code[a)] | PET6 wt-% | CS wt-% | EGMA wt-% | Code | PET6 wt-% | Biopar wt-% | EGMA wt-% |
|---|---|---|---|---|---|---|---|---|
| | EMGCS | — | 60 | 40 | MGB | — | 60 | 40 |
| a | ET6 | 100 | — | — | — | — | — | — |
| b | 7ET6-3C | 70 | 30 | — | 7ET6-3B | 70 | 30 | — |
| c | 8ET6-2G | 80 | — | 20 | — | — | — | — |
| d | 5ET6-2G-3C | 50 | 30 | 20 | 5ET6-2G-3B | 50 | 30 | 20 |
| e | 75ET6-1G-15C | 75 | 15 | 10 | 75ET6-1G-15B | 75 | 15 | 10 |
| f | 85ET6-15C | 85 | 15 | — | 85ET6-15B | 85 | 15 | — |
| g | 6ET6-1G-3C | 60 | 30 | 10 | 6ET6-1G-3B | 60 | 30 | 10 |
| h | 65ET6-2G-15C | 65 | 15 | 20 | 65ET6-2G-15B | 65 | 15 | 20 |
| i | 9ET6-1G | 90 | — | 10 | — | — | — | — |

[a)] ET6 = 95 wt-% PE/5 wt-% T6 = ET6; E = PE; C = CS; G = EGMA; B = Biopar.

Mixtures were prepared following three extrusion steps. As in the previous Section (2.4.3), it was prepared a masterbatch of corn-starch with EGMA (EMGCS) and Biopar with EGMA (MGB). The second step was the blending of the PE matrix with the additive prodegradant T6 at the proportion of 9.5:0.5 (ET6). Finally, in the third extrusion step, materials of the first and

second step were blended with addition of compatibilizer to adjust the desired compositions (Tab. 2.10). The extruded blends were stored under vacuum in a freezer to prevent possible oxo-degradation due to the presence of prodegradant on them.

Films of about 200-400 μm were obtained by blow extrusion in a SHOUMAN machine (model SH-F16) with L/D ratio of 25/1 and head diameter of 40 mm. Samples were processed with screw speed at 30 rpm and temperature zones at 150 °C, 150 °C and 140 °C. Films were storage at the same conditions of pellets up to characterization.

## 2.5. Thermal aging and Biodegradation procedures

### 2.5.1. *Thermal aging*

Thermal aging was performed in two different conditions depending on the type of parameter selected to evaluate the progress of thermo-oxidation:

i) Carbonyl index (COi), hydroperoxide index (ROOi) and activation energy (Ea) evaluation were carried out by Fourier Transform Infrared Spectroscopy (FTIR). Samples were fixed on cardboard supports (Fig. 2.3 a) and placed inside a static air-oven up to 120 days. In this way, degradation of each sample as a function of time could be analysed always at the same position. Degradation was studied at three different temperatures: 45 °C, 55 °C and 65 °C. These temperatures were chosen because represent the common temperatures founded in composting process;

ii) In the thermal-degradation performed at 55 °C up 60 days in a static air-oven, the specimens of each sample (*ca.* 40 μm of thickness) were placed on polystyrene Petri dishes (Fig. 2.3 b). The properties changes were evaluated at specific times corresponding to middle (defined by $CO_i$) and end of degradation. The assessments were in terms of mechanical and thermal properties as well as molecular weight (MW) as determined by high pressure liquid chromatography (HPLC) and gel content by solvent extraction;

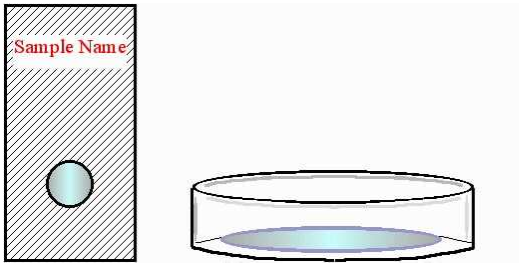


a) b)

**Figure 2.3.** Supports used on aging test: a) for FTIR analysis, and b) Petri dish, Ø = 10 cm.

To analyse the low molecular weight polymers produced during the thermal aging, samples were submitted to an extraction with boiling acetone under reflux for 3 hours using a Soxhlet extractor. The obtained extracts were dried to constant weight that was recorded with an electronic balance. Molecular weight was evaluated by means of HPLC analysis.

#### *2.5.1.1 Activation energy*

The reaction rates can raise many folds by increasing temperature. This is a consequence of the increase in movement of reactant molecules and more frequent collisions between them with the temperature. The minimum amount of kinetic energy that these molecules will need to have in order to react and transform reagents in products is called activation energy (*Ea*). Higher values of *Ea* denote that larger amounts of energy are needed to initiate a reaction. This means that the reaction will be more susceptible to the influence of temperature. The influence of temperature on the *Ea* is described by Arrhenius equation (Eq. 2.1). At higher temperatures, a larger number of molecules will have the minimum *Ea* to react. Taking the natural logarithm of both sides (Eq. 2.2), and determining ***k*** experimentally at several temperatures, *Ea* can be calculated from the slope of a plot of ln ***k*** *vs.* 1/T. An accurate determination of the activation energy requires at least three runs completed at different reaction temperatures. The temperature intervals should be at least 5 °C.[81]

$$k\,(T) = A \cdot e^{-Ea/RT} \qquad \text{(Eq. 2.1)}$$

$$\ln k = \ln A - Ea/RT \qquad \text{(Eq. 2.2)}$$

Where, *k* is the rate constant and is specific for each reaction changing with the temperature; A is the frequency factor that is a number representing the chance that collisions would occur with the proper orientation for reaction; R is the gas constant, which value is 8.314 J/mol·K and T is the absolute temperature in Kelvin.

#### *2.5.1.2 Gel Content*

Gel content was evaluated as the percentage of insoluble material after extraction (Eq. 2.3) in a Soxhlet extractor for 13 hours in a mixture of xylenes isomers and ethyl benzene solvents using Whatman cellulose extraction thimbles.[82] After extraction, the material was dried in a vacuum oven until constant weight. For each sample, four replicates were used for statistical evaluation.

$$\text{Gel content (\%)} = \frac{\text{Weight sample after extraction}}{\text{Initial weight sample}} * 100 \qquad \text{(Eq. 2.3)}$$

## 2.6. Biodegradation

Biodegradation at screening level of PE-PHB based materials, was carried out in both aquatic media (AM) and soil burial (SB). Samples used in these experiments are described in Table 2.11 and Table 2.12 records the characterizations performed on them.

Both aquatic and soil burial aerobic biodegradation tests are based on the headspace $CO_2$ test (Sturm $CO_2$). Briefly, the $CO_2$ is evolved inside a sealed biometer from biodegradation of samples, which is trapped by an

absorber (that in the present study was a solution of KOH at 0.06N), and quantities by titrimetry.[83]

**Table 2.11.** Samples in the aquatic medium (AM) and soil burial (SBi) biodegradation tests in. [a)]

| Sample | AM | | | SBi | | |
|---|---|---|---|---|---|---|
| | PS | TAS | KE | PS | TAS | KE |
| PEL | X | X | — | — | — | — |
| 2B | X | X | — | — | — | — |
| 3T6 | X | X | X | X | X | — |
| 2B-3T6 | X | X | X | X | X | — |
| 3T7 | X | X | X | X | X | — |
| 2B-3T7 | — | — | X | X | X | — |

[a)] PS: Pristine Sample; TAS: Thermo Aged Sample; KE: Acetone Extract; see Table 2.6.

**Table 2.12.** Characterization of samples submitted to biodegradation tests. [a)]

| Sample | $CO_2$ evolved | FTIR | TGA | DSC | SEM | EDS |
|---|---|---|---|---|---|---|
| PEL | AM/SBi | — | AM/SBi | AM/SBi | AM/SBi | — |
| 2B | AM/SBi | — | AM/SBi | AM/SBi | AM/SBi | — |
| 3T6 | AM/SBi | SBi | AM/SBi | AM/SBi | AM/SBi | AM |
| 2B-3T6 | AM/SBi | SBi | AM/SBi | AM/SBi | AM/SBi | AM |
| 3T7 | AM/SBi | SBi | AM/SBi | AM/SBi | AM/SBi | — |
| 2B-3T7 | AM/SBi | SBi | AM/SBi | AM/SBi | AM/SBi | — |

[a)]AM: Aquatic Medium; SB: Soil Burial; FTIR: Fourier Transform Infrared Spectroscopy; TGA: Thermogravimetric Analysis; DSC: Differential Scanning Calorimetry; SEM: Scanning Electron Microscopy; EDS: Elemental microanalysis.

At specific times, biometers were opened and aliquots of 10 mL of KOH, containing soluble inorganic carbon, were transferred to a Becker. To this solution, a volume of 1 mL of $BaCl_2$ at 2.6 wt-% was added to precipitate and form insoluble inorganic carbon. In this way, KOH was back titrated by using HCL 0.1N up to phenolphthalein end point. Subsequently, biometer

was recharged with a new KOH solution and immediately closed. This cycle of procedure was repeated periodically up to the end of experiment.

The above procedure is based on the following reactions:

$$CO_2 + 2\ KOH \rightarrow K_2CO_3\ (soluble) + H_2O \qquad (Eq.\ 2.4)$$

$$K_2CO_3 + BaCl_2 \rightarrow BaCO_3\ (insoluble) + 2\ KCl \qquad (Eq.\ 2.5)$$

To determine complete or ultimate aerobic biodegradability (mineralization to $CO_2$), it is necessary to now the initial amount of organic carbon in the sample. In the case of plastic materials the amount of total organic carbon ($TOC_S$) can be obtained by CHN elemental analysis (Carlo Erba Elemental analyzer MOD 1106). In the present study this analysis was performed in the Department of Pharmaceutical Sciences, University of Pisa.[*] It is possible to estimate the theoretical amount of $CO_2$ ($ThCO_2$) of the test plastic sample, knowing the amount of TOC as illustrated by Equations 2.6-2.7.

$$C_S = TOC_S * W_S \qquad (Eq.\ 2.6)$$

Where $C_S$ is the amount of carbon in the sample, $TOC_S$ the relative amount of total organic carbon in the sample at time 0 and $W_S$ the total amount of sample.

As to evolve 44 g of $CO_2$ it is needed 12 g of carbon (C), Equation 2.7 calculates the amount of $ThCO_2$.

$$ThCO_2 = C_S * 44/12 = TOC_S * W_S * 3.67 \qquad (Eq.\ 2.7)$$

The extension of biodegradation defined as mineralization percent ($D_t$) is calculated subtracting the accumulated $CO_2$ content evolved into the biometers of sample ($(CO_2)_S$) from that of blank ($(CO_2)_B$). The difference

[*] The author thanks Prof. Marco Macchia and Dr. Caterina Orlando.

found is divided by the $ThCO_2$, as specified in the standards ASTM D5209 and D5338 (Eq. 2.8).[84, 85]

$$\% Dt = 100*((CO2)_S - (CO2)_B)/ThCO_2 \quad \text{(Eq.2.8)}$$

### 2.6.1. *Aerobic aquatic biodegradation*

Aerobic aquatic biodegradation followed a usual procedure of BIOLAB-DCCI-UNIPI.[86, 87] It combines characteristics of some standards as recorded in Table 2.13.[84, 88-90] The absence of agitation, the cyclic light (from day to night) and the way of trapping the headspace $CO_2$ evolved from biodegradation are the principal differences between Standard tests and that of BIOLAB.

The inoculum used was originally taken from a river "Fiume Morto" that receives domestic sewage water from the north quarter of Pisa (Italy).[80] However, in the present study the inoculum (IRU) was obtained from a medium used in a previously experiment of biodegradation with the same family of materials.[86] The procedure of biodegradation of samples in aquatic media was carried out in three steps as resumed in Figure 2.4.

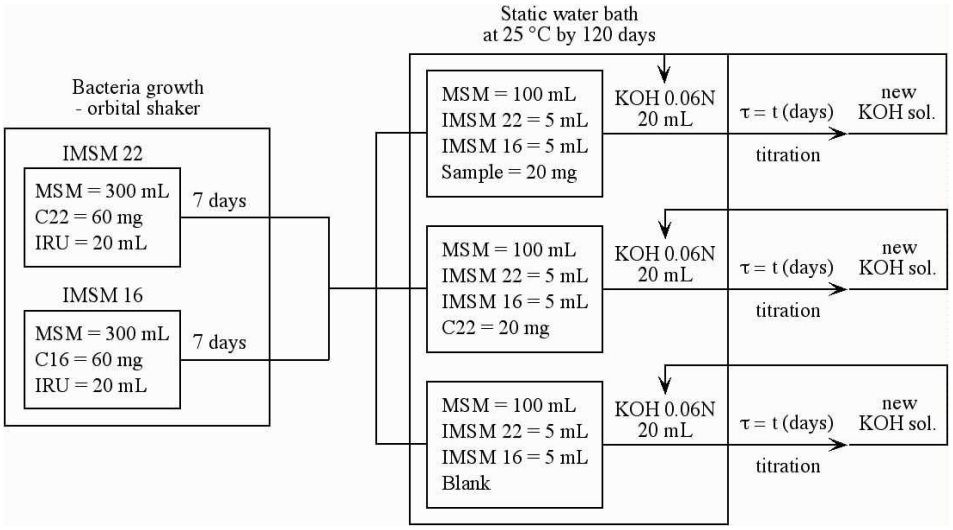


**Figure 2.4.** Flow-sheet of aquatic biodegradation.

**Table 2.13.** Characteristics of standard methods for aerobic biodegradation in aquatic medium and that used in the present study.

| Features | ASTM D5209 | ASTM E1720 | OECD 301-B | ISO 14593 | BIOLAB |
|---|---|---|---|---|---|
| Size vessels (mL) | 4000 | 160 | 2000-5000 | 160 | 300 |
| System | closed | sealed | closed | sealed | sealed |
| Aeration | yes | no | yes | no | no |
| Agitation | yes | yes | yes | yes | no |
| Headspace/liquid | 1:1.7 | 3:5 | 3:5 | 1:2 | 2:1 |
| Light | n.s. | dark | dark/diffuse | dark/diffuse | day-night |
| Inoculum source | activated sludge | sewage | DS | DS | sewage |
| Inoculum pre-adapted | no | no | optionally | optionally | yes |
| Inoculum amount | 1 wt-% | variable | ≤ 30 mg/L | 4 mg/L | 10 % (v/v) |
| Nitrogen source | $(NH4)_2SO_4$ | $NH_4Cl$ | $NH_4Cl$ | NH4Cl | $NH_4Cl$ |
| Positive control | n.s. | SS | n.s. | optionally | no |
| Reference material | n.s. | SA, GL | SA, SBo, AN | AN, SBo | docosane |

[a)] Closed is a system with a continuous entrance of $CO_2$-free air; n.s. = not specified; DS means a inoculum that may be derived from a variety of sources: activated sludge, sewage effluents, surface water, soils or from their mixtures; SS: sodium stearate: SA: sodium acetate; GL: glucose; SBo: sodium benzoate; AN: aniline

The first step corresponds to the preparation of inoculum. So, an aliquot of 20 ml of IRU was pre-exposed to the mineral salt medium (MSM) (Tab. 2.14) containing an organic matter. The aim was to increase the microorganism population. Hence, it was added in two separately Erlenmeyers of 500 ml containing MSM one of the two hexadecane (C16) or docosane (C22) as unique carbon source. The mediums (IMSM16 and IMSM22) were incubated for 7 days in an orbital shaker (IKA Labortecnik KS250 basic) (Fig. 2.4).

In the second step, Biometers were prepared in duplicate (Fig. 2.4 and 2.5) totalizing 32 flasks taking account of one blank, one reference and fourteen samples. The flask volume ($V_F$) of each system was 300 ml which was added 100 ml of MSM ($V_S$) ($V_F$:$V_S$ = 2:1Biometers were closed with silicon rubber stopper in which was hanged a conical-bottom polypropylene tube (BD Falcon$^{TM}$ – 50 mL, $\phi$ = 30 mm and adjusted length = 10 cm). In this tube was added 20 mL of KOH *ca*. 0.06 N to trap evolved $CO_2$. Biodegradation followed in a static water bath at 25 °C and day-night light for 125 days.

The last step was the determination of $CO_2$ by titrimetry. About 10-11 cycles of titration-recharging were performed corresponding the times of mineralization measurement.

Samples from Biometers at the end of experiment were characterized by means of SEM, Microanalysis, TGA and DSC.

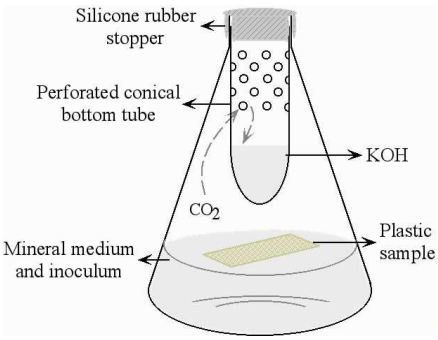


**Figure 2.5.** Biometer used on aquatic biodegradation.

**Table 2.14.** Composition of the mineral salt medium (MSM) used in the aquatic aerobic biodegradation experiments.

| Compound | Concentration ($g.L^{-1}$) | Preparation of 1 L of medium (mL) | |
|---|---|---|---|
| A. Phosphate buffer | | Solution A | 10 |
| $KH_2PO_4$ | 8.50 | Solution B | 1 |
| $K_2HPO4$ | 21.75 | Solution C | 1 |
| $Na_2HPO_4.7H_2O$ | 33.40 | Solution D | 1 |
| $NH_4Cl$ | 2.00 | | |
| B. Calcium chloride | | | |
| $CaCl_2.2H_2O$ | 36.40 | | |
| C. Magnesium sulfate | | | |
| $MgSO_4.7H_2O$ | 22.50 | | |
| D. Ferric chloride | | | |
| $FeCl_3.6H_2O$ | 0.25 | | |

### 2.6.2. *Soil Burial*

Loam used in the soil burial test was taken from Pinus and Quercia woods in the south quarter of Pisa at October 2006 (total nitrogen 1.34g/kg and S.O. 2.95% evaluation were performed on the Department of Agronomy & Agroecosystem Management, University of Pisa[*]). The procedure of aerobic biodegradation of samples in soil burial was carried out in three steps.

The first step consisted on the preparation of soil. Initially, stones, plant remains, *etc* from loam were removed manually and left in static oven at 50 °C by *ca*. 48 h. Dried loam was sieved through a 2 mm mesh prior to use. Following, the moisture content of the soil was adjusted at 50 wt-%. After that, it was mixed with perlite in the proportions of 2:1 soil:perlite (WSP).

In the second step, the biometers (Fig. 2.6) were prepared for the aerobic soil burial biodegradation in duplicate, totalizing 20 flasks taking into

[*] The author thanks Dr. Simone Magni.

account one blank, one reference and eight samples. Biometers of 750 mL were filled with three layers of materials. The first one was 15 g of perlite (PER), the following was 50 g of WSP where it was placed a piece of sample (*ca*. 250 mg) in the middle, and finally 15 g of PER. The layers in the blank consisted only of PER/WSP/PER at the same amount of the sample test. Finally, the preparation reference material was similar to that of sample test but in its place was used a cellulose paper. Once prepared the three layers, a beaker containing 40 mL of KOH (*ca*. 0.06 N) was positioned on the surface layer of perlite, to trap evolved $CO_2$ from biodegradation and the biometer was closed hermetically. Biodegradation followed in the dark at room temperature for 180 days.

The last step corresponds to the evaluation of the amount of $CO_2$ evolved from biodegradation. So, at periodical intervals of time the biometer was opened and the beaker with KOH was removed. An aliquot of 10 mL was withdrawal from it and back titrated with HCl 0.1 N. Subsequently, KOH solution in the beaker was replaced by new one inside of the biometer.

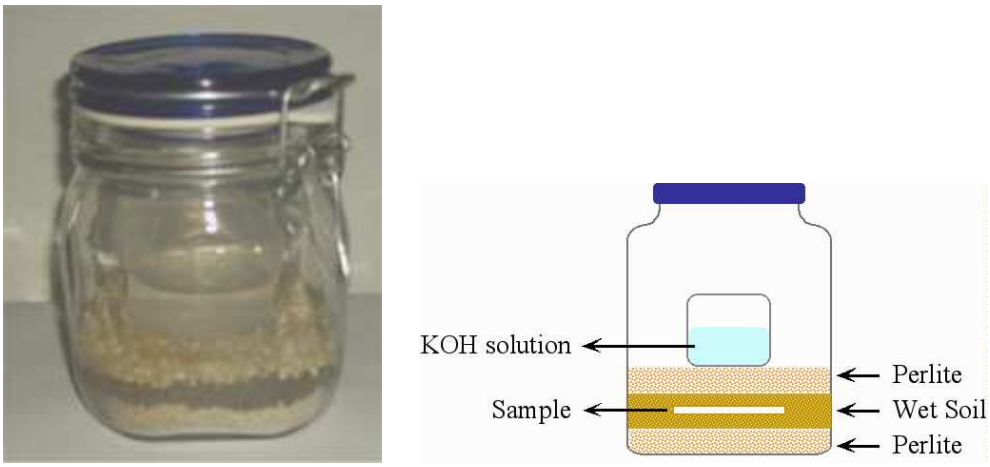


**Figure 2.6.** Biometer used in soil burial experiments.

Another study performed from soil burial biodegradation had the objective the evaluation of both morphological and thermal properties changes as a function of time. Two similar biometers to that shown in Figure 2.6 were used in this study but their volume was 5 L. The area of their base

allowed placing four films disk with 10 cm of diameter. In one biometer was placed the four samples of the family PS (see Table 2.11). In the other one, it was placed the four samples of the family TAS. The assembly of these biometers differed in other two aspects. One refers to the number of medium layers. This means that only the base of perlite followed by the soil layers were used. Besides, the beaker with the $CO_2$ absorber was not necessary. Sampling for characterization was fulfilled at each two months up to complete six months. Pieces of buried film samples were removed from biometer and were washed with distillated water. The excess of surface water was removed with tissue paper and placed inside desiccators containing saturated solutions of magnesium nitrate for at least 48 h before testing. SEM, TGA, and DSC characterized the conditioned samples.

## 2.7. Characterization

### 2.7.1. *Melt Flow Index (MFI)*

Melt flow index (CEAST type 6941.000 – die diameter and length 2.095 mm and 8.0 mm respectively) (MFI) values were obtained from the average of five measurements at temperature of 190°C with a weight of 2.16 Kg. ASTM D1238-04c Procedure A is a manual cut-off operation based on time used for materials having flow rates that fall generally between 0.15 and 50 g/10 min.[91]

### 2.7.2. *Thermogravimetric Analysis (TGA)*

TGA experiments were performed in the thermogravimetric analyzer Series Q500 of the TA Instruments. Generally, sample size was between 10-20 mg. Two different range of temperatures were scanned at $10°C \cdot min^{-1}$ under nitrogen atmosphere at 60 $mL \cdot min^{-1}$ flow rate. These range of temperatures were from 30 °C to 810 °C and from 30 °C to 600 °C depending of the presence or not of the prodegradant in the formulations, respectively.

### 2.7.3. *Differential Scanning Calorimetry (DSC)*

Two DSC instruments from Mettler-Toledo were used. TA 4000 System consisting of the DSC-30 module and TA72 GraphWare software was employed for the evaluation of the thermodynamic parameters of PE-PHB-compatibilizer formulations. Samples of 10–15 mg were weighed in 40 μL aluminium pan and an empty pan was used as reference. DSC temperature calibration was performed using indium, lead and zinc standards and energy calibration by using indium standard. Measurements were performed under nitrogen flow rate of 80 $mL \cdot min^{-1}$ according to the following protocol:

1. First heating scan from -50 °C to 205 °C at 10 $°C \cdot min^{-1}$ and 2 min of isotherm at the end;
2. First cooling scan from 205 °C to -50 °C at 100 $°C \cdot min^{-1}$ and 4 min of isotherm at the end;
3. Second heating scan from -50 °C to 205 °C at 10 $°C \cdot min^{-1}$ and 2 min of isotherm at the end;
4. Second cooling scan from 205 °C to -50 °C at -10 $°C \cdot min^{-1}$ and 4 min of isotherm at the end;
5. Third heating scan from -50 °C to 230°C at 10 $°C \cdot min^{-1}$.

In the evaluations of the formulations families containing prodegradant additive, it was employed a DSC822$^e$ (700 °C) module with FRS5 sensor and operated by means of STAR$^e$ software. Measurements were performed under nitrogen flow rate of 160 $mL \cdot min^{-1}$ according to the following protocol:

1. First heating scan from -50°C to 150°C at 10$°C \cdot min^{-1}$ and 2 min of isotherm at the end;
2. First cooling scan from 150°C to -50°C at -10$°C \cdot min^{-1}$ and 4 min of isotherm at the end;
3. Second heating scan from -50°C to 150°C at 10$°C \cdot min^{-1}$.

### 2.7.4. *Scanning Electron Microscopy (SEM)*

The cross-section morphologies of films were recorded using a JEOL (JSM-5600LV) scanning electron microscope (SEM) at the required magnification and with accelerating voltage of 14kV. The film samples frozen in liquid nitrogen were fractured and sputtered with gold before SEM observation.*

### 2.7.5. *Microanalysis (EDS)*

Microanalysis of the samples containing prodegradant was investigated via SEM (JSM-5600LV) equipped with Energy Dispersive X-ray Microanalysis Spectroscopy (EDS) an OXFORD Instrument. Samples analyzed were original film and from aqueous medium biodegradation.

### 2.7.6. *Wide Angle X-ray Scattering (WAXS)*

Wide-angle X-ray diffraction patterns were performed at room temperature with a Kristalloflex 810 diffractometer (SIEMENS) using a Cu Kα (λ=1.5406 Å) as X-ray source. Scans were run in the high angle region $2° < 2\theta < 36°$ at scan rate of 0.016°/min and a dwell time of 1s.

### 2.7.7. *Size Exclusion Chromatography (SEC)*

Molecular weight (MW) and molecular weight distribution (ID) of acetone extracts were measured in a Jasco PU-1580 intelligent HPLC pump connected to Jasco RI-2031 plus intelligent refractive index and Jasco UV-1575 intelligent ultraviolet detectors and equipped with two PLgel 3µm

* SEM, EDS and WAXS were performed in the Department of Chemical Engineering, Industrial Chemistry and Materials Science, University of Pisa and the Author thanks Dr. Piero Narducci.

mixed-E columns (Polymer laboratories UK). Chloroform was used as eluent at 1.0 mL·min$^{-1}$ flow rate. Monodisperse polystyrene standards were used for calibration. Samples solutions were prepared in chloroform for HPLC at 0.2 wt-%. Before use, samples were filtered in with PTFE filter pore size 0.2 µm.

### 2.7.8. *Transmission Fourier Transform Infrared Spectroscopy (FTIR)*

FTIR measurements were carried out in a Jasco FTIR model 410 spectrophotometer. FTIR absorbance spectra were taken as an average of 16 scans with 2 cm$^{-1}$ of resolution in the region of 5000 to 400 cm$^{-1}$.

Carbonyl index was calculated as the rate between the absorbance of peak at 1715 cm$^{-1}$, corresponding to carbonyl ketone group, and the absorbance of $CH_2$ scissoring peak at 1463 cm$^{-1}$. The relationship used for the calculation of hydroperoxide index was between the peak at 3380 cm$^{-1}$ corresponding to OH group and the $CH_2$ scissoring peak at 1463 cm$^{-1}$.[33, 39, 92]

### 2.7.9. *Dynamic Mechanical Thermal Analysis (DMTA)*

The viscoelastic behaviour of the films in nitrogen atmosphere was analyzed with DMTA V instrument (Rheometric Scientific). Experiments were carried out on a single cantilever arrangement in bending mode in the temperature range from –130 °C to 140 °C at a heating rate of 4 °C·min$^{-1}$. Samples were scanned with an imposed frequency of 1 Hz and strain of 0.15% corresponding to linear viscoelasticity range. Typical dimensions of the samples are 20 mm x 5 mm x 0.4 mm.

### 2.7.10. *Gravimetric Analysis*

Weight gain of samples from thermal aging study was recorded at specific times in a common laboratory balance with four decimal scales.

### 2.7.11. *Photoacoustic Fourier Transform Infrared Spectroscopy (PAS-FTIR)*

Photoacoustic infrared spectra were recorded using a Bruker IFS 66 Spectrometer equipped with an MTEC (Model 200) photoacoustic cell under helium purge gas. The spectroscopic runs were in the mid-IR region of 4000 to 400 with 8 $cm^{-1}$ of resolution and 128 scans. Scan velocity was fixed in 2.2 kHz. Carbon black spectrum was collected as reference.[*]

### 2.7.12. *Mechanical Tests*

The tensile tests were performed on PE based films according to two standard test methods using a universal testing machine Instron (model 5564) with a load cell of 2 kN and pneumatic grips. Specimens were preconditioned inside desiccators containing saturated solutions of magnesium nitrate (*ca*. 53% RH) by 48h at 25°C (ASTM E104-02)[93]. At least 12 specimens for each sample formulation were tested and the average value has been reported. A digital micrometer was used to monitor film thickness.

Films from compression moulding followed ASTM D1708-06a.[94] Samples were cut into microtensile test specimens (width 4.64 mm). Measurements were performed with a crosshead speed set at 1 $mm \cdot min^{-1}$ and initial gauge length of 22.2 mm.

Films from blow moulding followed ASTM D882-02[95]. Specimens of 70 mm length and 10 mm width were cut out from films. Initial gauge length was 50 mm and crosshead speed was 10 $mm \cdot min^{-1}$.

[*] PAS-FTIR was performed in the Department of Chemical and Industrial Chemistry, University of Genova and the Author thanks Prof. Paolo Piaggio.

# 3. RESULTS

The results chapter was divided in three main topics each one corresponding to the following studies:

4. Compatibilization of Polyethylene-Poly(3-hydroxybutyrate) Based Blends;
5. Effect of Prodegradant Additive in the Polyethylene-Poly(3-hydroxybutyrate)-Poly(ethylene-*co*-glycidyl methacrylate) Blends;
6. Polyethylene-Starch Materials: Compatibilization and Prodegradant Effect.

## 3.1. Compatibilization of Poly(ethylene)-Poly(3-hydroxybutyrate) Based Blends

The greatest environmental pressure for the packaging chain comes from legislation. According to the European Environmental Agency packaging waste is the major and growing waste stream[1]. Polyethylene (PE) represents a family of polyolefins widely used in food packaging. Although PE was first produced over 50 years ago, manufacturing and processing developments continue to improve its properties, performance, and packaging applications[14]. Some of advantages that justify its application in this segment of market are: the low cost, the excellent chemical resistance, and the very good processability. However, it is a non-biodegradable polymer, which characterizes an issue concerned to the waste management. One of the possible solutions, other than recycling and reuse, is to formulate new materials by blending PE with biodegradable polymer[96].

Poly(3-hydroxybutyrate) (PHB) is a bacterial aliphatic polyester, which is biodegradable and ecological. PHB has mechanical properties comparable to that of polypropylene (PP). However, due to its high cost and brittleness, it is less attractive to the packaging marked[60].

The combination of PE characteristics with that of PHB by blending them can result in a new material for use in packaging eco-compatible. The literature for this type of blend is very modest, meaning a field still to be

explored. PE and PHB are immiscible due to their polarity characteristics. To promote adhesion between the interphase of them, it is necessary at least a copolymer as a third component, which contain in its chain both polar and non-polar comonomers. Iordanskii *et al.* proposed environmentally friendly membranes for separation processes based on PHB-LDPE blends. They found that water permeability depends of blend composition in the range of 2:98-32:68[73]. However, they did not consider that the pathway formed in the interfaces of the two immiscible components could contribute to diffusion process. Rosa *et al*. performed a more detailed study on PHB-LDPE blends[74]. The independent variables were composition and the presence or absence of oxidate polyethylene wax in the formulations. Although the two components has been shown to be immiscible by SEM photomicrographs, elongation at break of PHB matrix increased with the addition of LDPE from 0.6 % to 19 % for PHB and 50PHB:50LDPE, respectively. On the other hand, Young's modulus of LDPE matrix increased from 41 MPa to 142 MPa with addition of 50 wt-% of PHB.

The present study about compatibilization of PE-PHB based blends followed a systematic screening statistical design experiment (DEX). The independent variables were the proportion between the three blend components and the type of compatibilizer. These compatibilizers were EVA, EGMA and EMAC.

### 3.1.1. *Morphology*

SEM micrographs of cryogenic fractures of PE-PHB based blends (see Tables 2.2 – 2.4 for nomenclature) as a function of type and amount of compatibilizer are shown in Figure 3.1-3.4.

All binary blends, independently if it is PE (75E25B – Fig. 3.1 a) and b)) or PHB (25E75B – Fig. 3.1 c) and d) as matrix, showed typical morphological features of immiscible systems. It can be observed that dispersed phase is not homogeneous and its interfacial adhesion with matrix is poor. The same observation was found by Rosa *et al*.[74] and Kim *et al*.[97]. As both components are mechanically diverse the surfaces of cryogenic

fractures will show distinct behaviour. Binary blend with PE matrix (Fig. 3.1 a) and b)) presents ductile fracture while that with PHB matrix (Fig. 3.1 c) and d)) is brittle. The aspect of the dispersed phase follows the same behaviour of that of matrix. This means, that the surface of PHB dispersed phase is smooth while that of PE dispersed phase is roughest. In both blends the amount of dispersed phase is the same. However, lower magnification micrographs (Fig 3.1 a) and c)) suggest that the blend containing dispersed phase PHB seems to be at lower amount or to have a better miscibility. This can be probably due to the fragility of PHB, which can be broken and part of its particle can remain immersed in PE matrix without to pull out (Fig. 3.1 b)).

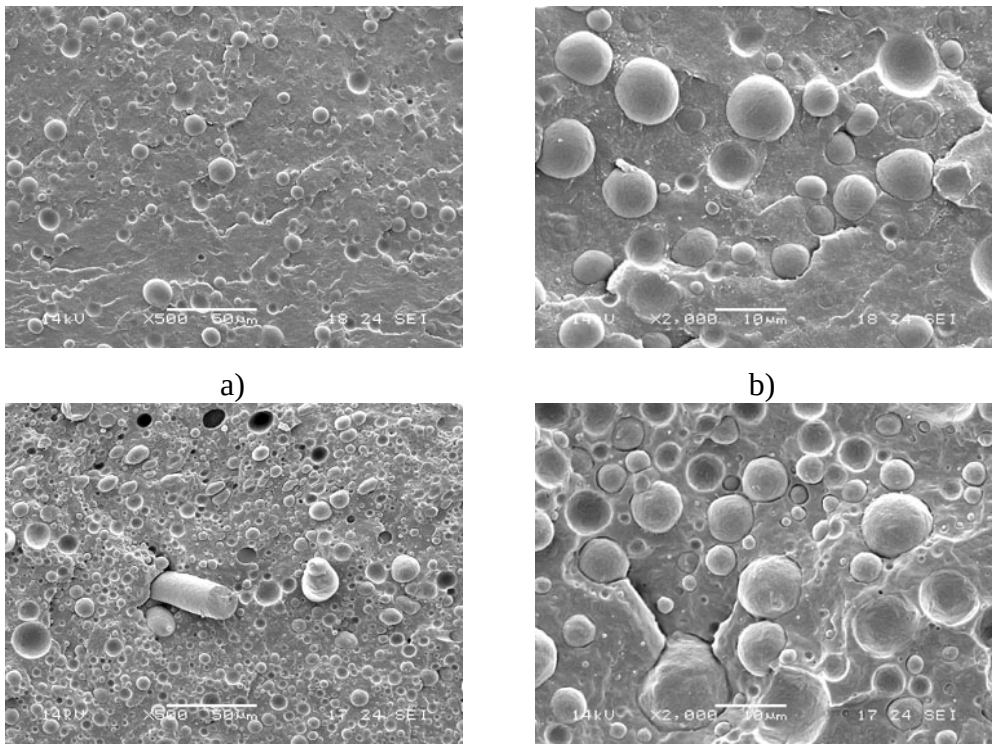


a) b)

c) d)

**Figure 3.1.** SEM micrographs of PE-PHB binary blends. a) 75E25B–500X; b) 75E25B–2000X; c) 25E75B–500X; d) 25E75B–2000X.

The compatibilizer EVA contain 33 wt-% of vinyl acetate (VA) comonomer. Figure 3.2 a) shows that the binary blend of PE with 10 wt-% of EVA has only one phase characterizing their compatibility. On the other hand, the dispersed phase EVA in binary blend with PHB as matrix, at the same amount (Fig. 3.2 b)), is heterogeneous in size and with poor adhesion. The choice of the EVA as compatibilizer of PE-PHB blends was based on the fact that VA comonomer is miscible with the PHB[98]. As the amount of compatibilizer used was 10 wt-%, it can be supposed that only a small fraction of PHB, proportional to *ca*. 3 wt-% of VA, could be compatibilized. In fact, Yoon *et al*. verified this dependence of the PHB-EVA compatibility with amount of VA[99]. They found thermal properties and crystallization behaviour that PHB is immiscible with EVA containing 70 wt-% of VA but miscible when the VA is present at 85 wt-%.

The proportions between PE-PHB in the ternary blends shown in Figure 3.2 c) and d) are equivalent to that of binary ones presented above (Fig. 3.1). The morphology of PE-PHB-EVA with PE as matrix (Fig. 3.2 c)) is very similar to that of equivalent binary blend (Fig. 3.1 a)) indicating that 10 wt-% of EVA (33 wt-% VA) compatibilizer was not sufficient to promote a satisfactory adhesion between PE and PHB components. A much more dramatic effect was observed for the equivalent ternary blend with PHB as matrix (Fig. 3.2 d)). The PE dispersed phase seems to be present in the blend in a different proportion of its counterpart binary blend (Fig. 3.1 c)). This is probably due to PE and EVA compatibility resulting in an apparent higher proportion in the blend. Besides, the presence of EVA seems to promote the coalescence of PE phase, probably due to the changes in its melt viscosity. So, it can be supposed that when PE is continuous phase, EVA can compatibilize it to some extension with PHB, depending on its proportions with VA comonomer amount.

The compatibilizer polyethylene-*co*-glycidyl methacrylate (EGMA) contain 8 wt-% of glycidyl methacrylate (GMA) comonomer. EGMA has an epoxy pendant group that can react with carboxyl chain end groups of PHB[100]. This reaction comes in the presence of temperature. So, the

hypothesis was that EGMA could compatibilize PE-PHB by reactive blending.

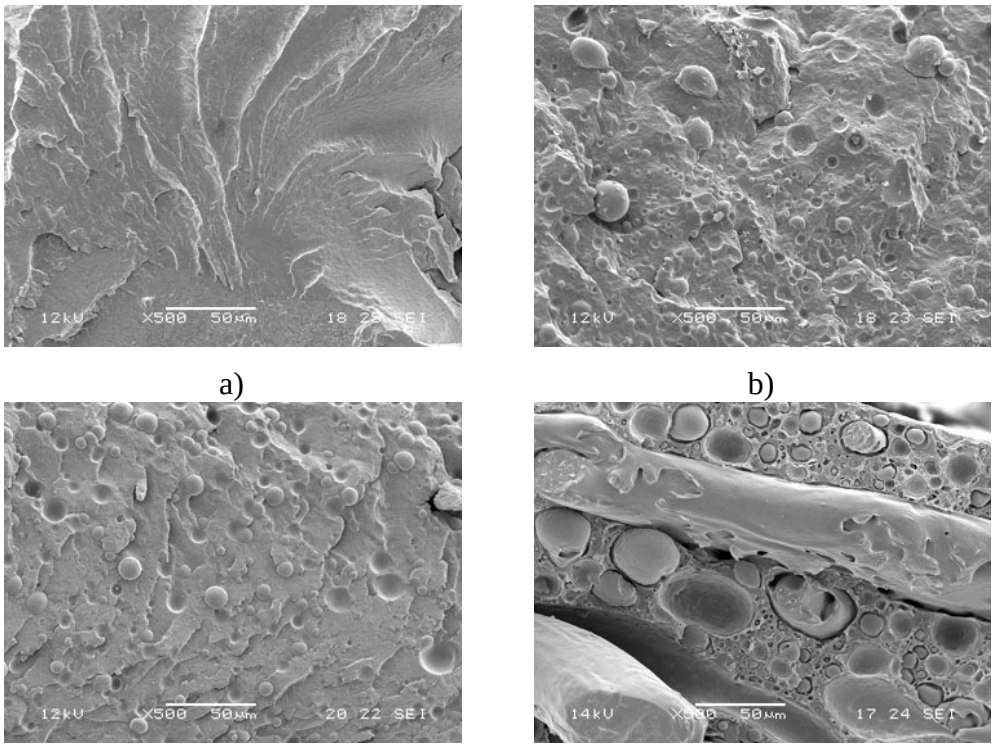


**Figure 3.2.** SEM micrographs of PE-PHB blends compatibilized with 10 wt-% of EVA at 500X. a) 90E-10V; b) 90B-10V; c) 68E22B10V; d) 22E68B10V.

Figure 3.3 shows cryogenic fractures of PE-PHB based blends compatibilized with EGMA. The compositions of these blends (binary and ternary) are the same to those of PE-PHB blends compatibilized with EVA (Fig. 3.2). Binary blend of PE with 10 wt-% of EGMA presents only one phase (Fig. 3.3 a)) indicating that both components are miscible. On the other hand, it can be observed two phases in the fracture of PHB-EGMA blends, at the same composition (Fig. 3.3 b)). The expected compatibility between PHB and PGMA, based on the results of Lee *et al.*[100], was not achieved probably due to the proportion between epoxy groups of EGMA and carboxyl end group of PHB. Nevertheless, confronting the morphologies of PHB-EVA

(Fig. 3.2 b)) and PHB-EGMA (Fig. 3.3 b)) blends it can assume that a small fraction of the EGMA dispersed phase reacted with PHB matrix.

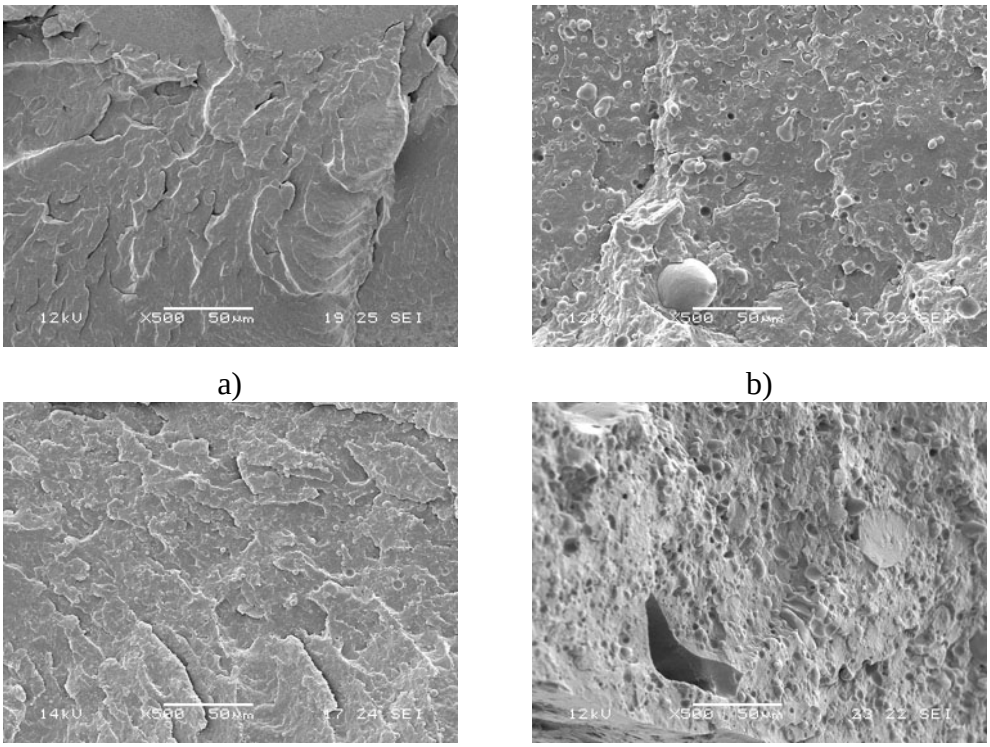


**Figure 3.3.** SEM micrographs of PE-PHB blends compatibilized with 10 wt-% of EGMA at 500X. a) 90E10G; b) 90B10G; c) 68E22B10G; d) 22E68B10G.

The fracture of both ternary PE-PHB based blends with 10 wt-% of EGMA showed two phase. The dispersed phase was more homogeneous for PE matrix based blend (Fig. 3.3 c)) than for PHB one (Fig. 3.3 d)). On the other hand, it can be concluded that the EGMA promote a better dispersion and interfacial interactions between both PE and PHB than EVA (Fig. 3.2 with Fig. 3.3). Besides, as the polar chain segments of compatibilizers are present in minor amount than that of the non-polar ones, the better results were found for blends with PE matrix.

Poly(ethylene-*co*-methyl acrylate) (EMAC) contain 20 wt-% of methyl acrylate (MA) comonomer and was the third material used to compatibilize

PE-PHB blends. The selection of this compatibilizer was based on the results found by An *et al.*[101]. They prepared blends of PHB-PMA by solution-casting method to study their miscibility by thermal and optical analysis. The behaviour of cold crystallization temperature ($T_{cc}$) as a function of blend composition led them to the assumption that both components form miscible blends in the whole range. Besides, the small angle x-ray (SAXS) demonstrated that the amorphous MA is incorporated within PHB spherulites.

Figure 3.4 shows both PE and PHB binary blends with 40 wt-% of EMAC. The blend 60B40EM (Fig. 3.4 a) and b)) point out that the adhesion between components is poor with irregular dimensions and forms of the dispersed phase. So, PHB and EMAC are not compatible at this composition. Another factor that could cause this morphology would be the difference in melts viscosity combined with compression moulding performed to obtain the films. On the other hand, PE and EMAC are compatible as suggests the surface fracture showed in Figure 3.4 c). At higher magnification (Fig. 3.4 c)) it is observed the good adhesion between the two phases. As yet considered in the PHB-EMAC binary blend, the PE-EMAC blend presents dispersed phase with irregularities in the form and size too. In these family of blends compatibilized by EMAC the level of shear developed inside the internal mixer was not sufficient to provide a good dispersion.

In the PE-PHB-EMAC ternary blends shown in Figure 3.5, the amount of compatibilizer used was 15 wt-% corresponding to *ca*. 3 wt-% of MA that might compatibilize PHB. This effect can be observed when the blend matrix is PE. In fact, the size and homogeneity of dispersed phase in the blend 64E21B15EM (Fig. 3.5 a)) is better than that of system with PHB as matrix (Fig. 3.5 b)). Probably a small fraction of PHB was compatibilized with PE in the 64E21B15EM.

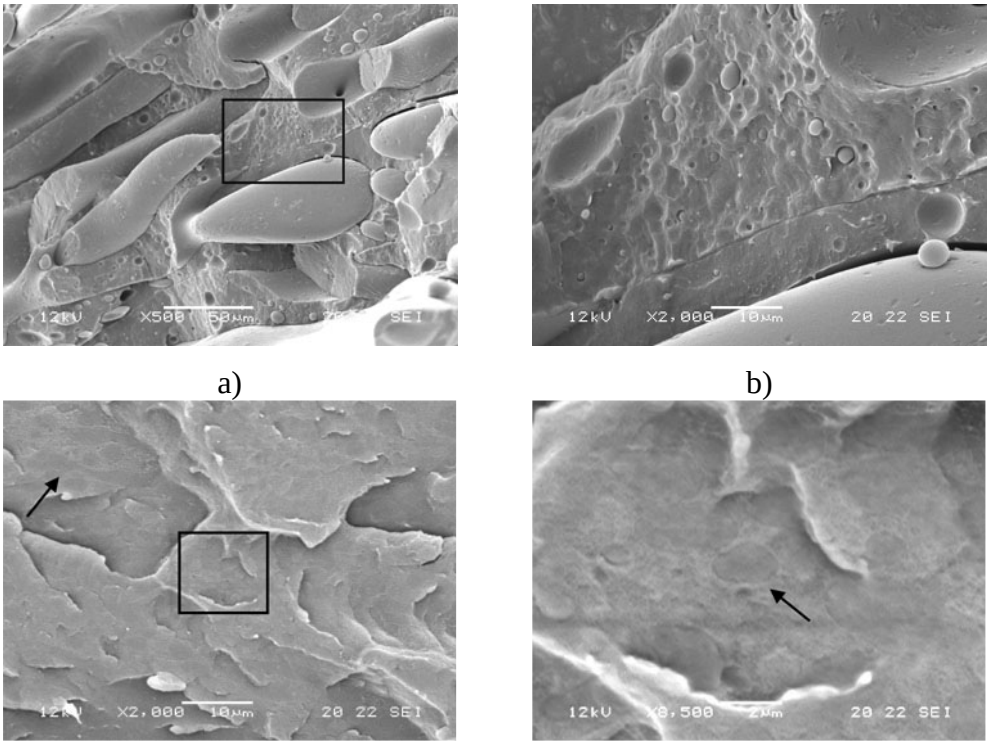


a) b)

c) d)

**Figure 3.4.** SEM micrographs of PE and PHB binary blends with 40 wt-% of EMAC. a) 60B40EM – 500X; b) 60B40EM – 2000X; c) 60E40EM – 2000X; d) 60E40EM – 8500X.

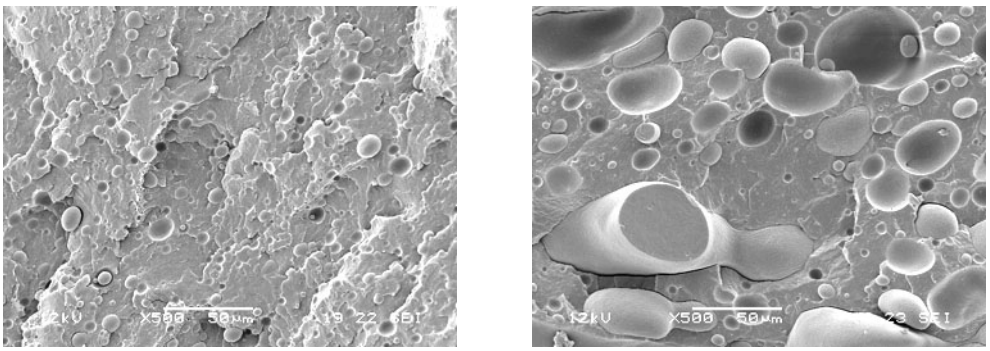


a) b)

**Figure 3.5.** SEM micrographs of PE-PHB blends compatibilized with 15 wt-% EMAC at 500X. a) 64E21B15EM; b) 21E64B15EM.

### 3.1.2. *Thermal properties*

Thermal characterization of polymer blends is a well-known method to determine the miscibility of polymer blends[102]. Thermal properties of PE-PHB films were assessed by thermogravimetry (TGA), differential scanning calorimetry (DSC) and dynamic mechanical thermal analyser (DMTA).

#### *3.1.2.1 Thermogravimetry (TGA)*

TGA provides important data parameters relating to thermal stability of polymers[103] that is very useful in polymer processing and formulation. One of them is the decomposition temperature ($T_d$), which is defined as the onset temperature at the beginning of the weight loss. In the present study, $T_d$ was defined as the temperature at 1 wt-% of weight loss[104]. Another parameter is the peak degradation temperature ($T_p$), which is related to the reaction mechanism. The $T_p$ data are obtained from the first derivate of TGA (DTGA) trace and corresponds to the temperature at the maximum degradation rate. The experiments of this study were conducted under nitrogen atmosphere in the range temperature of 25-600°C and the pyrolysis residue was measured at 600 °C. The replica was carried out only in three samples to evaluate the experimental error, due to the long time of the TGA analysis. The selected samples representing materials containing one, two and three components were PE, 25E75B, and 24E71B5V, which errors at 95 % of confidence of Student's *t*-test were 0.3 %, 20 %, and 5 %, respectively. The more significant error was found for the incompatible binary blend PE-PHB with PHB as matrix. As was observed in Figure 3.1 d), the PE dispersed phase is not homogeneous in size and presented poor adhesion to the PHB matrix. These characteristics of 25E75B combined with the small size of samples used in the TGA analysis can explain the significant measured error.

Thermogravimetric data of PE-PHB blends compatibilized with EVA, EGMA and EMAC are presented in Tables 3.1-3.3, respectively. The $T_d$ of PE, PHB, and of the compatibilizers EVA, EGMA and EMAC are 391 °C, 265 °C, 306 °C, 392 °C and 372 °C, respectively. The PHB $T_d$ value is in

agreement with that reported by Lee *et al.*[105], which found $T_d$ value equal to 267 °C defined at 5 wt-% of weight loss. Moreover, Huang and Kang[106] found for LDPE a $T_d$ value of 432 °C through the bi-tangent method. In the present study, the same value of PE $T_d$ was obtained by using the same approach of Huang and Kang. However, at this temperature the weight loss of PE was *ca.* 8 wt-% that is so much to be considered an onset decomposition temperature. As was observed in the work of Fernandes *et al.*[104] the use of bi-tangent method is only appropriate when the degradation rates (slope) are equivalent. This means, when this method is applied for the same family of materials with similar decomposition mechanism of reaction.

**Table 3.1.** TGA data of PE-PHB blends compatibilized with EVA.[a)]

| Trial | Sample[b)] | $T_d$ (°C) | $T_{p1}$ (°C) | $T_{p2}$ (°C) | $R_{600}$ (%) |
|---|---|---|---|---|---|
| | EVA | 306 | 352 | 494 | 0.5 |
| a | PE | 391 | — | 472 | 0.4 |
| b | PHB | 265 | 298 | — | 0.8 |
| c | 90E10V | 346 | 356 | 478 | 0.6 |
| d | 90B10V | 245 | 290 | 352/467 | 0.4 |
| e | 75E25B | 271 | 292 | 472 | 0.4 |
| f | 25E75B | 253 | 295 | 474 | 0.5 |
| g | 68E22B10V | 273 | 291 | 474 | 0.5 |
| h | 22E68B10V | 265 | 296 | 473 | 0.6 |
| i | 71E24B5V | 273 | 294 | 472 | 0.4 |
| j | 24E71B5V | 261 | 294 | 472 | 0.5 |

[a)] $T_d$ is the decomposition temperature defined at 1 wt-% of weight loss; $T_p$ is the first derivative peak; and $R_{600}$ is the residual weight at 600°C. [b)] See Table 2.2 for code definition.

PHB was 126 °C less stable than PE. The thermal decompositions of binary blends with PHB as matrix and with 10 wt-% of EVA and EGMA compatibilizers were *ca*. 20 °C lower than pristine PHB. On the other hand, $T_d$ value of binary blend of PHB with 40 wt-% of EMAC did not present any changes in relation to pristine PHB.

The $T_d$ values of binary blends with PE as matrix presented a different behaviour. The $T_d$ of 90E10G (Tab. 3.2) blend was practically invariable

because both components (PE and EGMA) have equivalent thermal stability. Conversely, the $T_d$ value of 90E10V (Tab. 3.1) was 40 °C higher than that of pristine EVA that is the less stable component of this blend. In this case, it can be supposed that the good dispersion of EVA in the PE matrix (Fig. 3.2 a)) allows a matrix protecting effect. This effect was less pronounced in the binary blend with EMAC, which $T_d$ value of 60E40EM blend (Tab. 3.3) was only 7 °C higher than that of the less stable compatibilizer.

**Table 3.2.** TGA data of PE-PHB blends compatibilized with EGMA.[a)]

| Trial | Sample[b)] | $T_d$ (°C) | $T_{p1}$ (°C) | $T_{p2}$ (°C) | $R_{600}$ (%) |
|---|---|---|---|---|---|
| | EGMA | 392 | 567 | — | 0.5 |
| a | PE | 391 | — | 473 | 0.4 |
| b | PHB | 265 | 298 | — | 0.8 |
| c | 90E10G | 396 | — | 479 | 0.3 |
| d | 90B10G | 241 | 287 | 460 | 0.4 |
| e | 75E25B | 271 | 292 | 472 | 0.4 |
| f | 25E75B | 253 | 295 | 474 | 0.5 |
| g | 68E22B10G | 270 | 291 | 471 | 0.5 |
| h | 22E68B10G | 262 | 295 | 466 | 0.7 |
| i | 71E24B5G | 272 | 293 | 471 | 0.8 |
| j | 24E71B5G | 260 | 293 | 470 | 0.5 |

[a)] $T_d$ is the decomposition temperature defined at 1 wt-% of weight loss; $T_p$ is the first derivative peak; and $R_{600}$ is the residual weight at 600°C. [b)] See Table 2.3 for code definition.

Lee *et al.*[100,105] studying the thermal stabilization of PHB by poly(glycidyl methacrylate) (PGMA) found that the blends containing PGMA in the range of 5-30 wt-% were more stable than PHB matrix. They explained this effect as a result of thermal cross-linking reactions of the epoxy group of PGMA with the carboxyl chain ends of PHB formed during its thermal degradation. The lower value of 90B10G $T_d$ (Tab. 3.2) than that of PHB can be explained by the same considerations made above for the 25E75B. In the 90B10G blend the amount of the GMA segment compatible with PHB is only 0.8 wt-% (in 10 wt-% of EGMA) and so predominate the effect of incompatible PE segment of the EGMA copolymer. Although some

cross-linked reactions of PHB end group with GMA epoxy group may have occurred, as suggested in the Figure 3.3 b), it was not sufficient to stabilize PHB matrix. The similar behaviour was found for the 90B10V blends (Tab. 3.1) and it can be explained in the same way because the amount of VA segment of the compatibilizer miscible with PHB is only 3.3 wt-% (in 10 wt-% of EVA).

**Table 3.3.** TGA data of PE-PHB blends compatibilized with EMAC.[a]

| Trial | Sample[b)] | $T_d$ (°C) | $T_{p1}$ (°C) | $T_{p2}$ (°C) | $R_{600}$ (%) |
|---|---|---|---|---|---|
| | EMAC | 372 | — | 466 | 0.3 |
| a | PE | 391 | — | 473 | 0.4 |
| b | PHB | 265 | 298 | — | 0.8 |
| c | 60E40EM | 379 | — | 472 | 0.6 |
| d | 60B40EM | 265 | 296 | 461 | 0.5 |
| e | 75E25B | 271 | 292 | 472 | 0.4 |
| f | 25E75B | 253 | 295 | 474 | 0.5 |
| g | 64E21B15EM | 261 | 294 | 474 | 0.4 |
| h | 21E64B15EM | 240 | 292 | 476 | 0.3 |
| i | 68E22B10EM | 266 | 290 | 472 | 0.6 |
| j | 22E68B10EM | 242 | 292 | 472 | 0.3 |
| l | 71E24B5EM | 267 | 293 | 479 | 0.2 |
| m | 24E71B5EM | 245 | 292 | 472 | 0.3 |

[a)] $T_d$ is the decomposition temperature defined at 1 wt-% of weight loss; $T_p$ is the first derivative peak; and $R_{600}$ is the residual weight at 600°C. [b)] See Table 2.4 for code definition.

Figure 3.6 shows $T_d$ temperatures of PE-PHB based blends as a function of composition and type of compatibilizer. The $T_d$ values of the blends with PE as matrix (Fig. 3.6 a)) are slightly superior to that of PHB and *ca.* 120 °C lower than PE (391 °C, which is not shown). An exception was found in the blends compatibilized with EMAC (Tab.3.3), which $T_d$ values tend to decrease slightly with increasing of EMAC amount in the blend.

As previously observed in the SEM photomicrographs (Figs. 3.2-3.5) it could be expected that the better distribution and lower size dispersed phase observed in the PE-PHB-EGMA blend could explain its superior

performance in relation to PE-PHB-EVA and PE-PHB-EMAC. However, this was not found. In the discussion of PHB-compatibilizer binary blends (Tabs 3.1-3.3), it was suggested that structure chemical changes would be a possible responsible for the low $T_d$ values, independently of type of compatibilizer. The same can be proposed for the behaviour of $T_d$ in the ternary blends.

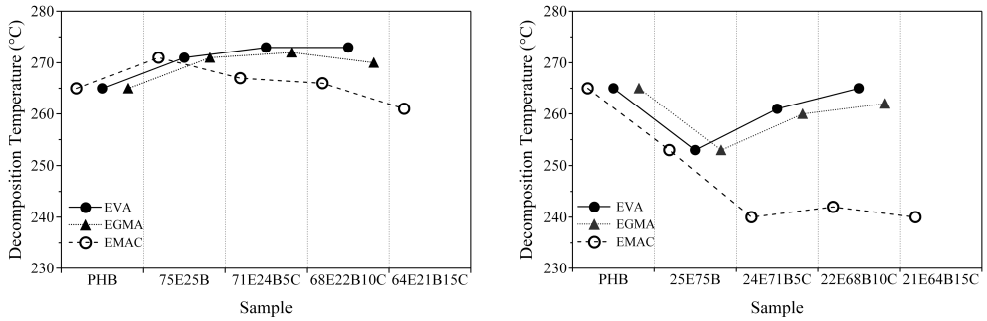


a) b)

**Figure 3.6.** Thermal stability of PE-PHB based blends as a function of composition and type of compatibilizer. a) PE matrix; and, b) PHB matrix.

In the ternary blends with PHB as matrix (Fig. 3.6 b)) the changes of $T_d$ values with composition and type of compatibilizer are not significant when EVA and EGMA are the compatibilizers used. On the other hand, the binary blend 25E75B and ternary blends with EMAC as compatibilizer presented the lower thermal stabilities. The source of these results might be the insufficient dispersion of the minor phase and/or the lack of adhesion between phases (Figs. 3.1 c) and 3.4-3.5).

As aforementioned, the peak of first derivate of the weight loss as a function of temperature ($T_{px}$) is related to the maximum rate of the volatile chemical formed. This rate depends of mechanism of decomposition reaction and of the mass transfer in the viscous media of the polymeric melt, for example. As already considered, the PE matrix protecting effect on the EVA component in their binary blend (90E10V) is confirmed by the temperature shift of 4 °C higher on EVA $T_{p1}$ (352 °C) in the blend (Tab. 3.1). In this case,

it can be supposed that the melt viscosity of more stable PE control diffusion of the decomposition chemicals (acetic acid in the first step) from EVA compatibilizer. On the other hand, a different behaviour was found for PHB-compatibilizer blends. Both 90B10V $T_p$ and 90B10G $T_p$ values (Tabs. 3.1-3.2) are respectively 8 °C and 11 °C lower than the less stable PHB (298 °C). PHB during melt processing in an internal mixer can have reduced its molecular weight (MW) up to 50 % in the presence of very low amount of humidity[107]. This MW decreasing comes from a random chain scission reaction (*cis*-elimination) forming carboxylic acid end groups[108]. This group can react with epoxy one of GMA or attack VA developing new chemical groups in the PHB main chain that might probably have less stability. The values of $T_p$ of ternary blends were practically invariable and equivalent to the less stable PHB. In this case, probably PE component gave some protection to the less stable components. The residue formed at 600 °C for all samples analysed were lower than 1 wt-%.

The two matrices of the compatibilized blends (PHB and PE) showed a white residue. Probably these residues are due to impurities because PE is decomposed in the pyrolysis without char formation, for example. The residue amounts were 0.4 wt-% and 0.8 wt-% for PE and PHB, respectively. In general, ternary blends showed an intermediate amount of residue, which increased with increasing amount of PHB in the blend.

Dodson *et al.* [109] analyzed blends behaviour using the additive rule in the TGA traces, which simulated trace is constructed by adding the weighted contributions of each homopolymer trace as indicated in the Equation 3.1 for two components. In this method it is supposed that the simulated TGA trace represents the behaviour that should be expected from the system when no interactions are present between the blend components.

$$W_{A\text{-}B} = (1\text{-}x)\, W_A + x\, W_B \qquad \text{(Eq. 3.1)}$$

Where W represents the TGA trace, A-B, A, B indices refer to blend and single components, respectively, and x is the weight fraction of component B in the blend.

Experimental and simulated TGA traces of PE-PHB binary blends are illustrated in Figure 3.7, which are compared with pristine components. The experimental trace of 25E75B blend presents a slow initial slope and a profile very different from the corresponding simulated trace and that of PHB matrix (zoom inside Fig. 3.7 a)). The change in the onset thermodegradation slope suggests a change in the reaction mechanism and probably a modification in the chemical structure. Another hypothesis that could be formulate to explain why the experimental traces began at lower temperature than the simulated one could be that of decomposition acceleration effect promoted by specific interaction among blend components and degradation species being formed (macro and small radicals, small molecules). Taking into account that the experimental 25E75B trace begin at temperature lower than the less stable PHB component, it can be supposed that these species were formed during blend melt processing. The plateau of the second step of experimental trace at lower weight loss in relation to predicted one suggests a blend composition with less PE component in relation to the nominal value. This observation can be related to the heterogeneity of dispersed phase as previously remarked.

The thermodegradation behaviour changes significantly when PE is the blend matrix (zoom inside Fig. 3.7 b)). In this case, 75E25B blend was slightly less stable than would be expected from the simulated trace. As the predicted weight loss of the second degradation step was superior to that of experimental one, it could be assumed that the apparent lower stability of 75E25B blend from that expected is due to a lower amount of the more stable PE in the blend than the nominal value. Again, this achievement may be related to the homogeneity of dispersed phase as depicted in Figure 3.1 a) and b).

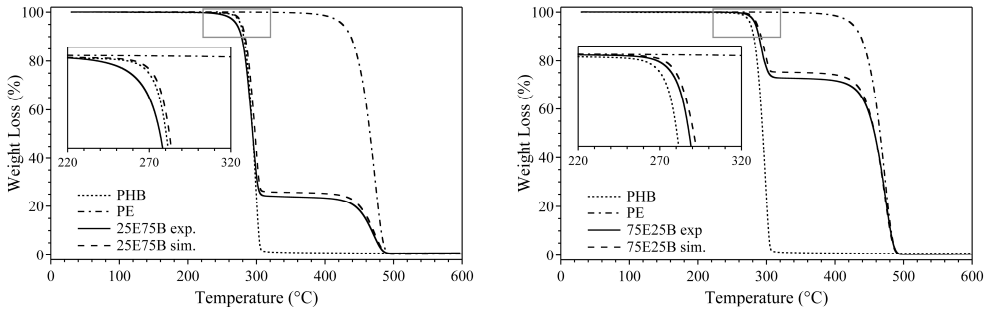


a) b)

**Figure 3.7.** Experimental and simulated TGA traces of blends and pristine components. Binary blends 25E75B a) and 75E25B b).

All experimental ternary blends traces (Fig. 3.8) indicate that them are less stable than expected, regardless of the polymer matrix used. However, when PHB is the blend matrix, ternary blends were less stable than PHB as discussed previously for the changes of $T_d$ as a function of the blend composition and type of compatibilizer. The 22E68B10V blend (Fig. 3.8 c)) was an exception, which experimental trace nearly overlaps the simulated one. This behaviour can have its origin in the melt processing. The melt flow index (MFI) of the compatibilizer EVA is the highest of all components used in the present study (43 g/10 min), which can reduce the shear effect on PHB melt processing degradation[107]. Consequently, the PHB macromolecule in the ternary blend compatibilized with EVA will undergo less chemical modification, which will influence its thermal stability. Although the lowest MFI is that of EGMA (5 g/10 min), its shear effect on melt processing degradation of PHB is compensated by the cross-linking reaction. The experimental traces of 22E68B10EM ternary blend (Fig. 3.8 e)) is very similar to that of 25E75B binary blend (Fig. 3.7 a)). This result substantiate the previously discussion about the shear effect on PHB melt processing degradation and the phase adhesion. The MFI of EMAC (6 g/10 min) is lower than that of PE and PHB (7.9 and 7.4 g/10 min, respectively), which can increase melt viscosity contributing to the PHB degradation.

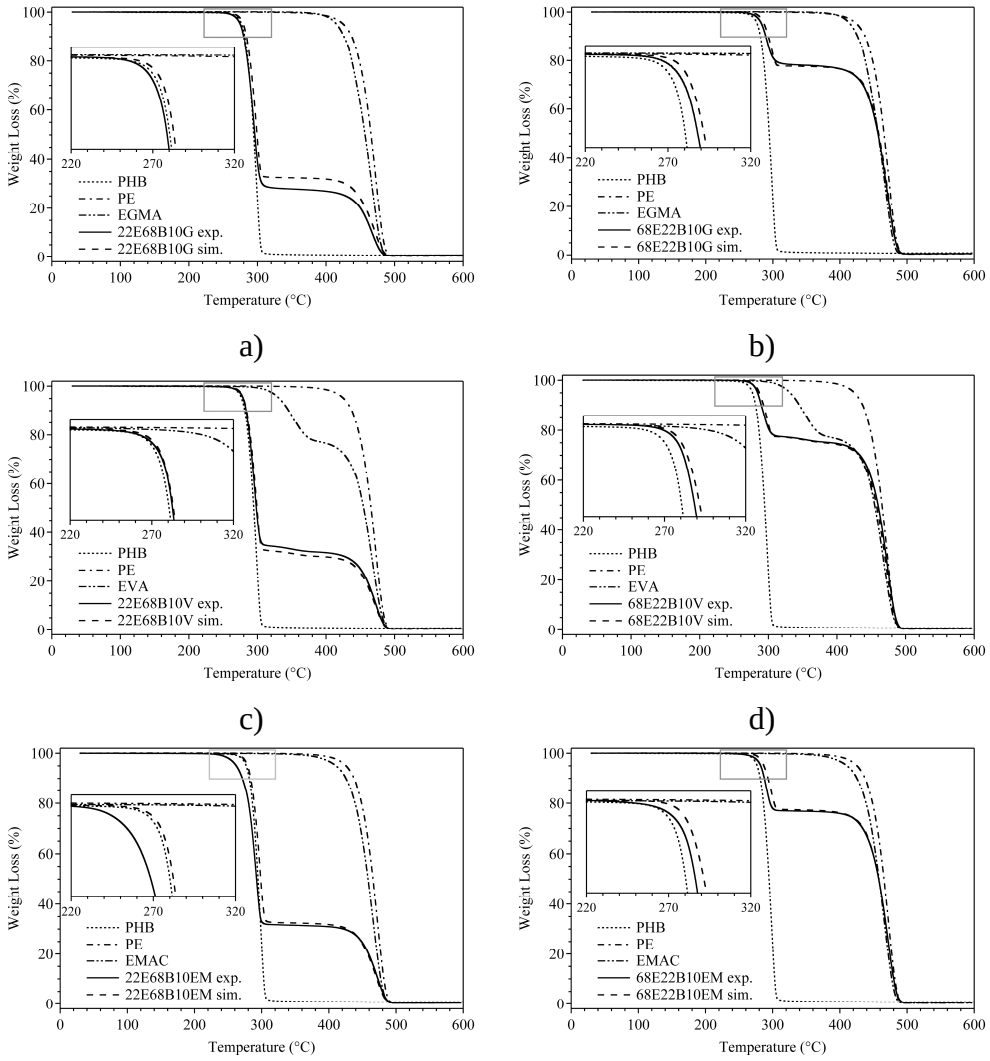


**Figure 3.8.** Experimental and simulated TGA traces of blends and pristine components. Ternary blends with EGMA, 22E68B10G a) and 68E22B10G b); with EVA, 22E68B10V c) and 68E22B10V d); and with EMAC, 22E68B10EM e) and 68E22B10EM f).

### *3.1.2.2 Differential scanning calorimetry (DSC)*

The glass transition temperature ($T_g$) is the most common way to study miscibility of polymer blends using DSC. However, this criterion is not useful in the present blend system studied considering that both PE and PHB are very crystalline and that $T_g$ of PE is not feasible to be detected in a heat flow calorimeter even after a quenching. In this case, it is the parameters of crystalline phase that can give information about the compatibility between blend components[102]. DSC analysis was performed in five scans. Figure 3.9 illustrates the characteristic DSC traces of PE and PHB pristine blend matrices as a function of thermal treatments. The second cooling scan was the quenching treatment and it is not shown. The traces of blends are intermediate to that of pristine matrices. PE transitions were slightly influenced by the thermal treatments on contrary to the behaviour of PHB that was sensible to them.

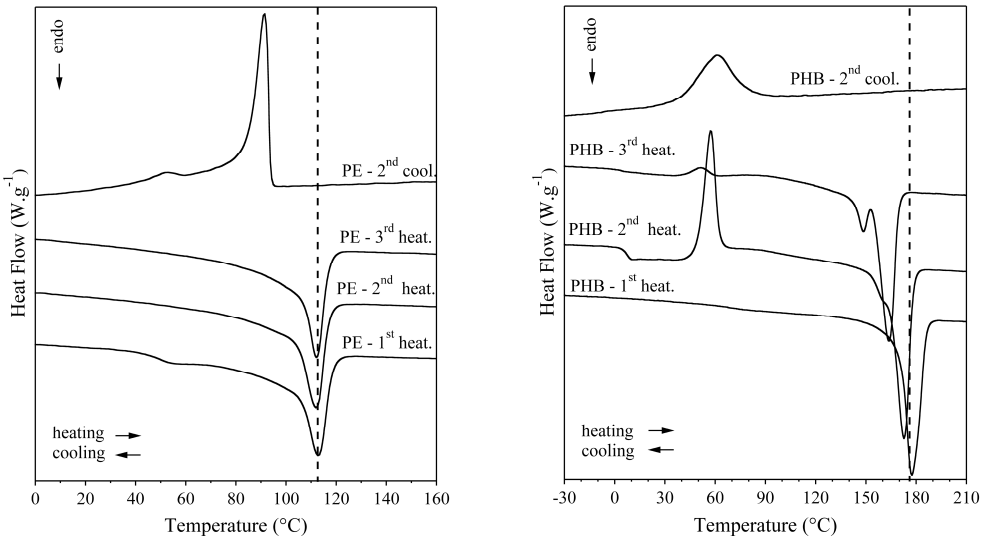


a) b)

**Figure 3.9.** DSC traces of pristine blend matrices as a function of thermal treatments. a) PE; and b) PHB.

The first heating characterize the phase transitions of a state of "equilibrium" taking into account the fact that the blends were maintained for some days (annealing) at ambient condition prior analysis. Thermodynamic parameters from the first heating scan of PE-PHB blends compatibilized with EVA, EGMA and EMAC are shown in Tables 3.4-3.6. In order to assess the degree of crystallinity ($X_c$) of samples, the enthalpy of 100 % crystalline PHB was taken as 146 $J \cdot g^{-1}$ and the enthalpy of 100 % crystalline PE was taken as 290 $J \cdot g^{-1}$ [110, 111]. The normalized enthalpy of transitions was calculated on the basis of nominal weight fraction of the component in the blend.

**Table 3.4.** Thermodynamic parameters (1st heating scan) of PE-PHB blends compatibilized with EVA.

| Sample | $T_{m\,1}$ (°C) | $\Delta T_{m\,1}$ (°C) | $X_{c\ PE}$ (%) | $T_{m2}$ (°C) | $\Delta T_{m2}$ (°C) | $X_{c\ PHB}$ (%) |
|---|---|---|---|---|---|---|
| PE | 113 | 125 | 43 | — | — | — |
| PHB | — | — | — | 178 | 136 | 68 |
| EVA | 64 | 67 | — | — | — | — |
| 90E10V | 117 | 116 | 47 | — | — | — |
| 90B10V | — | — | — | 179 | 87 | 64 |
| 75E25B | 112 | 113 | 45 | 179 | 65 | 80 |
| 25E75B | 113 | 120 | 49 | 181 | 70 | 70 |
| 68E22B10V | 113 | 130 | 50 | 179 | 60 | 72 |
| 22E68B10V | 112 | 118 | 60 | 178 | 70 | 68 |
| 71E24B5V | 113 | 117 | 48 | 179 | 52 | 62 |
| 24E71B5V | 113 | 104 | 54 | 180 | 75 | 71 |

[a] $T_m$ is the melting temperature; $\Delta T_m$ is the melting range and $X_c$ is the degree of crystallinity.

The melting temperature ($T_m$) of pristine PE and PHB are 113 °C and 178 °C, respectively. In general, the $T_m$ and the corresponding enthalpy (result not shown) of PE comonomer in the copolymers EVA, EGMA and EMAC, were lower than the values found for the homopolymer due to crystal imperfections created by the random presence of the second comonomer. The

amount of these comonomers decreased from EVA > EMAC >> EGMA with correspondent increasing of the PE comonomer $T_m$.

DSC traces of binary blends with PE as matrix and compatibilizer as dispersed phase showed only one endothermic peak, which PE $T_m$ values of the copolymer are *ca*. 4 °C higher than that of pristine PE. The increasing of $T_m$ values may be due to both a reduction in the melting entropy ($T_m = \Delta H_m/\Delta S_m$) or a superheating phenomenon[112]. The addition of a less crystalline copolymer will increase the chain entanglements in the amorphous phase of the blend slowing the crystal-melting rate in relation to the heating rate. On the other hand, DSC traces of binary blends with PHB as matrix showed two endothermic peaks assigned to PE comonomer of the compatibilizer and to PHB. In these cases, the $T_m$ of PHB remained unchanged and that of PE in the compatibilizer presented distinct behaviours.

**Table 3.5.** Thermodynamic parameters (1st heating scan) of PE-PHB blends compatibilized with EGMA.

| Sample | $T_{m\,1}$ (°C) | $\Delta T_{m\,1}$ (°C) | $X_{c\ PE}$ (%) | $T_{m2}$ (°C) | $\Delta T_{m2}$ (°C) | $X_{c\ PHB}$ (%) |
|---|---|---|---|---|---|---|
| PE | 113 | 125 | 43 | — | — | — |
| PHB | — | — | — | 178 | 136 | 68 |
| EGMA | 117 | 132 | — | — | — | — |
| 90E10G | 117 | 108 | 48 | — | — | — |
| 90B10G | 110 | 28 | — | 178 | 64 | 64 |
| 75E25B | 112 | 113 | 45 | 179 | 65 | 80 |
| 25E75B | 113 | 120 | 49 | 181 | 70 | 70 |
| 68E22B10G | 113 | 99 | 48 | 180 | 47 | 57 |
| 22E68B10G | 113 | 92 | 60 | 178 | 81 | 72 |
| 71E24B5G | 112 | 130 | 47 | 179 | 64 | 71 |
| 24E71B5G | 111 | 99 | 69 | 179 | 72 | 63 |

[a)] $T_m$ is the melting temperature; $\Delta T_m$ is the melting range and $X_c$ is the degree of crystallinity.

No PE melting peak was observed in the 90B10V blend (Tab. 3.4). The melting enthalpy in EVA is very small. So, with the small sample size used in DSC analysis make difficult its detection in the blend. A PE $T_m$ depression of

7 °C was detected in 90B10G blend (Tab. 3.5). This behaviour is typical of miscible blend[102]. Finally, no changes in the PE $T_m$ of system 60B40EM was observed. The morphological and TGA findings (Fig. 3.4 a) and Tab. 3.3) of this blend suggested that EMAC was the less compatible of the three copolymers used. So, the invariability of PE $T_m$ is another indication of its incompatibility with PHB.

**Table 3.6.** Thermodynamic parameters (1st heating scan) of PE-PHB blends compatibilized with EMAC.

| Sample | $T_{m\,1}$ (°C) | $\Delta T_{m\,1}$ (°C) | $X_{c\ PE}$ (%) | $T_{m2}$ (°C) | $\Delta T_{m2}$ (°C) | $X_{c\ PHB}$ (%) |
|---|---|---|---|---|---|---|
| PE | 113 | 125 | 43 | — | — | — |
| PHB | — | — | — | 178 | 136 | 68 |
| EMAC | 90 | 38 | — | — | — | — |
| 60E40EM | 116 | 64 | 33 | — | — | — |
| 60B40EM | 89 | 95 | — | 178 | 65 | 64 |
| 75E25B | 112 | 113 | 45 | 179 | 65 | 80 |
| 25E75B | 113 | 120 | 49 | 181 | 70 | 70 |
| 64E21B15EM | 116 | 120 | 51 | 181 | 42 | 59 |
| 21E64B15EM | 117 | 36 | 32 | 179 | 66 | 61 |
| 68E22B10EM | 116 | 108 | 52 | 181 | 48 | 66 |
| 22E68B10EM | 115 | 104 | 69 | 177 | 66 | 61 |
| 71E24B5EM | 116 | 99 | 44 | 179 | 47 | 67 |
| 24E71B5EM | 117 | 86 | 46 | 177 | 67 | 62 |

[a)] $T_m$ is the melting temperature; $\Delta T_m$ is the melting range and $X_c$ is the degree of crystallinity.

PE $T_m$ values remained constant in ternary blends of PE-EVA-PHB and PE-EGMA-PHB. However, when EMAC was used as compatibilizer, the PE $T_m$ values shifted in general from 113 °C to 117 °C. $T_m$ values of PHB in binary and ternary blends were equivalent to that of pristine PHB, except for blends containing EMAC. In these blends the $T_m$ of PHB also shifted to higher values. Probably the phase separations of the EMAC will causes PHB phase constrains reducing melting entropy.

The melting range of PE ($\Delta T_{m1}$) in binary blends 90E10V, 90E10G and 60E40EM were respectively 9 °C, 17 °C and 60°C nearer than that of pristine PE. Moreover, the PHB melting range ($\Delta T_{m2}$) values were closer than that of pristine PHB and *ca.* 60 °C. The melting range of ternary blends showed the same trend than that of binary mixtures, a narrowing in the melting range of both PE and PHB. These results suggest that the presence of compatibilizer copolymers accelerate the rate of crystallization of the polymeric matrix.

The thermodynamics characteristics of blends taken from the first heating indicate a quasi-stable phase formed that can be supposed to be the maximum limit of these characteristics. So, the value of the degree of crystallinity ($X_c$) evaluated in this heating rate will give a better approximation of the effect of blend composition and of type of compatibilizer on this property, which can be used to correlate with the other properties. Figures 3.10-11 present the changes of PE and PHB $X_c$, calculated from the 1st heating scan, respectively, in the PE-PHB based blends as a function of composition and type of compatibilizer. It can be observed that PE $X_c$ value (Fig. 3.10) increases with decreasing of PE amount in the blend. On the other hand, PHB $X_c$ value (Fig. 3.11) was superior for the binary blend with PE as matrix and apparently stabilize at around 65%. In both cases, the effect of the type of compatibilizer does not represent a significant variable.

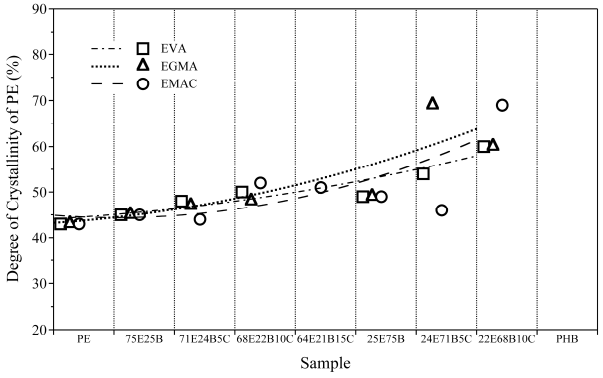


**Figure 3.10.** Degree of crystallinity of PE in the PE-PHB based blends as a function of composition and type of compatibilizer taken from the 1st heating scan.

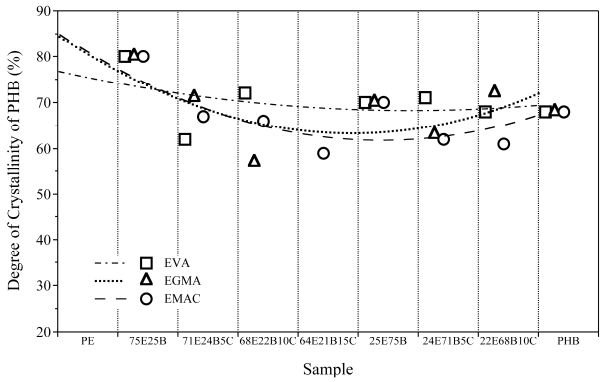


**Figure 3.11.** Degree of crystallinity of PHB in the PE-PHB based blends as a function of composition and type of compatibilizer taken from the 1st heating scan.

DSC traces from the second heating scan of PE-PHB based blends, after quenching, are shown in the Figure 3.12. The thermodynamic parameters are summarized in Tables 3.7-3.9.

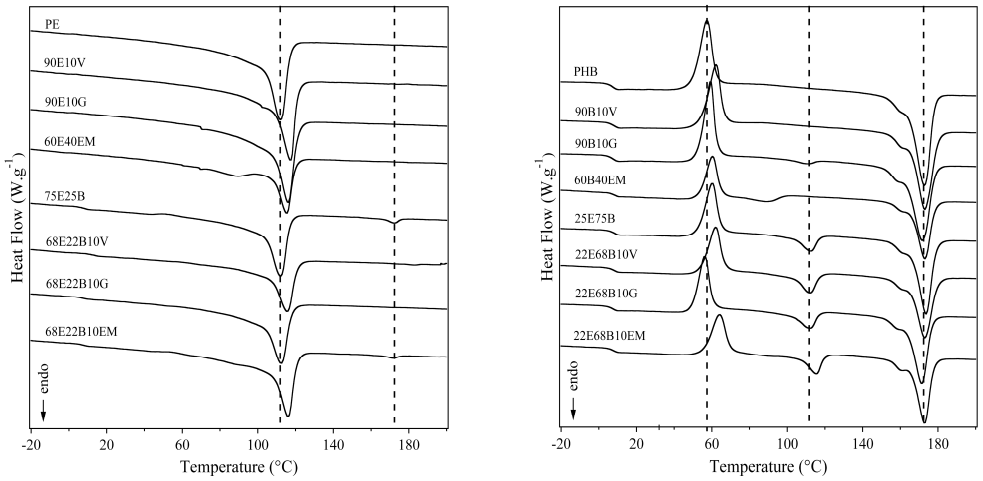


a) b)

**Figure 3.12.** Typical DSC traces from the second heating scan of PE-PHB based blends. a) PE matrix; and b) PHB matrix.

Melting peak of PE in the binary blends with compatibilizers moved up of *ca*. 3°C. The same behaviour was detected in the ternary blends compatibilized with EVA and EMAC (Fig. 3.12 a)). Invariable melting peak

was observed for 75E25B and 68E22B10G. Basically, no changes in the PHB $T_m$ values were verified for blends with PHB as matrix. These temperature were around 172 °C which were *ca*. 7 °C lower than the values found in the 1st heating scan (177-181 °C – Tab. 3.4-3.6). This decrease of PHB $T_m$ can be assigned to the PHB thermal degradation. Binary and ternary blends containing both PE and PHB showed two endothermic melting peaks corresponding to PE and PHB transition in the blend, respectively. Although the melting peak of PHB is practically independent of composition and type of compatibilizer that of the dispersed phase of PE decreased slightly for the systems compatibilized with EVA and EGMA but increased for that compatibilized with EMAC.

**Table 3.7.** Thermodynamic parameters (2nd heating scan) of PE-PHB blends compatibilized with EVA.[a)]

| Sample | $T_{cc,\ PHB}$ (°C) | $T_{m\ PE}$ (°C) | $T_{m\ PHB}$ (°C) | $X_{c\ PE}$ (%) | $X_{c\ PHB}$ (%) |
|---|---|---|---|---|---|
| PE | — | 112 | — | 43 | — |
| PHB | 58 | — | 172 | — | 60 |
| EVA | — | 68 | — | — | — |
| 90E10V | — | 116 | — | 45 | — |
| 90B10V | 63 | — | 172 | — | 59 |
| 75E25B | nd | 112 | 172 | 39 | 70 |
| 25E75B | 61 | 113 | 173 | 12 | 60 |
| 68E22B10V | nd | 115 | nd | 41 | nd |
| 22E68B10V | 61 | 111 | 172 | 19 | 60 |
| 71E24B5V | nd | 113 | 171 | 42 | nd |
| 24E71B5V | 61 | 111 | 173 | 16 | 62 |

[a)] $T_{cc}$, and $T_m$ are cold crystallization and melting temperatures, respectively; $X_c$ is the degree of crystallinity; and, nd = not detected.

In the DSC traces of samples with PHB as matrix, it can be observed the presence of both the PHB glass transition and its exothermic cold crystallization peak (Fig. 3.12 b)). The presence of these PHB transitions in the second heating scan is due to the fact that crystallization of PHB is slower than that of PE and with the quenching treatment PHB has more difficulty to

crystallize. The cold crystallization temperature ($T_{cc}$) of pristine PHB was at 58 °C followed by an endothermic melting peak centred at 172 °C. PHB $T_{cc}$ in the blends in general were *ca*. 3°C higher than the pristine matrix, except the blend 22E68B10G that presented its cold crystallization peak at slightly lower temperature than that of pristine PHB. This blend has indicated to have the better compatibility between components due to the reaction of cross-linking between PHB and EGMA. In the other systems the presence of more rigid phases (PE crystal, VA and MA segments) could be the cause of the higher $T_{cc}$. However, this shifting of $T_{cc}$ to higher temperature is in agreement with the results found by An *et al.* in their study on PHB/PVAc blends[113].

**Table 3.8.** Thermodynamic parameters (2nd heating scan) of PE-PHB blends compatibilized with EGMA. [a)]

| Sample | $T_{cc,\ PHB}$ (°C) | $T_{m\ PE}$ (°C) | $T_{m\ PHB}$ (°C) | $X_{c\ PE}$ (%) | $X_{c\ PHB}$ (%) |
|---|---|---|---|---|---|
| PE | — | 112 | — | 43 | — |
| PHB | 58 | — | 172 | — | 60 |
| EGMA | — | 115 | — | — | — |
| 90E10G | — | 116 | — | 46 | — |
| 90B10G | 60 | — | 172 | — | 61 |
| 75E25B | nd | 112 | 172 | 39 | 70 |
| 25E75B | 61 | 113 | 173 | 12 | 60 |
| 68E22B10G | nd | 112 | — | 43 | nd |
| 22E68B10G | 57 | 111 | 172 | 17 | 63 |
| 71E24B5G | nd | 112 | — | 40 | nd |
| 24E71B5G | 56 | 111 | 172 | 25 | 54 |

[a)] $T_{cc}$, and $T_m$ are cold crystallization and melting temperatures, respectively; $X_c$ is the degree of crystallinity; and, nd = not detected.

The glass transition temperature ($T_g$) was taken as the inflection point in the DSC traces. In the Figure 3.13 is shown the graphic of PHB $T_g$ taken from the second heating scan as a function of composition and type of compatibilizer. The tendencies of PHB $T_g$ were equivalent in both matrix. The $T_g$ of pristine PHB from the second heating scan was 6.5 °C. This value is in accordance with literature, which PHB $T_g$ values can be found from 1 to

7 °C depending of melt processing, molecular weight, thermal history in the DSC analysis *etc*. [107, 114, 115]. In the binary blend with PE as matrix (75E25B, Fig. 3.13 a)), the PHB $T_g$ value increased of *ca*. 1 °C. The same result was found for ternary blends compatibilized with EVA in both PE and PHB matrix. EVA $T_g$ value is *ca*. -20 °C. As vinyl acetate (VA) is compatible with PHB[98] it could be expected a decrease of at least 2 °C (estimated by Fox equation) on PHB $T_g$. On the other hand, the PHB $T_g$ could remain invariable if no compatibilization was performed by EVA. So, the hypothesis is that there is an additional effect that can be that of the more rigid phase of PE crystals. The blend systems compatibilized by EGMA and EMAC did not presented significant changes in the PHB $T_g$ regardless the matrix used.

**Table 3.9.** Thermodynamic parameters (2nd heating scan) of PE-PHB blends compatibilized with EMAC. [a)]

| Sample | $T_{cc,\ PHB}$ (°C) | $T_{m\ PE}$ (°C) | $T_{m\ PHB}$ (°C) | $X_{c\ PE}$ (%) | $X_{c\ PHB}$ (%) |
|---|---|---|---|---|---|
| PE | — | 112 | — | 43 | — |
| PHB | 58 | — | 172 | — | 60 |
| EMAC | -— | 90 | — | — | — |
| 60E40EM | — | 115 | — | 35 | — |
| 60B40EM | 61 | 89 | 173 | — | 57 |
| 75E25B | nd | 112 | 172 | 39 | 70 |
| 25E75B | 61 | 113 | 173 | 12 | 60 |
| 64E21B15EM | nd | 116 | nd | 45 | nd |
| 21E64B15EM | 63 | 115 | 175 | 17 | 57 |
| 68E22B10EM | nd | 116 | 172 | 45 | 4 |
| 22E68B10EM | 64 | 115 | 173 | 20 | 56 |
| 71E24B5EM | nd | 116 | 172 | 36 | 60 |
| 24E71B5EM | 61 | 115 | 173 | 15 | 59 |

[a)] $T_{cc}$, and $T_m$ are cold crystallization and melting temperatures, respectively; $X_c$ is the degree of crystallinity; and, nd = not detected.

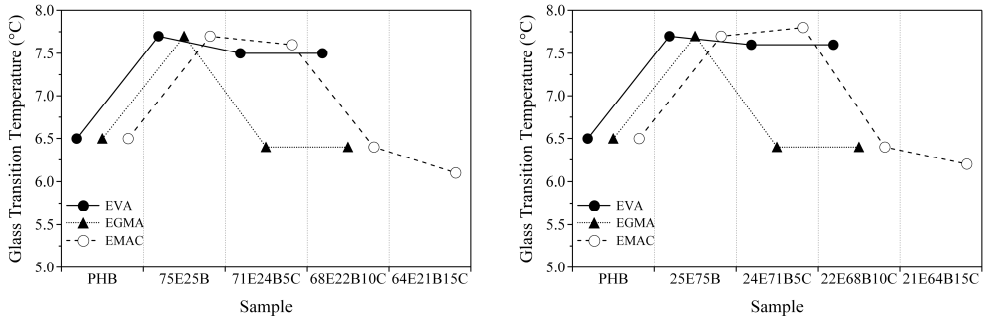


**Figure 3.13.** Glass transition temperature of PHB in PE-PHB blends compatibilized with EVA, EGMA and EMAC ($2^{nd}$ heating scan). a) PE matrix; and b) PHB matrix.

Data taken from the $3^{rd}$ DSC heating scan after a cooling at 10 °C·min$^{-1}$ for PE-PHB blends are shown in Tables 3.10-3.12. $T_g$ values of PHB after other two cycles of heating and cooling were lower than data obtained the $2^{nd}$ heating scan independently of blend composition and type of compatibilizer. In the $2^{nd}$ heating scan after a quenching the amount of amorphous phase is higher because PHB crystallization rate is lower than that of quenching. So, the lower values after a cooling rate of 10 °C·min$^{-1}$, when PHB material partially crystallize (Fig. 3.9 b) - $2^{nd}$ cooling), it could be expected a PHB $T_g$ values higher than that after quenching (Fig. 3.13). PHB $T_g$ values decreased of *ca.* 3°C and this result can be attributed to a decrease in the molecular weight of PHB by thermodegradation.

PHB cold crystallization temperatures were lower than that observed after quenching ($2^{nd}$ heating scan) for pristine PHB and blends compatibilized with EVA and EGMA. A contrary behaviour was observed for blends compatibilized with EMAC. Although in all cases the PHB $T_g$ values were lower (that can anticipate the temperature of cold crystallization) in the case of blends compatibilized with EMAC, it can be supposed that with cyclic thermal treatment performed in DSC favoured the phase separation and difficult in this way PHB crystallization. Besides, cold crystallization was not detected in the blends with PE as matrix.

**Table 3.10.** Thermodynamic parameters (3rd heating scan) of PE-PHB blends compatibilized with EVA.[a)]

| Sample | $T_{g\ PHB}$ (°C) | $T_{cc\ PHB}$ (°C) | $T_{m\ PE}$ (°C) | $T_{m\ PHB}$ (°C) | $X_{c\ PE}$ (%) | $X_{c\ PHB}$ (%) |
|---|---|---|---|---|---|---|
| PE | — | — | 113 | — | 44 | — |
| PHB | 4 | 52 | — | 164 | — | 61 |
| EVA | — | — | 70 | — | — | — |
| 90E10V | — | — | 116 | — | 46 | — |
| 90B10V | 5 | 63 | — | 164 | — | 58 |
| 75E25B | 5 | nd | 113 | 165 | 40 | 60 |
| 25E75B | 4 | 58 | 112 | 165 | 14 | 58 |
| 68E22B10V | 5 | nd | 112 | nd | 44 | nd |
| 22E68B10V | 1 | 60 | 112 | 164 | 20 | 58 |
| 71E24B5V | 5 | nd | 112 | nd | 42 | nd |
| 24E71B5V | 4 | 63 | 111 | 165 | 17 | 60 |

[a)] $T_g$, $T_{cc}$, and $T_m$ are glass transition, cold crystallization, and melting temperatures, respectively; $X_c$ is the degree of crystallinity and nd = not detected.

**Table 3.11.** Thermodynamic parameters (3rd heating scan) of PE-PHB blends compatibilized with EGMA.[a)]

| Sample | $T_{g\ PHB}$ (°C) | $T_{cc\ PHB}$ (°C) | $T_{m\ PE}$ (°C) | $T_{m\ PHB}$ (°C) | $X_{c\ PE}$ (%) | $X_{c\ PHB}$ (%) |
|---|---|---|---|---|---|---|
| PE | — | — | 112 | — | 44 | — |
| PHB | 4 | 52 | — | 164 | — | 61 |
| EGMA | — | — | 115 | — | — | — |
| 90E10G | — | — | 117 | — | 48 | — |
| 90B10G | 3 | 57 | 110 | 161 | — | 59 |
| 75E25B | 5 | nd | 113 | 165 | 40 | 60 |
| 25E75B | 4 | 58 | 112 | 165 | 14 | 58 |
| 68E22B10G | 4 | nd | 112 | nd | 48 | nd |
| 22E68B10G | 3 | 52 | 112 | 160 | 24 | 67 |
| 71E24B5G | 4 | nd | 113 | nd | 42 | nd |
| 24E71B5G | nd | 53 | 112 | 160 | 38 | 54 |

[a)] $T_g$, $T_{cc}$, and $T_m$ are glass transition, cold crystallization, and melting temperatures, respectively; $X_c$ is the degree of crystallinity and nd = not detected.

Melting temperatures of PE were practically invariable in relation to the values obtained in the 2nd heating scan. However, PHB $T_m$ values decreased of *ca*. 8°C. As in the others thermodynamic parameters the lowering of PHB $T_m$ values can be a consequence of its thermodegradation with the cyclic thermal treatments in DSC.

**Table 3.12.** Thermodynamic parameters (3rd heating scan) of PE-PHB blends compatibilized with EMAC.[a)]

| Sample | $T_{g\ PHB}$ (°C) | $T_{cc\ PHB}$ (°C) | $T_{m\ PE}$ (°C) | $T_{m\ PHB}$ (°C) | $X_{c\ PE}$ (%) | $X_{c\ PHB}$ (%) |
|---|---|---|---|---|---|---|
| PE | — | — | 113 | — | 44 | — |
| PHB | 4 | 52 | — | 164 | — | 61 |
| EMAC | — | — | 90 | — | — | — |
| 60E40EM | — | — | 115 | — | 38 | — |
| 60B40EM | 5 | 63 | 90 | 165 | — | 57 |
| 75E25B | 5 | nd | 113 | 165 | 40 | 60 |
| 25E75B | 4 | 58 | 112 | 165 | 14 | 58 |
| 64E21B15EM | 6 | nd | 116 | nd | 46 | nd |
| 21E64B15EM | 5 | 65 | 115 | 166 | 21 | 55 |
| 68E22B10EM | 5 | nd | 116 | 161 | 48 | 2 |
| 22E68B10EM | 4 | 65 | 116 | 165 | 24 | 54 |
| 71E24B5EM | 5 | nd | 116 | 164 | 40 | 3 |
| 24E71B5EM | 4 | 63 | 116 | 166 | 16 | 58 |

[a)] $T_g$, $T_{cc}$, and $T_m$ are glass transition, cold crystallization, and melting temperatures, respectively; $X_c$ is the degree of crystallinity and nd = not detected.

PHB crystalline content in ternary blends measured in the 2nd (Tab 3.7 – 3.9) and 3rd (Tab 3.10 – 3.12) heating scans presented lower values than that calculated in the 1st heating. PHB $X_c$ values were in the range of 54-70 % for blends containing EGMA and EVA and 4-60 % for blends containing EMAC The crystalline content of pristine PE measured in the 1st heating was 43 %. PE-compatibilizer binary blends presented equivalent PE $X_c$ values. On the other hand, ternary blends showed higher PE $X_c$ values than pristine PE, which values moved up to 60 % for 22E68B10V and 22E68B10G blends and 69 % for 22E68B10EM blend.

### *3.1.2.3 Dynamic mechanical thermal analysis*

DMTA measures the response of a material to sinusoidal stress over a range of temperature and frequencies, and it is sensitive to chemical and physical structures of polymers and their composites. The main variables obtained from DMTA are the storage modulus (*E'*), which represents the elastic component, the loss modulus (*E''*) representing the viscous component, and Tan δ (the damping factor), given as the ratio of E''/E'. The loss factor (Tan δ) gives the fractional energy lost in a system due to deformation. It is often proportional to the imperfections in the elasticity of a polymer. Tan δ is a sensitive indicator of all types of molecular motions and phase transitions[116].

Figure 3.14 shows the *E'* and *tan δ* versus T at 1 Hz for pristine PE and PHB. In general, low-density polyethylene (LDPE) shows relaxations nominated α, β and γ in decreasing order of temperature[117]. The α-transition is an amorphous phase process[112] and results from a complex multi-relaxation process, which is mainly concerned with the molecular motion of the crystalline region of LDPE[118, 119]. Generally, α-transition is attributed to the vibrational or reorientational motion within the crystals. In addition, α-transition temperature depends on the side-branch content, crystallization method and some possible mechanisms of re-crystallization[120-122]. The β-transition has been extensively studied. Many discussions and ambiguous explanations about its origin have been published[120, 122-125]. This relaxation originates in the amorphous phase and some authors attribute this relaxation in PE to the glass transition[112]. Finally, the γ relaxation is also related to local-mode, non-cooperative relaxation process in the amorphous phase. According to literature, α-transition occurs as result of the motions of chain units within the crystal, and the molecular mechanism involved is the same observed in γ-relaxation. The difference would be that in γ-relaxation this mechanism could be the result of the relaxation of chain units in the amorphous region[119-121]. For some authors, γ-transition is associated with the glass transition of the amorphous regions, so in this cases the $T_g$ of PE would be around -112 °C[120, 121].

The *tan* $\delta$ temperatures of α, β and γ relaxation for PE are 82 °C, -8 °C and -112 °C, respectively (Fig. 3.14 a)). A shoulder at *ca*. 50 °C is defined as α' relaxation. Equivalent values for α, β and γ transitions on PE were found by Chen *et al.*[126]. Another important point to take into account is the observable variation in α-transition according to the degree of crystallinity. In general, linear polyethylene with high degree of crystallinity shows strong α-relaxation. In fact, from DSC results PE sample showed a degree of crystallinity of *ca.* 43 %.

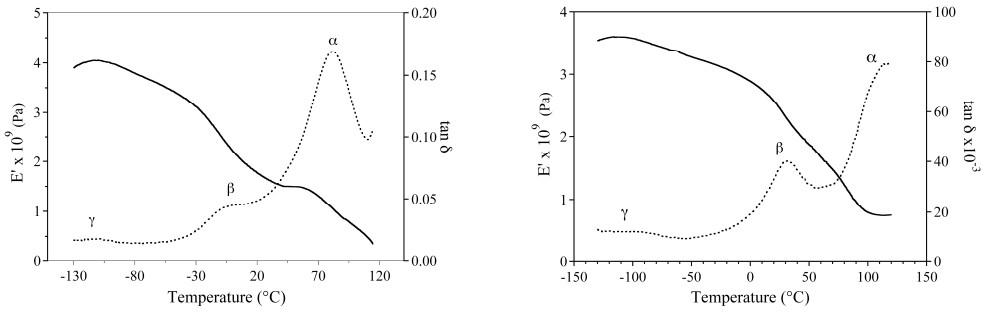


a) b)

**Figure 3.14.** DMTA tensile storage modulus and *tan* $\delta$ at 1 Hz for pristine PE (a) and (b) PHB.

PHB relaxations α and β were found at 118 °C and 32 °C, respectively (Fig. 3.14 b)). Cimmino *et al.*[119] reported the values of *ca*. 100°C and 25 °C for these relaxations, respectively. Besides, they registered a γ relaxation for PHB, which appeared in the range of -80 to -100 °C and was attributed to the presence of moisture in the sample. Apparently, this relaxation exists in the same range of temperature but it is not well defined as a peak in the present study.

Tables 3.13 – 3.15 show DMTA data for PE-PHB based blends compatibilized with EVA, EGMA and EMAC, respectively. As shown in Table 3.13, the tensile modulus at -110 °C ($E_{-110}$) of PE and PHB are 4 GPa and 3.6 GPa, respectively. The value of $E_{-110}$ of binary blends prepared with PE and PHB was equivalent to that of PE, independently of which of them was the matrix (75E25B or 25E75B). Although the $E_{-110}$ value of PE is slightly higher than that of PHB, when was blended with the compatibilizer

this property presented values lower than that of equivalent blends with PHB as matrix. It was observed in the morphological study (Fig. 3.2-3.4) that the binary blends of PE with compatibilizers were more homogeneous than that with PHB. So, this result can be an indication of the better compatibilization for systems with PE as matrix. This behaviour was also verified for the ternary blends compatibilized with EVA and EGMA. In the case of ternary blends, the lower values found of $E_{-110}$ were 2.8 GPa, 2.7 GPa and 2.2 GPa for 68E22B10V, 68E22B10G and 64E21B15EM, respectively. Up to now the worst compatibilizer was EMAC. However, the result of $E_{-110}$ found for 64E21B15EM, suggest that a higher amount of EMAC in the ternary blend or of MA in the copolymer can compatibilize better the system PE-PHB.

**Table 3.13.** DMTA data of PE-PHB blends compatibilized with EVA.[a)]

| Sample [b)] | $E_{-110}$ (GPa) | $E_{25}$ (GPa) | $T_1$ (°C) | tan δ (°C) | | | |
|---|---|---|---|---|---|---|---|
| | | | | $T_\alpha$ | $T_{\alpha'}$ | $T_\beta$ | $T_\gamma$ |
| PE | 4.0 | 1.69 | -112 | 82 | 50 | -8 | -112 |
| PHB | 3.6 | 2.45 | -104 | 118 | — | 32 | — |
| EVA | 7.6 | 0.42 | -48 | — | — | -7 | — |
| 75E25B | 4.2 | 1.91 | -107 | 82 | 50 | -4 | -115 |
| 25E75B | 4.0 | 1.96 | -103 | 80 | 46 | -4 | -115 |
| 90E10V | 3.2 | 2.21 | -97 | 88 | 58 | 2 | -111 |
| 90B10V | 3.8 | 1.99 | -98 | 71 | 31 | -13 | — |
| 68E22B10V | 2.8 | 0.25 | -98 | 88 | 86 | 0 | -115 |
| 22E68B10V | 3.6 | 1.59 | -99 | 63 | 39 | -8 | -110 |
| 71E24B5V | 3.4 | 1.95 | -98 | 84 | 60 | -5 | -110 |
| 24E71B5V | 3.9 | 1.79 | -99 | 49 | 34 | -6 | -110 |

[a)] $E_{-110}$ and $E_{25}$ are the modulus at -110 °C and at 25 °C, respectively; $T_1$ is the temperature where modulus starts to decrease; $T_\alpha$, $T_{\alpha'}$, $T_\beta$ and $T_\gamma$ are the temperatures at the α, α', β and γ relaxation, respectively. [b)] See Table 2.2 for code definition.

At 25 °C the storage modulus of PE and PHB are 58% and 32% lower than at –110 °C. The behaviour of the blends depends of composition and type of compatibilizer. The higher values for ternary blends 24E71B5V, 24E71B5G and 71E24B5EM were 1.79 GPa, 1.70 GPa, and 1.75 GPa, respectively. The first two were found for the system with PHB as matrix and

the last one for that with PE as matrix. In all cases, the amount of everyone compatibilizer was 5 wt-%. These values are 27% and 31% lower than that of PHB and 3% higher than PE, respectively.

$T_1$ corresponds to the temperature where modulus starts to decrease. From Table 3.13 it was observed that 75E25B and 25E75B presented $T_1$ values between that of each single component (PE and PHB). Besides, the values for binary blends 90E10V, 90B10V and ternary blends are higher than that of pristine polymers PE and PHB (*ca.* 14 °C), which is probably caused by the addition of 10 % of EVA that have a $T_1$ higher than that of the other polymers used (-48 °C). The γ-transition temperatures (related to the PE $T_g$) of all samples was observed with low intensity at around -115 °C, which is in agreement with values found in literature[127]. PE $T_g$ of all samples was equivalent to that of pristine PE.

**Table 3.14.** DMTA data of PE-PHB blends compatibilized with EGMA.[a)]

| Sample [b)] | $E_{-110}$ (GPa) | $E_{25}$ (GPa) | $T_1$ (°C) | tan δ (°C) | | | |
|---|---|---|---|---|---|---|---|
| | | | | $T_\alpha$ | $T_{\alpha'}$ | $T_\beta$ | $T_\gamma$ |
| PE | 4.0 | 1.69 | -112 | 82 | 50 | -8 | -112 |
| PHB | 3.6 | 2.45 | -104 | 118 | — | 32 | — |
| EGMA | 2.4 | 1.12 | -106 | 73 | 57 | -1 | -110 |
| 75E25B | 4.2 | 1.91 | -107 | 82 | 50 | -4 | -115 |
| 25E75B | 4.0 | 1.96 | -103 | 80 | 46 | -4 | -115 |
| 90E10G | 2.4 | 0.22 | -108 | 67 | 46 | -9 | -115 |
| 90B10G | 3.3 | 1.87 | -105 | 125 | — | 30 | -103 |
| 68E22B10G | 2.7 | 0.39 | -111 | 85 | 56 | 0 | -100 |
| 22E68B10G | 3.1 | 1.19 | -108 | 103 | 43 | -5 | -101 |
| 71E24B5G | 3.0 | 0.65 | -107 | 85 | 52 | -4 | -105 |
| 24E71B5G | 3.7 | 1.70 | -105 | 122/68 | 29 | -1 | -106 |

[a)] $E_{-110}$ and $E_{25}$ are the modulus at -110 °C and at 25 °C, respectively; $T_1$ is the temperature where modulus starts to decrease; $T_\alpha$, $T_{\alpha'}$, $T_\beta$ and $T_\gamma$ are the temperatures at the α, α', β and γ relaxation, respectively. [b)] See Table 2.2 for code definition.

Table 3.14 shows data relative to PE-EGMA-PHB family of materials. As it was observed, binary and ternary blends containing EGMA showed lower values of modulus at –110 °C than pristine PE and PHB. For modulus

at 25 °C, the highest decreases were observed for the system with PE as matrix and EGMA. T1 of all blends remained between that of pristine components PE and PHB. It can be clearly seen that α and β transitions remained at temperatures between that of PE and PHB showing that some compatibility probably occurred, confirming in this way the results obtained from SEM analysis (Fig. 3.2 – 3.4).

**Table 3.15.** DMTA data of PE-PHB blends compatibilized with EMAC.[a)]

| Sample [b)] | $E_{-110}$ (GPa) | $E_{25}$ (GPa) | $T_1$ (°C) | tan δ (°C) | | | |
|---|---|---|---|---|---|---|---|
| | | | | $T_\alpha$ | $T_{\alpha'}$ | $T_\beta$ | $T_\gamma$ |
| PE | 4.0 | 1.69 | -112 | 82 | 50 | -8 | -112 |
| PHB | 3.6 | 2.45 | -104 | 118 | — | 32 | — |
| EMAC | 3.3 | 1.61 | -104 | 23 | — | -9 | -105 |
| 75E25B | 4.2 | 1.91 | -107 | 82 | 50 | -4 | -115 |
| 25E75B | 4.0 | 1.96 | -103 | 80 | 46 | -4 | -115 |
| 60E40EM | 2.5 | 1.24 | -107 | 91 | 51 | -5 | -105 |
| 60B40EM | 3.2 | 0.68 | -109 | 27 | — | -15 | -110 |
| 64E21B15EM | 2.2 | 0.26 | -108 | 98 | 59 | -10 | -112 |
| 21E64B15EM | 3.1 | 1.56 | -107 | — | 34 | -13 | -106 |
| 68E22B10EM | 3.8 | 1.50 | -109 | 94 | 44 | -8 | -112 |
| 22E68B10EM | 3.0 | 1.45 | -108 | nd | 31 | -13 | -105 |
| 71E24B5EM | 4.1 | 1.75 | -105 | 66 | 29 | -11 | -112 |
| 24E71B5EM | 3.2 | 1.04 | -112 | 70 | 30 | -13 | -105 |

[a)] $E_{-110}$ and $E_{25}$ are the modulus at -110 °C and at 25 °C, respectively; $T_1$ is the temperature where modulus starts to decrease; $T_\alpha$, $T_{\alpha'}$, $T_\beta$ and $T_\gamma$ are the temperatures at the α, α', β and γ relaxation, respectively. [b)] See Table 2.2 for code definition.

Table 3.15 are reported DMTA data of PE-EMAC-PHB materials. As it was observed, the modulus at glass of PE-EMAC sample was more affected than that PHB-EMAC in relation to pure components PE and PHB, respectively. In fact, considering ternary blends, when PE was the matrix, an increase from 5 wt-% to 10 wt-% and 15 wt-% in EMAC amount decrease the modulus from 4.1 GPa to 3.8 GPa and 2.2 GPa, respectively. When PHB was the matrix no significant changes were observed with an increase in the EMAC content. Moreover, in this family of materials higher values of

modulus at glass ($E_{-110}$) were obtained for ternary blends than for PE-EGMA-PHB blends. The lowest values of modulus at 25 °C were obtained for 60B40EM and 64E21B15EM blends. The $T_1$ of binary and ternary blends remained between that of PE and PHB. Temperatures of γ-transition of binary and ternary blends containing EMAC remained between that of PE and PHB.

### 3.1.3. *Crystallinity of PE-PHB based blends by x-ray diffraction*

Wide-angle X-ray (WAXS) diffraction patterns were performed on PE-PHB blends. Figures 3.15 – 3.16 show the WAXS diffraction patterns of pristine samples, binary and ternary blends.

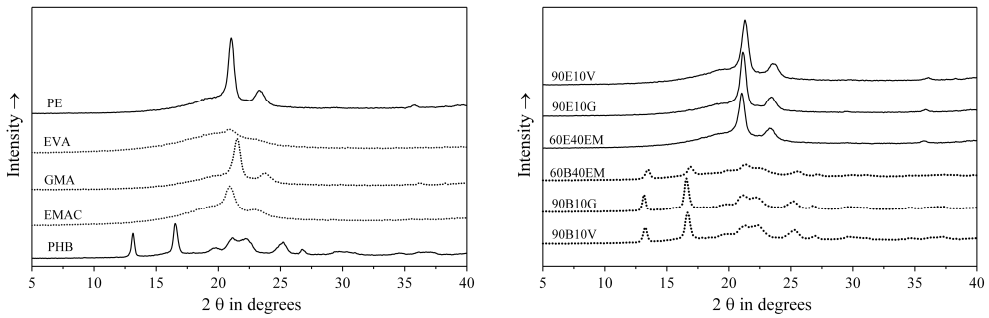


a) b)

**Figure 3.15.** WAXS diffraction patterns of pristine blend components a) and their binary formulations b).

As it can be observed in Figure 3.15 a), the pattern of PHB exhibit the characteristic peaks of a semi-crystalline material. Moreover, it is clearly seen that the positions and intensities of the diffraction peaks remained unchanged when PHB was blended with EVA and EGMA (Fig. 3.15 b)), which means that the addition of EVA and EGMA do not result in any change of crystalline structure of PHB. The same behaviour was found by An *et al.*[128] studying the crystallization behaviour of PHB/PVAc blends in all range of compositions. However, when PHB was blended with EMAC the intensities of the diffraction peaks decreased and a small shift in the peak positions was observed. The diffraction patterns of binary 25E75B, 75E25B

and ternary blends are shown in Figure 3.16. The patterns of all blends are intermediate to that of pristine PE and PHB.

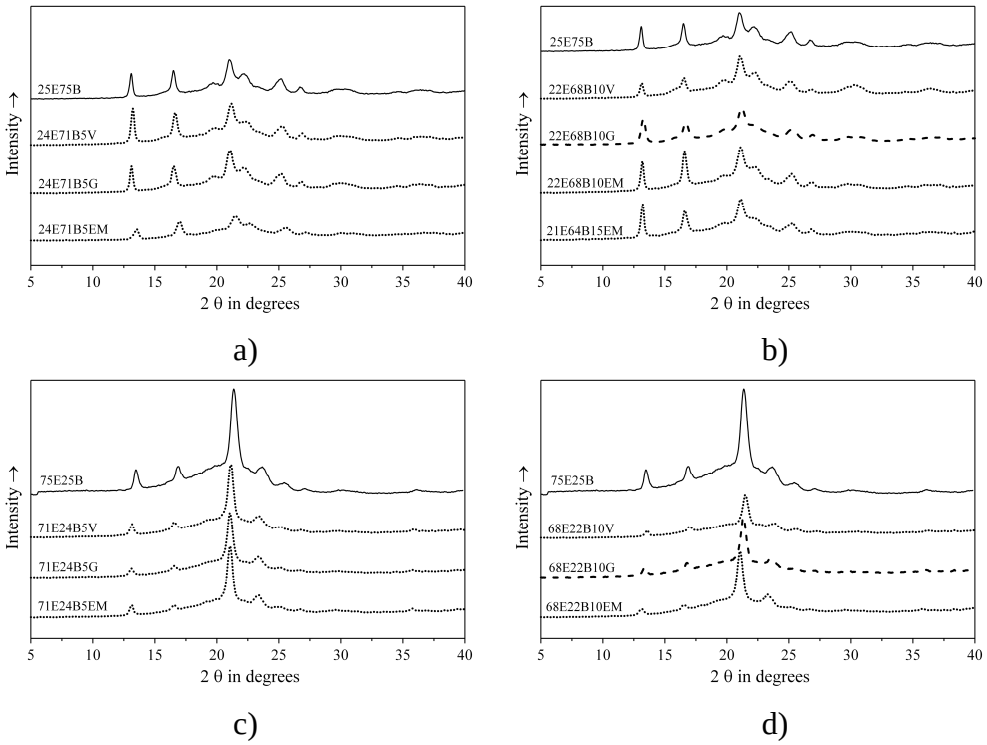


**Figure 3.16.** WAXS diffraction patterns of binary and ternary blends.

### 3.1.4. *Infrared spectroscopy (FTIR)*

FTIR measurements were carried out on PE-PHB films. The spectra of pure PE and PHB are shown in Figure 3.17 and the characteristic absorption bands are listed in Table 3.16. Figure 3.18 shows the FTIR spectra of binary and ternary blends. The profiles of spectra show that the absorptions of all blend components overlap which is a challenging in their interpretation. Apparently, there is no shift in the absorptions related to PHB in the PE-PHB films.

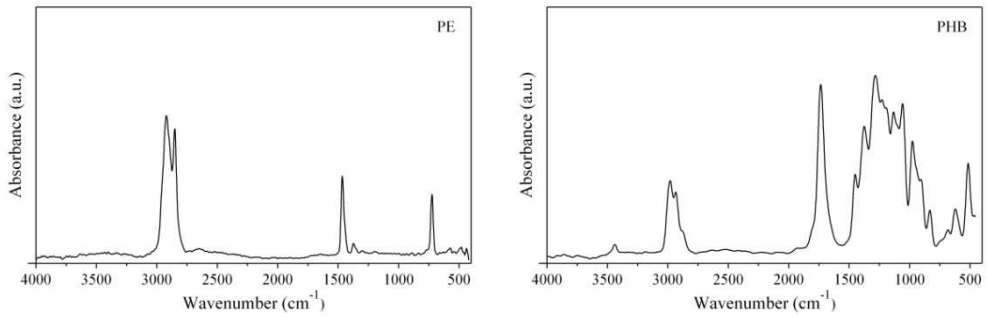


a) b)

**Figure 3.17.** FTIR spectra of (a) PE and (b) PHB.

**Table 3.16.** Assignments of FT-IR absorptions peaks for PE and PHB.

| PE | | PHB | |
|---|---|---|---|
| $cm^{-1}$ | Assignment | $cm^{-1}$ | Assignment |
| | | 825 | $CH_3$ rocking |
| 720 | Skeletal vibration $CH_2$ | 896 | $CH_3$ rocking |
| 1465 | $CH_3$ bending $CH_2$ rocking | 929 | $CH_3$ rocking |
| 2850 | C-H stretching | 979 | C-C stretching |
| 2930 | C-H stretching | 1057 | C-O symmetric stretching |
| | | 1100 | OH stretching |
| | | 1132 | C-O-C symmetric stretching |
| | | 1184 | C-O-C asymmetric stretching |
| | | 1228 | Conformational band of the helical chains |
| | | 1278 | $CH_2$ wagging |
| | | 1289 | $CH_2$ wagging |
| | | 1379 | $CH_3$ symmetric wagging |
| | | 1453 | $CH_3$ asymmetric |
| | | 1724 | C=O stretching |
| | | 2875 | $CH_3$ (C-H symmetric stretching) |
| | | 2934 | $CH_2$ (C-H asymmetric stretching) |
| | | 2976 | $CH_3$ (C-H asymmetric stretching) |
| | | 3437 | OH stretching (H bridges) |

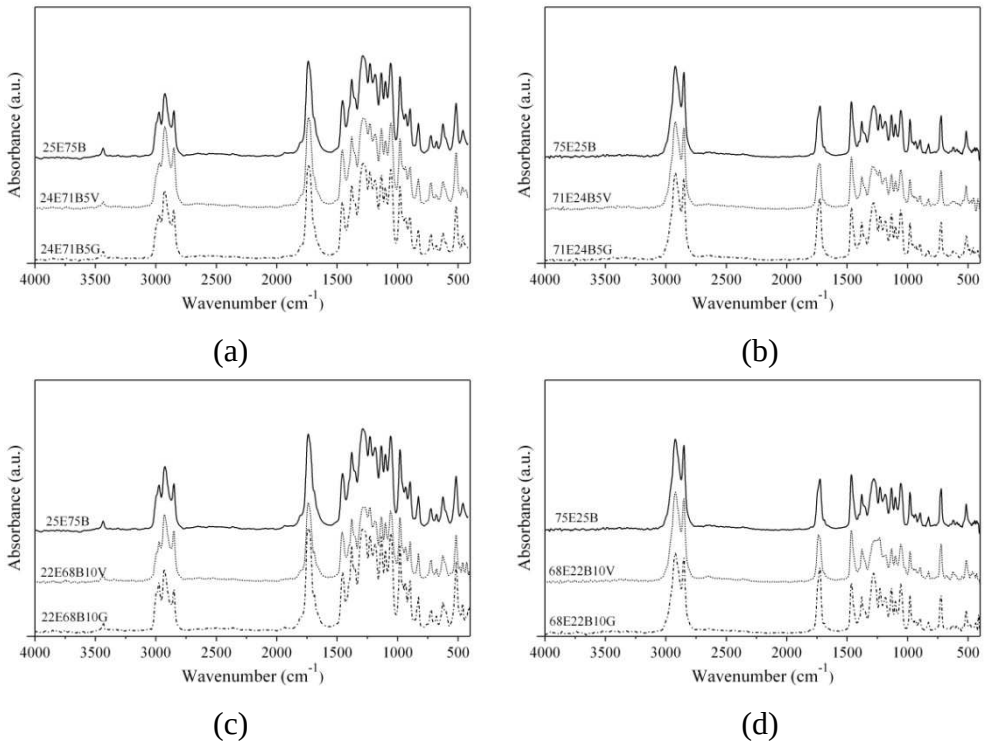


**Figure 3.18.** FTIR spectra of binary and ternary PE-PHB based blends.

### 3.1.5. *Mechanical properties*

The tensile curves obtained for the three families of PE-PHB blends were characteristic of brittle materials, with high values of Young modulus (YM) and low strain at break (SB) values. Even though brittle behaviour was seen for all the samples, some important differences with the composition were observed. In Tables 3.17 – 3.19 are presented the results of tensile tests performed on PE-PHB based blends. YM was taken as the tangent at 0.3 MPa of stress in the stress-strain traces.

As a general trend, the three families of materials showed the same behaviour. It was observed that YM depends of both the matrix used (PE or PHB) and the amount of compatibilizer in the blend. As reported by Zainuddin *et al* [129] the continuous phase in a polymeric blend improve the mechanical properties of the blend. Therefore, blends with PE as matrix showed YM near to that of pristine PE (190 MPa) and blends with PHB as matrix showed YM near to that of pristine PHB (2060 MPa) (Tab. 3.17). In

blends with PE as matrix, the addition of 5 wt-% and 10 wt-% of EVA caused a decreasing in the YM from 260 MPa (75E25B) to 210 MPa (19 % lower) and 160 MPa (38 % lower), respectively. In addition, the decrease in the YM of samples with PHB as matrix was of 21 % (5 wt-% EVA) and 28 % (10 wt-% EVA). ST of samples was very low, with values near to that of pristine PHB. Moreover, blends with PHB as matrix presented very low elasticity, with SB values of 1-2 % and high error values.

**Table 3.17.** Mechanical properties of PE-EVA-PHB blends. [a)]

| Trial | Code | YM (MPa) | ST (MPa) | SB (%) |
|---|---|---|---|---|
| a | PE | 190 ± 5 | — | > 100 |
| b | PHB | 2060 ± 3 | 18 ± 11 | 2 ± 18 |
| c | 90E10V | 140 ± 6 | — | > 100 |
| d | 90B10V | 1640 ± 4 | 21 ± 3 | 7 ± 34 |
| e | 75E25B | 260 ± 3 | 6 ± 6 | 11 ± 18 |
| f | 25E75B | 1300 ± 5 | 15 ± 3 | 2 ± 7 |
| g | 68E22B10V | 160 ± 6 | 5 ± 10 | 25 ± 34 |
| h | 22E68B10V | 930 ± 3 | 8 ± 5 | 2 ± 10 |
| i | 71E24B5V | 210 ± 5 | 6 ± 3 | 53 ± 9 |
| j | 24E71B5V | 1030 ± 3 | 8 ± 5 | 2 ± 14 |

[a)] YM is the Young modulus; ST and SB are the stress and strain at break. Errors were calculated at 95 % of confidence of Student's *t*-test.

YM of PE-PHB-EGMA and PE-PHB-EMAC materials presented the same behaviour. This means, YM values near to that of PE for blends with PE as matrix and near to that of PHB with PHB as matrix. Comparing the three families of PE-PHB blends, samples obtained with EGMA showed the higher values of YM in relation to the equivalent blends formulations compatibilized with EVA or EMAC. Exception was for the 24E71B5EM blend, which presented higher YM values than that of 24E71B5V and 24E71B5G. In addition the errors at 95 % of confidence of Student's *t*-test in the ST and SB of samples were more significant than the errors in the YM values. This was expected as ST and SB are failure properties, so any

imperfection presented by the sample can cause an early broke of the specimen during the test.

**Table 3.18.** Mechanical properties of PE-EGMA-PHB blends. [a)]

| Trial | Code | YM (MPa) | ST (MPa) | SB (%) |
|---|---|---|---|---|
| a | PE | 190 ± 5 | — | > 100 |
| b | PHB | 2060 ± 3 | 18 ± 11 | 2 ± 18 |
| c | 90E10G | 180 ± 4 | — | > 100 |
| d | 90B10G | 1690 ± 5 | 19 ± 5 | 2 ± 6 |
| e | 75E25B | 260 ± 3 | 6 ± 6 | 11 ± 18 |
| f | 25E75B | 1300 ± 5 | 15 ± 3 | 2 ± 7 |
| g | 68E22B10G | 260 ± 2 | 7 ± 3 | 27 ± 11 |
| h | 22E68B10G | 1160 ± 4 | 13 ± 11 | 1 ± 9 |
| i | 71E24B5G | 300 ± 3 | 7 ± 2 | 21 ± 14 |
| j | 24E71B5G | 990 ± 4 | 5 ± 40 | 1 ± 31 |

[a)] YM is the Young modulus; ST and SB are the stress and strain at break. Errors were calculated at 95 % of confidence of Student's *t*-test.

**Table 3.19.** Mechanical properties of PE-EMAC-PHB blends. [a)]

| Trial | Code | YM (MPa) | ST (MPa) | SB (%) |
|---|---|---|---|---|
| a | PE | 190 ± 5 | — | > 100 |
| b | PHB | 2060 ± 3 | 18 ± 11 | 2 ± 18 |
| c | 60E40EM | 90 ± 8 | — | > 100 |
| d | 60B40EM | 850 ± 4 | 8 ± 11 | 3 ± 15 |
| e | 75E25B | 260 ± 3 | 6 ± 6 | 11 ± 18 |
| f | 25E75B | 1300 ± 5 | 15 ± 3 | 2 ± 7 |
| g | 64E21B15EM | 150 ± 5 | — | > 100 |
| h | 21E64B15EM | 1050 ± 1 | 10 ± 4 | 3 ± 11 |
| i | 68E22B10EM | 190 ± 5 | 7 ± 3 | 53 ± 21 |
| j | 22E68B10EM | 1110 ± 2 | 10 ± 6 | 3 ± 12 |
| l | 71E24B5EM | 200 ± 6 | 7 ± 2 | 42 ± 18 |
| m | 24E71B5EM | 1230 ± 3 | 12 ± 3 | 2 ±17 |

[a)] YM is the Young modulus; ST and SB are the stress and strain at break. Errors were calculated at 95 % of confidence of Student's *t*-test.

## 3.2. PE-PHB-EGMA blends additivated with prodegradants

For sustainable development, all life segments that employ plastic materials as for example, agricultural, sanitary and packaging, have to take into account the time of its disintegration in the ambient.[130] PE is a well-established plastic in packaging due to its good property profile. In special, for food packaging it represents an ideal compromise between price and mechanical properties compared with other polymers. However, its slow degradability with consequent environmental concerns, represents an important drawbacks[131]. Several solutions have been applied to improve PE disintegration. For example, PE has been mixed with natural polymers such as starch and protein hydrolysate, and synthetic biodegradable or hydrolysable polymers.

LLDPE blended with protein hydrolysate (HP) from leather waste showed that mechanical properties of the blends decreased with HP addition. A blend composition containing 20% of HP showed a balanced mechanical and biodegradation properties.[132] Immiscible blends prepared with biodegradable aliphatic polyester (BDP) and linear low density polyethylene (LLDPE) were proposed as a way to broaden the range of applicability of BDP with lower cost material.[97] Their rheological properties lie between both of the components following the additive rule.

LLDPE was blended with decanol esterified styrene maleic anhydride copolymer (SMA) to improve its degradability. Although SMA is hydrophobic, anhydride group in presence of alkaline medium, like that found in some soils, hydrolyses. So, turn the LLDPE blends into a hygroscopic material. Increasing SMA amount from 0 to 40 % in the blend decreases elongation at break of LLDPE from ca. 900 % to 500 % respectively. However, elastic modulus showed an increasing of about 72 % with the addition of 40 % of SMA.[133]

Alternatively, PE disintegration has been activated by addition of prodegradants. Bonhomme *et al.*[134] investigated green polyethylene films from EPI group. Both abiotic oxidation and biodegradation showed that the abiotic peroxidation process is the determining step and that colonization of

microorganisms occurred on all samples, respectively. Chiellini *et al.*[135] reported that about 60 % of PE mineralization can be found in compost biodegradation, after thermal degradation, over a period of 18 months for samples containing TDPA® prodegradants.

PE-PHB based blends containing prodegradants were not found in the academic and technical literature. The second part of the present thesis was the formulation of PE based blends containing PHB and prodegradants. The compatibilizer EGMA was selected from the previous study and used in a fixed amount of 10 wt-% in relation to PE matrix PE:EGMA (9:1). This blend was nominated PEL. Section 2.4.2 describes in detail the experimental design and the formulations containing PE, PHB and prodegradants. PE-PHB thin films were obtained by blow extrusion. These films were first of all completely characterized in relation to morphology, thermal and mechanical properties and subsequently submitted to a thermal aging and biodegradation experiments.

### 3.2.1. *Characterization*

#### *3.2.1.1 Morphology*

Phase morphologies of PE-PHB based blends after cryogenic fracture and gold metallization were observed in a scanning electron microscope (SEM). The micrographs of fractured surfaces are shown in Figures 3.19 – 3.23. Apparently, all PE-PHB based blends do not present phase separation at the level of magnification applied. Their surfaces present ductile fracture typical of the PE. The amount of the dispersed phase of PHB is very small (2 wt-%) because it was calculated to be proportional to the amount of GMA present in the copolymer EGMA. So, probably the proportion was sufficient to give the expected compatibilization between PE and PHB. The dispersion of the pro-degradant additive was facilitated giving homogeneous fractured surface because the matrix of the masterbatch is PE.

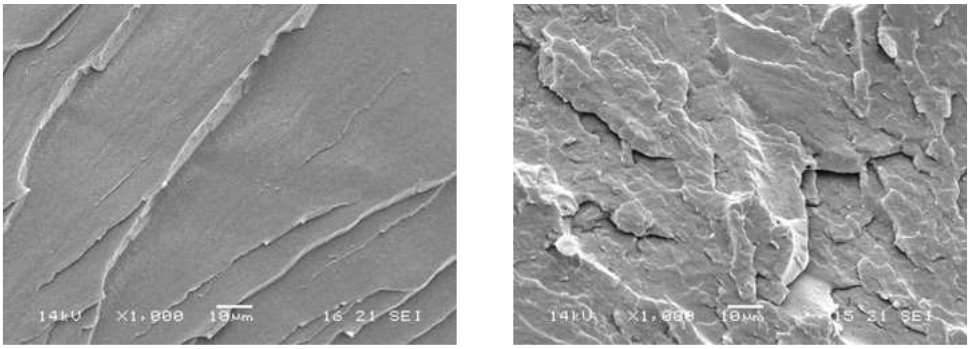

a) b)

**Figure 3.19.** SEM of cryogenic fracture of a) PEL and b) 2B at 1000X. See Table 2.6 for sample code nomenclature.

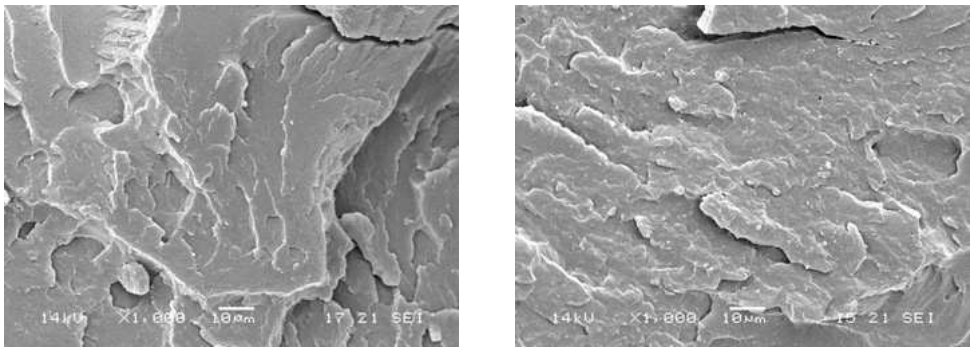

a) b)

**Figure 3.20.** SEM of cryogenic fracture of a) 2B3T63T7 and b) BT6T7 at 1000X.

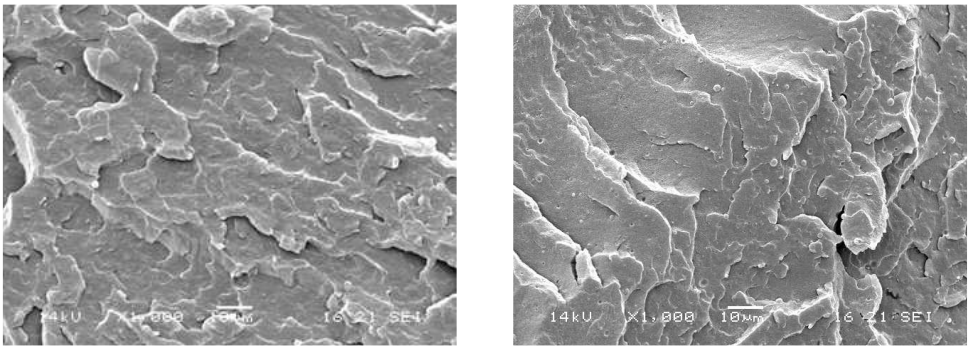

a) b)

**Figure 3.21.** SEM of cryogenic fracture of a) 3T6 and b) 2B3T6 at 1000X.

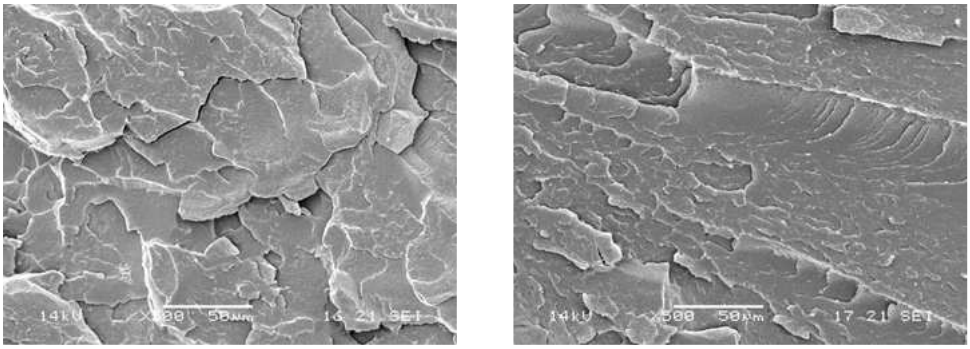

a) b)

**Figure 3.22.** SEM of cryogenic fracture a) 3T7 at 500X; b) 2B3T7 at 1000X.

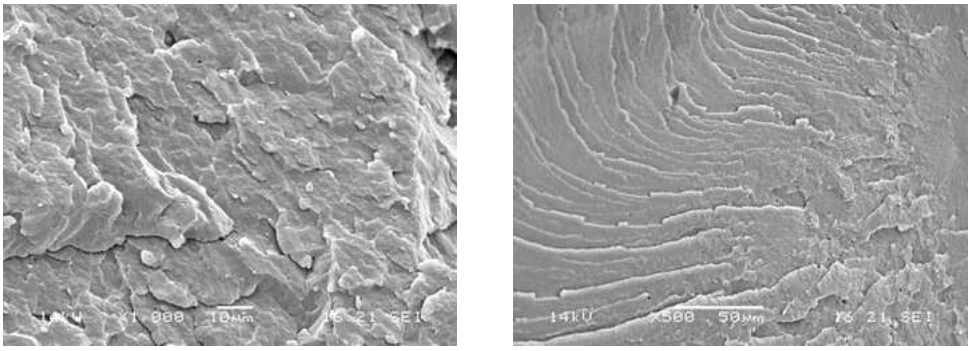

a) b)

**Figure 3.23.** SEM of cryogenic fracture of a) 3T63T7 at 100X; b) 3T63T7 at 500X.

### *3.2.1.2 Melt flow index (MFI)*

MFI is largely used for the characterization of various polymers. It can be also a good tool for the monitoring of the melt stability of polyolefins in multiple extrusion experiments[76, 78, 136]. Table 3.20 record the MFI of PE-PHB blends. PE based blends presented MFI lower than 1.36 g·10 $min^{-1}$ found on formulation containing the higher amount of the three components (2B3T63T7). Anyway, this value is appropriated for blow moulding, generally applied on packaging manufacture. The highest MFI values were measured for PHB and EGMA. Consequently, all samples presented MFI

higher than that of pristine PE (0.80 g·10 $min^{-1}$). For instance, the MFI of PEL was 45 % higher than that of PE. This increase was due to the 10 wt-% of EGMA presented in PEL, which has a MFI of 5 g·10 $min^{-1}$. In general, the blends presented a MFI ranging from 0.95 g·10 $min^{-1}$ (2B) to 1.36 g·10 $min^{-1}$ (2B3T63T7).

**Table 3.20.** MFI of PE-PHB based blends as a function of composition.

| Sample | MFI (g·10 $min^{-1}$) | Error | Sample | MFI (g·10 $min^{-1}$) | Error |
|---|---|---|---|---|---|
| PHB | 7.40 | 0.97 | 3T7 | 1.18 | 0.03 |
| PE | 0.80 | — | 2B3T7 | 0.99 | 0.01 |
| EGMA | 5.00 | — | 3T63T7 | 1.20 | 0.01 |
| PEL | 1.16 | 0.00 | 2B3T63T7 | 1.36 | 0.04 |
| 2B | 0.95 | 0.01 | BT6T7 | 1.00 | 0.01 |
| 3T6 | 1.15 | 0.02 | BT6T7 | 0.97 | 0.01 |
| 2B3T6 | 1.29 | 0.01 | BT6T7 | 1.08 | 0.02 |

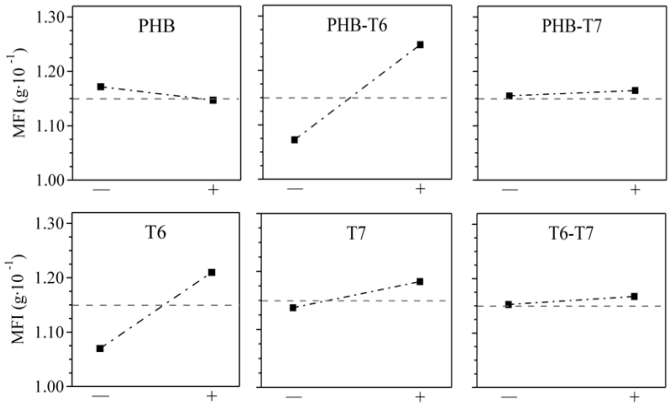


**Figure 3.24.** DEX interaction plot of the factors PHB, T6 and T7 on MFI of PE based blends.

Figure 3.24 represents the design plots, which is appropriate for analyzing data from a designed experiment (DEX), with respect to important factors. So, the effects of each factor (variable) and of its interaction are plotted versus level. The DEX interaction plot is a complement to the traditional analysis of variance (ANOVA) of designed experiments. From the

analysis of effects it is easy to note that component T6 cause the mainly effect increasing the MFI of the blends, the same occurs when PHB-T6 were used together. However, PHB alone do not cause an increasing in the MFI of blends and this is the evidence that the increasing in MFI is just an effect caused by T6 additive. The other variables do not produce a significant change on MFI.

#### *3.2.1.3 Mechanical properties*

It is known from literature that orientation of films during blow processing will affect their mechanical properties[137]. PE-PHB thin films (about 50-80μm) obtained by blow extrusion were submitted to tensile tests in the parallel and transverse to the blow direction. Table 3.21 lists the Young modulus (YM), the tensile stress at break (ST) and the strain at break (SB) of samples measured at parallel and transverse to the blow mounding direction. The respective error was evaluated at 95 % of confidence of Student's *t*-test. In general, the YM was calculated as the tangent at 1 % of strain in the stress x strain curves. YM in the parallel direction ($YM_P$) for samples containing PHB presented higher values than that of corresponding blend without it. PHB component alone have an YM of about 2060 MPa (calculated as the tangent at 0.3 MPa stress). So, PHB increases the $YM_P$ of blends even at low amounts (2 wt-%). However, opposing behaviour for YM in the transverse direction to the blow ($YM_T$) was observed. This means that basically all samples presented $YM_T$ values higher than that of $YM_P$. Exception was verified for the $YM_T$ values of blends containing PHB, which were equal or lower than that of the corresponding formulation without PHB. For example, 2B3T6 blend $YM_T$ was 11 % lower than that of 3T6 sample and 2B3T7 blend $YM_T$ was 16 % lower than that of 3T7 sample. The highest YM values of blends in the transversal direction of blow can be due to a physical "crosslinking" promoted by the oriented PE crystal. So, in the case of samples containing PHB, this physical crosslinking would be reduced and consequently the chain orientation effect in the $YM_T$.

**Table 3.21.** Mechanical Properties of PE-PHB based blend films.[a)]

| Sample | $YM_P$ (MPa) | $YM_T$ (MPa) | $ST_P$ (MPa) | $ST_T$ (MPa) | $SB_P$ (%) | $SB_T$ (%) |
|---|---|---|---|---|---|---|
| PEL | 147 ± 3 | 193 ± 15 | 18 ± 0 | 9 ± 1 | 356 ± 39 | 457 ± 129 |
| 2B | 167 ± 7 | 193 ± 15 | 17 ± 1 | 9 ± 1 | 254 ± 68 | 315 ± 127 |
| 3T6 | 186 ± 11 | 185 ± 10 | 20 ± 2 | 6 ± 0 | 244 ± 54 | 62 ± 15 |
| 2B3T6 | 182 ± 19 | 165 ± 10 | 15 ± 1 | 9 ± 1 | 405 ± 44 | 422 ± 80 |
| 3T7 | 154 ± 8 | 209 ± 18 | 16 ± 1 | 8 ± 1 | 222 ± 43 | 46 ± 16 |
| 2B3T7 | 159 ± 8 | 175 ± 8 | 16 ± 1 | 8 ± 1 | 286 ± 27 | 285 ± 159 |
| 3T63T7 | 147 ± 7 | 178 ± 12 | 16 ± 1 | 8 ± 0 | 321 ± 22 | 183 ± 72 |
| 2B3T63T7 | 200 ± 10 | 225 ± 15 | 17 ± 1 | 7 ± 1 | 271 ± 37 | 61 ± 44 |
| BT6T7 | 155 ± 8 | 200 ± 11 | 15 ± 1 | 8 ± 0 | 306 ± 58 | 39 ± 15 |

[a)] $YM_P$ and $YM_T$ are the Young Modulus in the parallel and transverse direction of blow, respectively. $ST_P$ and $ST_T$ are the Stress at break in the parallel and transversal direction and $SB_P$ and $SB_T$ are the Strain at break in the parallel and transversal direction.

Tensile stress at break of all samples was significantly lower in the transverse direction ($ST_T$) than in the parallel one ($ST_P$). $ST_P$ values ranged from 15 MPa (2B3T6 and BT6T7) to 20 MPa (3T6) while $ST_T$ values ranged from 7 MPa (2B3T63T7) to 9 MPa (PEL, 2B and 2B3T6). Values of transverse strain at break ($SB_T$) were significantly lower than the parallel one ($SB_P$) even if the error values are significant. Moreover, SB presented significant errors values principally in the transverse direction. Mechanical properties at break are very sensible to imperfections inside the matrix, which can lead to severe variabilities.

To have an insight about the statistical dispersion on the mechanical data, the fractured surfaces from tensile test were analysed by electron scanning microscopy (SEM). Figure 3.25 shows typical photomicrographs of the fractured surfaces represented by the samples PEL, 2B, 3T6, and 2B3T6. The SB value of sample 3T6 was one of the lowest measured. This result can be attributed to the brittle character of this material as suggested its fractured surface and not to imperfections. On the other hand, the fractured surfaces of the blends, principally containing PHB, indicate that during blow moulding

the alignment of the blend components form elongated phase separation, which can initiate a failure.

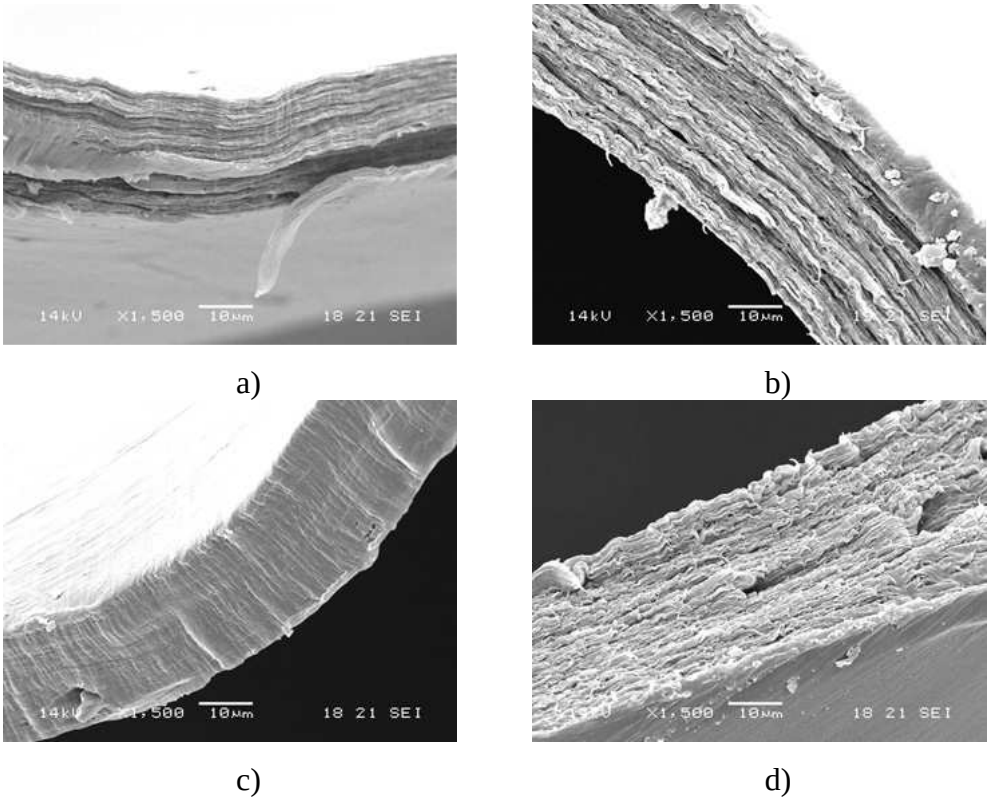


a) b)

c) d)

**Figure 3.25.** SEM of fractured surfaces from tensile test of PE-PHB films in the transverse direction to the blow at 1500X of magnification. a) PEL; b) 2B; c) 3T6; and d) 2B3T6.

### *3.2.1.4 Thermogravimetry (TGA)*

Figure 3.26 shows the TGA and DTGA traces at nitrogen atmosphere of prodegradants T6 and T7. These additives are proprietary concentrates of a transition metal chemical (in the present study the elements cobalt and calcium were detected by microanalysis) in a matrix of PE (masterbatch). Table 3.22 reports the decomposition temperature ($T_d$), peak temperature ($T_p$), mass loss ($\Delta M$) and residue at 800 °C of blend films obtained by blow extrusion. PHB film by blow extrusion was not possible to be obtained and

its data refers to film obtained by compression moulding after its processing in an internal mixer. The data of T6 and T7 correspond to their pellets. The $T_d$ error value of 1.1 % was calculated for BT6T7 sample, which measurement was replicated four times.

The weight loss of the additive T7 begin at a temperature 149 °C (Tab. 3.22) lower than that of T6. T7 $T_d$ value was the same in both nitrogen and air atmosphere. So, it is probable that only the temperature affects the degradation of the transition metal substance. In addition, T6 presents two steps of weight loss and T7 three steps. T7 $T_p$ of the first step of weight loss is centered at 356 °C corresponding to a less stable component in this additive, which is not present in T6. Roy *et al.*[40] studied the effect of cobalt carboxylates on the photo-oxidative degradation of LDPE. As the $T_d$ value depends of the way as it is calculated, the best thermodegradation property for comparison is the $T_p$. So, these authors found the temperature of 367 °C for the $T_p$ of cobalt stearate that is the closest one of the T7 $T_p$. In both additives, the main step of weight loss was due to the PE chain degradation and was centered at 474 °C. The residues at 800 °C of both T6 and T7 additives were ca. 19 wt-% and 15 wt-%, respectively, in both nitrogen and air atmosphere.

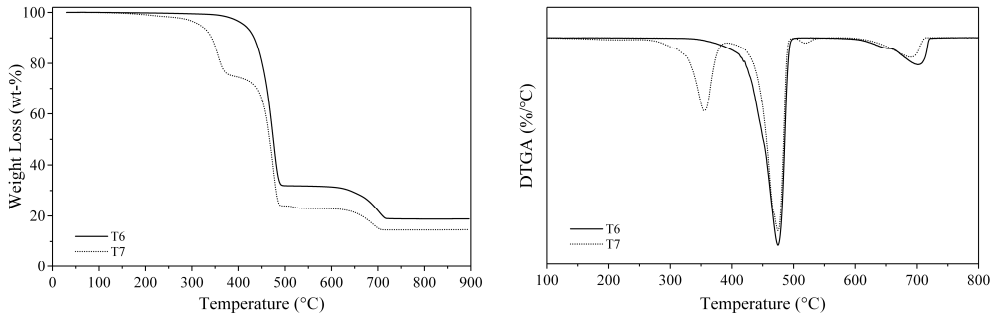


a) b)

**Figure 3.26.** TGA (a) and DTGA (b) traces of the prodegradants additives.

PEL $T_d$ value was 391 °C and the values for blends containing prodegradants were *ca.* 1 %, 4 % and 10 % lower for 3T6, 3T7 and 3T63T7 blends, respectively. The addition of PHB also decreased the $T_d$ of blends.

The $T_d$ value of 2B sample was 22 % lower than that of PEL. Consequently, the decrease in $T_d$ values was still more evident in samples containing both PHB and prodegradant. These blends presented a decrease in $T_d$ values of 23 %, 33 % and 39 % for 2B3T6, 2B3T7 and 2B3T63T7 blends, respectively. The effect in thermal stability was more evident when T7 was present together with PHB.

**Table 3.22.** TGA data of PE-PHB-prodegadant blends as a function of composition.[a)]

| Sample | $T_d$ (°C) | $T_{p1}$ (°C) | $\Delta M_1$ (%) | $T_{p2}$ (°C) | $\Delta M_2$ (%) | $T_{p3}$ (°C) | $\Delta M_3$ (%) | $R_{800}$ (%) |
|---|---|---|---|---|---|---|---|---|
| T6 | 353 | — | — | 474 | 68.2 | 701 | 13.0 | 18.9 |
| T7 | 204 | 356 | 23.2 | 474 | 51.0 | 690 | 8.4 | 14.6 |
| PHB | 265 | 275 | 99.6 | — | — | — | — | 0.2 |
| PE | 390 | — | — | 468 | 99.9 | — | — | 0.1 |
| PEL | 391 | — | — | 474 | 99.9 | — | — | 0.0 |
| 2B | 305 | 307 | 1.7 | 474 | 98.1 | — | — | 0.1 |
| 3T6 | 386 | — | — | 475 | 99.3 | — | — | 0.7 |
| 2B3T6 | 301 | 221 | 0.8 | 473 | 98.2 | 619 | 0.4 | 0.5 |
| 3T7 | 377 | — | — | 471 | 99.0 | — | — | 0.4 |
| 2B3T7 | 263 | 246 | 2.0 | 468 | 97.1 | 624 | 0.2 | 0.6 |
| 3T63T7 | 354 | — | — | 474 | 97.9 | 667 | 0.7 | 1.4 |
| 2B3T63T7 | 239 | 226 | 2.0 | 476 | 96.5 | 617 | 0.6 | 1.1 |
| BT6T7 | 353 | 216 | 0.8 | 466 | 98.3 | 607 | 0.4 | 0.8 |

[a)] $T_d$ is the onset decomposition temperature defined at 1 wt-% of weight loss; $T_p$ is the first derivative peak; $\Delta M$ is the mass loss; and $R_{800}$ is the residual weight at 800°C.

In blends formulation, $T_{p1}$ correspond to the temperature of the maximum degradation rate of PHB and $T_{p2}$ to the temperature of maximum degradation rate of PE. $T_{p1}$ changed significantly depending on the blend composition. $T_{p1}$ of 2B blend was 12 % higher than that of PHB. This increase in thermal stability of PHB can be attributed to two possibilities. The first one would be that of the protective effect of the more stable PEL components. The other one is related to difference in the samples processing.

This means, PHB was firstly processed in an internal mixer and then by compression moulding while 2B blend were processed in a twin screw extruder followed by blow extrusion. Comparing the $T_{p1}$ values of blends containing prodegradants with that of 2B it was observed a decrease of 28 %, 20 %, 26 % and 30 % for 2B3T6, 2B3T7, 2B3T63T7 and BT6T7 blends, respectively. This changes means that the mechanism of PHB degradation changed depending of the presence of prodegradant and that is a function of the blend composition.

$T_{p2}$ values of the majority of blends did not present significant differences with composition, which were centered in the same range of temperature of that of prodegradants. 2B3T7 and BT6T7 blends presented $T_{p2}$ values of 468 °C and 466 °C, respectively that are equivalent to that of pristine PE.

$T_{p3}$ corresponds to temperature of the maximum degradation rate of the third step of weight loss in the prodegradants. Pristine T6 and T7 presented $T_{p3}$ values of 701 °C and 690 °C, respectively. In the blends, the $T_{p3}$ values were lower than that of pristine T6 and T7. Probably, this decrease is a result of the partially degraded blends during the extrusion process. As above mentioned, blends containing prodegradants were first obtained in a twin-screw extruder and after films were obtained by blown extrusion. In this process the high shear and elevated temperatures can promote a degradation of the materials containing T6 and T7. The steps of weight loss ($\Delta M_1$, $\Delta M_2$ and $\Delta M_3$) were proportional to the amounts of the respective components in each blend and the residue of all blends increased with the addition of prodegradants.

#### *3.2.1.5 Differential scanning calorimetry (DSC)*

DSC traces of 1$^{st}$ heating and 1$^{st}$ cooling scan of PE-PHB-prodegradant blends are shown in Figure 3.27 and thermodynamic parameters of blends and of single components are reported in Tables 3.23 – 3.24. Basically, all samples presented a single endothermic peak centered around 109 °C that corresponds to melting temperature ($T_m$) of the PEL (the blend PE-EGMA)

(Fig. 3.27 a)). The same invariability was verified on cooling scan (Fig. 3.27 b)). All samples presented a single broad crystallization peak centered at around 98 °C with an enthalpy ($\Delta H_m$) ranging from 123 J/g (3T63T7) to 135 J/g (BT6T7). The crystallization started around 110 °C (Tab. 3.24).

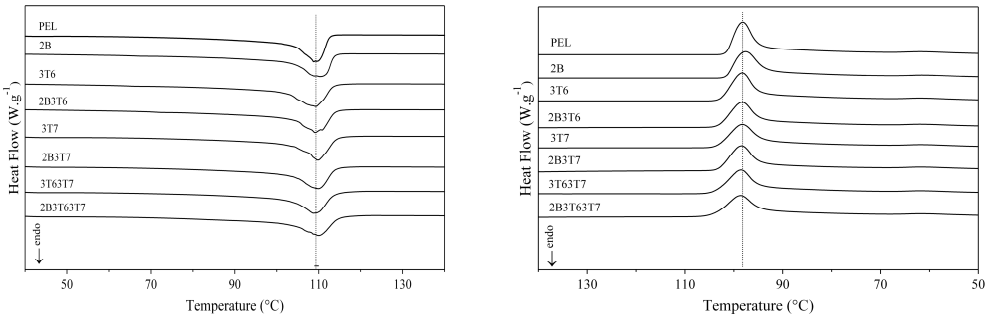


a) b)

**Figure 3.27.** DSC traces of (a) 1st heating scan and (b) 1st cooling scan of PE-PHB-prodegradant blends.

**Table 3.23.** Thermodynamic parameters from 1st heating scan of blends.[a)]

| Sample | $T_m$ (°C) | $\Delta T_m$ (°C) | $\Delta H_m$ ($J \cdot g^{-1}$) | $X_c$ (%) |
|---|---|---|---|---|
| PE | 111 | 102 | 126.9 | 43.8 |
| EGMA | 104 | 94 | 102.7 | 35.4 |
| T6 | 123 | 120 | 100.2 | 34.6 |
| T7 | 123 | 132 | 101.2 | 34.9 |
| PEL | 108 | 98 | 131.7 | 45.4 |
| 2B | 110 | 99 | 120.4 | 41.5 |
| 3T6 | 109 | 101 | 123.7 | 42.7 |
| 2B3T6 | 109 | 102 | 123.8 | 42.7 |
| 3T7 | 109 | 102 | 128.3 | 44.2 |
| 2B3T7 | 110 | 102 | 128.5 | 44.3 |
| 3T63T7 | 108 | 102 | 129.1 | 44.5 |
| 2B3T63T7 | 110 | 103 | 130.7 | 45.1 |
| BT6T7 | 108 | 100 | 124.3 | 42.9 |

[a)] $T_m$ is melting temperature; $\Delta T_m$ and $\Delta H_m$ are range and enthalpy of melting; and $X_c$ is the degree of crystallinity.

Roy *et al*.[40] found for cobalt stearate a $T_m$ of *ca.* 122 °C. This value overlap the $T_m$ values found for T6 and T7 prodegradants (123 °C) that contain PE as matrix. PEL blend showed a $T_m$ value lying between those of PE and EGMA. In addition, all blends showed $T_m$ near that of PEL, this could be due to the small amount of additives present in the blends (2-3 wt-%), which should not be enough to shift the $T_m$ value of PE matrix. The crystalline content of all blends remained in the range of 41.5 % (2B) to 45.1 % (2B3T63T7).

Thermodynamic parameters relative to the first DSC cooling scan of PE-PHB-prodegradant blends are reported in Table 3.24. $T_c$ value of PEL matrix was not affected by the addition of PHB, T6 and T7 additives. Probably, this result is due to their low amount in the formulations. The same was verified for the others parameter. The degree of crystallinity ($X_c$) was in general *ca*. 43 %. The exception was for BT6T7 blend, which $X_c$ value was *ca.* 8 % higher than the other ones.

**Table 3.24.** Thermodynamic parameters from 1st cooling scan of blends.[a)]

| Sample | $T_c$ (°C) | $T_{on}$ (°C) | $\Delta T_c$ (°C) | $\Delta H_c$ ($J \cdot g^{-1}$) | $X_c$ (%) |
|---|---|---|---|---|---|
| PE | 95 | 109 | 91 | 129.2 | 44.5 |
| EGMA | 90 | 103 | 102 | 113.0 | 38.9 |
| T6 | 108 | 121 | 134 | 84.0 | 29.0 |
| T7 | 114 | 119 | 130 | 98.3 | 34.0 |
| PEL | 98 | 108 | 91 | 129.3 | 44.6 |
| 2B | 98 | 110 | 91 | 123.4 | 42.5 |
| 3T6 | 98 | 109 | 90 | 126.9 | 43.8 |
| 2B3T6 | 98 | 109 | 91 | 125.3 | 43.2 |
| 3T7 | 98 | 109 | 92 | 124.6 | 43.0 |
| 2B3T7 | 98 | 111 | 93 | 127.0 | 43.8 |
| 3T63T7 | 98 | 110 | 91 | 122.9 | 42.4 |
| 2B3T63T7 | 99 | 112 | 95 | 124.5 | 43.0 |
| BT6T7 | 99 | 110 | 94 | 135.0 | 46.4 |

[a)] $T_c$ is crystallization temperature; $T_{on}$ is the temperature at the beginning of crystallization; $\Delta T_c$ and $\Delta H_c$ are range and enthalpy of crystallization; and $X_c$ is the degree of crystallinity.

### 3.2.2. *Thermal-oxidation of PE-PHB-prodegradat blends*

Several definitions of degradation are found in literature. Within this Thesis, the term degradation will follow the definition given by Krzan *et al.*[23] and by Amass *et al.*[138]. According to Krzan *et al.*[23] degradation of environmental degradable polymers take place by means of various mechanisms (photolytic, thermal, mechanical, hydrolytic, oxidative, biological) that in general is a combination of them with the ultimate degradation (known as biodegradation or "mineralization") carried out exclusively by biological processes. Biodegradation was defined by Amass *et al.*[138] as an event which takes place through the action of enzymes and/or chemical decomposition associated with living organisms (bacteria, fungi, etc.) or their secretion products.

It is usually think that oxidation increases the biodegradation of inert polymers. The polymer oxidation increases the amount of low molecular weight material by breaking bonds, increasing the surface area, through embrittlement and by increasing the hydrophilicity by the introduction of carbonyl groups. As soon as carbonyl groups are formed, they may be attacked by microorganism and the macromolecules decompose into shorter chains[139].

The products of oxidative degradation of PE include water, carbon monoxide, carbon dioxide, alcohols, ketones, hydroperoxides, peroxides and carboxylic acids[40, 140]. In a secondary process, microorganisms may utilize the degradation products and low molecular weight polymer in anabolic and catabolic cycles leading the polymer to a completely biodegradation[25, 141]. However, PE can undergo a variety of different chemical reactions during extrusion and thermal aging. During these process thermo-oxidative and thermo-mechanical degradation take place and the radicals thus formed play an important role in the chain scission, chain branching or crosslinking. Crosslinking leading to an increase of the molecular weight of the polymer is generally favoured compared to thermo-oxidative induced chain scission[76, 78, 142].

The thermal oxidation is affected by several factors such as crystallinity and molecular orientation of films[39]. In diffusion-controlled processes, the rate of oxidation increases with increasing of oxygen permeability through the material. Therefore, the oxidation in crystalline regions where the oxygen diffusion is limited or absent is practically inexistent[143]. Consequently, the oxidation reactions take place especially on the surface of the films, where oxygen is more abundant. However, much of the oxidation occurs through radical chain reactions, involving low molecular weight radicals produced by thermal cleavage. The crystallinity and the molecular orientation also determine the mobility of the radicals and hence control the rate of termination through recombination and/or disproportionation. Increased crystallinity and/or increased orientation reduce the radical mobility and therefore reduce the rate of termination, allowing an increase in the propagation of chemical reactions leading to molecule scission, and this effect is opposite to that caused by reduced oxygen mobility[144].

The aim of this study was to evaluate de oxidation behaviour of PE-PHB films blends containing commercial prodegradants additives through the assessment of some parameters: i) the formation of carbonyl and hydroperoxide groups; ii) the activation energy necessary to promote the oxidation; iii) the crosslinking formation through the amount of gel formed on samples; and iv) the influence of oxidation on molecular weight, thermal the and mechanical properties of films.

Thermo-oxidation of PE-PHB-prodegradant blends was evaluated in two different conditions as explained in Section 2.5.1. Briefly, in the first condition, PE-PHB-prodegradant blends was thermo aged in a static oven for up to 120 days at three different temperatures: 45 °C, 55 °C and 65 °C. These temperatures were chosen because represent the common temperatures found in composting process[145]. In this experiment, the assessed parameters were the carbonyl and hydroperoxide formation as a function of aging time and temperature. Moreover, the activation energy (*Ea*) of PE-PHB-prodegradant blends was also calculated. In the second group of experiment, samples were submitted to a thermo-oxidation at 55 °C for 60 days and characterized in relation to the carbonyl index ($CO_i$), amounts of acetone extractable fractions

and their molecular weights, thermal properties by means of TGA, DSC and mechanical properties from tensile tests.

#### *3.2.2.1 FTIR analysis of thermo-oxidized blends*

The mechanism of polyolefin oxidation is not a trivial argument and over the years different approaches were used to study the thermo-oxidation of these materials. Volatile products from thermal-oxidation at high temperatures of PE-starch films were identified and measured by gas chromatography[131]. Moreover, gas-chromatography/mass-spectrometry has been used in the identification of degradation products from enhanced environmentally degradable PE[146]. Jipa *et al.*[147], Jacobson *et al.*[148] and Broska *et al.*[149, 150], reported the use of chemiluminescence as a tool for determine the amount of hydroperoxides accumulated in a oxidized polymer. This technique is based on the phenomena that polyolefins emit a weak light, luminescence, when heated in air and this luminescence effect is linked to the polymer oxidation[36, 151]. The number of photons emitted from a polyolefin can be counted during the degradation time and this number can be related to the amount of hydroperoxides and thereby the degree of aging[151]. A simple method to monitoring the rate of degradation of films is by monitoring the accumulation of non-volatile oxidation reaction products. The concentration of these products is followed by the growth of the carbonyl (C=O), hydroperoxide (ROO) and hydroxyl (OH) bands in the infrared spectrum. The C=O band can belong to a large number of chemicals from many different products[15, 33].

In this work, samples were thermo-oxidized in cardboard supports (Fig. 2.3a), which permitted to measure the growing of the functional groups always at the same film position. The increasing in the carbonyl and hydroperoxide absorption bands was measured during the time and the results were reported as carbonyl ($CO_i$) and hydroperoxide ($ROO_i$) index. Carbonyl index was calculated as the rate between the absorbance of peak at 1715 $cm^{-1}$, corresponding to carbonyl ketone group, and the absorbance of $CH_2$ scissoring peak at 1463 $cm^{-1}$[33, 39, 41, 152, 153]. The relationship used for the

calculation of hydroperoxide index was between the peak at 3380 $cm^{-1}$ corresponding to OH group and the $CH_2$ scissoring peak at 1463 $cm^{-1}$[154].

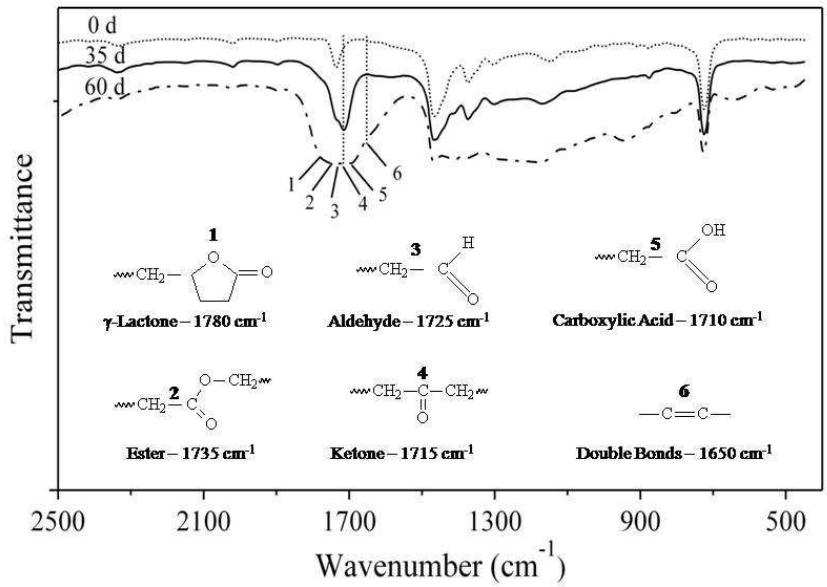


**Figure 3.28.** FTIR-spectra of 3T7 blend after 0, 35 and 60 days of thermal degradation at 55 °C.

Figure 3.28 shows the FTIR spectra of 3T7 blend at 0, 35 and 60 days of thermal aging in a static oven at 55°C. The spectra showed clearly the evolution of polymer degradation and the formation of various bands that are assigned to different products formed during PE oxidation. In the spectra of original 3T7 formulation (0 days) and in that aged for 35 days, it was not observed the band related to carbon double bonds (1650 $cm^{-1}$). However, this band clearly increased in samples aged for 60 days at 55 °C. The presence of these double bonds can be explained by the breakdown of peroxy radical[76], and can also indicate oxygen deficient conditions during PE oxidation, which can lead to disproportionation reactions of alkyl radicals contributing to the formation of carbon double bonds as shown in the Scheme 3.1 a) and b). Also, the β-scission of the alkoxy radical and the breakdown of the peroxy radical can lead to the formation of aldehydes (Sch. 3.1 c) and d)) [155], but this type of reaction product is more usual in polypropylene (PP) than in PE. In addition, it can be clearly seen the differences between the spectra of the

original 3T7 and that of aged blend. In the FTIR of non degraded 3T7 sample, a peak was observed in the range of 1770 $cm^{-1}$ and 1700 $cm^{-1}$ with a maximum at 1735 $cm^{-1}$, which was assigned to ester groups. Moreover, the band at 1715 $cm^{-1}$, attributed to aliphatic ketone group, is small in the pristine sample. During aging this band increases gradually and after 60 days of temperature exposure the peak broadening from 1765-1684 $cm^{-1}$ to 1876-1549 $cm^{-1}$ as a result of the overlapping of the peaks corresponding to the functional groups of different degradation products. Lacoste *et al.*[156] and Commereuc *et al.*[157] reported that during PP oxidation hydroperoxide groups clearly dominate over carbonyl species whilst in PE oxidation[158] carboxylic acid an ketone groups predominate. The mainly products formed during 3T7 degradation are easily observed in Figure 3.28. The principal bands are: 1780 $cm^{-1}$ assigned to γ-lactone; 1735 $cm^{-1}$ to ester groups; 1725 $cm^{-1}$ to aldehydes; 1715 $cm^{-1}$ to aliphatic ketone; 1710 $cm^{-1}$ to carboxylic acid and the absorption at 1650 $cm^{-1}$ to carbon double bonds[76].

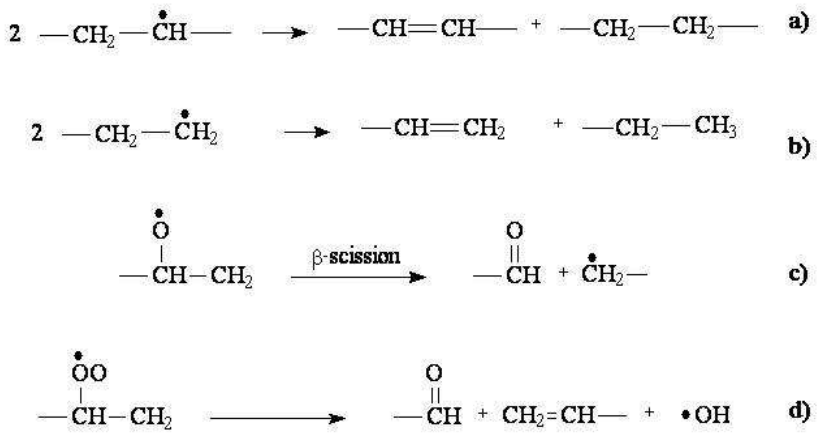


**Scheme 3.1.** Thermo-oxidation mechanism of polyolefinic materials.

Figures 3.29 and 3.30 show the spectra of 3T6, 2B3T6 and 2B3T7 blends, respectively, in the range of 1900-1550 $cm^{-1}$ at different times of thermal degradation (0, 25, 35, 45 and 60 days). Two bands were used to control PE oxidation, at 1735 $cm^{-1}$ and 1715 $cm^{-1}$ from ester and aliphatic

ketone groups, respectively. Significant difference can be observed between blends without (3T6 - Fig. 3.29 a)) and with PHB (2B3T6 – Fig. 3.29 b)).

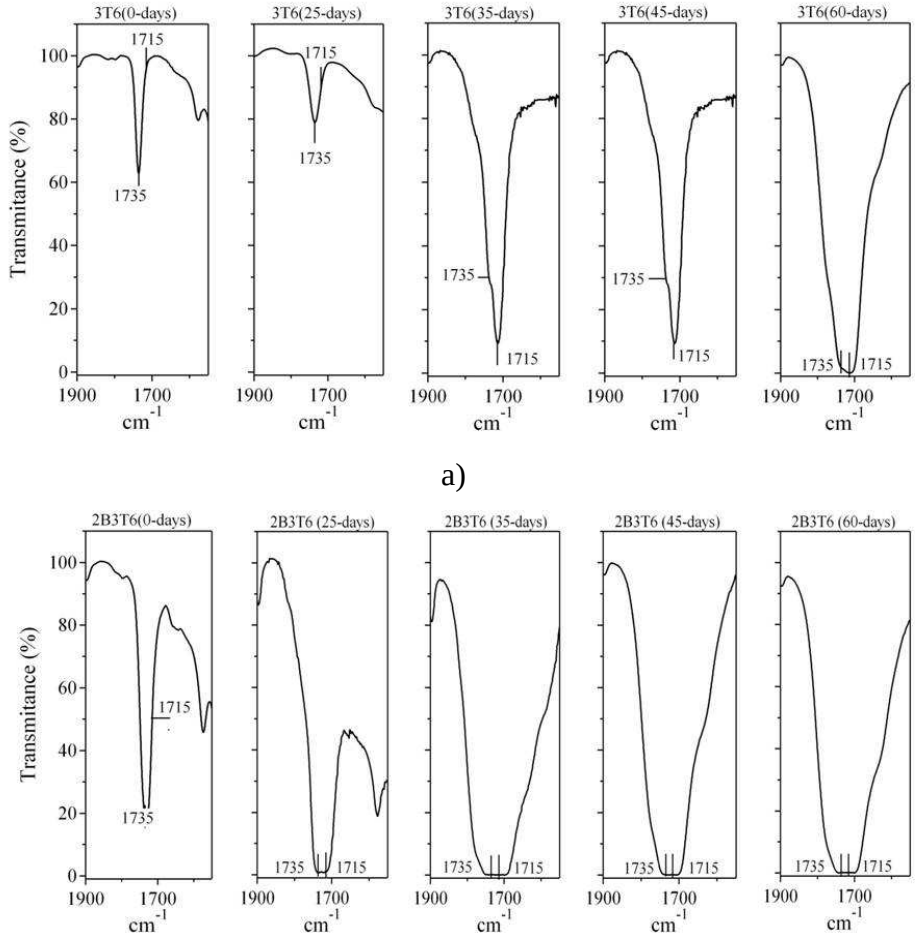


**Figure 3.29.** FTIR bands in the range of 1900-1550cm$^{-1}$ from aged a) 3T6 and b) 2B3T6.

At the beginning of the degradation process, 3T6 blend presents principally the peak at 1735 cm$^{-1}$ and that at 1715 cm$^{-1}$ is very weak. Ketone band starts to increase just after 25 days of aging, which overcome that of ester band after 35 days in the oven. At same time, 2B3T6 blend presents at the beginning a high band at 1715 cm$^{-1}$ and that at 1735 cm$^{-1}$ increased quickly with time. A different behaviour was observed for 2B3T7 sample

(Fig. 3.30), where ketone band starts to increase only after 25 days of thermal aging and much more slowly than 2B3T6 blend.

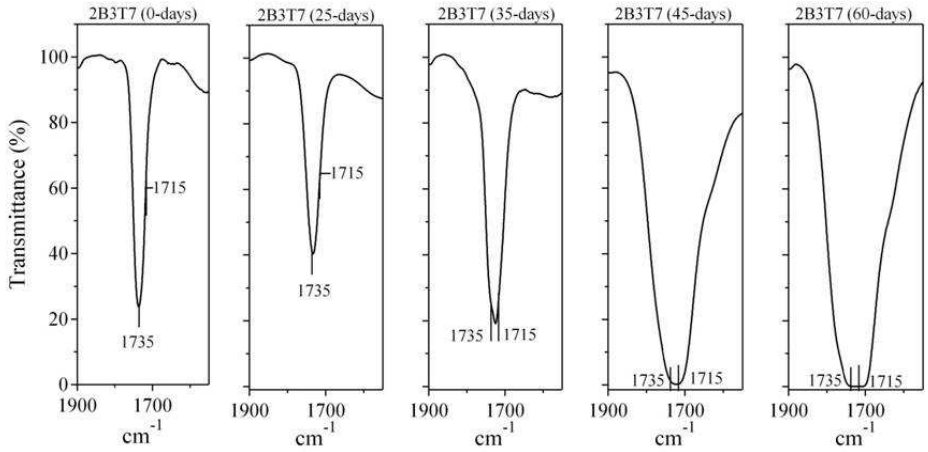


**Figure 3.30.** FTIR bands in the range of 1900-1550cm$^{-1}$ from aged 2B3T7 films.

As observed in Figures 3.29 –3.30 the main products of PE degradation are ketones (1715 cm$^{-1}$), ester (1735 cm$^{-1}$) and carboxylic acids (1710 cm$^{-1}$). The ketones formed can react by a Norrish type II mechanism[159] following abstraction of hydrogen from a γ carbon or decompose into a fragment with an unsaturated polymer chain-end and a second fragment with an end carbonyl group[25]. In this study, absorptions at 910 cm$^{-1}$ ($CH_2$=C-) and at 1650 cm$^{-1}$ (-C=C-) (Fig. 3.28) associated with an unsaturated polymer chain are in agreement with the mechanism shown in the Scheme 3.2.

As aforementioned, in polyolefin oxidation, the majority of the oxidation products are the result of hydroperoxide decomposition[160]. Hydroperoxy groups form the most part the primary products of thermo-oxidative degradation processes. These groups are unstable and are easily converted to alkoxy radicals giving hydroxyl and carbonyl groups[33]. The carbonyl groups are responsible for the majority of the products of oxidation in PE. So, their concentration can be used to monitor the progress of thermodegradation[155].

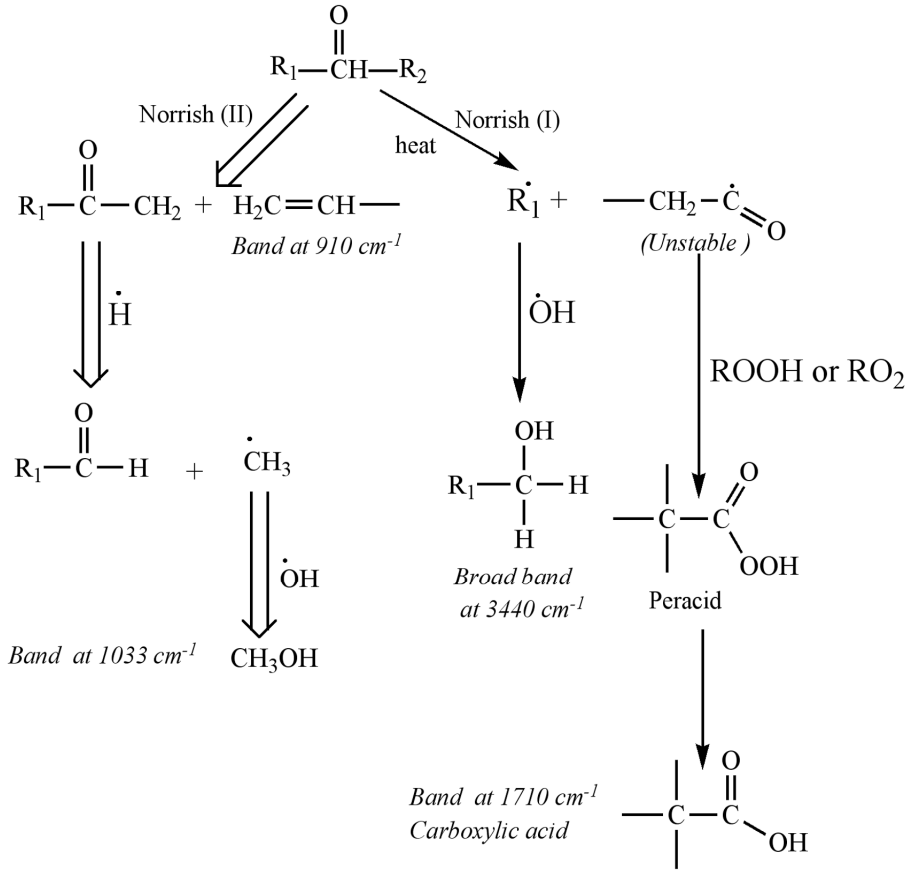


**Scheme 3.2.** Carbonyl reactions in PE through Norrish type I and II degradations[25, 159].

Figures 3.31 – 3.33 show the hydroperoxy ($ROO_i$) and carbonyl ($CO_i$) indexes of samples aged at 45 °C, 55 °C and 65 °C as a function of aging time. The $ROO_i$ and $CO_i$ were also measured for PE compatibilized with EGMA (PEL) and with PHB (2B), but no significant change in these indexes was observed during the aging time. On the other hand, blend samples containing prodegradants had these indexes increased with aging time and their velocity was more fast for higher aging temperature. These results demonstrate that the prodegradants have an important role in the thermodegradation of PE.

Thermo-oxidation of 3T6 at 45 °C presented an apparent time lag of *ca*. 50 days while at 65 °C this time was at *ca*. 15 days of aging, detected by $CO_i$. As general rule, the $ROO_i$ presents the same tendency in the temperature-time

behaviour of that verified for $CO_i$. An exception was observed for 3T7 blend, where the hydroperoxidation from aging at 55 °C was higher than that from aging at 65 °C. The time lag for equivalent formulation containing PHB (2B3T6 – Fig. 3.31 c) and d)) was lower. This time was ca. 40 days, 20 days and 15 days for aging temperatures at 45 °C, 55 °C and 65 °C, respectively. So, the presence of PHB contributes additionally to the thermo-oxidation of PE. The plateau of the $ROO_i$ and $CO_i$ values did not show a tendency with temperature. However, the $CO_i$ values were slightly higher for PE blends without PHB.

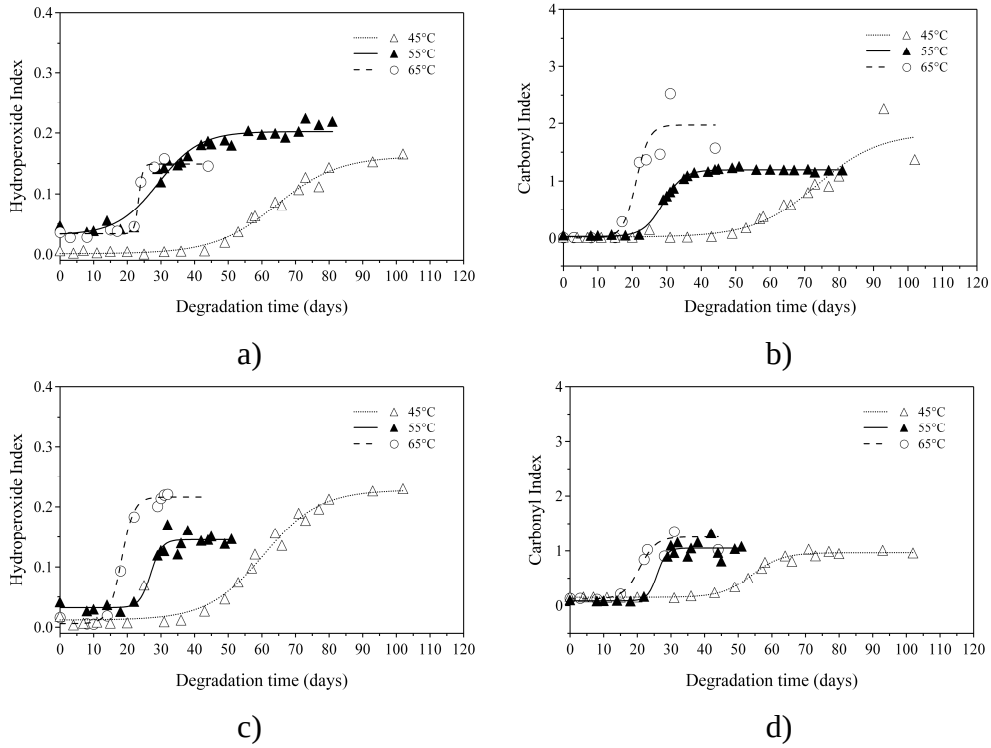


**Figure 3.31.** $ROO_i$ and $CO_i$ as a function of time from aging at 45 °C, 55 °C and 65 °C of blends 3T6 (a, b) and 2B3T6 (c, d).

The plateau values of both $ROO_i$ and $CO_i$ for PE blends containing T7 were higher than the equivalent one with T6 (Fig. 3.32). Besides, their time lag was also higher with apparent activation at 80 days, 45 days and 17 days for the blend 3T7 aged at 45 °C, 55 °C and 65 °C, respectively (Fig. 3.32 a) and b)). The corresponding blend with PHB (2B3T7 – Fig. 3.32 c) and d))

showed a time lag of about 10 days earlier. The plateau values of both $ROO_i$ and $CO_i$ were equivalent for both 3T7 and 2B3T7. Besides, apparently they increase with the temperature increasing of aging. The exception was verified for the treatment at 55 °C that gave higher $ROO_i$ and lower $CO_i$ values. The experiment performed at this temperature was in an oven at least three times higher than that at 45 °C and 65 °C in volume. So, this can be a variable not controlled that was more significant in the blend system containing T7 probably due to its higher reactivity than that T6.

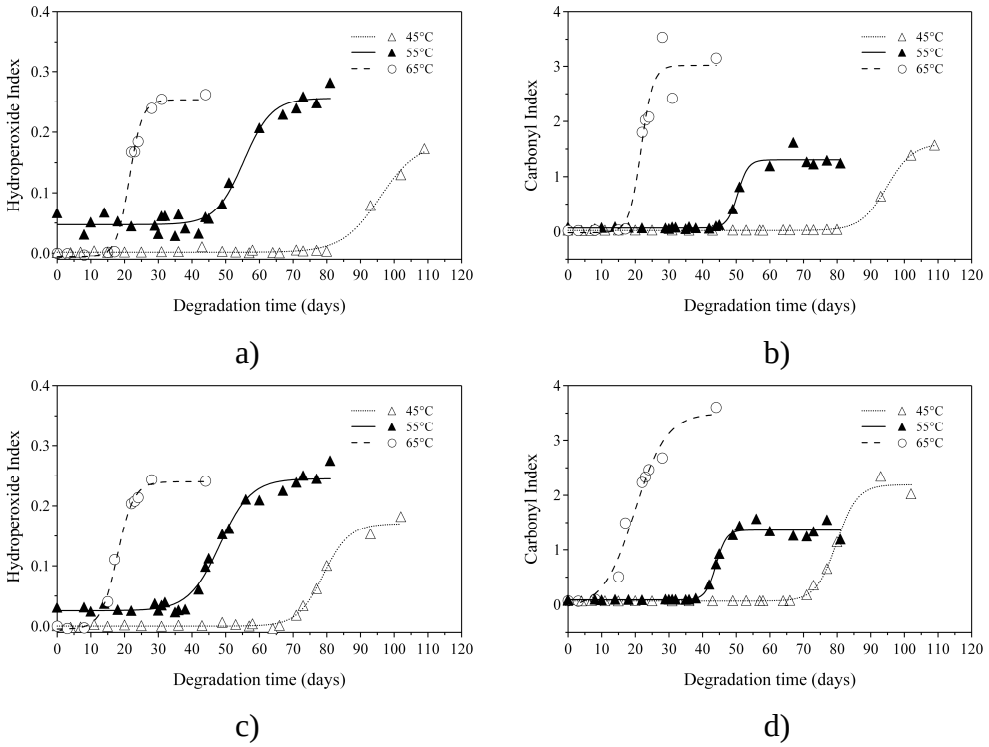


**Figure 3.32.** $ROO_i$ and $CO_i$ index as a function of aging time at 45 °C, 55 °C and 65 °C of blends 3T7 (a, b) and 2B3T7 (c, d).

$ROO_i$ and $CO_i$ of formulations containing the two types of prodegradants without (3T63T7) and with PHB (2B3T63T7 and BT6T7) are reported in Figure 3.33. These systems suggest that the presence of T6 and T7 together has an antagonist effect. The time lag of thermo-oxidation was higher than 100 days for samples aged at 45 °C. Decreasing the amount of both additives in the blend (BT6T7 – Fig. 3.33 e) and f)) the time lag was

lower confirming the antagonistic effect of both additives together. However, samples aged at 65 °C presented time lag equivalent to the systems analysed previously. In these systems the results at 55 °C presented the same behaviour observed previously.

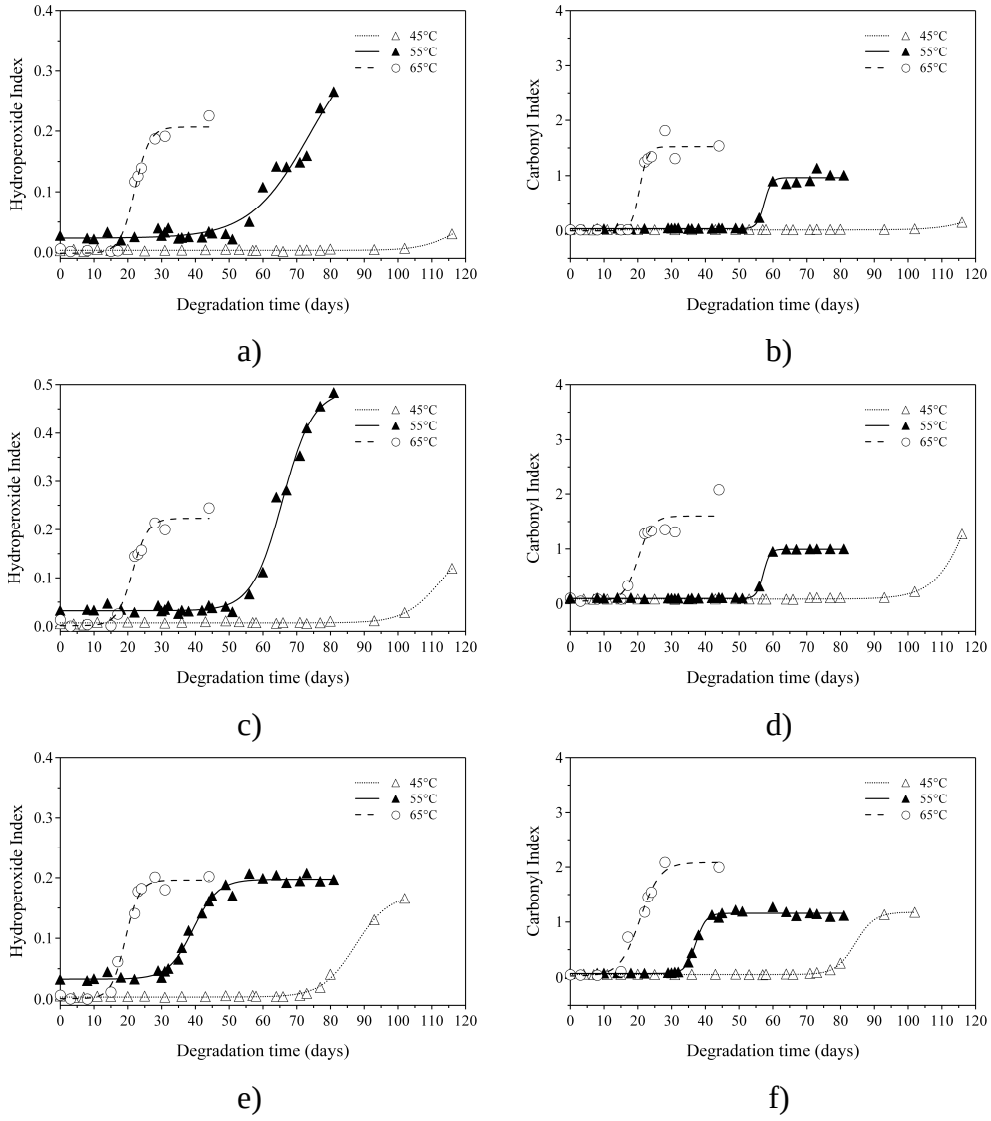


**Figure 3.33.** $ROO_i$ and $CO_i$ index as a function of aging time at 45 °C, 55 °C and 65 °C of blends 3T63T7 (a, b), 2B3T63T7 (c, d) and BT6T7 (e, f).

The reaction rates can raise many folds by increasing temperature. This is a consequence of the increase in movement of reactant molecules and more frequent collisions between them with the temperature. The minimum amount of kinetic energy that these molecules will need to have, in order to react and transform reagents in products, is called activation energy (*Ea*). Higher values of *Ea* denote that larger amounts of energy are needed to initiate a reaction. This means that the reaction will be more susceptible to the influence of temperature.

The rate constants (*k*) and *Ea* of samples obtained from Arrhenius equation are reported in the Table 3.25. As expected, the *k* values are dependent of the temperature. Blends without prodegradants (PEL and 2B), did not thermo-degraded in the range of temperature and period of time studied (120 days). The *Ea* values ranged from *ca*. 81 kJ/mol for 3T6 to *ca*. 22 kJ/mol for 2B3T7. This result is in accordance with that of carbonyl index. Besides, the blends containing PHB presented lower values of *Ea* than the corresponding formulation without it.

**Table 3.25.** Rate constants (*k*) and activation energy (*Ea*) of samples obtained from Arrhenius equation.

| Sample | $k_1$ (45°C) | $k_2$ (55°C) | $k_3$ (65°C) | *Ea* (kJ/mol) |
|---|---|---|---|---|
| 3T6 | 0.0324 | 0.0734 | 0.1981 | 80.74 |
| 2B3T6 | 0.0264 | 0.0990 | 0.0871 | 53.89 |
| 3T7 | 0.0556 | 0.0664 | 0.3115 | 76.34 |
| 2B3T7 | 0.0999 | 0.1128 | 0.1602 | 20.98 |
| 3T63T7 | — | 0.0938 | 0.1624 | 50.60 |
| 2B3T63T7 | 0.0526 | 0.0928 | 0.1516 | 47.28 |
| BT6T7 | 0.0637 | 0.1088 | 0.1430 | 36.25 |

### 3.2.2.2 *Characterization of PE-PHB-prodegradant blends thermo-aged at 55 °C*

As previously pointed out, several chemical modifications are observed in the polymeric chains during a thermo-oxidation reaction. Consequently, the polymeric chains will reduce its molecular weight (MW) and will form new functional groups as ketones, alcohols, hydroperoxides, peroxides, carboxylic acids and so on.[25, 140, 146, 161, 162]. The effect of the thermo-oxidation in the physical-chemical properties of samples can be related with the $CO_i$. In this way, the measurement of the oxidation level of samples (in relation to the formation of C=O at 1715 $cm^{-1}$ ($CO_i$)) was performed by means of FTIR on samples that have been degraded in static oven at 55 °C for 60 days using Petri dishes supports (Fig. 2.3 b)). The samples were removed from the oven at 0, 25, 35, 45 and 60 days of degradation and characterized regarding their $CO_i$, amount and molecular weight of acetone extractable fractions, TGA, DSC, gel content and mechanical properties. In addition, the weight gain was measured at shorter intervals of time. Measurements were carried out in triplicate and errors were calculated at 95 % of confidence of Student's *t*-test.

#### ***Carbonyl index ($CO_i$)***

In Figure 3.34 are represented the changes of the $CO_i$ (1715 $cm^{-1}$/1463 $cm^{-1}$) with time for samples aged in Petri dishes at 55 °C for 60 days indicating the level of data dispersion. As expected, samples without prodegradants did not show any significant difference in the aliphatic ketone formation. On the other hand, all samples containing both T6 and T7 showed sigmoid thermo-oxidation behaviour and the time lag was between 25 and 35 days. After this induction period, 2B3T6 sample (Fig.3.34 b)) was activated to oxidation earlier than the other PE based blends, reaching the $CO_i$ plateau at 45 days of thermo-degradation; all the other samples presented an intermediate oxidation level at this aging time. In general, additivated PE blends with prodegradant has nearly arrived to their maximum $CO_i$ at 60 days

of thermal aging. Moreover, the highest oxidation level was achieved by sample containing PHB (2B3T7), which $CO_i$ value was *ca*. 3.

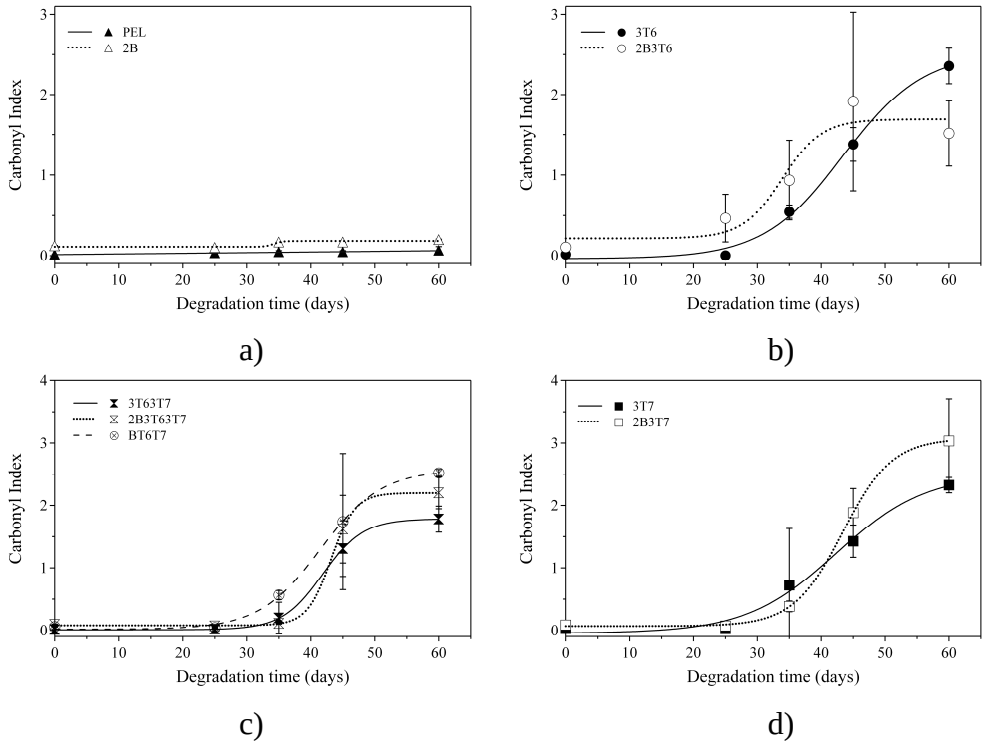


**Figure 3.34.** Carbonyl index as a function of aging time at 55 °C of PE-PHB-prodegradant films.

***Weight gain***

Figure 3.35 shows the weight changes of PE based blend films during the thermo-oxidation at 55 °C. PEL and 2B samples did not present any significant weight changes and then the results are not reported. It can be clearly observed that all PE blends containing prodegradant has its weight augmented during thermal aging. The origin of the increase in the initial weight is the oxygen uptake via hydroperoxide formation[15]. The weight gain presented the same trend of $CO_i$. This means, that the graphic of weight changes as a function of time also presented a sigmoid behaviour. Up to 30 days of aging basically no changes in sample weight was verified. After 60

days of thermal aging, the weight gain was from *ca.* 30 wt-% (2B3T63T7) to *ca.* 45 wt-% (3T6).

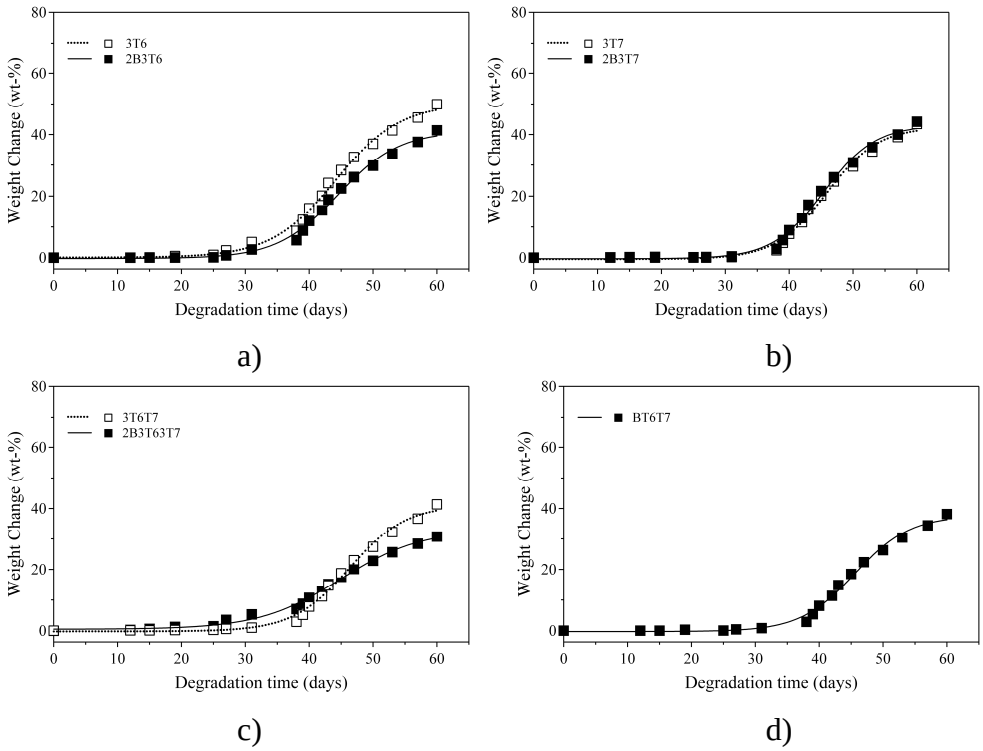


**Figure 3.35.** Weight changes of PE-PHB-prodegradant blend films by the oxygen uptake during oxidation process at 55°C.

***Acetone extraction***

In general, chain scission is the dominant thermo-degradation mechanism in polymers and is revealed by a fall in the average molecular weight (MW)[163, 164]. Acetone extractable fraction (KE) means the low MW chemicals that were extracted with boiling acetone by 3 hours. Residual mass (RM) corresponds to the residual fraction of material after the extraction in boiling acetone, which was dried to constant weight. Extraction was performed in the samples before aging, after 45 days and 60 days of thermo-oxidation. The time of 45 days nearly corresponds to the intermediate level of thermo-degradation.

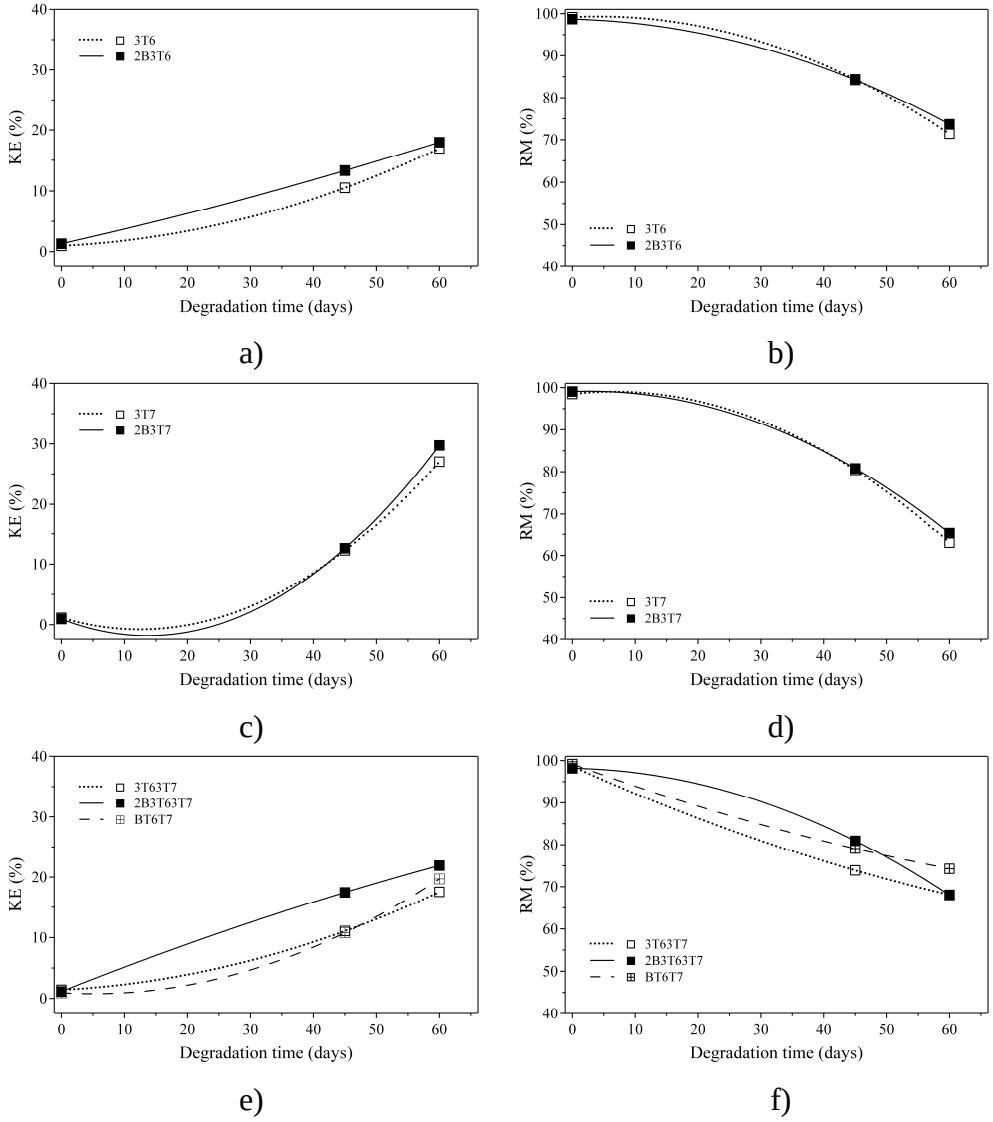


**Figure 3.36.** Acetone extractable fractions (KE) and residual mass (RM) from samples thermo-oxidized at 55°C for 60 days.

Figure 3.36 shows the KE and RM of thermo-oxidated PE-PHB-prodegradant blend films. From samples containing T6 and PHB it was extracted up to 15 wt-% (Fig. 3.36 a)). The highest amount of KE was around 30 wt-% for PE blends containing 2 wt-% of PHB and 3 wt-% of T7 (2B3T7 - Fig. 3.36 c)). PE blends containing PHB and both T6 and T7 at highest concentration (3 wt-%) presented 20 wt-% of KE after 60 days of thermo-aging (2B3T63T7 - Fig. 3.36 e)). This means that after 2 months at 55 °C at

least 20-30 wt-% of low MW chemicals was formed. Proportionally, RM decreased in the acetone extraction.

Average MW of the acetone soluble fraction was analyzed by GPC. Figure 3.37 represents typical GPC traces of KE fractions from UV detector (260 nm). This wavelength was selected because represent the λ max of absorption band of the majority of chromophore groups which were supposed to be present in the thermo-oxidized samples[165].

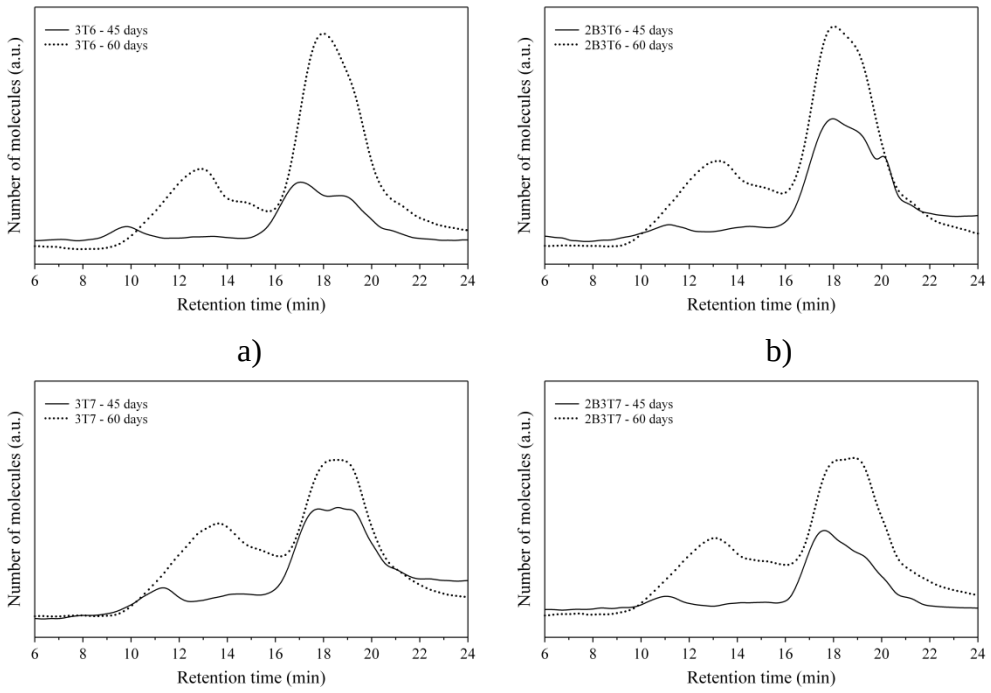


**Figure 3.37.** GPC traces of PE-PHB-prodegradant blends from thermo-degradation during 45 days and 60 days at 55 °C.

The average numeric molecular weight ($M_n$) of KE fractions are reported in Table 3.26. All samples showed the same trend where both retention time and peak intensity increased with aging time. This means that during thermal degradation, different reaction products were formed along of time. According to Craigh *et al.*[166], a large shift to lower MW weights is observed when a large amount of chain scission occurs and that the appearance of a high molecular weight tall indicates significant cross-linking.

In addition, an increasing of the thermal aging promoted a broadening of the peaks. This peak broadening probably was due to different low MW products formed during the thermo-degradation.

Figure 3.38 displays broad peaks with corresponding deconvolution, which peaks are reported in Table 3.26. According with Hakkarainen *et al.*[161], at lower oxygen concentration the probability that two neighbouring alkyl radicals will survive long enough to react with each other instead of reacting with oxygen is higher and the molecular enlargement reactions are more dominant leading to broadening of the MW distribution.

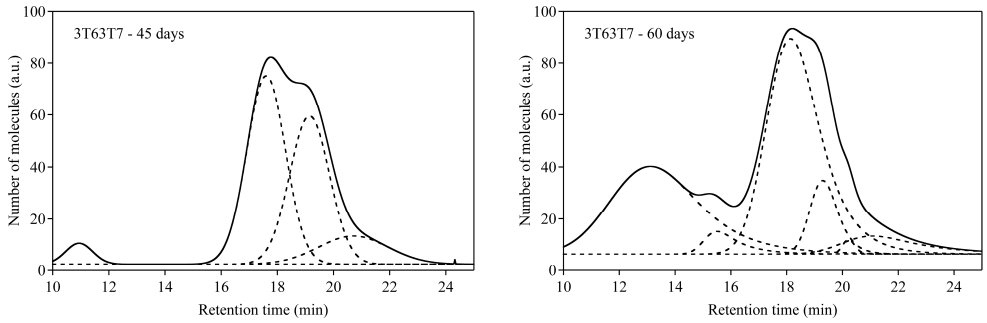


a) b)

**Figure 3.38.** GPC traces of 3T63T7 blend from thermo-degradation during a) 45 days and b) 60 days at 55 °C.

**Table 3.26.** $M_n$ of acetone extracted chemicals from PE-PHB-prodegradant blends aged at 55 °C [a)].

| Sample | Aged for 45 days | | | Aged for 60 days | | | |
|---|---|---|---|---|---|---|---|
| | $M_{n1}$ (kDa) | $M_{n2}$ (kDa) | $M_{n3}$ (kDa) | $M_{n1}$ (kDa) | $M_{n2}$ (kDa) | $M_{n3}$ (kDa) | $M_{n4}$ (kDa) |
| 3T6 | 1.5 | 0.3 | — | 70.3 | 7.2 | 0.7 | 0.2 |
| 2B3T6 | 1.3 | 0.3 | 0.1 | 50.0 | 7.2 | 0.8 | 0.3 |
| 3T7 | 17.0 | 1.0 | 0.3 | 34.0 | 3.7 | 0.6 | 0.2 |
| 2B3T7 | 13.0 | 0.9 | 0.3 | 9.1 | 0.4 | 0.7 | 0.2 |
| 3T63T7 | — | 0.9 | 0.2 | 39.3 | 5.2 | 0.6 | 0.3 |
| 2B3T63T7 | 22.0 | 0.8 | 0.2 | 70.0 | 4.5 | 0.8 | 0.2 |
| BT6T7 | 16.3 | 0.9 | 0.2 | 36.2 | 5.0 | 0.6 | 0.2 |

[a)] Mn lower than 0.1 kDa were not considered.

***Gel content***

During processing and thermal aging, PE is subjected to different temperatures and shear rates allowing chemical reactions to occur. Degradation can be initiated by oxygen, shear, heat, catalyst, additives or any combination of these factors[76]. The gel content, or insoluble fraction, is produced in PE by crosslinking and it is one of the products of PE thermal aging. The thermal oxidation includes initiation, propagation, chain branching and termination steps[76]. At the firs degradation step, alkyl radicals are formed, but under oxygen deficient conditions not all alkyl radicals ($R^{\bullet}$) can be transformed to peroxide ($ROO^{\bullet}$) radicals. Depending on thermal conditions and the type of additive used, PE can undergo different radical reactions such as chain scission and chain branching, leading to cross-linking as previously described and illustrated in the Scheme 3.3. Cross-linking via an oxidation reaction is due to the recombination of alkyl radicals $R^{\bullet}$ with each other, with $RO^{\bullet}$ or $ROO^{\bullet}$ radicals[76, 78].

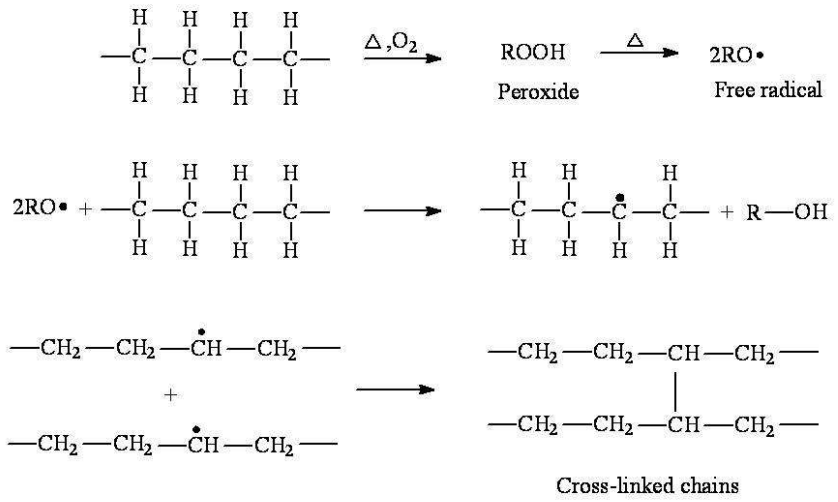


**Scheme 3.3.** General mechanism of PE cross-linking.

Table 3.27 report the insoluble fraction (gel) in xylene-ethyl benzene extraction as a function of aging time at 55°C. Four samples were replicated to assess the standard deviation of the measurement, which was *ca.* 3 wt-%.

PEL, 3T6 and 3T7 blends presented 21 wt-%, 23 wt-% and 26 wt-% of gel content before aging, respectively. The high values of gel for all samples before aging, is probably a consequence of the repeated times of melt processing to obtain blend films. During processing, PE base blends found conditions of poor oxygen, shear and elevated temperature. So, radical reactions leading to chain cross-linking could take place prematurely due to the presence of prodegradants. For all samples, the exposure to temperature-time conditions leads to an increase of cross-linked polymer content. Pristine PEL increased from 21 wt-% to 60 wt-% and 75 wt-% after 0, 35 and 60 days of aging, respectively. Data from Table 3.27 suggest that cross-linking is one of the dominant reaction mechanisms in PE-PHB based blends during thermal aging.

**Table 3.27.** Gel content (wt-%) of PE-PHB-prodegradant based blends aged at 55°C for 0, 35 and 60 days.

| Sample | Aging time (days) | | |
|---|---|---|---|
| | 0 | 35 | 60 |
| PEL | 21 | 60 | 75 |
| 2B | 15 | 64 | 70 |
| 3T6 | 23 | 53 | 74 |
| 2B3T6 | 42 | 49 | 76 |
| 3T7 | 26 | 34 | 70 |
| 2B3T7 | 22 | 30 | 77 |
| 3T63T7 | 32 | — | 73 |
| 2B3T63T7 | 30 | 32 | 69 |
| BT6T7 | 34 | 29 | 83 |

***Thermal properties***

A general strategy used in the evaluation of degradation caused by natural or artificial aging is the specimen exposition at different times in the degradation condition and then to examine their properties by mechanical or chemical tests. Polymer degradation often occurs as a heterogeneous process controlled by oxygen diffusion[167-169]. This means that the main oxidation

will occurs in the surface of the films. So, while through FTIR analysis important information about the degradation at surface of materials can be obtained, the TGA and DSC measurements provide essential information from the bulk. Both TGA and DSC were used to assess the thermal properties of aged PE based blend films.

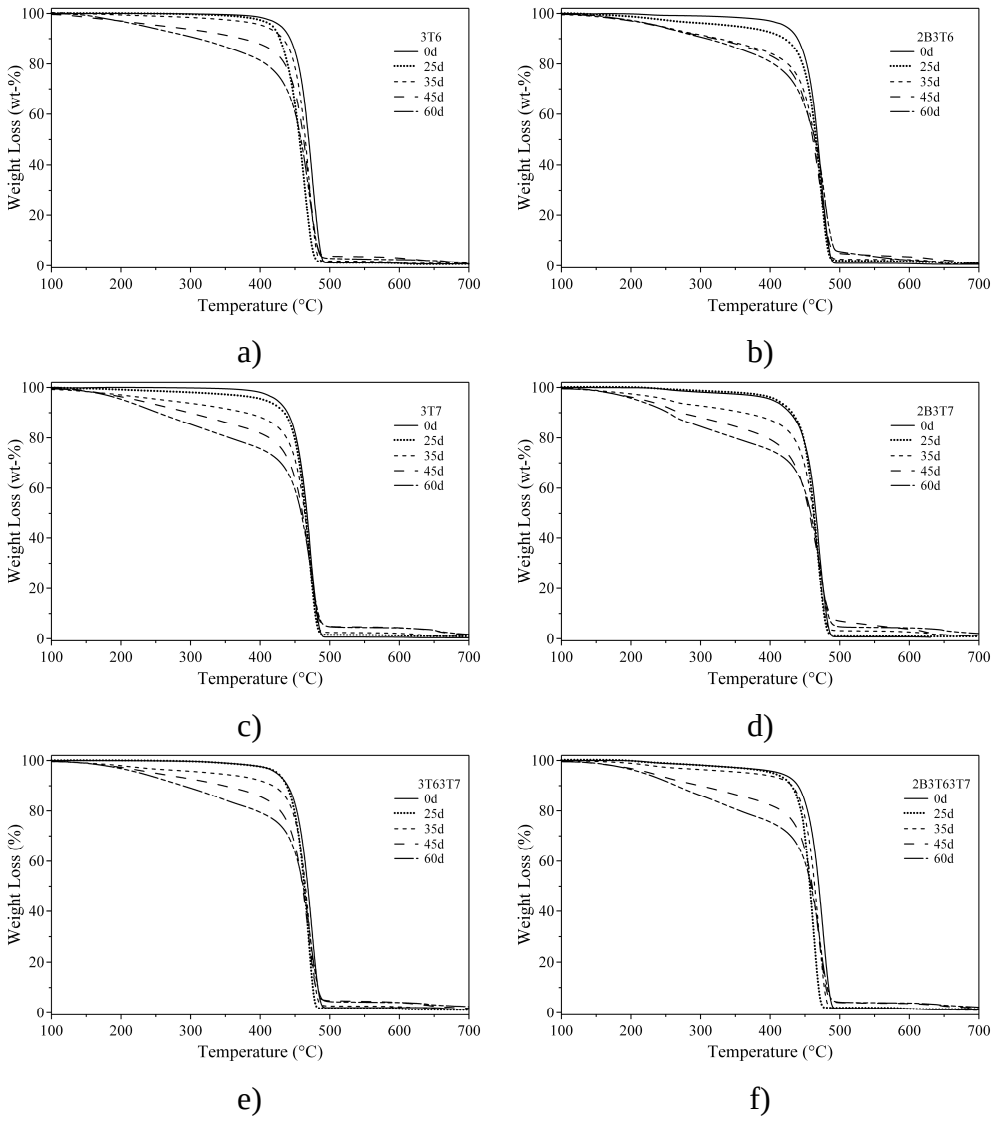


**Figure 3.39.** TGA traces of PE-PHB-prodegradant blends thermal aged at 55 °C up to 60 days.

Figure 3.39 shows TGA traces of samples containing prodegradants without (Fig. 3.39 a), c) and e)) and with PHB (Fig. 3.39 b), d) and f)) and thermo-degraded at 55 °C for up to 60 days. Thermal stability of aged blends decreased with increasing of aging time. Moreover, blends that have been pre-oxidized presented more than one step of weight loss found in pristine materials. These steps are small and overlapped corresponding to the evolution of low MW chemicals formed during the degradation.

This behaviour is illustrated by DTGA trace of 2B3T63T7 blend film in the Figure 3.40. This sample aged for 60 days presented at least six-overlapped weight loss steps. DTGA traces suggest three weight loss steps prior to major degradation step of PE ($T_p$ at 472 °C and *ca.* 67 wt-% of weight loss) that is followed by other two. Each of these steps correspond to 13.7 wt-%, 8.7 wt-%, 6.6 wt-%, 66.6 wt-%, 1.4 wt-% and 1.2 wt-% with increasing of the temperature. The sum of the three initial steps is 29 wt-%. This results are in good agreement with the KE, which was found 23 wt-% of low MW products extracted with boiling acetone after its aging for 60 days.

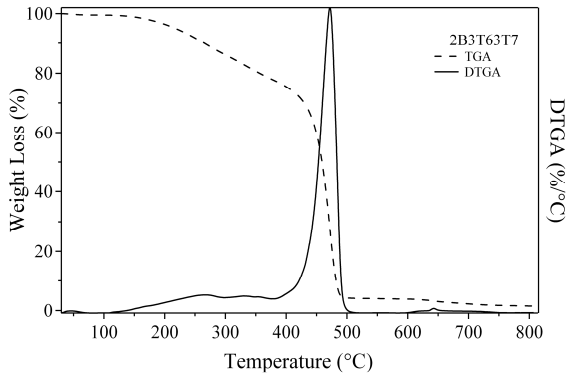


**Figure 3.40.** TGA and DTGA traces of 2B3T63T7 blend aged at 55 °C for 60 days.

Table 3.28 shows the values of TGA decomposition temperature ($T_d$) defined at 1 wt-% of weight loss from blends aged at 55 °C. Blends containing prodegradants decreased its thermal stability in relation to the original material. For example, BT6T7 blend presented $T_d$ values of 358 °C, 335 °C, 163 °C, 150 °C, and 142°C for samples aged by 0, 25, 35, 45 and 60

days, respectively. However, the DTGA peak temperature ($T_p$) values corresponding to the degradation of PE main chain remained practically unaltered during the aging process (Tab. 3.29).

**Table 3.28.** Decomposition temperature ($T_d$ in °C) of aged PE based blends.[a)]

| Sample | Degradation time (days) | | | | |
|---|---|---|---|---|---|
| | 0 | 25 | 35 | 45 | 60 |
| PEL | 391[b)] | 388 | 390 | 385 | 378 |
| 2B | 305 | 294 | 287 | 342 | 304 |
| 3T6 | 386 | 358 | 243 | 132 | 153[b)] |
| 2B3T6 | 301 | 190 | 135 | 146 | 152[b)] |
| 3T7 | 377 | 212 | 121 | 140 | 117 |
| 2B3T7 | 263 | 277 | 142 | 134 | 131 |
| 3T63T7 | 354 | 348 | 145 | 137 | 137 |
| 2B3T63T7 | 239 | 247 | 190 | 135 | 133[b)] |
| BT6T7 | 358 | 335 | 163 | 150 | 142[b)] |

[a)] $T_d$ is decomposition temperature defined at 1 wt-% of weight loss; [b)] The standard deviation from four replicates was *ca.* 3 °C.

**Table 3.29.** $T_p$ (°C) of PE weight loss from aged PE-PHB based blends.

| Sample | Degradation time (days) | | | | |
|---|---|---|---|---|---|
| | 0 | 25 | 35 | 45 | 60 |
| PEL | 474 | 475 | 474 | 474 | 475 |
| 2B | 474 | 473 | 465 | 473 | 466 |
| 3T6 | 475 | 464 | 471 | 471 | 472 |
| 2B3T6 | 473 | 473 | 476 | 473 | 478 |
| 3T7 | 471 | 471 | 472 | 471 | 472 |
| 2B3T7 | 468 | 469 | 470 | 474 | 472 |
| 3T63T7 | 474 | 469 | 470 | 469 | 471 |
| 2B3T63T7 | 476 | 462 | 470 | 469 | 472 |
| BT6T7 | 473 | 455 | 473 | 469 | 469 |

**Table 3.30.** Weight loss (wt-%) of PE degradation step from aged PE-PHB based blends.

| Sample | Degradation time (days) | | | | |
|---|---|---|---|---|---|
| | 0 | 25 | 35 | 45 | 60 |
| PEL | 99.9 | 99.4 | 99.3 | 99.1 | 96.9 |
| 2B | 98.1 | 97.9 | 96.4 | 97.9 | 94.5 |
| 3T6 | 99.3 | 98.1 | 87.4 | 85.5 | 79.9 |
| 2B3T6 | 98.2 | 93.7 | 89.2 | 81.1 | 76.8 |
| 3T7 | 99.0 | 96.5 | 88.1 | 80.4 | 70.8 |
| 2B3T7 | 97.1 | 97.1 | 88.4 | 76.4 | 68.4 |
| 3T63T7 | 97.9 | 98.0 | 92.2 | 84.2 | 72.4 |
| 2B3T63T7 | 96.5 | 96.1 | 93.3 | 81.9 | 66.4 |
| BT6T7 | 98.3 | 97.0 | 90.1 | 82.9 | 73.8 |

Table 3.30 shows weight loss (ΔM) of PE degradation step from aged PE-PHB based blends. This step in the blends decreases as a function of aging time, evidencing that chain scission occurred with the formation of the low MW products as verified in Figure 3.36. In addition, the decrease in the ΔM related to PE was influence by the presence of PHB. For the majority of blends, the value of PE ΔM was lower than that of equivalent blend without PHB. Residue of blends at 800 °C are shown in Table 3.31. The residues of samples at different aged times did not show any significant differences.

**Table 3.31.** Residue (wt-%) at 800°C from aged PE based blends.

| Sample | Degradation time (days) | | | | |
|---|---|---|---|---|---|
| | 0 | 25 | 35 | 45 | 60 |
| PEL | 0.0 | 0.2 | 0.2 | 0.2 | 0.2 |
| 2B | 0.1 | 0.2 | 0.5 | 0.2 | 0.7 |
| 3T6 | 0.7 | 0.8 | 0.9 | 0.6 | 0.9 |
| 2B3T6 | 0.5 | 0.8 | 0.9 | 1.0 | 0.8 |
| 3T7 | 0.4 | 0.7 | 0.6 | 0.9 | 0.9 |
| 2B3T7 | 0.6 | 0.9 | 0.7 | 1.3 | 1.1 |
| 3T63T7 | 1.4 | 1.2 | 1.2 | 1.2 | 1.7 |
| 2B3T63T7 | 1.1 | 1.5 | 0.9 | 1.1 | 1.5 |
| BT6T7 | 1.1 | 1.8 | 1.1 | 1.0 | 1.1 |

DSC traces of original and aged samples from the 1st heating scan are shown in Figure 3.41. It can be observed that there is an enlargement of melting transitions with aging time and in some cases this effect appears as a shoulder (2B3T6). These results could be attributed to changes in crystallite sizes, molecular weight differences (due to chain breaking) and secondary re-crystallization. The presence of shoulders have been previously observed in the aged PE[41, 92, 170-172]. According with Martins *et al.*[173] the crystallinity degree increased with increasing gel content. In these cases, the melting transition detected by DSC scan became broader proportionally to the PE cross-linking increasing. As aforementioned (Tab 3.27) the gel content of samples that have been pre-oxidized increases with thermo-degradation, which confirms this hypothesis.

$T_m$ values are reported in Table 3.32. The original materials showed melting transitions in the range of 108 °C to 110 °C. The $T_m$ values of samples presented a slightly increase with aging time. Original PEL $T_m$ value was 108 °C, which increased to 111 °C for sample aged for 60 days. The highest increase observed was for $T_m$ value of 3T7, which was 109 °C prior aging and resulted 114 °C after 60 days of aging.

**Table 3.32.** DSC 1st heating scan $T_m$ (°C) from aged PE based blends.

| Sample | Degradation time (days) | | | | |
|---|---|---|---|---|---|
| | 0 | 25 | 35 | 45 | 60 |
| PEL | 108 | 109 | 109 | 109 | 111 |
| 2B | 110 | 109 | 109 | 109 | 108 |
| 3T6 | 109 | 109 | 111 | 111 | 112 |
| 2B3T6 | 109 | 110 | 114 | 113 | 113 |
| 3T7 | 109 | 110 | 112 | 112 | 114 |
| 2B3T7 | 110 | 108 | 112 | 112 | 113 |
| 3T63T7 | 108 | 108 | 113 | 112 | 112 |
| 2B3T63T7 | 110 | 111 | 110 | 112 | 114 |
| BT6T7 | 108 | 108 | 111 | 112 | 112 |

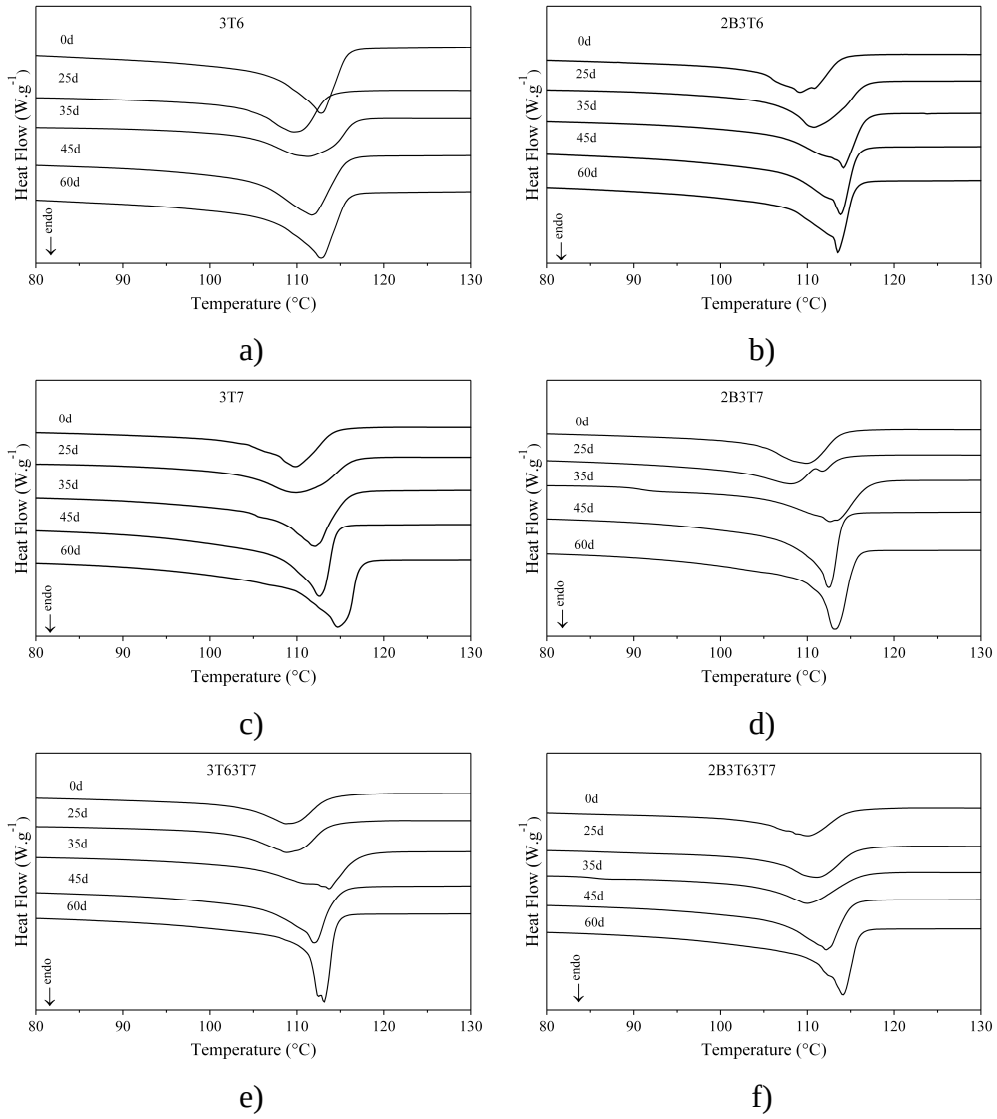


**Figure 3.41.** DSC traces of the 1st heating scan of PE-PHB blends aged at 55 °C up to 60 days.

In Figure 3.42 the crystallinity degree ($X_c$) from melting transition, registered in the 1st heating scan, is correlated with aging time at 55 °C. Un-aged samples presented $X_c$ values between 41 and 45 %. During the thermo-oxidation, PE based blends had their $X_c$ increased up to 45 days. After that, $X_c$ apparently decreased for higher aging times. The highest increases were observed for samples containing prodegradants at 45 days of aging. Some authors consider this increase in crystallinity with aging time as a

consequence of the oxidation of the amorphous phase in the polymer[174] and to the development of a secondary crystallization induced by the formation of shorter segments with greater mobility, originated from chain cleavage during the aging process[174-176]. Khraishi *et al.*[177] have pointed out that the new formed crystalline regions have lower fusion temperatures. In Figure 3.41 e), it can be seen that 3T63T7 samples at 35 days and 60 days of thermo-aging presented both shoulder at left side of PE melting peak (Fig. 3.41 c)) and two peaks centered at 110 °C and 112 °C (Fig. 3.41 e)).

$X_c$ from melting transition, registered in the 2nd heating scan for blends aged at 55 °C are reported in Table 3.33.

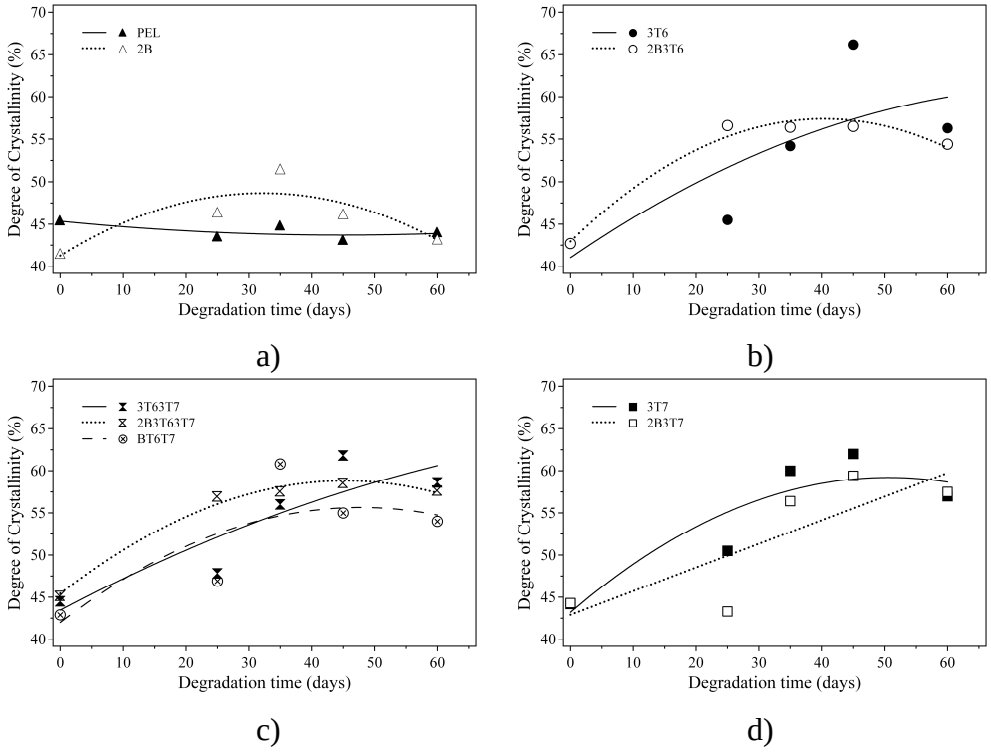


**Figure 3.42.** Degree of crystallinity calculated from the 1st heating scan of aged PE based blends.

**Table 3.33.** Degree of crystallinity (%) from 2st heating scan of aged PE based blends.

| Sample | Degradation time (days) | | | | |
|---|---|---|---|---|---|
| | 0 | 25 | 35 | 45 | 60 |
| PEL | 44.7 | 44.8 | 45.2 | 43.2 | 43.4 |
| 2B | 43.7 | 44.2 | 52.6 | 47.2 | 42.1 |
| 3T6 | 44.5 | 44.5 | 43.5 | 48.2 | 45.5 |
| 2B3T6 | 44.6 | 48.0 | 47.8 | 46.0 | 46.1 |
| 3T7 | 43.3 | 48.7 | 49.3 | 51.0 | 47.1 |
| 2B3T7 | 43.4 | 44.3 | 49.5 | 48.0 | 47.4 |
| 3T63T7 | 42.8 | 48.6 | 51.2 | 52.2 | 46.5 |
| 2B3T63T7 | 42.8 | 49.5 | 46.5 | 47.2 | 47.0 |
| BT6T7 | 44.8 | 47.3 | 51.5 | 47.4 | 54.0 |

As observed in the 1st heating, $X_c$ values of samples from melting transition registered in the 2nd heating scan increased with the aging time up to 45 days and then decreased. The $X_c$ values were lower in relation to that obtained in the 1st heating scan. For example, 3T7 $X_c$ values calculated from the 2nd heating scan where 2 %, 4 %, 18 %, 18 % and 18 % lower than that calculated from the 1st heating at 0, 25, 35, 45 and 60 days of aging, respectively. According to Craig *et al.*[143], when samples that have been pre-oxidized are treated by melt-cooling cycle, the crystallinity of the new solidified material will depend not only on the polymer and the cooling conditions but also on the molecular changes that occurred during the oxidation process. In this way, the shorter chains produced by scission events will crystallize more readily whereas cross-links and molecular defects will not be able to crystallize and will be rejected from the newly formed crystals. Thus there are opposing effects, one that promotes greater crystallization and the other inhibiting crystallization.

***Mechanical properties***

Another way to characterize the thermo-degradation of polymeric materials is through the loss in their mechanical properties[38, 178, 179]. Hence,

tensile tests can be used as a parameter to determine the oxidation end point in degradable PE. According with ASTM D5510[178], the embrittlement endpoint of oxidatively degradable plastics is achieved when 75 % of the specimens tested presented elongation at break of 5 % or less. In addition, it is generally accepted that failure of the degraded polymers involves fracture in materials that has become brittle by the molecular degradation caused by oxidation[167, 180]. The properties of thermoplastics depend very significantly on their chain length and it is, therefore, to be expected that chain scission and cross-linking reactions will have a strong effect on property changes. Table 3.34 shows the change in the thickness of films during 60 days at 55 °C. The thickness of all films did not present significant changes during thermo-degradation process.

**Table 3.34.** Thickness (mm) of PE-PHB based blends thermal-aged at 55 °C for 60 days.[a)]

| Sample | Degradation time (days) | | | | |
|---|---|---|---|---|---|
| | 0 | 25 | 35 | 45 | 60 |
| PEL | 0.10 | 0.09 | 0.10 | 0.10 | 0.10 |
| 2B | 0.06 | 0.05 | 0.06 | 0.06 | 0.06 |
| 3T6 | 0.05 | 0.05 | 0.07 | 0.06 | 0.07 |
| 2B3T6 | 0.10 | 0.10 | 0.17 | 0.13 | 0.09 |
| 3T7 | 0.06 | 0.07 | 0.06 | 0.09 | 0.08 |
| 2B3T7 | 0.07 | 0.04 | 0.05 | 0.05 | 0.05 |
| 3T63T7 | 0.08 | 0.07 | 0.08 | 0.07 | 0.07 |
| 2B3T63T7 | 0.07 | 0.07 | 0.07 | 0.07 | 0.08 |
| BT6T7 | 0.07 | 0.06 | 0.05 | 0.05 | 0.06 |

[a)] The standard deviation from five replications was *ca*. 0.01 %.

The results of tensile tests performed on PE-PHB films are shown in Figures 3.43 – 3.45. It can be observed that in the two group of samples without prodegradants (PEL and 2B), the Young modulus (YM), tensile stress at break (ST) and strain at break (SB) values did not change significantly with aging time, while in blends containing prodegradants a significant fall in ST and SB properties was recorded. On the other hand, the

YM of samples containing prodegradants increased with the aging time. The highest YM (*ca.* 330 MPa) were observed for samples containing higher amounts of prodegradants (6 wt-%) 3T63T7 and 2B3T63T7 at 45 days of temperature exposure (Fig. 3.43 c)). The increase in the YM can be explained through the increase in the crystallinity of samples. More crystalline materials are more fragile, hard, deform little and need higher energy to deform[175]. Similar results were found by Tavares *et al.*[152] and Gulmine *et al.*[175] studying the effect of accelerated aging on the surface mechanical properties of PE and the correlations between structure and accelerated artificial ageing of XLPE, respectively. These authors found that with increasing of the aging time the samples presented an increase in YM that was attributed to the increase in the crystalline content of samples.

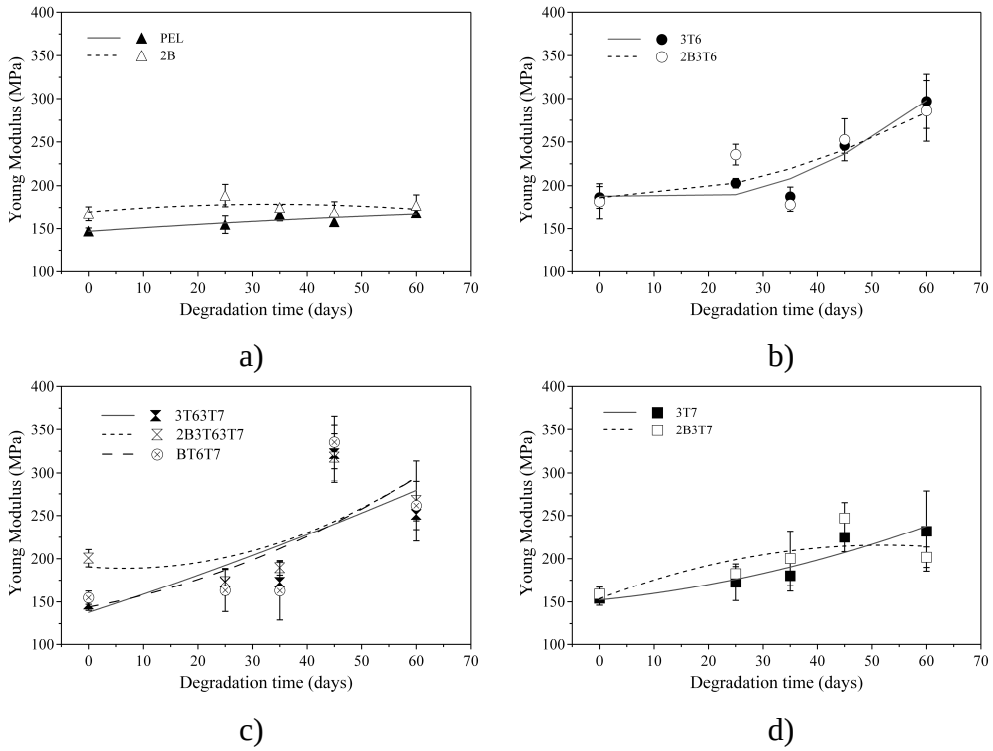


**Figure 3.43.** Young's modulus of aged PE-PHB based blends for 60 days at 55 °C.

As observed in Figure 3.42, the crystallinity of samples containing prodegradants is higher, and consequently the chains do not have the necessary mobility. According with Gulmine and Akcelrud[175], an increase in the crystallinity of the materials during aging should lead to higher values of tensile stress at break due to the reinforcement induced by ordering and crystallinity during stretching. However, this was not observed in this work. In Figure 3.44, the highest ST values were obtained for sample not aged and ST values decreased with aging time. Roy *et al.*[40] studying the effect of cobalt carboxylated on the degradation of PE obtained similar results, a decrease in ST and SB of samples with UV irradiation exposure.

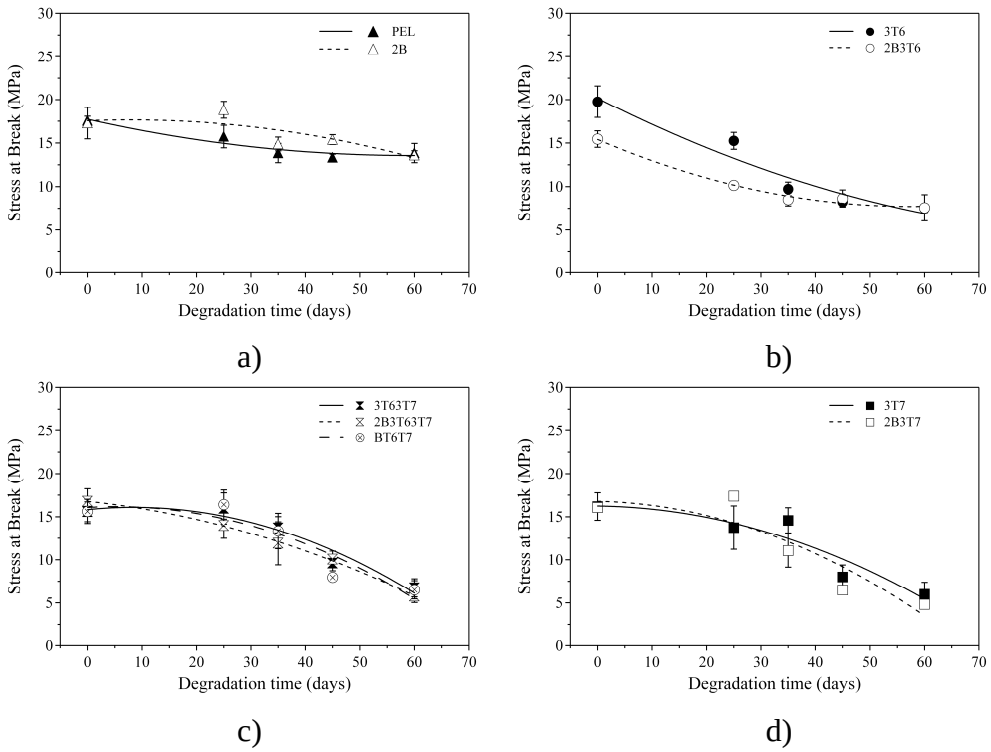


**Figure 3.44.** Stress at break (ST) of aged PE-PHB based blends for 60 days at 55 °C.

As it can be seen in Figure 3.45, the SB of samples decreased quickly with aging time. Roy *et al.*[181] in their study about the degradation of LDPE containing cobalt stearate argue that significant decay in LDPE properties start at a $CO_i$ greater than 6 ($CO_i$ was calculated as the relation between the band at 1740 $cm^{-1}$ and the band at 2020 $cm^{-1}$). PE-PHB blends presented a

significant decay in SB of samples after 25 days of thermo-degradation ($CO_i$ of about 0.5). At 45 days of thermo-degradation at 55 °C ($CO_i$ of about 2.5), all samples containing prodegradants had reached the embrittlement endpoint according to ASTM D5510[178]. The drop in SB values was faster for 3T6 and 2B3T6 samples than for other blends. As for instance, 3T6 sample decreased its SB values from 245 % measured in the original films to 82 %, 32 %, 5% and 3 % after 25, 35, 45 and 60 days of thermo-degradation, respectively. For 2B3T7 blend this decrease was still quick, the films decreased its SB values from 405 % measured in the original films to 22 %, 21 %, 5% and 3 % after 25, 35, 45 and 60 days of thermo-degradation, respectively. On the other hand, 3T63T7 blend presented a decrease from 321 % measured in the original films to 281 %, 171 %, 5% and 3 % after 25, 35, 45 and 60 days of thermo-degradation, respectively.

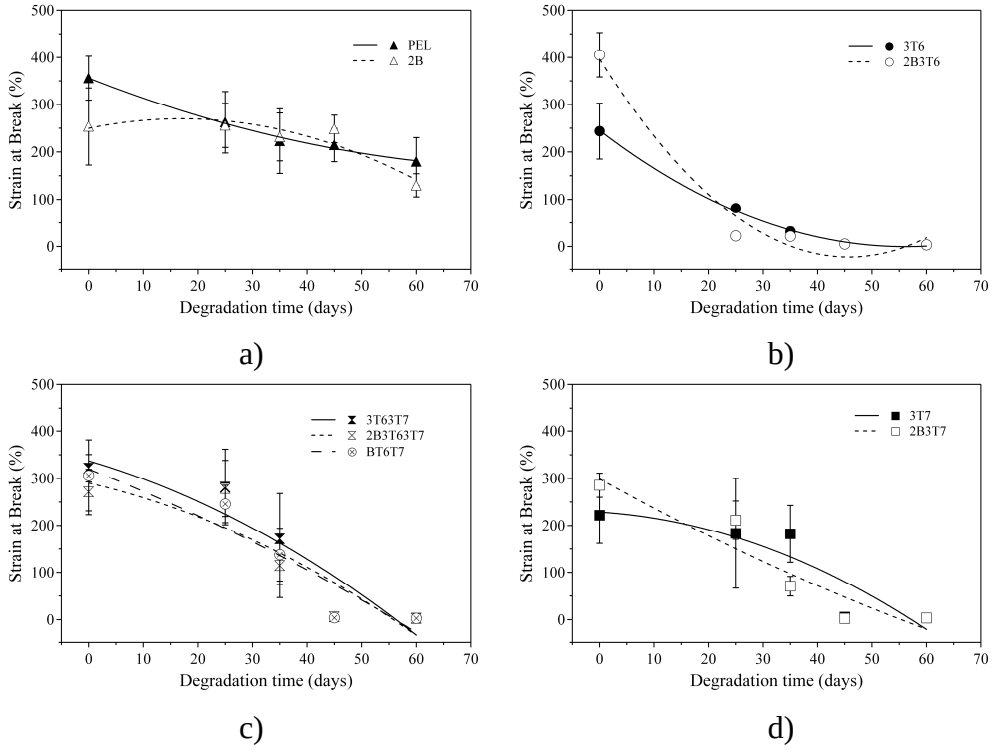


**Figure 3.45.** Strain at break (SB) of aged PE-PHB based blends for 60 days at 55 °C.

The reduction in the mechanical performance (ST and SB) of samples match very well with the chemical degradation of materials, followed through the carbonyl formation (Fig. 3.34) and the increase in the amount of low MW products formed during aging (Fig. 3.36). In PE-PHB films containing prodegradants, the significant decrease in the tensile stress and strain at break occurred at 25 days of aging (Fig. 3.45), which is the time when $CO_i$ starts to increase significantly. At this time, probably the amount of low MW polymer chains starts to increase contributing to the reduction in the tensile stress (Fig. 3.44) and strain at break of samples (Fig. 3.45). In addition, the simultaneous occurrence of chemical modifications as oxidation and cross-linking contribute to the development of surface tension and cracking[152] with a consequent reducing in the ST and SB of samples.

Moreover, the increase in the crystallinity brings the formation and propagation of cracks, decreasing the strain at break of samples. This can be explained because the increase in crystallinity is, of course, accompanied by a corresponding decrease in the amorphous content. For semi-crystalline polymers such as PE, which $T_g$ is below room temperature, the amorphous phase is very deformable and the reduction in the fraction of the material that is in this state will inevitably reduce the overall deformability of the material and cause it to become more brittle[182]. The increasing number of cross-links also reduces ductility, and the increase in chain scission reduces the network of entanglements that the amorphous phase requires for its mechanical integrity[166, 167, 182].

### 3.2.3. *Biodegradation*

In most cases, plastic materials should survive a predetermined service life before physical degradation starts. This means that no significant changes in their physical and mechanical properties during its service life are expected to take place. However, after the material has served to its primary purpose, rapid biodegradation and disintegration should occur. Hence, all biodegradable polymers are in a delicate balance between the achievement of useful technological performance and a rapid and effective biodegradability. This work was performed as a complementary study of the previous one. These studies together can be used as a model for the prediction of the behaviour of oxo-biodegradable materials, where both lifetime and mineralization time can be determined.

The biodegradation of polymers proceeds via hydrolysis and oxidation. The rate of degradation is sensitive to microbial population, moisture, temperature and oxygen in the environment[183, 184]. Microbial degradation occurs when fungi and bacteria attack the plastic material under aerobic or anaerobic conditions. Besides, microbial activity can change the structure of the compounds in the medium, thus causing chemical degradation[184]. In addition, bio-surfactants that act as emulsifiers are supposed to play an important role in the biodegradation of hydrophobic compounds[184]. Most of the biodegradable synthetic polymers and biopolymers contain hydrolysable groups along the main chains. Initial studies of biodegradation mechanisms were motivated by biomedical applications of biodegradable polymers. In recent years polymer waste management through biodegradation and bioconversion has become more important[185]. Considering the great variation in natural conditions, the biodegradability of polymers varies significantly on a global scale, as well as within smaller ecosystems.

PE-PHB based blends containing prodegradant additives (T6 and T7) previously exposed to thermal aging at 55 °C for 60 days were submitted to biodegradation experiments in two different environments, aquatic and soil burial (Tab. 3.35). Samples not thermal-aged were also biodegraded for comparison. Blends were assessed with respect to the extent of

mineralization through carbon dioxide evolved. In addition, the ability of blends to support microbial growth when used as the only source of carbon was evaluated through SEM analysis. During biodegradation experiments, EDS and DSC were used to verify possible release of additives in aquatic media, and crystallization, respectively. Changes in the degradation behaviour of blends and in its polymeric matrix structure were evaluated through TGA and FTIR, respectively.

**Table 3.35.** Samples used in biodegradation experiments in aquatic medium (AM) and soil burial (SBi).

| | AM | | | SBi | | |
|---|---|---|---|---|---|---|
| Sample [a)] | PS | TAS | KE | PS | TAS | KE |
| PEL | X | X | — | — | — | — |
| 2B | X | X | — | — | — | — |
| 3T6 | X | X | X | X | X | — |
| 2B3T6 | X | X | X | X | X | — |
| 3T7 | X | X | X | X | X | — |
| 2B3T7 | — | — | X | X | X | — |

[a)] See Table 2.6 for code definition; PS: Pristine Sample; TAS: Thermo Aged Sample; KE: Low molecular weight compounds extracted from TAS with boiling acetone.

Samples of PE based blends oxidized and also their thermo-oxidation products (acetone extractable fractions) were assessed by means of the rate of biodegradation. In this way, samples PELt, 2Bt, 3T6t and 2B3T6t correspond to PEL, 2B, 3T6 and 2B3T6 that had been pre-oxidized at 55°C for 60 days before the biodegradation experiments, respectively. Samples 3T6e, 2B3T6e, 3T7e and 2B3T7e correspond to the acetone extractable fractions of 3T6, 2B3T6, 3T7 and 2B3T7, respectively.

For aerobic aquatic biodegradation, docosane was used as reference material. In soil burial experiments, the biodegradation of pure Whatman cellulose filter paper (PWC) was used as reference. Docosane and PWC

biodegradation were also an important control to assess the microbial activity during all the experiment.

#### *3.2.3.1 CHN analysis*

The amount of total organic carbon (TOC) of PE-PHB based blends was obtained by CHN elemental analysis. The results are reported in Table 3.36. The total carbon present in the each sample was used to calculate the mineralization of the respective material as described in Section 2.6.

**Table 3.36.** Elemental analysis of PE-PHB based blends

| Sample[a)] | C (wt-%) | H (wt-%) | Sample | C (wt-%) | H (wt-%) |
|---|---|---|---|---|---|
| PWC | 41.40 | 5.94 | 2B3T6 | 71.25 | 11.70 |
| PEL | 85.65 | 14.82 | 2B3T6t | 73.72 | 11.40 |
| PELt | 85.24 | 15.43 | 2B3T6e | 80.04 | 14.03 |
| 2B | 83.56 | 13.72 | 3T7 | 82.53 | 14.68 |
| 2Bt | 84.28 | 15.40 | 3T7t | 77.57 | 12.95 |
| 3T6 | 83.93 | 15.14 | 3T7e | 72.45 | 12.16 |
| 3T6t | 67.34 | 11.50 | 2B3T7 | 84.28 | 14.80 |
| 3T6e | 71.46 | 11.84 | 2B3T7t | 74.89 | 11.50 |
| | | | 2B3T7e | 67.29 | 11.60 |

[a)] See Table 2.6 for code definition.

#### *3.2.3.2 Aerobic aquatic biodegradation*

Aerobic aquatic biodegradation experiments are a common screening test[184] used before other biodegradation tests in order to check the potential extent of biodegradability of different materials, soluble, insoluble or low soluble in water[83, 186, 187]. This type of experiment is known for its severe conditions during tests, which means that a positive results in these

experiments is an evidence that the readily biodegradability of a material may occurs quickly in the environment. However, a negative or a low degradability result in the test does not mean that the material is not biodegradable when exposed to natural environments.

***Morphology***

SEM is a significant and reliable tool to measure the morphological changes of degraded polymer. Surface morphology of films changed after biodegradation. SEM micrographs of surface of films of PE-PHB based blends submitted or not to a previous thermo-oxidation process before and after 125 days of incubation in aquatic medium (AM) at 25 °C are shown in Figures 3.46 – 3.49.

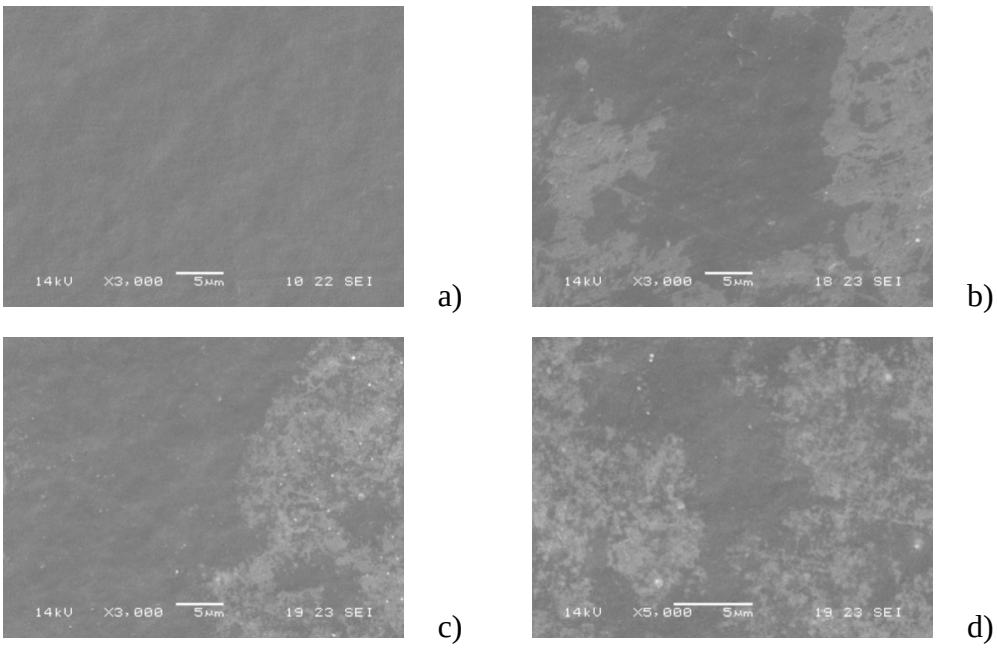


**Figure 3.46.** SEM of PE-PHB blend surfaces: a) PEL pristine – 3000X; b) PEL125d – 3000X; c) PELt – 3000X; d) PELt –125d – 5000X.

Figure 3.46 shows that PEL matrix previously exposed or not to a thermal aging did not support any microorganism growth and no clear signs of bioerosion could be found on the surface of PEL films.

The thermal treatment and the water exposition of the PE-PHB based blends lead to a partial disintegration of the films surfaces. This phenomena can be clearly seen in Figure 3.47 b)-d) and 3.48 b) where some holes can be observed in the surface of the films. According with Kumar *et al*.[188] these holes formed on surface of oxidized films are due to the removal of volatile oxidation products that have been formed during thermo-degradation. However, these cavities can also bee observed in samples incubated in AM for 125 days which have not been pre-oxidized (Fig. 3.47 b)). PHB can degrades in water. Majid *et al*.[189] studying the kinetics of hydrolytic degradation of PHB at 37 °C in buffer solution showed that its degradation in water occurs by surface hydrolysis. Probably the presence of these holes in 2B sample is due to both the PHB degradation in water and the PHB consumption by microbes during biodegradation. It is well known that PHB alone is a totally biodegradable polymer. Bucci *et al*.[190] demonstrated the easy of PHB packaging biodegradation after 90 days in AM, containing sewage inoculum. Zhao *et al*.[191] showed that pure PHB degraded rapidly, and after 21 days of exposure in soil-mineral solution, its weight reached 53.6% of the initial value. This surface disintegration can also be seen in samples without PHB containing T6 and T7 (Figure 3.48 - 3.49). Moreover, it can be clearly seen in Figure 3.48 b) the presence of microorganisms in the film surface, demonstrating that the prodegradants used were no toxic to sewage microorganisms. These results are in agreement with that found by Bonhomme *et al.*[134]. These authors studied the biodegradation of PE by both biotic oxidation in air oven and in the presence of selected microorganisms. They observed that the colonisation of microorganisms occurred in both samples that had been pre-oxidized or not.

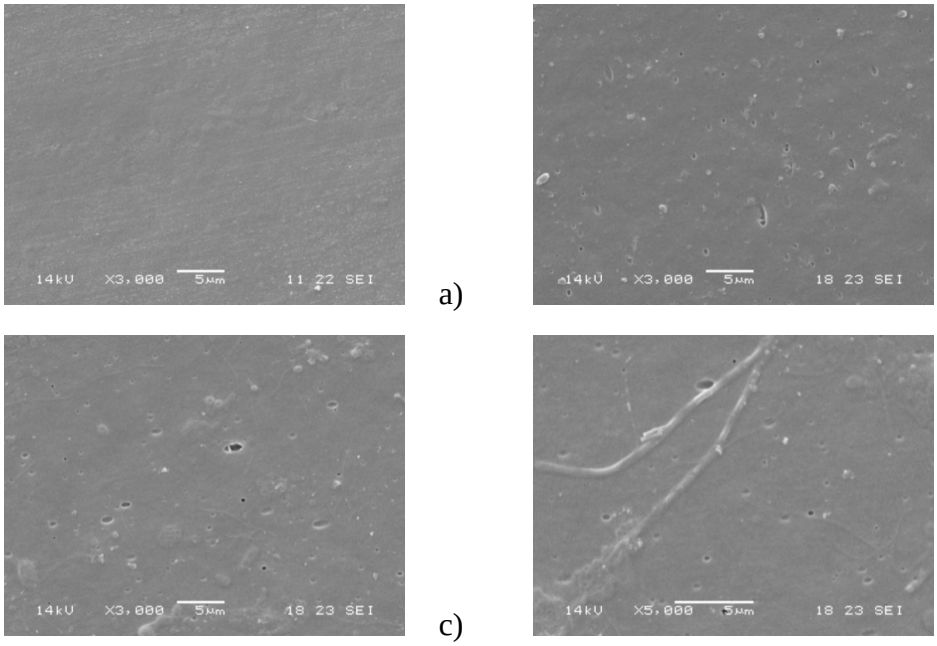


**Figure 3.47.** SEM of PE-PHB blend surfaces: a) 2B pristine – 3000X; b) 2B-125d – 3000X; c) 2Bt– 3000X; d) 2Bt–125d – 5000X.

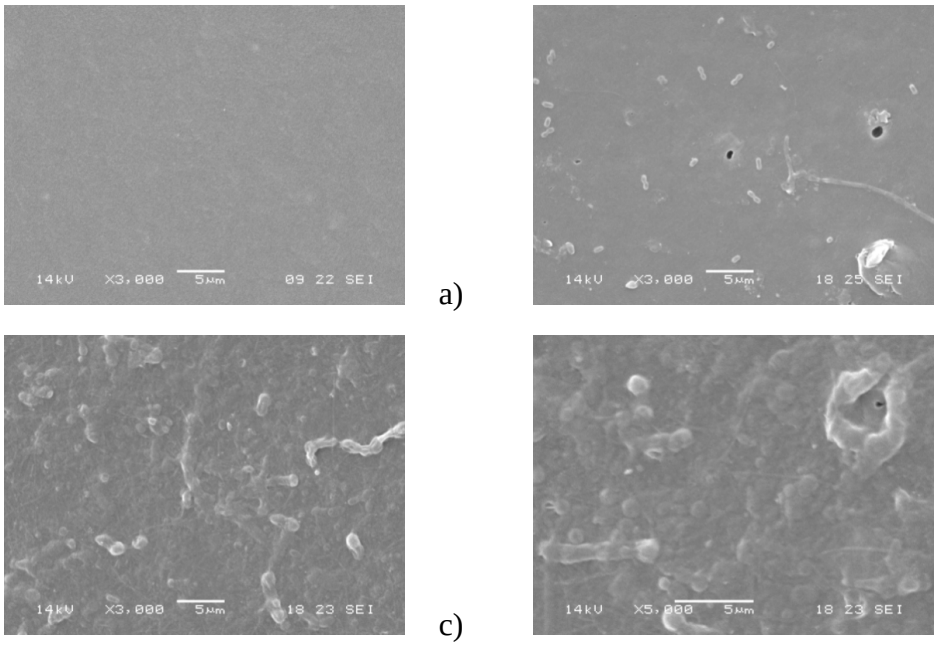


**Figure 3.48.** SEM of PE-PHB blend surfaces: a) 3T6 pristine – 3000X; b) 3T6-125d – 3000X; c) 3T6t– 3000X; d) 3T6t–125d – 5000X.

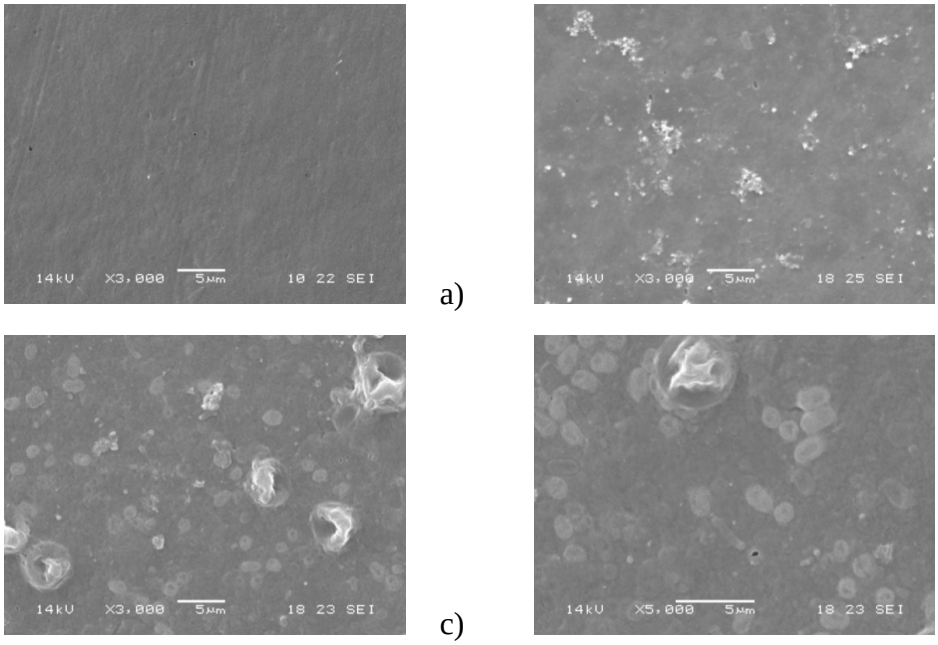


**Figure 3.49.** SEM of PE-PHB blend surfaces: a) 2B3T6 pristine – 3000X; b) 2B3T6-125d – 3000X; c) 2B3T6t– 3000X; d) 2B3T6t–125d – 5000X.

***Microanalysis (EDS)***

Scanning electron microscopy in combination with energy dispersive X-ray microanalysis (SEM/EDS) was used to characterize composition and homogeneity in the sample films before and after 125 days of aquatic biodegradation. The application this technique facilitates a concurrent analysis of both elemental composition and morphology of samples.

Figures 3.50 – 3.51 show the back scattering image and composition of pristine T6 and T7 additives. Besides, the results of the composition of T6, T7 and the PE-PHB based blends in terms of prodegradants are summarized in Table 3.37. Both T6 and T7 prodegradants presented calcium (Ca) and cobalt (Co) in their composition. T7 have less carbon and more transition metals than T6. Moreover, it can be seen that even after 125 days of incubation of samples in aquatic media, prodegradants did not released from the film. It can be noted that after incubation the carbon content of PE samples decreased probably due to the mineralization of samples. Besides,

the oxygen amount in samples increased 67 wt-% for 3T6 and 71 wt-% for 2B3T6 sample. Jakubowicz[37] studying the degradability of biodegradable PE in microbial activated soil at a constant incubation temperature of 60 °C reported that some additional oxidation takes place during biodegradation experiments. Albertsson *et al.*[25] reported the alkane chain oxidation to carboxylic acid and also to the ester formation due to microbial action of alkanes. Small traces of Si were found in both T6 (*ca.* 0.3 wt-%) and T7 (*ca.* 1 wt-%).

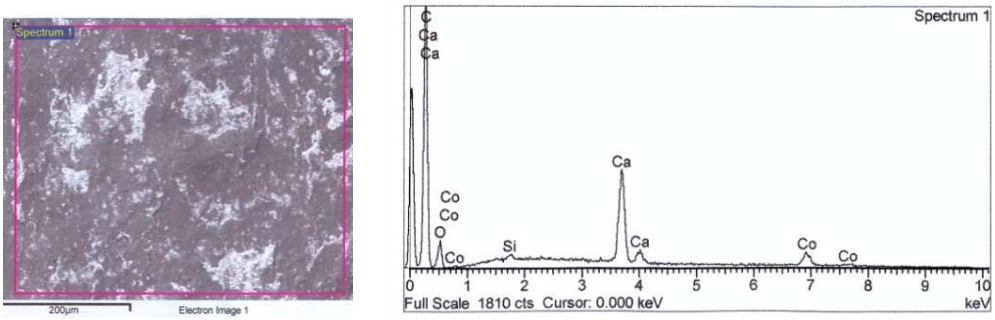


a) b)

**Figure 3.50.** Back scattering image of pristine T6 additive (a) and composition (b).

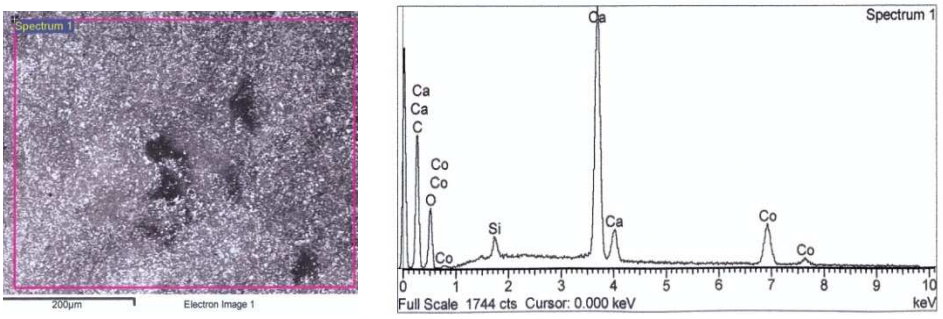


a) b)

**Figure 3.51.** Back scatteting image of pure T7 additive (a) composition (b).

**Table 3.37.** Elemental microanalysis of T6, T7 prodegradants and PE-PHB based blends.

| Sample | Carbon (wt-%) | Oxygen (wt-%) | Calcium (wt-%) | Cobalt (wt-%) |
|---|---|---|---|---|
| T6 | 63.5 | 22.1 | 9.4 | 4.7 |
| T7 | 34.8 | 33.4 | 19.3 | 11.5 |
| BT6T7 | 91.7 | 7.1 | 1.12 | nd[a)] |
| 3T6 | 92.9 | 6.2 | 0.9 | — |
| 3T6-125d | 88.9 | 10.2 | 0.9 | — |
| 2B3T6 | 91.9 | 7.0 | 1.1 | — |
| 2B3T6-125d | 86.7 | 12.1 | 1.2 | — |

[a)] nd = not detected.

Figures 3.52 – 3.53 present the back scattering images and composition of 3T6 blend before and after the exposition of the film for 125 days in a mineral salt medium. In Figures 3.54 – 3.55 are shown the back scattering images and composition of 2B3T6. It can be seen that the prodegradants are homogeneously dispersed in the film surface.

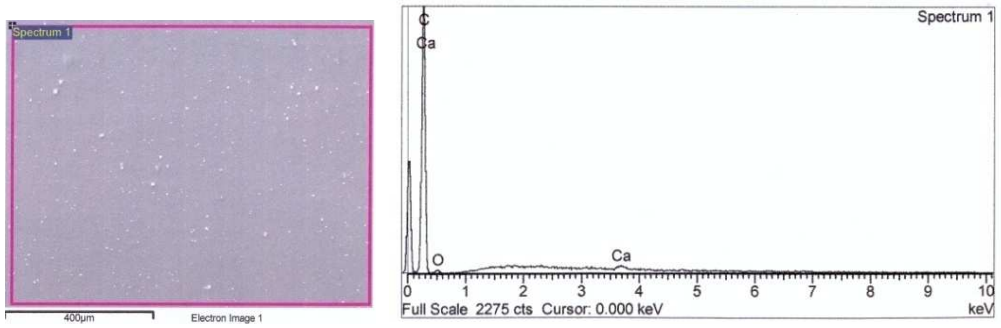


a) b)

**Figure 3.52.** Back scattering image of 3T6 before biodegradation (a) and composition (b).

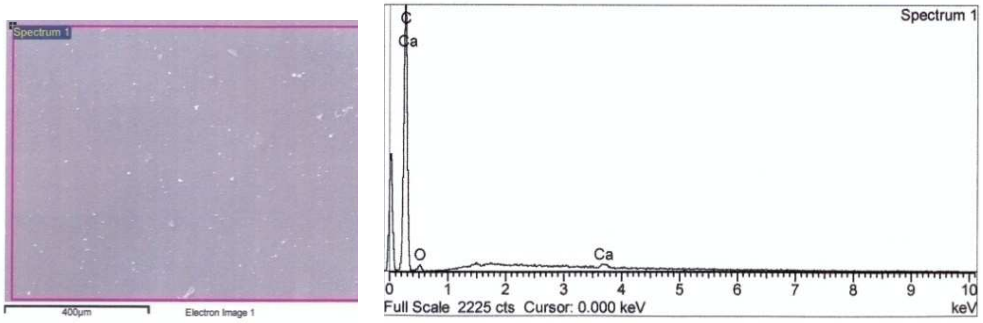


a) b)

**Figure 3.53.** Back scattering image of 3T6 after 125 days of biodegradation (a) and composition (b).

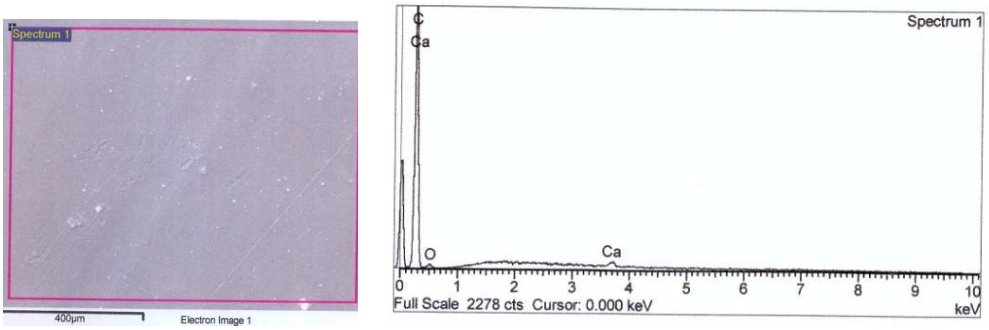


a) b)

**Figure 3.54.** Back scattering image of 2B3T6 before biodegradation (a) and composition (b).

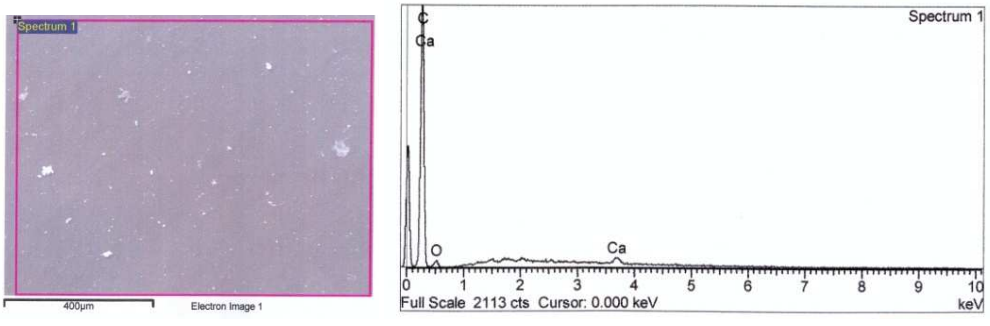


a) b)

**Figure 3.55.** Back scattering image of 2B3T6 after 125 days of biodegradation (a) and composition (b).

***Carbon Dioxide Evolved***

The mineralization of samples was assessed through aquatic aerobic biodegradation experiments. During degradation tests, docosane was utilized as reference material due to its recognized biodegradability[86]. Figure 3.56 shows the mineralization behaviour of docosane during 125 days of biodegradation. As it can be seen, biodegradation began immediately after the test was launched. Besides, within the time of degradation, docosane mineralization arrives at more than 50 % evidencing the activity of the microorganisms.

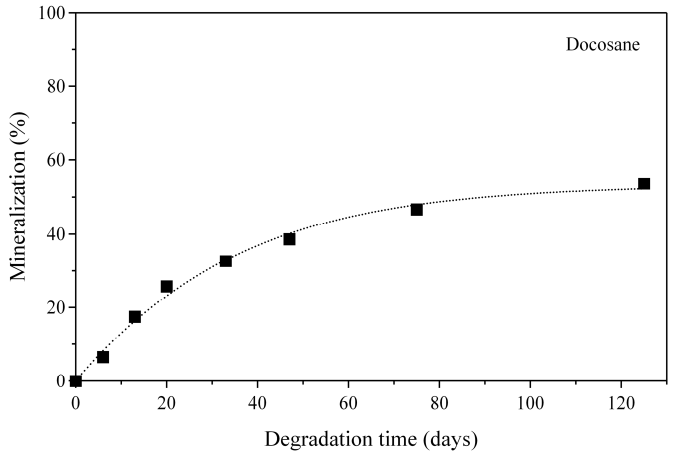


**Figure 3.56.** Mineralization behaviour of docosane during 125 days in aquatic aerobic biodegradation experiments.

Figure 3.57 shows the mineralization of PE-PHB based blends without prodegradants during biodegradation in aquatic media. Samples without prodegradants were used to compare their effect on biodegradationof blends. It is known that the characteristic hydrophobicity of PE constitutes a high obstacle for its biodegradation[192]. As it can be observed, both PEL and PELt samples showed low mineralization values. These values yields up to a maximum of 5 % for PEL and 2 % for oxidized PELt after 40 days of biodegradation and stagnated at these levels up to the incubation of 125 days in aquatic media. This probably occurs because PE consists of molecules

with an extremely high molecular weight (MW), typically several hundreds of thousands Daltons formed by -$CH_2$- units[38]. So, the MW itself represents a serious problem because as a molecule of this size cannot enter in the cell, it is inaccessible to intracellular enzyme systems.

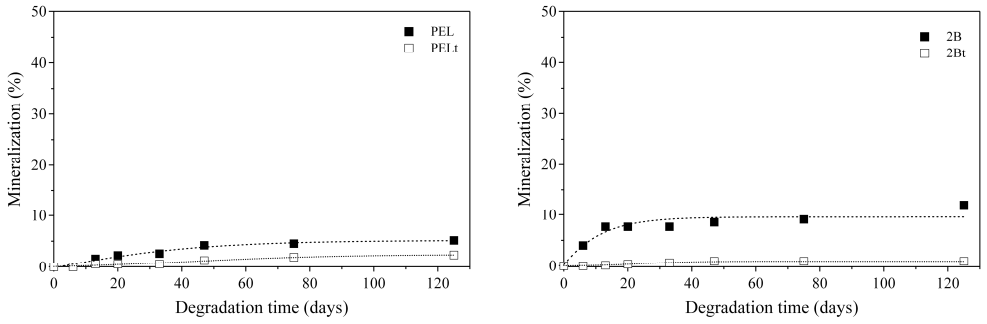


a) b)

**Figure 3.57.** Mineralization behaviour of PE-PHB based blends during 125 days in aquatic aerobic biodegradation experiments: (a) PEL, and (b) 2B.

For other macromolecular substrates, in general microorganisms often find the solution in the production of extracellular enzymes, which cut macromolecules to smaller fragments that can finally cross a cell wall and a cytoplasmic membrane. The PE molecule contains only non-polar C-C and C-H bonds which do not provide centers for nucleophilic or electrophilic attack, and the possibilities for its chemical reactivity are strongly limited, mainly to radical reactions[38]. Moreover, thermo-aged samples had an enormous amount of gel (21 wt-% for PEL and 75 wt-% for PELt). In this way, it can be supposed that hydrophobic PE molecules are densely linked limiting the diffusion of water and possible reactive molecules produced by microorganisms. So that, in these cases only the surface of the films, which have a limited number of free chain ends could be available for the enzymatic action. Hence, in PELt and 2Bt blends with 75 wt-% and 70 wt-% of gel and 44 % and 43 % of crystallization, respectively, there is practically no water and oxygen diffusion. Huang and Edelman working with gelatine observed that cross-linking decrease biodegradation rates[185]. Molitoris *et al.*[193]

demonstrated that a high degree of cross-linking can inhibit the biodegradation process of PHAs. In addition, the degradation rate of PHB was found to be dependent on sample crystallinity[65]. On the other hand, 2B sample presented a higher mineralization value than 2Bt, which was *ca.* 10 %. This increase in relation to 2Bt is probably due to both the biodegradation of PHB fraction present in the surface of the film and the small amount of cross-linking. As the gel content presented for 2B sample (15 wt-%) is much lower than for 2Bt (70 wt-%), the PHB present in the surface of 2B film could be more susceptible to microbial attack than PHB present in 2Bt sample, which probably had already been degraded during the thermo-aging.

Figure 3.58 shows the mineralization of samples containing prodegradants. It can be observed that samples containing prodegradants that had been exposed to a thermal oxidation and the low MW PE components (extracts) of these samples presented a fast growth in the mineralization during the firsts days of incubation. On the other hand, pristine samples presented a stationary induction time of 20 days (Fig. 3.58 a)) and 40 days (Fig. 3.58 b)) before the beginning of the biodegradation. Besides, thermo-degraded samples presented higher mineralization values than pristine ones. As discussed before, thermal aged samples (TAS) presented a high amount of low MW compounds. Hence, the elevated mineralization can be a consequence of the assimilation by microorganisms of these low MW compounds. These compounds could be released to aquatic media from oxidized PE based films and in this way they could be easily consumed by microorganisms. The mineralization of PE-PHB based blends without prodegradants, which have been pre-exposed to a thermal aging or not arrived at maximum values of about 6 wt-%. On the other hand, the highest values of mineralization were obtained for the low molecular weight compounds extracted from TAS with boiling acetone (KE). For these samples, the extent of mineralization reached 22 % for 2B3T6e and 32 % for 2B3T7e (Fig. 3.58 b) and d)). Probably this occurred because at the beginning of the biodegradation, a high amount of MW compounds supported the microorganism growth and consequently caused an increase in the mineralization amount. These compounds were probably the low MW

degradation products of PE chains terminated with carboxylic and aldehydes groups already observed in the FTIR analysis.

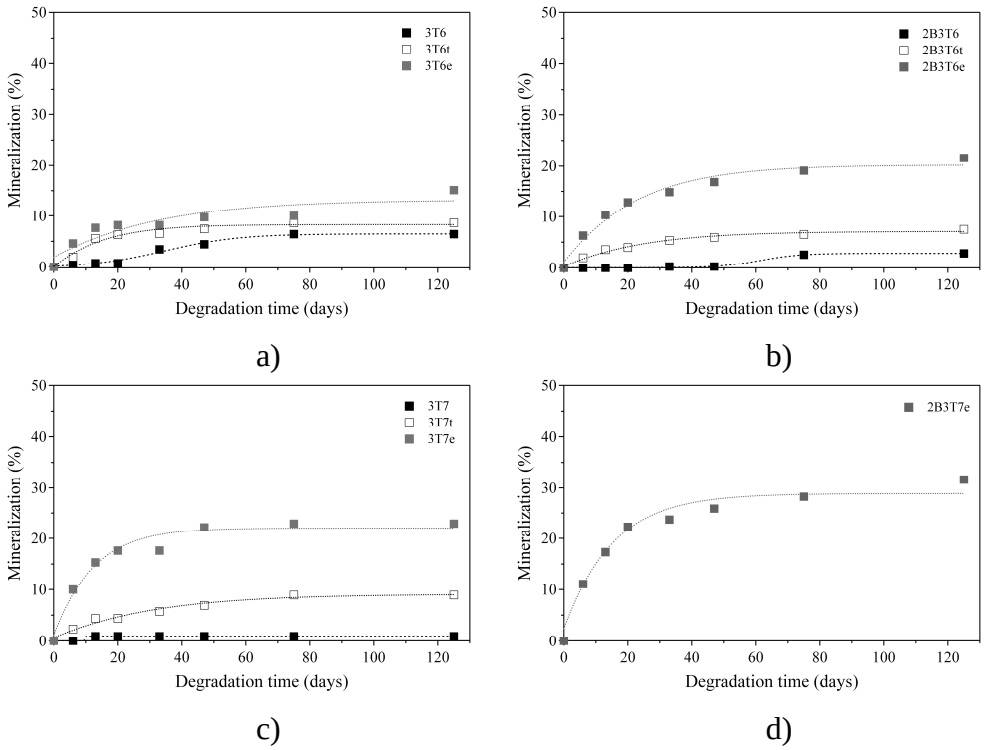


**Figure 3.58.** Mineralization behaviour of PE-PHB based blends during 125 days in aquatic aerobic biodegradation experiments: (a) 3T6, (b) 2B 3T6, (c) 3T7 and (d) 2B3T7.

Koutney *et al.*[194] followed the release of low molecular compounds to water media from thermo and photo-oxidized HDPE and LDPE samples both containing a balance of antioxidants and pro-oxidants by NMR. These substances were subsequently completely consumed by *Rhodococcus rhodochrous* strain during 4 days of cultivation. The same samples without oxidation pre-treatment did not release any substances. Jakubowicz *et al.*[37] in their study about the degradability of biodegradable PE in microbial activated soil at a constant incubation temperature of 60 °C concluded that when the material is degraded into low molecular mass products, it is bioassimilated quickly. Albertsson *et al.*[195] argue that the low molecular weight products are preferentially removed directly from the surface of the

polymer by metabolizing organisms and subjected to bioaccumulation and/or biotransformation. Moreover, at the end of the incubation period (125 days) the KE samples, which are formed of low MW compounds presented the highest mineralization values.

Chiellini *et al*.[86] assessing the mineralization of LDPE containing prodegradants (the films and the KE) in river water found that the oxidation level of samples can influence significantly the biodegradation of them. In their study, the highest mineralization values (*ca.* 30 % for films and *ca.* 40 % for KE) were obtained for samples at the end of oxidation process. It can be noted that the results as demonstrated in Figure 3.58 indicate that the mineralization of materials occurred up to ca. 70 days of biodegradation achieving a plateau, which followed until 125 days. This could be explained taking into consideration the weakness of the microorganism communities used. The same behaviour was reported by Chiellini et al.[135] studying the biodegradation of PE oxidized samples in forest soil and mature compost. These authors observed that at the beginning of experiment a very fast period of biodegradation of about 30 days was recorded and at the end of which carbon dioxide production reached a plateau corresponding to about 4 wt-% of mineralization and remained at this value. This period without significant mineralization remained until 160 days and then the authors tried to revitalize the microbial community by a new inoculation with a small amount of fresh forest soil, agitation and moistening.

***Thermogravimetry Analysis (TGA)***

Data related to TGA analysis of blends are reported in Table 3.38. The degradation temperature ($T_d$) was defined as the temperature at 1 wt-% of weight loss. $T_{di}$ errors were calculated using four replicates of 3T6t and 2B3T6t samples. These samples represent the family of materials containing 3 wt-% of prodegradant T6 with and without PHB, which had been thermo-degraded for 60 days in an oven. The errors at 95 % of confidence of Student's *t*-test were 2.9 % and 2.4 % for 3T6t and 2B3T6t, respectively.

Before TGA analysis, samples were conditioned in a desiccator containing silica gel for at least 72 h.

**Table 3.38.** TGA data of PE-PHB blends before and after 125 days of aquatic biodegradation.[a)]

| Sample[b)] | $T_{di}$ (°C) | $T_{d125}$ (°C) | $R_{800i}$(°C) | $R_{800e}$ (%) |
|---|---|---|---|---|
| PEL | 391 | 386 | 0.0 | 0.6 |
| PELt | 378 | 389 | 0.2 | 0.6 |
| 2B | 305 | 300 | 0.1 | 0.3 |
| 2Bt | 304 | 263 | 0.7 | 0.9 |
| 3T6 | 386 | 369 | 0.7 | 1.0 |
| 3T6t | 156 | 208 | 0.9 | 2.1 |
| 3T6e | na | 163 | na | 5.0 |
| 2B3T6 | 301 | 230 | 0.5 | 0.9 |
| 2B3T6t | 152 | 186 | 0.8 | 2.1 |
| 2B3T6e | na | 159 | na | 6.1 |
| 3T7 | 377 | 361 | 0.4 | 1.1 |
| 3T7t | 151 | 207 | 0.9 | 2.8 |
| 3T7e | na | 108 | na | 5.8 |
| 2B3T7e | na | 129 | na | 7.1 |

[a)] $T_d$ is the decomposition temperature defined at 1 wt-% of weight loss before ($T_{di}$) and after biodegradation experiments ($T_{d125}$) and $R_{800}$ is the residual weight of polymer blends at 800°C before ($R_{800i}$) and after biodegradation experiments (R800e), na = not analysed. [b)] See Table 2.6 for code definition.

PEL, PELt and 2B samples presented a variation of 5 °C, 11 °C and 5°C in their $T_d$ values, respectively. These are not significant changes considering the error of *ca*. 3 %. 2Bt, 3T6, 2B3T6 and 3T7 blends presented a decrease in $T_d$ values of 41 °C, 17 °C, 71 °C and 16°C, respectively. As clearly observed, the most significant decreases were obtained for samples containing PHB in their formulations. This decrease in $T_d$ can be probably explained as the result of the biodegradation of samples, which is supported by SEM experiments (Fig 3.47 and 3.49). It was also observed that, 3T6 blend, which presented a decrease of 17 °C also supported microbial growth. However, other behaviour was showed by thermo-degraded 3T6t, 2B3T6t and 3T7t blends, which have $T_d$ values increased after a 125 days of

incubation. This increase in $T_d$ value could be occasioned by some cross-linking that could have happened during the incubation period. In addition, the residue of all blends at 800 °C systematically increased after biodegradation.

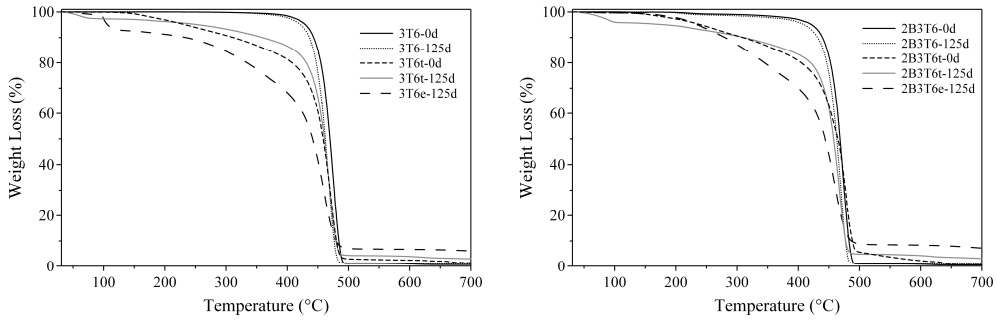


a) b)

**Figure 3.59.** Typical TGA traces of PE based blends before and after aquatic aerobic biodegradation: (a) 3T6 and (b) 2B3T6.

In Figure 3.59 are shown typical TGA traces of samples before and after biodegradation experiments. Pristine samples 3T6 and 2B3T6 showed a single step of weight loss after the biodegradation for 125 days, which correspond to 99 wt-%. TAS and KE samples presented three steps of weight loss. The first one below 100 °C was assigned to the water loss that may have remained in the samples even after the conditioning in silica gel ambient. These amounts are 2.8 wt-%, 4.2 wt-%, 7.2 wt-%, and 0.5 wt-% for 3T6t, 2B3T6t, 3T6e and 2B3T6e, respectively. The second step of weigh loss is an overlapping of several small weight loss steps which correspond to the low MW compounds formed during the thermo-degradation of samples appearing in a broad temperature range from 150-390 °C and corresponding to *ca.* 23-26 wt-%. These values are in agreement to the amounts of low MW compound extracted with acetone (Fig. 3.36). Finally the third step of weigh loss corresponds to the main stage attributed to PEL content in the samples. As expected, it is the highest one with amounts of about 65 wt-%.

Derivative TGA traces (DTGA) of PE-PHB based blends exposed to aquatic biodegradation, in the temperature range of 350-550 °C, are shown in

Figure 3.60. This temperature range was chosen in order to compare $T_p$ values of PEL fraction present in the samples after incubation with that of pristine PEL, which is around 474 °C. It can be clearly observed from DTGA traces that $T_p$ of samples decreased after the biodegradation. $T_p$ values remained between 449-470 °C depending on sample analysed. Main shifts of $T_p$ were observed for 2Bt (17 °C) and 2B3T6t (11 °C) blends. As above mentioned $T_p$ is related to the reaction mechanism of thermal degradation of samples. Hence, it can be supposed that a shift in $T_p$ means that the biodegradation of samples changed their chemical structures.

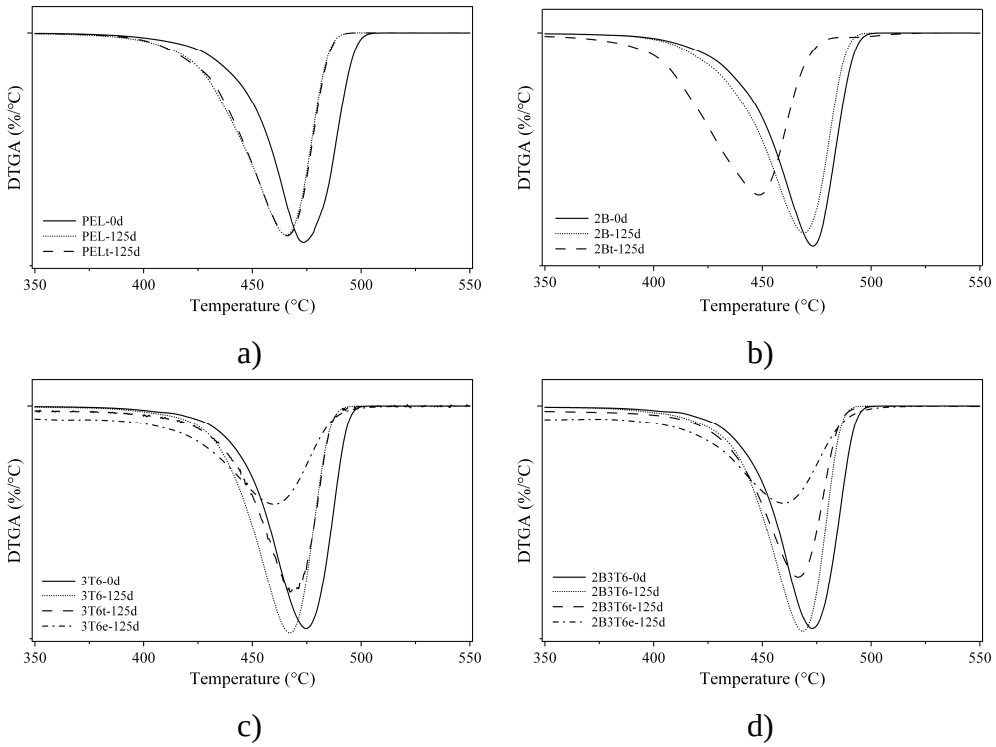


**Figure 3.60.** DTGA traces of PE based blends: (a) PEL, (b) 2B, (c) 3T6 and (d) 2B3T6 at the beginning after 125 days of aquatic biodegradation.

### *Differential Scanning Calorimetry*

Changes in the melting temperature ($T_m$) and crystallinity ($X_{cPE}$) of PE-PHB based blends before and after the exposure time in aquatic media have been studied by DSC. Figure 3.61 presents the DSC traces before and after biodegradation experiments. Table 3.39 reports $T_m$ and $X_{cPE}$ values of samples from DSC traces registered in the 1st heating scan at 10 °C.min$^{-1}$.

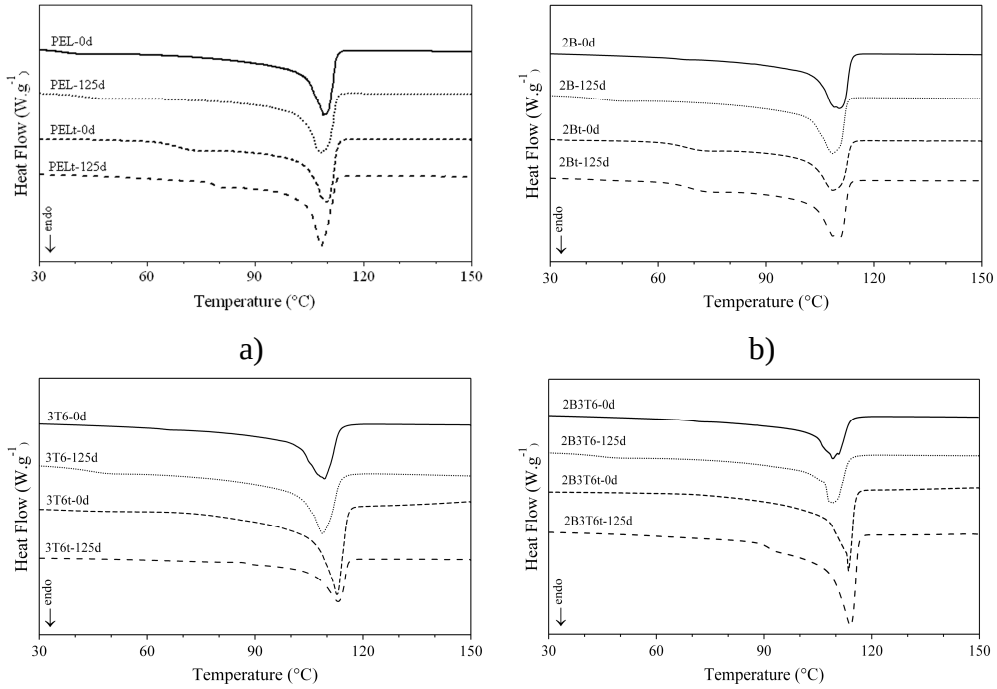


**Figure 3.61.** Typical DSC traces (1st heating scan) of PE blends: (a) PEL (b) 2B, (c) 3T6 and (d) 2B3T6.

DSC traces of samples showed a single endothermic peak ranging from 108 °C to 114 °C depending on sample composition. These values remained essentially unaltered during the biodegradation process. The crystallinity of samples were calculated using the enthalpy values (ΔHm) according with the equation below:

$$X_{cPE} = \Delta Hm/\Delta Hmi*100 \qquad \text{(Eq. 3.2)}$$

Where $X_{cPE}$ is the PE crystallinity degree of sample, ΔHm is the variation of enthalpy and ΔHmi is the change in the enthalpy of a perfect crystal of infinite size. For PE, ΔHmi = 290 $J.g^{-1}$[111]. As can be observed in Table 3.39 a slight increase in $X_{cPE}$ was found for the majority of the samples. This increase was not more than 10 %. On the other hand, 3T6t and 3T7t blends showed a remarkable decrease in $X_{cPE}$ values that was of 30 % and 25 %, respectively.

**Table 3.39.** Thermodynamic parameters (1st heating scan) of PE-PHB blends at the beginning and after 125 days in aquatic biodegradation.[a)]

| | $T_m$ (°C) | | $X_{cPE}$ (%) | |
|---|---|---|---|---|
| Sample[b)] | 0 d | 125 d | 0 d | 125 d |
| PEL | 108 | 108 | 45.4 | 46.6 |
| PELt | 110 | 108 | 44.0 | 45.0 |
| 2B | 110 | 108 | 41.5 | 43.7 |
| 2Bt | 108 | 110 | 43.2 | 48.4 |
| 3T6 | 109 | 109 | 42.7 | 49.8 |
| 3T6t | 112 | 113 | 56.3 | 25.2 |
| 2B3T6 | 109 | 109 | 42.7 | 49.7 |
| 2B3T6t | 113 | 114 | 54.4 | 67.7 |
| 3T7 | 109 | 110 | 44.3 | 54.5 |
| 3T7t | 114 | 117 | 57.0 | 32.7 |

[a)] $T_m$ is the melting temperature and $X_{cPE}$ is the degree of crystallinity of PE in the sample.

In Table 3.40 are registered $T_m$ and $X_{cPE}$ of samples from DSC traces recorded in the 2nd heating scan. No change was found in $T_m$ of PE-PHB blends with the time of biodegradation. In addition, the same behaviour was observed to that previously found for the 1st heating scan with regarding to the $X_{cPE}$ in the 2nd heating scan.

**Table 3.40.** Thermodynamic parameters (2nd heating scan) of PE-PHB blends at the beginning and after 125 days in aquatic biodegradation.[a)]

| | $T_m$ (°C) | | $X_{cPE}$ (%) | |
|---|---|---|---|---|
| Sample[b)] | 0 d | 125 d | 0 d | 125 d |
| PEL | 110 | 110 | 44.7 | 46.3 |
| PELt | 111 | 110 | 43.4 | 47.8 |
| 2B | 110 | 110 | 43.7 | 44.4 |
| 2Bt | 110 | 110 | 42.1 | 47.0 |
| 3T6 | 109 | 110 | 44.5 | 51.2 |
| 3T6t | 113 | 114 | 45.5 | 25.7 |
| 2B3T6 | 110 | 110 | 44.6 | 47.9 |
| 2B3T6t | 113 | 113 | 46.1 | 55.9 |
| 3T7 | 110 | 110 | 43.3 | 55.3 |
| 3T7t | 113 | 113 | 47.1 | 22.0 |

[a)] $T_m$ is the melting temperature and $X_{cPE}$ is the degree of crystallinity of PE in the sample.

### *3.2.3.3 Soil burial biodegradation*

Soil burial experiments represent a more significant approach to natural environments than that carried out in aquatic salt medium[38]. In addition, using a natural complex media, with broad mixed microbial communities it should be expected a higher mineralization of polymeric materials. So, after aquatic biodegradation, samples were also submitted to soil burial tests, in order to assess the biodegradability of PE-PHB based blends films in an approximately natural environment.

Forest soil used in biodegradation experiment was taken from Pinus and Quercia woods and has a total nitrogen content of 1.34g/kg and S.O. content of 2.95 wt-%. Before performing each characterization on PE-PHB based blends films that had been incubated in soil, all samples were washed

with distilled water until all visible residues were removed. Samples were then dried in a desiccator containing silica gel for at least 72 hours before analysis.

***Morphology***

Figure 3.62 shows the SEM photomicrographs of PE-PHB samples before and after 180 days of soil burial biodegradation.

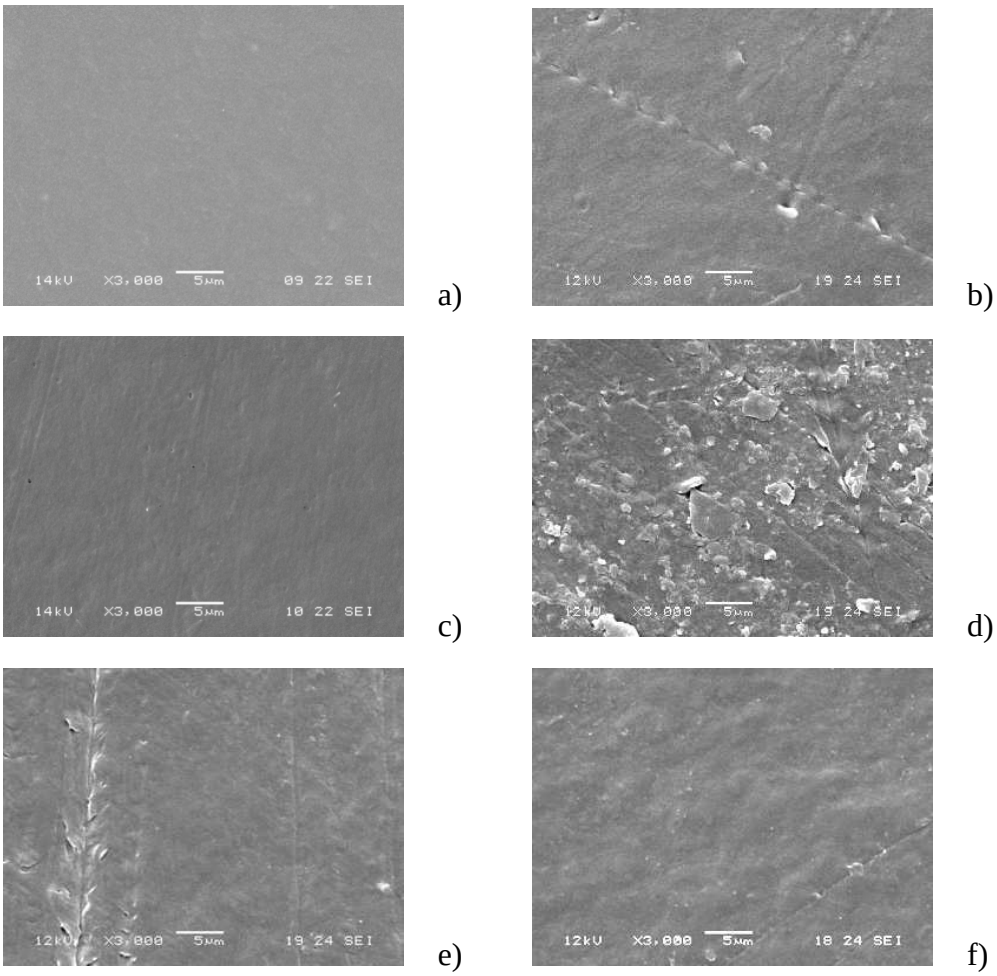


**Figure 3.62.** SEM of PE-PHB blends surface at magnification of 3000X: a) 3T6 initial; b) 3T6-6m; c) 2B3T6 initial; d) 2B3T6–6m; e) 3T7-6m; f) 2B3T7–6m.

As it can be observed, no microorganisms appear in the surface of the samples. Probably microbes were removed from the surfaces of the films during the washing step carried out before SEM analysis. The blends 3T6 (Fig. 3.62 a) and b)) and 2B3T6 (Fig. 3.62 c) and d)) showed a slight change in the surface morphology after biodegradation, evidencing that bioerosion occurred. Samples 3T7 and 2B3T7 (Fig. 3.62 e) and f)) also showed signals of bioerosion after six months of incubation in soil evidencing that microbiological action occurred on the pristine and oxidized PE-PHB blends. These results are the proof that prodegradants are not toxic to the community of microorganisms present in the soil. Koutny *et al.*[38] also arrived at this conclusions in their review concerning the biodegradation of PE films containing prodegradants.

***Carbon Dioxide Evolved***

The mineralization of PE-PHB based blends in soil burial were compared to that obtained for pure Whatman cellulose filter paper (PWC), which was used as the reference material. As observed in Figure 3.63 the biodegradation of PWC began after 10 days of exposure in soil. Moreover, the most significant biodegradation period was between 20-70 days. After this time the degradation rate decreased. However, even at a lower rate, PWC degradation occurred continuously until 140 days evidencing microbiological activities.

Figure 3.64 shows the mineralization behaviour of pristine and thermo degraded blends containing prodegradants with and without PHB. Pristine samples without PHB and 2B3T7 began to mineralize at 40 days of incubation in soil (Fig 3.64 a), c) and d)). Orhan and Buyukgungor[196] studying the biodegradation of LDPE/starch blends containing prodegradants in soil found a gradual increase of $CO_2$ evolution after 40 days of exposure in soil. On the other hand, 2B3T6 blend mineralization began at *ca.* 5 days of incubation (Fig 3.64 b)).

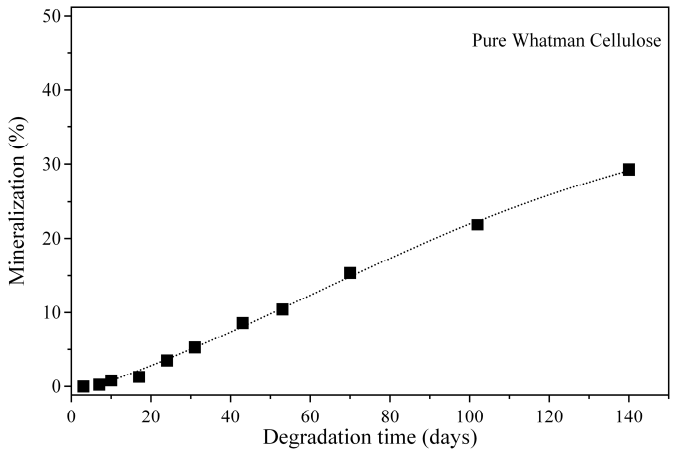


**Figure 3.63.** Mineralization behaviour of PWC up to 6 months of soil burial experiments.

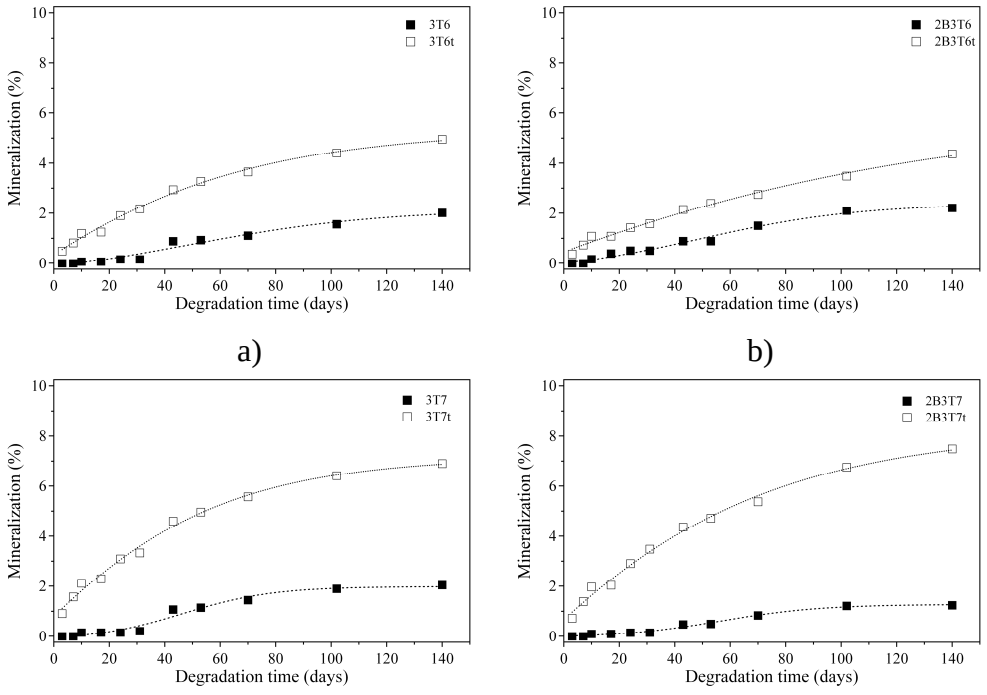


**Figure 3.64.** Mineralization behaviour of PE-PHB blends, with and without a previous thermal aging, during soil burial experiments: (a) 3T6, (b) 2B3T6, (c) 3T7, and (d) 2B3T7.

Samples that had been pre-oxidized showed the highest biodegradation values, which arrived up to 6 wt-% after 140 days of incubation in soil. Albertsson and Karlsson[197] found that PE subjected to 26 days of artificial UV radiation before being buried in soil evolved less than 0.5 wt-% of carbon as $CO_2$ after 10 years. In addition, for TAS the biodegradation began soon and presented the most significant increase until 70 days of incubation. At this time biodegradation rate decreased, but mineralization still occurred until the end of the experiment.

***Thermogravimetric Analysis (TGA)***

Changes in the thermal stability of PE-PHB blends submitted to soil burial experiments were assessed by TGA. Table 3.41 shows the decomposition temperature ($T_d$) and the residue at 800 °C ($R_{800}$) for samples after 0, 2, 4 and 6 months of biodegradation.

**Table 3.41.** TGA data of PE-PHB blends up to 6 months soil burial biodegradation [a)]

| Sample | 0 m | | 2 m | | 4 m | | 6 m | |
|---|---|---|---|---|---|---|---|---|
| | $T_d$ (°C) | $R_{800}$ (wt-%) | $T_d$ (°C) | $R_{800}$ (wt-%) | $T_d$ (°C) | $R_{800}$ (wt-%) | $T_d$ (°C) | $R_{800}$ (wt-%) |
| 3T6 | 386 | 0.7 | 348 | 0.8 | 355 | 1.1 | 327 | 2.6 |
| 3T6t | 156 | 0.9 | 156 | 5.1 | na | na | 186 | 6.6 |
| 2B3T6 | 301 | 0.5 | 234 | 0.7 | 285 | 0.7 | 302 | 0.9 |
| 2B3T6t | 152 | 0.8 | 172 | 4.2 | na | na | 168 | 1.4 |
| 3T7 | 377 | 0.4 | 357 | 0.7 | 364 | 0.8 | 354 | 1.3 |
| 3T7t | 117 | 0.9 | 180 | 1.6 | na | na | 178 | 1.7 |
| 2B3T7 | 263 | 0.4 | 250 | 1.0 | 246 | 0.8 | 244 | 1.0 |
| 2B3T7t | 131 | 0.6 | 185 | 7.4 | na | na | 187 | 3.8 |

[a)] $T_d$ is the decomposition temperature defined at 1 wt-% of weight loss and $R_{800}$ is the residual weight of polymer blends at 800°C and na = not analysed

In general, the $T_d$ values of pristine samples decrease with increasing of incubation time (Tab. 3.41). The behaviour of $T_d$ value for the 2B3T6 blend

seems to remain unaltered although the intermediate values were lower. This variability suggests that or sample composition or biodegradation is heterogeneous. On the other hand, samples that had been pre-oxidized before testing showed a significant increase in $T_d$ values. $T_d$ increased 30 °C, 61 °C, 16 °C and 56 °C in the 3T6t, 3T7t, 2B3T6t and 2B3T7t samples, respectively. This increase suggests that during soil incubation thermo degraded samples undergo some cross-linking and that this effect is more evident for samples containing T7 than T6 prodegradant. TGA residual weight was measured at 800 °C ($R_{800}$). $R_{800}$ increased with incubation time and this increase arrived up to 371 % for 3T6 and 730 % for 3T6t.

TGA traces of 3T6, 3T6t blends and the respective derivative traces (DTGA) are plotted in Figure 3.65.

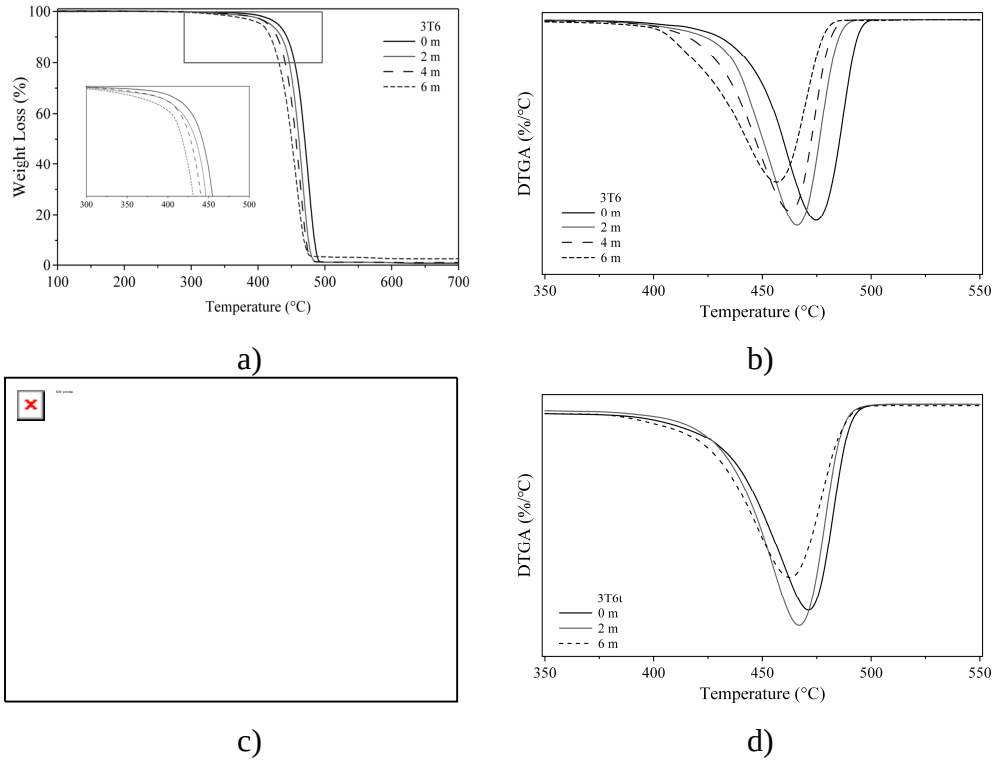


**Figure 3.65.** TGA (a,c) and DTGA (b,d) traces of PE based blends during soil burial experiments: (a,b) 3T6 and (c,d) 3T6t.

The effect of biodegradation on the thermo-degradation of buried materials is visible in the Figure 3.65. DTGA traces presented only one peak. However, DTGA peaks of pristine samples are closer than that of pre-oxidized one, which suggest overlapped degradation steps not resolved in the scan rate used in the TGA analysis. As aforementioned, these overlapped degradation steps correspond to the low MW compounds formed during the thermo-degradation of samples. In addition, for pristine 3T6 blend, the temperature of maximum degradation rate ($T_p$) of main stage (corresponding PE fraction in the blends) decreased after 6 months of incubation in soil. $T_p$ value of pristine 3T6 blend was around 475 °C decreased to 465 °C, 460 °C and 455 °C after 2, 4 and 6 months of incubation, respectively. These results suggest that PE matrix undergo chemical changes during biodegradation in soil.

Figure 3.66 shows DTGA traces of PE-PHB blends as a function of soil burial time. All blends presented the same behaviour of 3T6 and 2B3T6 films. This means, $T_p$ of PE phase decreases with increasing of incubation time. It was observed that $T_p$ values of blends without PHB decreased more than that of samples containing 2 wt-% of PHB. Probably this result is related to the ease assimilation of PHB by the microorganism. So, PE based blends containing PHB would have the PE matrix more accessible to the degradation. PE $T_p$ values decreased slowly in these cases.

**Table 3.42.** PHB weight loss step (ΔM %) data in PE-PHB blends soil burial biodegraded in the period of 6 months

| Sample | 0 m | 2 m | 4 m | 6 m |
|---|---|---|---|---|
| 2B3T6 | 1.6 | 2.1 | 2.7 | 1.6 |
| 2B3T7 | 2.1 | 2.7 | 2.7 | 2.6 |

Table 3.42 reports the PHB weight loss step data in PE-PHB blends for samples soil burial biodegraded in the period of 6 months. For samples that had been pre-oxidized was not possible to calculate the step of PHB weight loss due to the overlap of several steps of weight loss of the products formed

during the thermal aging. As it can be observed, the amount of PHB in the samples that originally was 2 wt-% remains practically unaltered during all the biodegradation time.

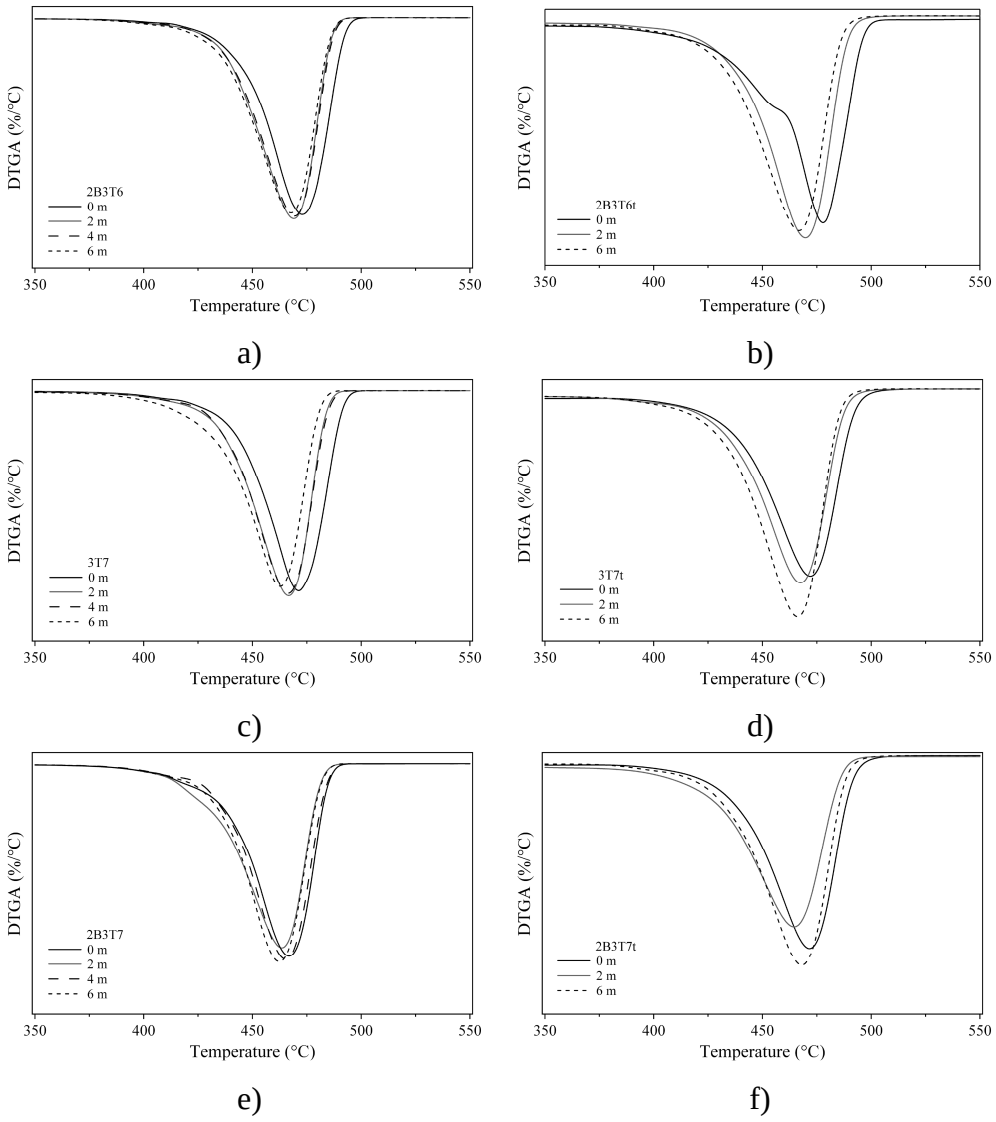


**Figure 3.66.** DTGA traces of PE based blends as a function of soil burial time: (a) 2B3T6, (b) 2B3T6t, (c) 3T7, (d) 3T7t , (e) 2B3T7 and (f) 2B3T7t.

### *Differential Scanning Calorimetry*

Figure 3.67 shows the DSC traces of the 1st heating scan of PE-PHB blends containing T6 additive incubated in soil for 6 months.

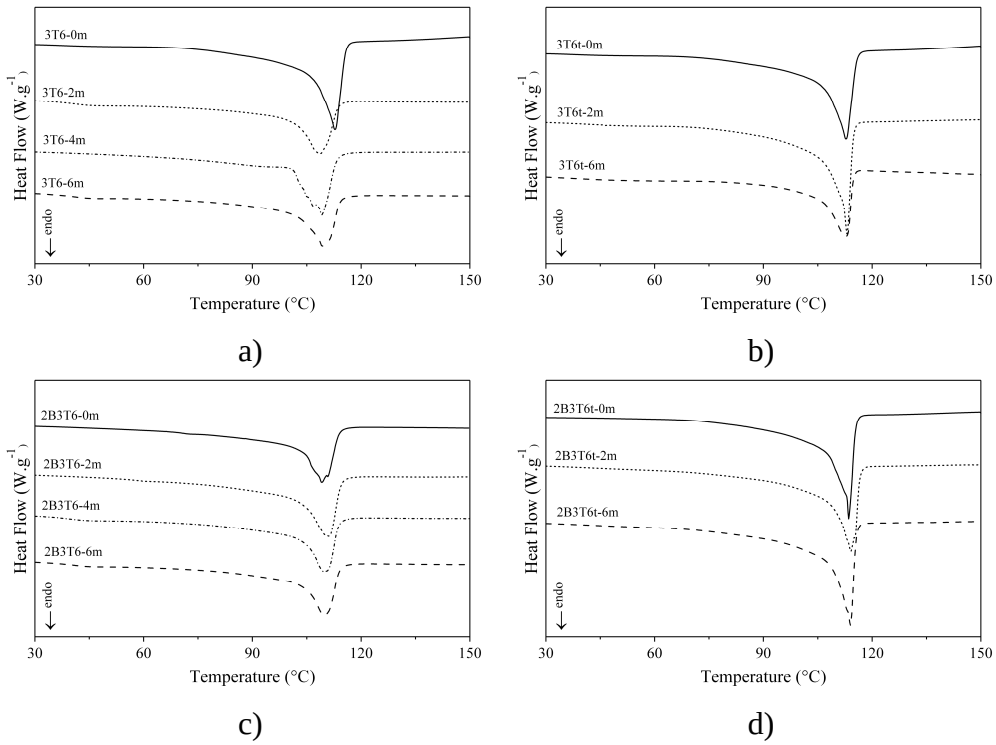


**Figure 3.67.** DSC traces (1st heating scan) of biodegraded PE based blends: (a) 3T6 (b) 3T6t, (c) 2B3T6 and (d)2B3T6t.

The amount of samples used in DSC experiments was *ca.* 5 mg, which means that was difficult to detect PHB transition. So, in this way the DSC traces were recorded from -30 °C to 150 °C in order to detect only PE matrix transitions. DSC traces showed an endothermic peak at around 110 °C for pristine samples and at 113 °C for pre-oxidized samples. This peak corresponds to the PE melting temperature and these values remained unaltered for the majority of the samples during biodegradation experiment. Nevertheless, sample 3T6 presented a decrease in $T_m$ with degradation time.

Table 3.43 registers the values of PE crystallinity degree ($X_{cPE}$) as a function of biodegradation time. The $X_{cPE}$ values of samples increase initially. Afterwards, it decreases and then it shows a slight tendency to increase again. Same behaviour was found by Contat-Rodrigo *et al.*[198] studying polypropylene with enhanced degradability in soil burial for 21 months. According to these authors, in semi crystalline polymers, degradation starts in the amorphous phase and in the interfacial regions, in which oxygen is soluble. This could explain the initial increase of crystallinity. As degradation takes place, the crystalline phase begins to disintegrate, thus reducing the crystalline content of the polymer. Another explanation suggested by these authors is that the crystalline content of a semi crystalline polymer is conditioned by the amorphous phase that restricts the crystallization process. So, a scission of the molecules of the amorphous regions, caused for example by oxidation, allows the crystallization to proceed to a higher extent. In this case, an increase in crystallinity could be considered as degradation.

**Table 3.43.** PE crystallinity degree ($X_{cPE}$ %) as a function of biodegradation time (1st heating scan).[a)]

| Sample | 0 m | 2 m | 4 m | 6 m |
|---|---|---|---|---|
| 3T6 | 42.7 | 46.6 | 48.1 | 44.9 |
| 3T6t | 56.3 | 60.4 | na | 55.5 |
| 2B3T6 | 42.7 | 51.3 | 45.1 | 46.2 |
| 2B3T6t | 54.4 | 57.2 | na | 60.6 |
| 3T7 | 44.3 | 44.2 | 55.9 | 47.9 |
| 3T7t | 57.0 | 60.9 | na | 58.4 |
| 2B3T7 | 44.3 | 47.5 | 42.3 | 58.8 |
| 2B3T7t | 57.5 | 69.3 | na | 65.3 |

[a)] na = not analysed

Figure 3.68 shows DSC traces of the first cooling scan of PE-PHB blends incubated in soil for 6 months. The temperatures of the maximum crystallization ($T_c$) are reported in Table 3.44. $T_c$ values around 99 °C have

been found for all the pristine samples and around 105 °C for pre-oxidized samples, regardless of the exposure time.

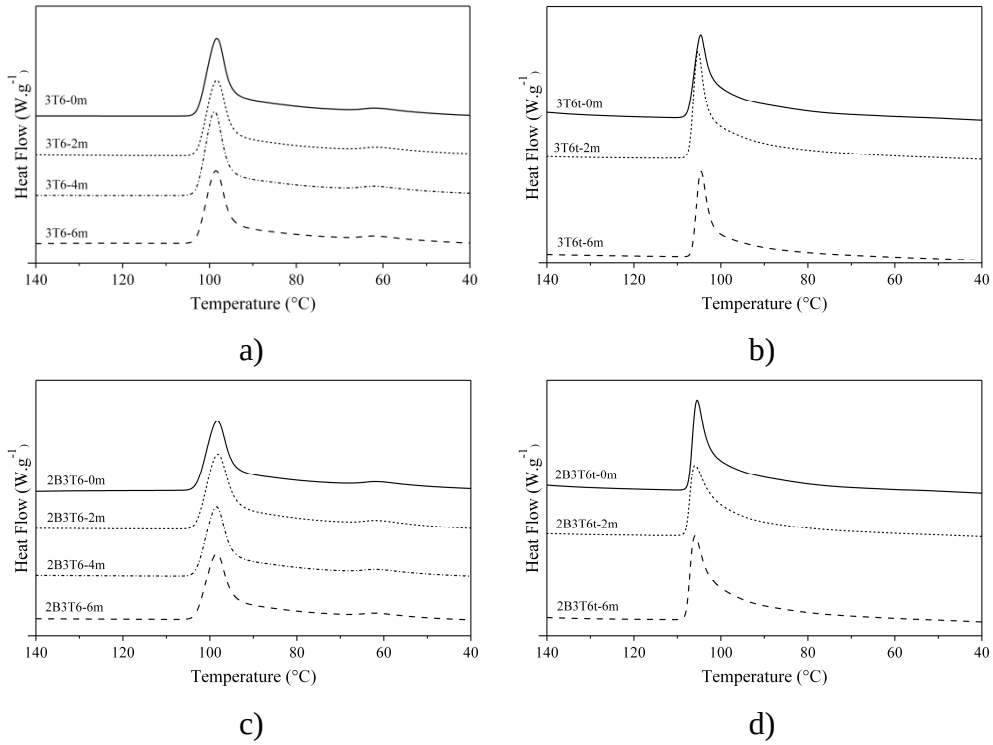


**Figure 3.68.** DSC traces (1st cooling scan) of biodegraded PE blends: (a) 3T6 (b) 3T6t, (c) 2B3T6 and (d)2B3T6t.

**Table 3.44.** PE crystallization temperature ($T_c$ °C) in PE-PHB blends as a function of biodegradation time (1st cooling scan).[a)]

| Sample | 0 m | 2 m | 4 m | 6 m |
|---|---|---|---|---|
| 3T6 | 98 | 98 | 99 | 99 |
| 3T6t | 05 | 105 | na | 105 |
| 2B3T6 | 98 | 98 | 98 | 99 |
| 2B3T6t | 06 | 106 | na | 106 |
| 3T7 | 98 | 99 | 100 | 100 |
| 3T7t | 04 | 104 | na | 105 |
| 2B3T7 | 98 | 99 | 99 | 99 |
| 2B3T7t | 04 | 104 | na | 102 |

[a)] na = not analysed

Table 3.45 shows the $T_m$ and $X_{cPE}$ calculated from the second heating scan as a function of biodegradation time. From these results it can be noted that $T_m$ values remained constant during all the degradation experiment and the crystalline content increased with biodegradation time.

**Table 3.45.** Thermodynamic parameters of PE in PE-PHB blends as a function of biodegradation time (2nd heating scan).[a]

| Sample | 0 m | | 2 m | | 4 m | | 6 m | |
|---|---|---|---|---|---|---|---|---|
| | $T_m$ (°C) | $X_{cPE}$ (%) | $T_m$ (°C) | $X_{cPE}$ (%) | $T_m$ (°C) | $X_{cPE}$ (%) | $T_m$ (°C) | $X_{cPE}$ (%) |
| 3T6 | 109 | 44.5 | 110 | 46.4 | 110 | 47.4 | 110 | 46.2 |
| 3T6t | 113 | 45.5 | 113 | 49.2 | na | na | 113 | 35.5 |
| 2B3T6 | 110 | 44.6 | 111 | 51.0 | 110 | 45.0 | 110 | 45.0 |
| 2B3T6t | 113 | 46.1 | 113 | 45.5 | na | na | 113 | 48.1 |
| 3T7 | 110 | 43.3 | 110 | 44.5 | 111 | 55.1 | 111 | 45.4 |
| 3T7t | 113 | 47.1 | 114 | 48.5 | na | na | 113 | 48.3 |
| 2B3T7 | 110 | 43.4 | 110 | 47.1 | 110 | 43.5 | 110 | 52.0 |
| 2B3T7t | 112 | 47.4 | 113 | 57.5 | na | na | 109 | 48.2 |

***Transmission Fourier Transform Infrared Spectroscopy (FTIR)***

FTIR spectra were performed from 500 to 4000 $cm^{-1}$. Figure 3.69 shows the FTIR spectra of samples as a function of soil burial biodegradation. FTIR spectra of 3T7 and 2B3T7 blends (Fig. 3.69 c) and d)) did not show any significant differences before and after incubation in soil for 6 months. However, 3T6 and 2B3T6 films showed consistent changes in the FTIR spectra after 180 days of incubation in the absorption bands at 1715 $cm^{-1}$ and 3500 $cm^{-1}$. The absorption band at 1715 $cm^{-1}$ is assigned to carbonyl groups. The appearance of this absorption suggests that 3T6 and 2B3T6 samples were oxidized during the incubation in soil. As aforementioned, Jakubowicz[37] studying the degradability of PE in soil reported that oxidation occurred during the biodegradation experiments. The band at 3500 $cm^{-1}$ can be attributed to the proteinic material[134].

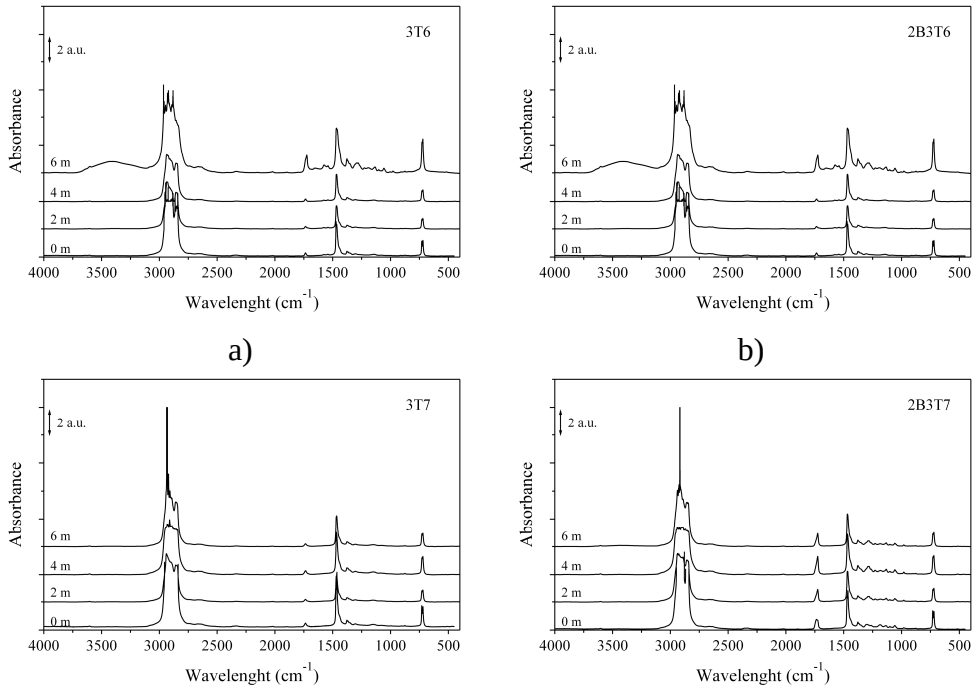


**Figure 3.69.** FTIR spectra of PE-PHB samples as a function of soil incubation time.

## 3.3. PE-Starch Based Composites

The firsts approaches to increase PE biodegradability were based on the replacement of 40 % of PE matrix by biodegradable fillers, especially starch. Even though this type of filler can be relatively rapid to degrade, it is now well accepted that it does not accelerate the biodegradation of the PE matrix itself[38]. One method to improve the biodegradability of PE materials is to add together with starch some other additives, as prodegradants, which can increase the rate of oxidation by air oxygen and cleavage PE chains under the influence of light and/or heat.

Starch is the lowest priced and most abundant worldwide commodity. It is the major form in which carbohydrates are stored[199]. Moreover, it is a well-known polymer, naturally produced by plants in the form of granules (mainly from potatoes, corn, and rice)[200-202]. Among other features, it is inexpensive and annually renewable[203]. Starch granules vary from plant to plant but are in general composed of a linear polymer, amylase (in most cases up about 20 wt-% of the granule), and a branched polymer, amylopectin. It is produced in most countries and is available at low cost in all countries.

Starch based products are an option for the replacement of oil based materials. However, the production of starch based materials without other additives presents some difficult such as the poor mechanical properties presented by the films[204-207]. Starch materials are fragile and their ability to develop large deformation are rather limited[43]. Starch films can be made from the native starch or its components, amylose and amylopectin, by various techniques such as thermoplastic processing and solution casting[153]. Films rich in amylose or amylopectin are reported to have different properties. Preponderance of amylose in starches gives stronger films, stable in water, while the branched structure of amylopectin generally leads to films that disperse quickly in water and with different mechanical properties, such as lower tensile stress.

Starch can also be used as the main polymer in macromolecular compositions, which can be processed as thermoplastics such as PE. In this case, the granular structure of starch is completely disrupted by the use of

plasticizers under heating, giving rise to a continuous phase in the form of a viscous melt, which can be processed following conventional plastic processing techniques such as injection moulding or extrusion. These types of starch compositions are commonly known as thermoplastic starches (TPS)[208-210]. Starch based biodegradable polymers can also be produced by blending or mixing them with synthetic polymers[51, 211]. The first attempt to obtain starch based materials concerned the utilisation of starch granules as fillers for synthetic polymer as PE[45, 53, 203]. By varying the PE amount, its miscibility with starch, the morphology and hence the properties of the films can be regulated. Of all the modifying approaches to render starch and PE more compatible, the more efficient is when a compatibilizer is introduced into the blends.

Although the literature of PE-starch films is abundant, the results show that the PE-starch films had good biodegradability but very poor compatibility[51], which will affect specially the mechanical performance of these materials. In order to improve PE-starch compatibilization, several studies report the properties of PE-starch materials compatibilized with copolymers as for instance the ethylene-acrylic acid copolymer (EAA)[212] or ethylene-vinyl acetate (EVA)[213]. In addition, very little quantity of studies was dedicated to PE-starch containing prodegradants. Kim *et al*.[214] prepared PE based blends containing hydroxypropylated starches (HPS) with different degrees of substitution (DS). They studied the effect of HPS DS on thermal and bio-degradation of blends in the period of 12 and 4 weeks, respectively. Thermal degradation in an oven at 70 °C began after 7 weeks for PE/HPS blends with higher DS (0.18 and 0.4). The same was observed on biodegradation. This means that PE/HPS blends with higher HPS DS biodegraded faster than the PE blended with not modified starch. Bikiaris *et al.*[212] prepared three families of PE based blends containing plasticized starch (PLST) and/or ethylene-acrylic acid copolymer (EAA). For all blends it was added 0.01 wt-% of Cobalt stearate prodegradant (Co). It was observed that the effect of EAA is of acceleration of thermal oxidation whereas that of PLST is of inhibition.

Besides, some commercial additives based on thermoplastic starch such as Mater-Bi are available. Mater-Bi is a trademark of Novamont and comprises four classes of biodegradable materials based on starch, which differ in synthetic components[215]. Mater-Bi products made basically of thermoplastic starch in combination with polymers such as poly(vinyl alcohol) or aliphatic polyesters present a biodegradation rate similar to that of cellulose and their mechanical properties similar to those of PE[215].

### 3.3.1. *Compatibilization of PE and starch*

As aforementioned, PE and starch are not compatible and therefore the first aim of this chapter is the investigation of the compatibility between PE and starch. Within this Thesis, PE-starch based materials will be defined as composites. According with Work *et al*.[216] a composite can be defined as a multi-component material comprising multiple different (non-gaseous) phase domain in which at least one type of phase domain is a continuous phase. The aim of this study was (1) to select the best type of starch to blend with PE (TPS or native corn starch (25% amylose)) (2) to improve PE-starch compatibilization through the introduction of a third component in the formulation. The third component selected for this purpose were two PE copolymers, EVA and EGMA. PE-Starch based composites followed a screening experiment consisting of a factorial $2^2$ design combined or not with a mixture design were the dependent variables in the factorial design were type of starch (Thermoplastic (TPS) or granules (CS)) and of compatibilizer (EVA and EGMA). The films of PE-TPS and PE-CS were obtained by compression moulding and characterized in terms of morphology and mechanical properties.

#### *3.3.1.1 Morphology*

The morphology of polymeric materials, blends or composites give very useful information about most of its properties, especially its mechanical properties depend on it[217, 218]. SEM micrographs of cryogenic fractures of

PE-Starch based composites (see Tables 2.8 – 2.9 for nomenclature) as a function of type (TPS or CS) and amount of starch (up to 30 wt-%) and compatibilizer (EVA or EGMA) are shown in Figures 3.70 – 3.75. It was observed visually that film samples without compatibilizer (7E3T and 7E3C) were not homogeneous. The different phases (TPS and PE) were clearly observed at naked eye. However, it can be seen in Figure 3.70 that binary composite 7E3T did not present any phase separation between the PE matrix and thermoplastic starch, even at higher concentrations of TPS (30 wt-%). This could be due to the heterogeneity of the dispersed phase and its size that in the small fracture surface prepared for the SEM observation. This means that it is possible that the surface prepared did not contained the two phases of the composite. Besides, the observed surface presents a homogeneous ductile fracture typically of PE. The photomicrograph of 7E3C sample was not performed because it was possible to see phase separation with naked eye.

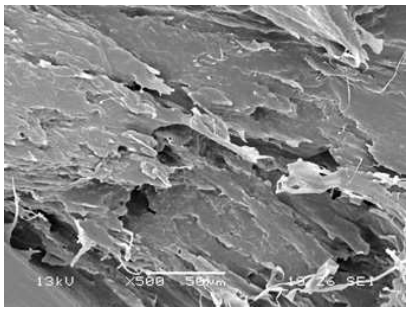


a)

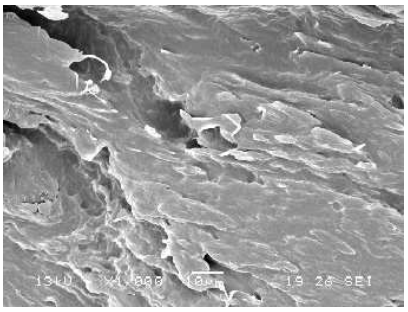


b)

**Figure 3.70.** SEM of PE-Starch materials: a) 7E3T-500X; b) 7E3T-1000X.

Figures 3.71 and 3.72 presents photomicrographs of PE-TPS compatibilized with EGMA and EVA containing 30 wt-% and 15 wt-% of TPS, respectively. It is clearly observed the phase separation and the lack of adhesion independently of the type of compatibilizer used in the formulation.

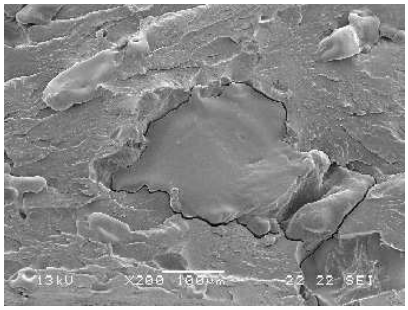


a)

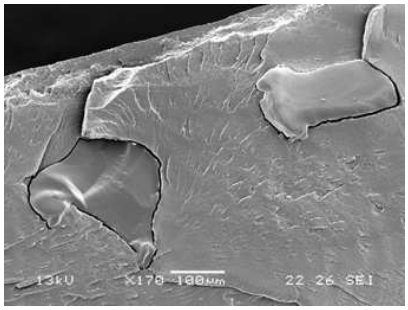


b)

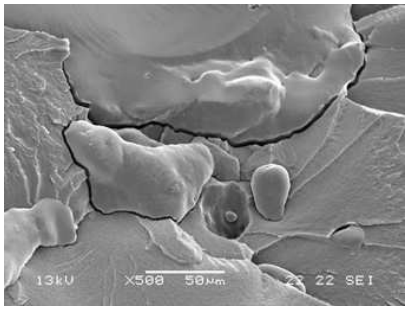


c)

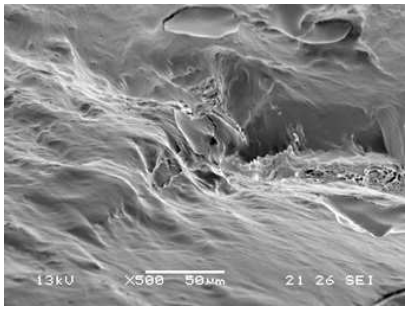


d)

**Figure 3.71.** SEM of PE-Starch materials: a) 5E2G3T-200X; b) 5E2V3T-170X; c) 5E2G3T-500X; d) 5E2V3T-1000X.

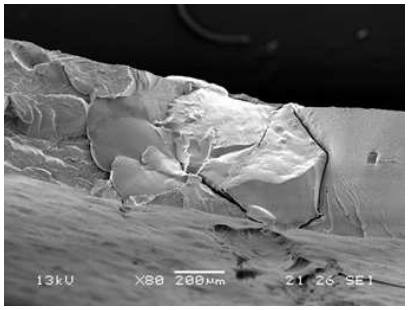


a)

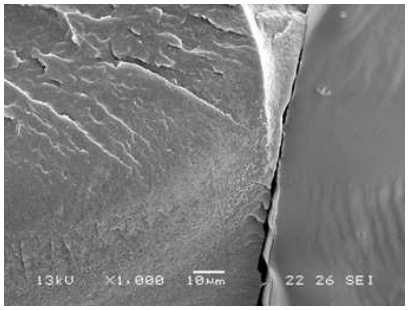


b)

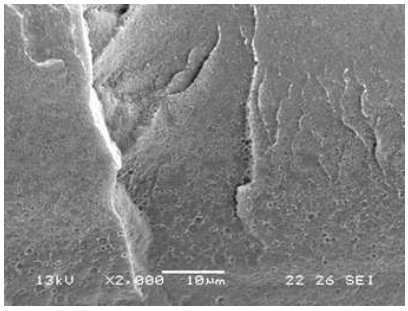


c)

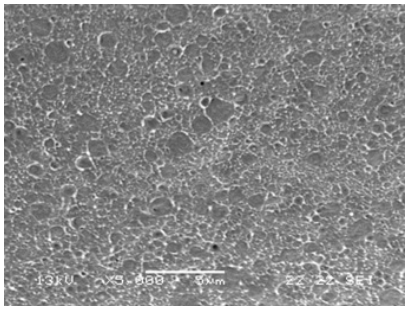

d)

**Figure 3.72.** SEM of PE-Starch materials: a) 75E1V15T-80X; b) 75E1V15T-1000X; c) 75E1V15T-2000X; d) 75E1V15T-5000X.

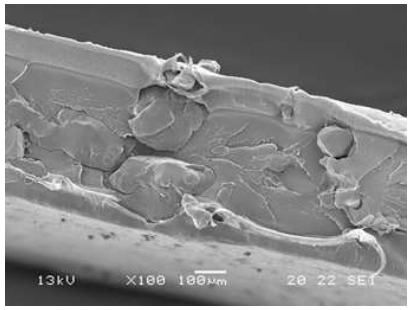


a)

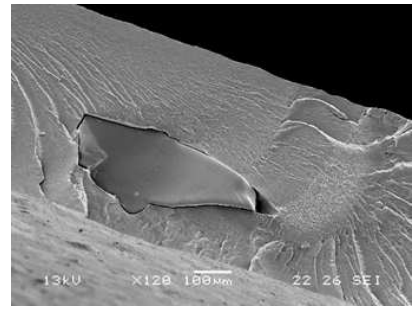


b)

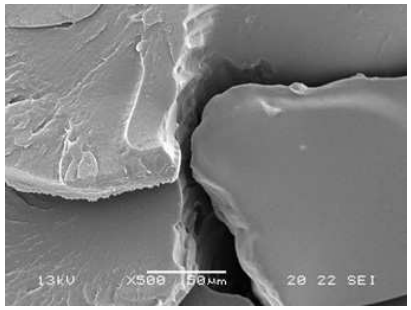


c)

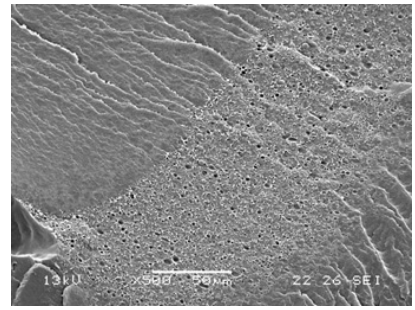


d)

**Figure 3.73.** SEM of PE-Starch materials: a) 65E2G15T-100X; b) 65E2V15T-120X; c) 65E2G15T-500X; d) 65E2V15T-500X.

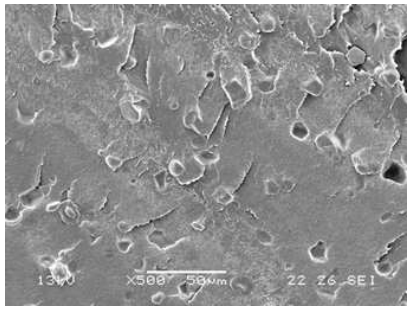


a)

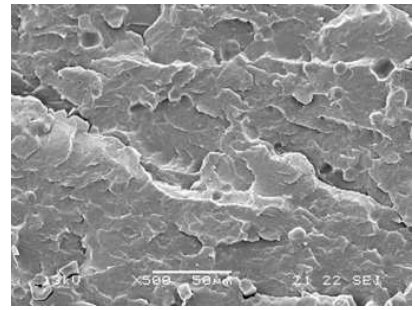


b)

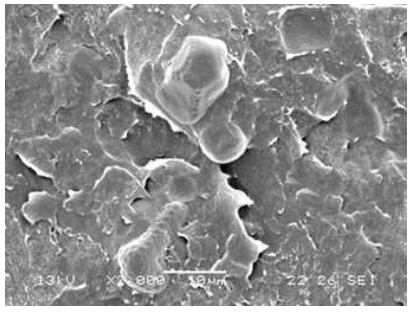


c)


d)

**Figure 3.74.** SEM of PE-Starch materials: a) 65E2G15C-500X; b) 65E2V15C-500X; c) 65E2G15C-2000X; d) 65E2V15C-2000X.

Figure 3.73 shows the photomicrographs of composites containing the maximum amount of compatibilizer (20 wt-%) and a low amount of TPS (15 wt-%). Although these formulations contain the highest compatibilizer-TPS proportion, it can still be observed phase separation. EVA compatibilizer contains carbonyl groups, which could form hydrogen bonds with the hydroxyl groups of starch. So, it was expected that its use could increase the compatibility between PE and starch[213]. The amount of vinyl acetate (VA) comonomer in the compatibilizer EVA is 33 wt-% of vinyl acetate (VA) and that of glycidyl methacrylate (GMA) comonomer in the compatibilizer EGMA is 8 wt-%, which corresponds at just 6.6 wt-% and 1.6 wt-% of VA and GMA, respectively in the blends 65E2V15T and 65E2G15T. In conclusion, the proportion of polar component of compatibilizer was very low to promote the compatibilization between PE and TPS.

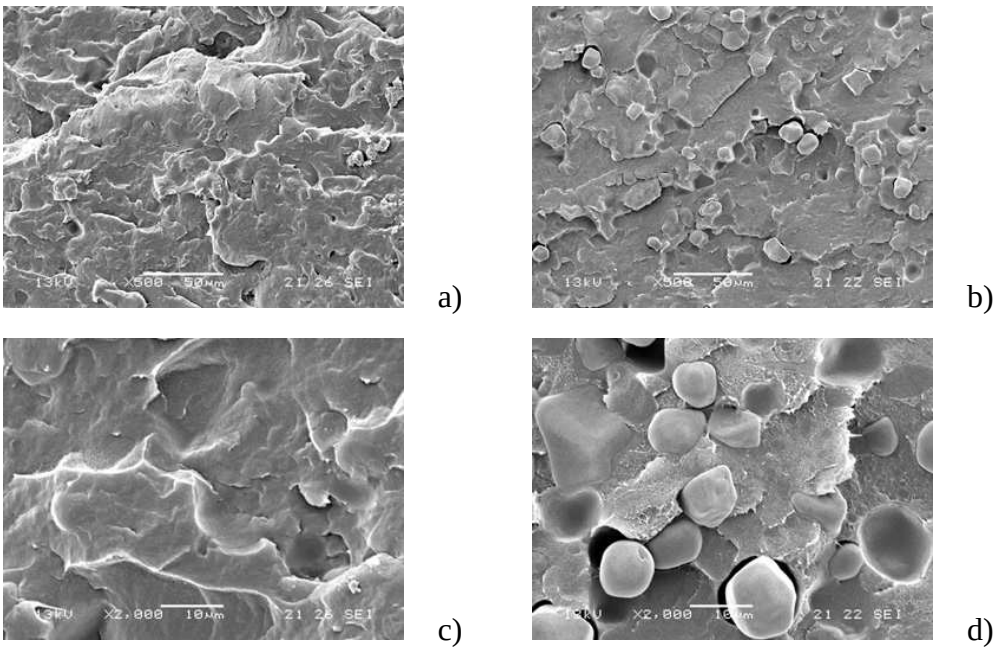


**Figure 3.75.** SEM of PE-Starch materials: a) 5E2G3C-500X; b) 5E2V3C-500X; c) 5E2G3C-2000X; d) 5E2V3C-2000X.

SEM of the fractures surfaces of composites containing 15 wt-% and 30 wt-% of corn-starch (CS) are showed in Figures 3.74 and 3.75. The fracture of both ternary PE-CS based composites with 15 wt-% and 30 wt-% of CS

showed two phase. Starch granules are visible on composites surfaces independently of composite formulation in terms of the type of compatibilizer used (EVA or EGMA) and composition. However, the systems containing CS-EGMA and CS-EVA indicate that starch phase is better dispersed than that of TPS. According with Prinos *et al.*[213], starch in its native form can be mixed with PE, but the greater dispersion of starch in the polymer matrix containing compatibilizer makes it more suitable.

#### *3.3.1.2 Mechanical properties*

Young modulus, tensile stress and strain at break values were determined from stress-strain traces of each sample of PE-starch based composites. For each sample 12 specimens were tested and errors were calculated at 95 % of confidence of Student's *t*-test. In Table 3.46 are specified the codes used in the graphic representation of mechanical properties.

**Table 3.46.** Codes used in the graphic representation of YM.[a)]

| Code | TPS/EGMA | TPS/EVA | CS/EGMA | CS/EVA |
|---|---|---|---|---|
| A | PE | PE | PE | PE |
| B | 7E3T | 7E3T | 7E3C | 7E3C |
| C | 8E2G | 8E2V | 8E2G | 8E2V |
| D | 5E2G3T | 5E2V3T | 5E2G3C | 5E2V3T |
| E | 75E1G15T | 75E1V15T | 75E1G15C | 75E1V15C |
| F | 85E15T | 85E15T | 85E15C | 85E15C |
| G | 6E1G3T | 6E1V3T | 6E1G3C | 6E1V3C |
| H | 65E2G15T | 65E2V15T | 65E2G15C | 65E2V15C |
| I | 9E1G | 9E1V | 9E1G | 9E1V |

[a)] See Tables 2.8-2.9 for code definition.

The mechanical properties of the four families of PE-starch based materials are reported in Tables 3.47 – 3.50. Binary blends of PE containing

different amounts (10 wt-% and 20 wt-%) of EGMA (Tab. 3.47) presented similar values of YM (*ca.* 66 MPa), ST (*ca.* 3.0 MPa), and SB (*ca.* 250 %).

**Table 3.47.** Mechanical properties of PE-TPS-EGMA materials.[a)]

| Code | Sample | YM (MPa) | ST (MPa) | SB (%) |
|---|---|---|---|---|
| A | PE | 171 ± 4 | 13.1 ± 0.8 | 638 ± 48 |
| B | 7E3T | 183 ± 8 | 10.6 ± 3.3 | 284 ± 410 |
| C | 8E2G | 66 ± 5 | 2.9 ± 0.2 | 246 ± 24 |
| D | 5E2G3T | 148 ± 9 | 5.2 ± 0.3 | 19 ± 7 |
| E | 75E1G15T | 57 ± 4 | 1.7 ± 0.1 | 10 ± 3 |
| F | 85E15T | 49 ± 27 | 1.1 ± 0.8 | 4 ± 2 |
| G | 6E1G3T | 109 ± 7 | 5.3 ± 0.3 | 31 ± 9 |
| H | 65E2G15T | 66 ± 4 | 1.6 ± 0.1 | 11 ± 3 |
| I | 9E1G | 67 ± 4 | 3.0 ± 0.3 | 248 ± 37 |

[a)] YM was calculated as the tangent at 1% of tensile strain.

PE-starch composites without compatibilizer presented different mechanical properties. Formulations with TPS (Tab. 3.47 and 3.48) increased the YM of the films and reduced the ST and SB values. Sample containing 30 wt-% of TPS (7E3T) presented satisfactory values of YM which were close to that of PE. Besides ST was slightly reduced in relation to PE and SB decreased considerable. On the other hand, films with CS (Tab. 3.49 - 7E3C) showed very poor mechanical properties. YM was 68 % lower than that of pure PE (171 MPa), ST decreased of 88 % and SB dropped from 638 % to values below 10 %. Prinos *et al.*[213] also observed a decreased in ST of their LDPE-Starch-EVA blends with increasing of starch content (4.5-9.5MPa). Moreover, these authors reported that when EVA is added in the blends, an increase in ST was observed compared with the uncompatibilized blends. Pedroso and Rosa[219] studying the effect of PE-*g*-GMA on the mechanical properties of LDPE-corn starch composites found ST values of 7 MPa for samples containing 30 wt-% of corn starch. In his work, Sailaja *et al.*[46] studied blends consisting of LDPE and esterified starches, starch acetate (Stac) and starch phthalate (Stph). Starch esters were melted with LDPE using LDPE-*co*-glycidyl methacrylate copolymer as compatibilizer. The

results indicate that, in general, LDPE-Stph blends perform better than LDPE-Stac blends. Esterified starch has better mechanical properties than unmodified starch when incorporated in LDPE. The tensile strength and modulus are close to that of pure LDPE for LDPE-Stph blends while the impact strength values are 80 % of that of pure LDPE for 20-40 % Stph loading. The elongation at break values was in the range of 60-70 % of that of pure LDPE for LDPE-Stph blends.

**Table 3.48.** Mechanical properties of PE-TPS-EVA materials.[a)]

| Code | Sample | YM (MPa) | ST (MPa) | SB (%) |
|---|---|---|---|---|
| A | PE | 171 ± 4 | 13.1 ± 0.8 | 638 ± 48 |
| B | 7E3T | 183 ± 8 | 10.6 ± 3.3 | 284 ± 410 |
| C | 8E2V | 188 ± 4 | 11.2 ± 0.7 | 660 ± 36 |
| D | 5E2V3T | 24 ± 3 | 0.9 ± 0.2 | 8 ± 4 |
| E | 75E1V15T | 44 ± 7 | 1.1 ± 0.2 | 6 ± 2 |
| F | 85E15T | 49 ± 27 | 1.1 ± 0.8 | 4 ± 2 |
| G | 6E1V3T | 60 ± 14 | 1.8 ± 0.6 | 66 ± 80 |
| H | 65E2V15T | 31 ± 4 | 0.9 ± 0.2 | 12 ± 5 |
| I | 9E1V | 62 ± 4 | 3.0 ± 0.1 | 271 ± 15 |

[a)] YM was calculated as the tangent at 1% of tensile strain.

Wang *et al*.[211] reported that when TPS amount is increased in TPS/PE blends, a considerable decrease in ST and SB of samples is observed, regardless of the presence of compatibilizer. They justified these results through the difference in polarities of both materials (PE and starch). According with these authors, starch granule is highly hydrophilic, containing hydroxyl groups on its surface, whereas LLDPE is mostly non-polar. Therefore, the strong interfacial bonds such as hydrogen bonds between starch and LLDPE are not produced and the mechanical properties of the TPS/LLDPE blends are rather poor. Surprisingly, in the present study the increase of TPS content in formulations compatibilized with both EGMA or EVA increases the ST and SB of samples. For example, 6E1V3T films presented YM, ST and SB values 194 %, 200 % and 550 % higher than that of films containing 15 wt-% of TPS (65E2V15T) (Tab. 3.48).

Table 3.50 shows the YM, ST and SB of PE-CS-EVA composites. YM of ternary composites changed from 42 MPa (5E2V3C) to 61 MPa for 75E1V15C.

**Table 3.49.** Mechanical properties of PE-CS-EGMA materials [a)]

| Code | Sample | YM (MPa) | ST (MPa) | SB (%) |
|---|---|---|---|---|
| A | PE | 171 ± 4 | 13.1 ± 0.8 | 638 ± 48 |
| B | 7E3C | 55 ± 2 | 1.6 ± 0.0 | 6 ± 0 |
| C | 8E2G | 66 ± 5 | 2.9 ± 0.2 | 245 ± 23 |
| D | 5E2G3C | 242 ± 8 | 9.6 ± 0.2 | 20 ± 0 |
| E | 75E1G15C | 216 ± 5 | 9.6 ± 0.1 | 28 ± 3 |
| F | 85E15C | 60 ± 1 | 2.0 ± 0.1 | 154 ± 50 |
| G | 6E1G3C | 240 ± 6 | 8.6 ± 0.1 | 15 ± 1 |
| H | 65E2G15C | 188 ± 2 | 8.8 ± 0.1 | 37 ± 4 |
| I | 9E1G | 67 ± 4 | 3.0 ± 0.3 | 248 ± 36 |

[a)] YM was calculated as the tangent at 1% of tensile strain.

**Table 3.50.** Mechanical properties of PE-CS-EVA materials [a)]

| Code | Sample | YM (MPa) | ST (MPa) | SB (%) |
|---|---|---|---|---|
| A | PE | 171 ± 4 | 13.1 ± 0.8 | 638 ± 48 |
| B | 7E3C | 55 ± 2 | 1.6 ± 0.0 | 6 ± 0 |
| C | 8E2V | 188 ± 4 | 11.2 ± 0.7 | 660 ± 36 |
| D | 5E2V3C | 42 ± 6 | 1.3 ± 0.1 | 67 ± 70 |
| E | 75E1V15C | 61 ± 3 | 2.0 ± 0.1 | 178 ± 16 |
| F | 85E15C | 60 ± 1 | 2.0 ± 0.1 | 154 ± 50 |
| G | 6E1V3C | 49 ± 2 | 1.5 ± 0.0 | 5 ± 0 |
| H | 65E2V15C | 52 ± 4 | 1.8 ± 0.1 | 186 ± 28 |
| I | 9E1V | 62 ± 4 | 3.0 ± 0.1 | 271 ± 15 |

[a)] YM was calculated as the tangent at 1% of tensile strain.

Ternary composites containing the higher amount of compatibilizer (20 wt-%) and of starch (30 wt-%) (Fig. 3.76 formulation D) showed superior YM for formulations containing CS (5E2G3C and 5E2V3C) in relation to the equivalent one containing TPS (5E2G3T and 5E2V3T). Besides, the compatibilizer EGMA appears in the formulations with better performance.

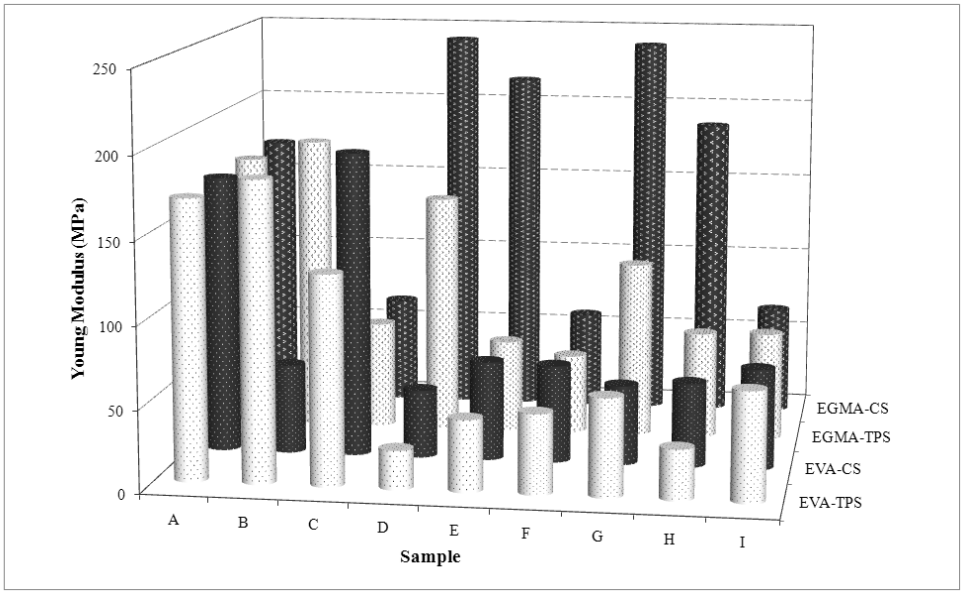


**Figure 3.76.** Young modulus of four families of PE-Starch based composites containing TPS or CS combined with EVA or EGMA as compatibilizers.

### 3.3.2. *PE-CS and PE-BTPS composites with prodegradant*

In the previous study related to the compatibilization of PE-starch composites, it was found that the better compatibilizer was EGMA. So, new series of materials based on PE-Starch-EGMA containing prodegradants were formulated. Initially, it was prepared the PE-T6 blend (ET6: 95 wt-% PE + 5 wt-% T6), which was used in the formulations with biodegradable polymers. Two families of materials containing natural corn-starch and Biopar (a bio-plastic resin consisting mainly of thermoplastic starch (TPS)) were prepared by extrusion. Films were obtained by blow extrusion and characterized by means of MFI, tensile tests, weight changes and TGA. The aim of this study was to assess the influence of starch in the PE based composites containing prodegradants.

### *3.3.2.1 Melt flow index (MFI)*

MFI values of both families of ET6 materials containing CS and Biopar as a function of composite composition are recorded in Table 3.51. To a facilitate comparison of both composite systems these data are shown in Figure 3.77 as a graphic.

**Table 3.51.** Melt flow index of PE-CS and PE-Biopar materials additivated with prodegradant [a)]

| Code | Sample ($g.10min^{-1}$) | MFI ($g.10min^{-1}$) | Sample | MFI |
|---|---|---|---|---|
| | PE | 0.80 ± — | — | — |
| | EGMA | 5.00 ± — | BIOPAR | 14.43 ± 0.60 |
| A | ET6 | 1.03 ± 0.01 | — | — |
| B | 7ET6-3C | 0.63 ± 0.05 | 7ET6-3B | 3.50 ± 0.31 |
| C | 8ET6-2G | 1.44 ± 0.04 | — | — |
| D | 5ET6-2G-3C | 0.97 ± 0.01 | 5ET6-2G-3B | 4.07 ± 0.09 |
| E | 75ET6-1G-15C | 1.02 ± 0.01 | 75ET6-1G-15B | 1.58 ± 0.02 |
| F | 85ET6-15C | 0.84 ± 0.09 | 85ET6-15B | 1.42 ± 0.03 |
| G | 6ET6-1G-3C | 0.71 ± 0.01 | 6ET6-1G-3B | 4.03 ± 0.09 |
| H | 65ET6-2G-15C | 1.24 ± 0.03 | 65ET6-2G-15B | 1.78 ± 0.02 |
| I | 9ET6-1G | 1.29 ± 0.05 | — | — |

[a)] ET6 = 95 wt-% PE/5 wt-% T6 = ET6; E = PE; C = CS; G = EGMA; B = BIOPAR; the errors were calculated at 95 % of confidence of Student's *t*-test.

ET6 composite presented an increase in the MFI of 29 % in relation to the original PE. Probably this increase is due to some degradation that occurred during the extrusion process. On the other hand, 7ET6-3C composite showed a decrease in MFI of 21 % and 39 % in comparison with original PE and ET6 composite, respectively. Moreover, it is worth noting that all ternary composites containing CS have reduced its MFI in relation to composites without it. Bagheri and Naimian[220] observed a linear relation between the corn starch content (up to 15 wt-%) in the LLDPE matrix and the MFI reduction. These authors also reported a decrease in the MFI of

composites when LLDPE containing photoinitiators (prodegradants) were melt processed with starch.

Composites containing 15 wt-% Biopar presented an increase in the MFI in relation to ET6 matrix. Anyway, this value is still appropriated for blow moulding, generally applied on packaging manufacture (Fig. 3.77). On the other hand, composites containing high amounts of Biopar (30 wt-%) were very difficult to handle during the extrusion process. In fact, these composites showed a significant increase in MFI. For example, the composite 7T6-3B presented an increase in the MFI of 340 % in relation to ET6 blend. Probably this increase was a result of the influence of the EGMA and Biopar because both presented the highests MFI (5 and 14 g.10 $min^{-1}$, respectively).

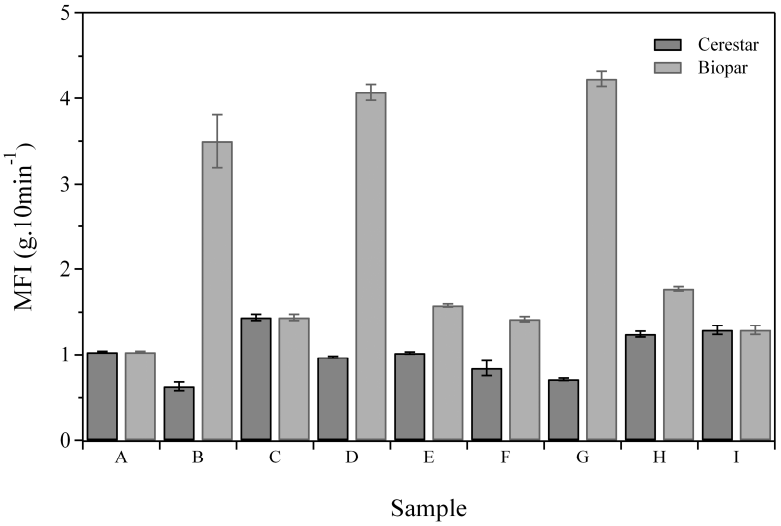


**Figure 3.77.** Changes in the MFI of ET6 samples containing CS and Biopar.

### *3.3.2.2 Thermogravimetry (TGA)*

Figure 3.78 exemplify typical TGA traces of PE-starch composites represented by CS, Biopar, PE-CS and PE-Biopar materials. CS presented three steps of weight loss (ΔM) (Fig. 3.78 a)). The first one below 100 °C corresponds to 9.2 wt-%, which is probably due to the water evaporation. The second and main step have a ΔM of 62.2 wt-% and the third of 16.3 wt-%.

On the other hand, Biopar presented at least four steps of ΔM (Fig. 3.78 b)) corresponding to 8.6 wt-%, 30.2 wt-%, 45.4 wt-% and 4.5 wt-%, respectively.

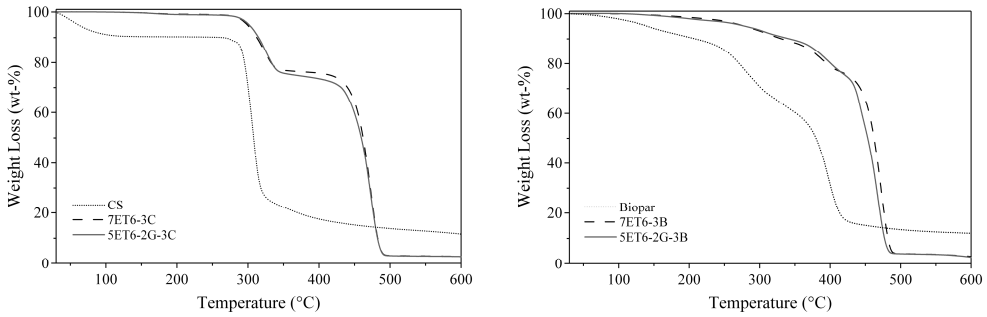


a) b)

**Figure 3.78.** TGA traces of a) PE-CS-prodegradant and b) PE-Biopar-prodegradant materials.

Blends containing CS showed two decomposition stages (Fig. 3.78 a)). The first one (250-360 °C) is due to starch decomposition as it is equivalent to that of pristine CS. The second stage, appearing at higher temperatures, is due to PE decomposition. Blends containing Biopar also showed several well defined decomposition steps before the degradation of PE main chain (468 °C).

### *3.3.2.3 Mechanical properties*

Tables 3.52 – 3.53 present the mechanical properties of PE-CS and PE-Biopar samples. Films containing CS presented higher values for YM than that containing Biopar. This results are in agreement with that presented by Sailaja *et al.*[46]. In their study about the mechanical properties of esterified tapioca starch-LDPE blends using LDPE-*co*-glycidyl methacrylate as compatibilizer, it was found that the YM of unmodified tapioca starch-LDPE blends progressively increase with the increasing in starch content. Pedroso and Rosa[221] studying polymeric materials prepared with virgin or recycled LDPE with corn starch pointed out that the starch must act as rigid filler in

the blends, since the main effect of rigid fillers is to increase the elastic modulus and the viscosity of a composite. As it was observed previously (Tab. 3.51), composites containing CS have decreased their MFI.

**Table 3.52.** Mechanical properties of PE-CS-prodegradant materials [a)]

| Code | Sample | YM (MPa) | ST (MPa) | SB (%) |
|---|---|---|---|---|
| A | ET6 | 196 ± 6 | 14.2 ± 0.9 | 337 ± 70 |
| B | 7ET6-3C | 174 ± 12 | 6.0 ± 0.5 | 51 ± 12 |
| C | 8ET6-2G | 134 ± 14 | 14.4 ± 1.6 | 294 ± 59 |
| D | 5ET6-2G-3C | 176 ± 14 | 7.0 ± 0.7 | 46 ± 14 |
| E | 75ET6-1G-15C | 148 ± 9 | 9.0 ± 0.6 | 113 ± 18 |
| F | 85ET6-15C | 177 ± 11 | 9.0 ± 0.4 | 91 ± 10 |
| G | 6ET6-1G-3C | 147 ± 8 | 6.0 ± 0.4 | 26 ± 4 |
| H | 65ET6-2G-15C | 157 ± 10 | 9.0 ± 0.4 | 104 ± 14 |
| I | 9ET6-1G | 157 ± 8 | 13.6 ± 0.5 | 379 ± 48 |

[a)] YM was calculated as the tangent at 1% of tensile strain.

**Table 3.53.** Mechanical properties of PE-Biopar-prodegradante materials[a)]

| Code | Sample | YM (MPa) | ST (MPa) | SB (%) |
|---|---|---|---|---|
| A | ET6 | 196 ± 6 | 14.2 ± 0.9 | 337 ± 70 |
| B | 7ET6-3B | 113 ± 12 | 8.0 ± 0.8 | 110 ± 16 |
| C | 8ET6-2G | 134 ± 14 | 14.4 ± 1.6 | 294 ± 59 |
| D | 5ET6-2G-3B | 99 ± 6 | 7.8 ± 0.5 | 127 ± 26 |
| E | 75ET6-1G-15B | 169 ± 7 | 11.0 ± 0.3 | 207 ± 19 |
| F | 85ET6-15B | 146 ± 6 | 11.1 ± 0.4 | 220 ± 25 |
| G | 6ET6-1G-3B | 105 ± 15 | 6.4 ± 0.8 | 93 ± 17 |
| H | 65ET6-2G-15B | 135 ± 7 | 11.1 ± 0.7 | 207 ± 59 |
| I | 9ET6-1G | 157 ± 8 | 13.6 ± 0.5 | 379 ± 48 |

[a)] YM was calculated as the tangent at 1% of tensile strain.

ST of samples containing CS was slightly lower than that with Biopar. Besides SB was significant lower in PE-CS than in PE-Biopar films. This decrease in ST of films can be attributed to the poor interfacial adhesion between PE and CS as previously observed (Fig. 3.75). Matzinos *et al.*[218] studying the production of LDPE/starch products through different process

reported a similar behaviour, a decrease in ST with the increase in starch content. They justified this behaviour considering that when starch is incorporated into the polymeric matrix an interface of weakness is also introduced. At this interface, cracks can be formed when the material is subjected to a certain stress.

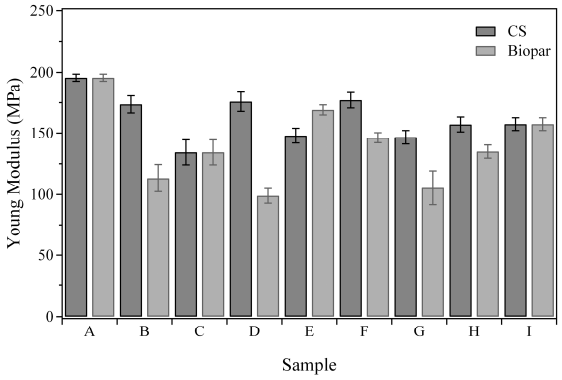


**Figure 3.79.** Variation in the Young modulus of PE-starch based composites.

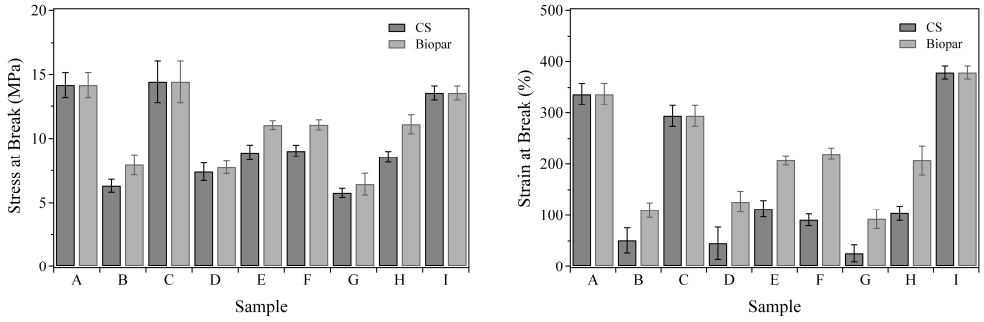


a) b)

**Figure 3.80.** Variation in the a) Tensile stress at break and b) Strain at break of PE-starch based composites.

### *3.3.2.4 Oxidation of PE-Starch based composites*

In order to verify if some synergism occurred when T6 were added together with starch or Biopar, samples were submitted to a thermal aging in

a static oven at 55 °C for 57 days. Oxidation of samples was assessed through weight changes during the aging, acetone extractable fractions and TGA.

Figure 3.81 shows the weight changes on ET6 composites without starch. Each value corresponds to the average of four samples. The weight changes errors for ET6, 8ET6-2G and 9ET6-1G were 0.2 %, 0.4 %, and 0.3 %, respectively at 95 % of confidence of Student's *t*-test. It can be observed that an increasing in the mass of samples starts at 30 days of thermal aging at 55 °C. This increasing in the weight of samples is due to the oxygen uptake during the oxidation process. The highest value of weight gain (WG) was obtained for 9ET6-1G sample, which yields up to 24 % after 57 days of aging.

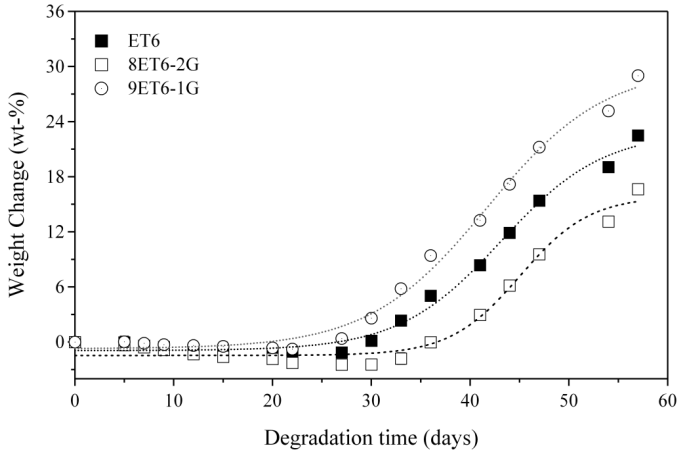


**Figure 3.81.** Weight variation of PE-T6 samples submitted to a aging process at 55°C for 60 days.

In Figure 3.82 are shown the weight variation of ET6-CS-prodegradant and ET6-Biopar-prodegradant composites. An initial weight loss was observed at the beginning of the aging. Because starch is hydrophilic, probably this weight loss was due to the evaporation of water at the beginning of the aging process. After this, the mass of samples formulated with CS starts to increase slightly. The beginning of weight gain is at *ca*. 30 days of thermal aging, which corresponds the time that PE oxidation process starts (Fig. 3.81).

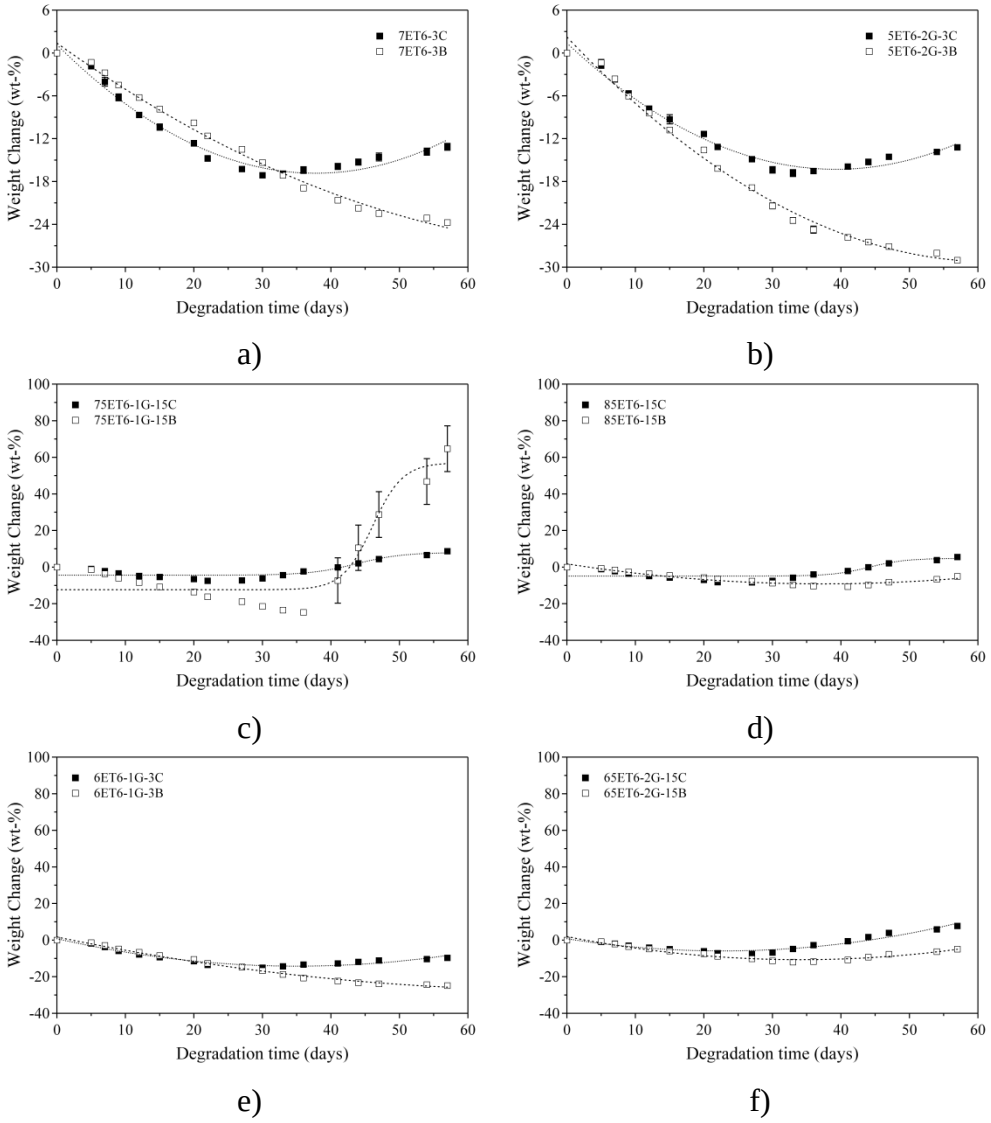


**Figure 3.82.** Weight variation of samples submitted to an aging process at 55°C for 60 days.

On the other hand, blends formulated with Biopar presented different behaviour. Samples containing the highest amount of Biopar (Fig. 3.82 a) and b)) showed a continuous decrease of weight. It is probable that oxidation occurs, but the hydrophilic character of Biopar seems to be prevalent, which at time of sample weighting there was a concurrent water loss, hence masking the weight increases due to oxygen uptake. In contradiction, the highest values of weight gain were obtained for the sample that corresponds

to the central point in the mixture design containing Biopar, 75ET6-1G-15B (Fig. 3.82 c)). In this case, its weight gain increased up to 60 % of its initial value.

Acetone extractable fraction (KE) values and the residual mass (RM) of ET6-CS and ET6-Biopar blends before and after thermal aging are shown in Figure 3.83.

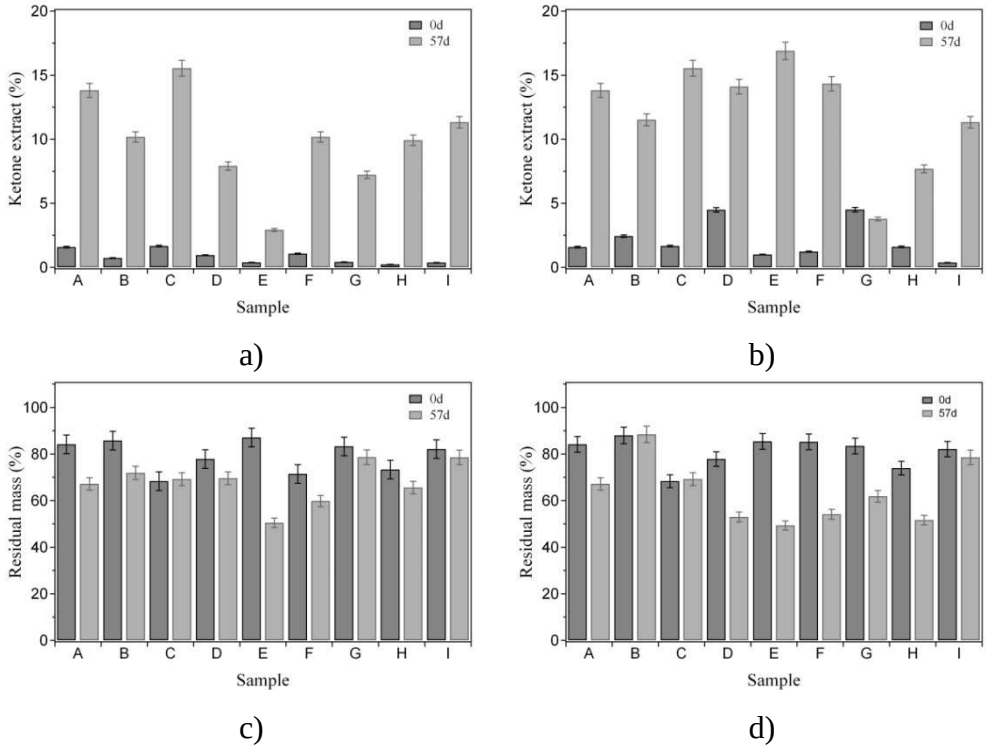


**Figure 3.83.** KE and RM of samples aged at 55 °C for 57 days: (a,c) PE-CS-prodegradant; and .(b,d) PE-Biopar-prodegradant.

Acetone extract values achieve the level of 15% after aging in comparison with 1-4 % obtained before the thermo-degradation, which is and evidence that oxidation occurred (Fig. 3.83 a) and b)). These values were slightly higher for samples containing Biopar (Fig. 3.83 b)) than that containing CS. In addition, 75ET6-1G-15B blend presented the highest value of acetone extract after 57 days aging, this was expected once 75ET6-1G-15B presented the highest increasing in the WG during aging (Figure 3.82c),

which means that a elevated oxidation of PE chain occurred in this formulation.

**Table 3.54.** TGA data of PE-CS-prodegradant composite aged at 55°C for 60 days.[a)]

| Sample | 0 d | | 20 d | | 57 d | |
|---|---|---|---|---|---|---|
| | $T_d$ (°C) | $R_{800}$ (wt-%) | $T_d$ (°C) | $R_{800}$ (wt-%) | $T_d$ (°C) | $R_{800}$ (wt-%) |
| ET6 | 394 | 0.8 | 393 | 1.0 | 159 | 2.0 |
| 7ET6-3C | 259 | 1.9 | 270 | 1.4 | 155 | 1.8 |
| 8ET6-2G | 369 | 1.1 | 374 | 0.6 | 154 | 1.0 |
| 5ET6-2G-3C | 245 | 1.8 | 275 | 1.8 | 153 | 1.6 |
| 75ET6-1G-15C | 276 | 1.0 | 280 | 1.4 | 152 | 1.4 |
| 85ET6-15C | 279 | 1.3 | 283 | 1.3 | 151 | 1.6 |
| 6ET6-1G-3C | 285 | 1.8 | 282 | 1.7 | 141 | 2.0 |
| 65ET6-2G-15C | 281 | 1.0 | 279 | 1.3 | 157 | 1.1 |
| 9ET6-1G | 370 | 1.1 | 384 | 1.2 | 151 | 0.1 |

[a)] $T_d$ is the decomposition temperature defined at 1 wt-% of weight loss and $R_{800}$ is the residual weight of polymer blends at 800°C.

**Table 3.55.** TGA data of PE-Biopar-prodegradant composite aged at 55°C for 60 days.[a)]

| Sample | 0 d | | 20 d | | 57 d | |
|---|---|---|---|---|---|---|
| | $T_d$ (°C) | $R_{800}$ (wt-%) | $T_d$ (°C) | $R_{800}$ (wt-%) | $T_d$ (°C) | $R_{800}$ (wt-%) |
| ET6 | 394 | 0.8 | 393 | 1.0 | 159 | 2.0 |
| 7ET6-3B | 176 | 1.1 | 147 | 1.1 | 146 | 1.2 |
| 8ET6-2G | 369 | 1.1 | 374 | 0.6 | 154 | 1.0 |
| 5ET6-2G-3B | 164 | 0.7 | 179 | 1.3 | 163 | 1.4 |
| 75ET6-1G-15B | 195 | 0.9 | 195 | 1.2 | 166 | 0.9 |
| 85ET6-15B | 216 | 1.2 | 224 | 1.3 | 162 | 1.0 |
| 6ET6-1G-3B | 176 | 1.4 | 213 | 1.1 | 160 | 0.8 |
| 65ET6-2G-15B | 206 | 0.9 | 212 | 1.0 | 167 | 0.8 |
| 9ET6-1G | 370 | 1.1 | 384 | 1.2 | 151 | 0.1 |

[a)] $T_d$ is the decomposition temperature defined at 1 wt-% of weight loss and $R_{800}$ is the residual weight of polymer blends at 800°C.

A way to confirm the oxidation of films is through the assessment of decomposition temperature ($T_d$) of degraded samples. In Tables 3.54 – 3.55 are shown the $T_d$ and the residue at 800 °C ($R_{800}$) of PE-starch-prodegradant based materials. In general, all composites presented a decrease in the thermal stability with aging time. This decrease in $T_d$ also confirms that even if low weight gain was observed during aging (Fig. 3.82), samples were oxidated. Moreover, $R_{800}$ of samples remained almost unchanged after 57 days of temperature exposure.

# CONCLUSIONS

## *Compatibilization of Poly(ethylene)-Poly(3-hydroxybutyrate) Based Blends*

A study of PE-PHB blends compatibilization was performed following a mixture statistical design. The independent variables were the proportion between the three blend components and the type of compatibilizer, which were EVA, EGMA and EMAC. PE-PHB based blends were characterized by using SEM, TGA, DSC, DMTA, WAXS, FTIR and tensile tests. The main conclusions of this work are summarised below.

- From SEM analysis it was seen that the compatibilizer EGMA promoted a better dispersion and interfacial adhesion between both PE and PHB than EVA or EMAC. Moreover, better results were obtained for blends with PE as matrix than those with PHB as matrix.

- Thermal stability of ternary blends with PE as matrix was not significantly influenced by EVA and EGMA compatibilizers. When PHB was used as matrix, the thermal stability of ternary blends formulated with both EVA and EGMA compatibilizers was slightly improved in relation to that of the binary blend 75B25E. On the other hand, the presence of EMAC reduced the thermal stability of all ternary blends regardless of the matrix used, PE or PHB. Moreover, the additive rule applied to the TGA traces was an efficient tool to infer about which phase dispersion plays the predominant effect in the blend thermo-degradation.

- DSC traces of binary and ternary PE-PHB blends formulated with compatibilizers showed two endothermic peaks assigned to PE and PHB. In addition, the PE $T_m$ value remained practically invariable while that of PHB decreased at each DSC heating run suggesting a thermo-degradation of the PHB at each DSC cycle. PE $T_m$ values of

ternary blends taken from the first heating remained equal to that of pristine PE when EVA and EGMA were used as compatibilizer. On the other hand, an increase of the PE $T_m$ value of *ca.* 4 °C was verified for formulations with EMAC. This was probably due to the phase separation present in the blends containing this compatibilizer. The phase separation could cause constrain in the PHB phase and consequently reduce the melting entropy.

- The type of used compatibilizer did not affect the PE crystalline content as measured by DSC. The crystalline content of PE changed as a function of its amount in the blend. Decreasing PE amount in the blends caused an increase in PE crystallinity, regardless of the compatibilizer used (EVA, EGMA or EMAC). On the other hand, the PHB crystalline content remained practically unaltered in all the composition range studied, with values of about 65 %.

- DMTA analysis showed that the blends containing EVA presented a $T_1$ (the temperature at which the modulus starts do decrease) 12 °C higher than the pristine components while blends formulated with EGMA and EMAC had a less significant increase in $T_1$ (*ca.* 7 °C). Moreover, blends compatibilized with EVA and EMAC did not present changes in the $T_g$ of PE. However, the $T_g$ of PE of all ternary blends formulated with EGMA increased to values around 12 °C, demonstrating that some partial compatibility between PE and PHB occurred when EGMA was used as compatibilizer.

- WAXS diffraction patterns of all blends were characteristic of semi-crystalline materials. Furthermore, the position and intensities of the diffraction peaks remained unchanged when PE-PHB were mixed with EVA and EGMA compatibilizers. However, when EMAC was mixed with PHB, the intensities of diffraction peaks decreased and a small shift in the peaks position to higher values was observed. In this way it was demonstrated that EMAC disturb the crystallization of PHB.

- The analyses of the tensile tests showed that the YM was influenced by both matrix used (PE or PHB) and by the amount of compatibilizer in the blend. For formulations with PE as matrix, the YM of binary and ternary blends remained in the same range of that found for pristine PE (YM < 300 MPa). On the other hand, for PHB as matrix, the YM of binary and ternary blends lied between that of PE (190 MPa) and PHB (2060 MPa). In addition, an increase in compatibilizer amount caused a decrease in the YM values of formulations with both polymers matrices.

The multi technique analysis carried out in PE-PHB films compatibilized with EVA, EGMA and EMAC demonstrated that these copolymers promoted some compatibility between PE and PHB. The order for the decreasing of compatibilization was EGMA > EVA > EMAC.

***PE-PHB-EGMA blends formulated with prodegradants***

Plastic materials should not present significant changes in their physical and mechanical properties during their service life. However, after the material has served to its primary purpose, rapid biodegradation and disintegration should occur. A study about PE-PHB-EGMA blends containing prodegradants was carried out following a central composite design (CCD) where the independent variables were the amounts of both the biodegradable polymer PHB and of prodegradant additives T6 and/or T7. This study was divided in three sections: the first one was related to the characterization of PE-PHB-prodegradant films obtained by melt blow extrusion. The second section regards the oxidation behaviour of PE-PHB-prodegradant blends. Finally, the third section regards the assessment of films biodegradability. These studies together can be used as a model for the prediction of the behaviour of oxo-biodegradable materials, where both lifetime and mineralization time can be determined. The main conclusions of this work are summarised below.

- The amount of PHB added in the formulations was proportional to the amount of the polar comonomer of compatibilizer. Hence, the blends did not show phase separation and presented good characteristics to be processed and used as packaging materials. The MFI of the samples were lower than 1.36 g/10min. The mechanical properties YM, ST and SB remained invariable in relation to the values measured for PEL (YM: 147-200 MPa, ST: 15-20 MPa and SB: 222-356 %). The lower thermal stability was found for the samples containing the highest amount of additives (2B3T63T6). These samples presented a $T_d$ value of 239 °C, which is higher than the temperatures used of PE processing. All samples showed the $T_m$ value of approximately 108 °C.

- In the aging study, it was observed that even when quite small amounts of prodegradants (3 wt-%) were added in the blends formulations, they were effective in promoting the degradation of the materials. The values of *Ea* were significantly different depending on the blend composition, measured by the rate of thermal degradation of the samples at three temperatures. The presence of PHB significantly decreased the *Ea* of the blends. The *Ea* values could be used to estimate the lifetime (or service life) of the films in indoor conditions. On the molecular level, the abiotic oxidation resulted in significant changes in both scission and crosslink concentrations of the samples measured by GPC and gel content. These results indicated that a strong thermal degradation occurred in all blends containing prodegradants along with a decrease in the MW of the samples and the introduction of polar groups such as carboxylic acids. In this way, the oxidation left the films more vulnerable to microbial attack. The TGA measurements showed a decrease in the thermal stability of the films exposed to thermo-oxidation as a consequence of the reduction in the MW of polymer chains. In addition, the DSC results demonstrated an increase in the crystallinity with the aging time, which was attributed to chain scission and secondary crystallization. Finally, the mechanical performance (ST

and SB) was reduced and an increase in the YM of the samples was in good agreement with the chemical degradation of the materials, followed through the formation of carbonyl groups.

- Biodegradation studies had shown the presence of microorganisms in the PE surface after biodegradation in aquatic media. Nevertheless, microbial growth was not detected in soil buried samples. This suggested that the microorganisms were leached out from the film surfaces during the washing step carried out on samples before the characterization. In addition, the mineralization of pristine PE-PHB films did not occur to any significant extent during incubation in aquatic media or soil burial. The highest mineralization values were obtained through the assimilation of the low molecular weight oxidation product as they were present in pre-oxidized samples. The decomposition temperature of the thermo aged samples increased after both 125 days in aquatic media and 6 months of incubation in soil. These results suggested that during biodegradation experiments these samples undergo some crosslinking and this effect was more evident for samples containing T7 than T6 prodegradant.

The most important finding of this study was that for all the blends, films containing prodegradants were unique to achieve an advanced state of embrittlement after 45 days aging. The disintegration into small fragments provides a potential solution to the problems of visual pollution by plastic litter commonly abandoned in the environment. Moreover, the biodegradation experiments showed that the oxidation process is the determining step in the oxo-biodegradation of PE based blends containing or not PHB, once biodegradation of pre-oxidized films starts without any induction period.

***PE-Starch based composites***

PE-Starch based composites are a promising family of materials, which have been commercially available since the 1970's. However, the incompatibility between the two components is still an important aspect. In this work, a screening experiment consisting of a factorial $2^2$ design combined or not with a mixture design was performed to formulate PE based blends containing starches in order to assess the PE-Starch compatibility. Subsequently, new families of PE materials containing starch and prodegradants were formulated and characterized. The main conclusions of this work are reported below.

- The best level of compatibility was detected for PE composites containing 20 wt-% of granular corn-starch and EGMA as compatibilizer. The tensile testes showed satisfactory YM and ST values, obtained when PE-CS were compatibilized with EGMA (PE-CS-EGMA). On the other hand, the other families of PE-CS presented lower mechanical performance.

- In PE-CS composites containing prodegradants, the presence of corn-starch in the ET6 matrix reduced the MFI of samples. On the other hand, composites containing 15 wt-% of Biopar presented an increase in the MFI in relation to ET6 matrix. Nonetheless, this value is still appropriate for blow moulding, generally applied in packaging manufacture of containers for food and food applications.

- Tensile tests performed on all the samples demonstrated that films formulated with CS presented higher values of YM than those formulated with Biopar. On the other hand, the SB of PE-Biopar samples was higher compared to that of PE-CS. Additionally, both families of materials (CS or Biopar in concentrations up to 15 wt-%) showed satisfactory ST.

- The effective oxidation of PE-CS and PE-Biopar samples was confirmed by the amount of extractable oxidized fractions and the decrease in the $T_d$ of all films.

An acceptable mechanical performance was obtained when PE-CS composites were formulated using EGMA copolymer as compatibilizer. Moreover, thermo-oxidation was effective in films containing T6 and starch based additives. However, considering the KE results, the thermo-oxidation was not improved by the addition of starch.

## REFERENCES


[1] McGlade, J., European packaging waste trends and the role of economic instruments, European Voice Conference Packaging Our Futures - Brussels, 1-2 March, European Environment Agency, 2004. http://www.eea.europa.eu/pressroom/speeches/01-03-2004 (30 November 2007).

[2] Ackerman, F., Environmental impacts of packaging in the U.S. and Mexico, E-Journal - Society for Philosophy and Technology 1997. http://scholar.lib.vt.edu/ejournals/SPT/v2_n2html/ackerman.html (31 January 2008).

[3] *Packaging Likes Polymers I – Economic and Technical Outline*, SpecialChem - Omnexus, 2004. http://www.omnexus.com/resources/articles/article.aspx?id=3323&or=s290621_101_&q=packaging+ (30 November 2007).

[4] Consumer Packaging Report 2007-08 'Imagining Tomorow', Rexan, 2007. http://www.rexam.com/files/pdf/Rexam_Consumer_Packaging_Report_2007.pdf (27 November 2007).

[5] Apresentação Apimec - Resultados 3T05 - Novembro, Suzano Petroquímica, 2005. www.suzanopetroquimica.com.br/navitacontent_/dbfiles/E2858FFD-AED4-4643-B69A007E03C9B115.arquivo.pdf?ECA8B964-B5FA-0FA2-4B5BBA813C4E953D (30 November 2007).

[6] CMAI 1998/99 World Polyolefins Analysis (pdf format), CMAI, 1999. http://www.cmaiglobal.com/News.aspx (31 January 2008).

[7] Psomiadou, E.; Arvanitoyannis, I.; Biliaderis, C. G.; Ogawa, H.; Kawasaki, N. Biodegradable films made from low density polyethylene (LDPE), wheat starch and soluble starch for food packaging applications. Part 2. Carbohydrate Polymers 1997, 33, (4), 227-242.

[8] Packaging and Packaging Waste - Official Journal L 365, (31/12/1994) 0010 – 0023, European Parliament and Council Directive 94/62/EC, 1994. http://eur-lex.europa.eu/LexUriServ/LexUriServ.do?uri=CELEX:31994L0062:EN:HTML (27 november 2007).

[9] Waste - Official Journal L 194, (25/07/1975) 0039 – 0041, European Parliament and Council Directive 75/442/EEC, 1975. http://eur-lex.europa.eu/LexUriServ/LexUriServ.do?uri=CELEX:31975L0442:EN:HTML (27 november 2007).

[10] Packaging and Packaging Waste - Statement by the Council, the Commission and the European Parliament - Official Journal L 047, 18/02/2004 P. 0026 – 0032, Directive 2004/12/EC of the European Parliament and of the Council of 11 February 2004 amending Directive 94/62/EC, 2004. http://eur-lex.europa.eu/LexUriServ/LexUriServ.do?uri=CELEX:32004L0012:EN:HTML (27 november 2007).

[11] Scott, G. \"Green\" Polymers. Polymer Degradation and Stability 2000, 68, (1), 1-7.

[12] Gross, R. A.; Kalra, B. Biodegradable polymers for the environment. Science (Washington, DC, United States) 2002, 297, (5582), 803-807.

[13] Yavuz, H.; Babac, C. Preparation and biodegradation of starch/polycaprolactone films. Journal of Polymers and the Environment 2003, 11, (3), 107-113.

[14] Tice, P., Packaging Materials: 4. Polyethylene for Food Packaging Applications, ILSI Europe, 2003. http://europe.ilsi.org/publications/Report+Series/foodpkgapps4.htm (29 december 2007).

[15] Adams, J. H. Analysis of the nonvolatile oxidation products of polypropylene. I. Thermal oxidation. Journal of Polymer Science, Polymer Chemistry Edition 1970, 8, (5), 1077-1090.

[16] Adams, J. H.; Goodrich, J. E. Analysis of nonvolatile oxidation products of polypropylene. II. Process degradation. Journal of Polymer Science, Polymer Chemistry Edition 1970, 8, (5), 1269-1277.

[17] Iring, M.; Foldes, E.; Barabas, K.; Kelen, T.; Tudos, F.; Odor, L. Thermal oxidation of linear low-density polyethylene. Polymer Degradation and Stability 1986, 14, (4), 319-332.

[18] Start, P., Surlyn®, Group of Prof. Kenneth A. Mauritz - School of Polymers and High Performance Materials - The University of Southern Mississippi, http://www.psrc.usm.edu/mauritz/surlyn.html (1 February 2008).

[19] The history of an idea, Tetra Pack, 2002. http://www.tetrapak.com/index.asp?page=crp_innovation& (1 February 2008).

[20] Lofgren, L.; Svensson, C. Packaging Materials of Laminate Type. US5133999, Jul 28, 1992.

[21] Khabbaz, F.; Albertsson, A. C.; Karlsson, S. Trapping of volatile low molecular weight photoproducts in inert and enhanced degradable LDPE. Polymer Degradation and Stability 1998, 61, (2), 329-342.

[22] Kyrikou, I.; Briassoulis, D. Biodegradation of agricultural plastic films: A critical review. Journal of Polymers and the Environment 2007, 15, (2), 125-150.

[23] Krzan, A.; Hemjinda, S.; Miertus, S.; Corti, A.; Chiellini, E. Standardization and certification in the area of environmentally degradable plastics. Polymer Degradation and Stability 2006, 91, (12), 2819-2833.

[24] Karlsson, S.; Albertsson, A.-C. Biodegradable polymers and environmental interaction. Polymer Engineering and Science 1998, 38, (8), 1251-1253.

[25] Albertsson, A. C.; Andersson, S. O.; Karlsson, S. The mechanism of biodegradation of polyethylene. Polymer Degradation and Stability 1987, 18, (1), 73-87.

[26] Pandey, J. K.; Reddy, K. R.; Kumar, A. P.; Singh, R. P. An overview on the degradability of polymer nanocomposites. Polymer Degradation and Stability 2005, 88, (2), 234-250.

[27] Shah, P. B.; Bandopadhyay, S.; Bellare, J. R. Environmentally degradable starch filled low density polyethylene. Polymer Degradation and Stability 1995, 47, (2), 165-173.

[28] Cinelli, P. Formulation and Characterization of Environmentally Compatible Polymeric Materials for Agriculture Applications. PhD, University of Pisa, Pisa, 1998.

[29] Jang, B. C.; Huh, S. Y.; Jang, J. G.; Bae, Y. C. Mechanical properties and morphology of the modified HDPE/starch reactive blend. Journal of Applied Polymer Science 2001, 82, (13), 3313-3320.

[30] Chandra, R.; Rustgi, R. Biodegradation of maleated linear low-density polyethylene and starch blends. Polymer Degradation and Stability 1997, 56, (2), 185-202.

[31] Saad, G. R.; Seliger, H. Biodegradable copolymers based on bacterial poly((R)-3-hydroxybutyrate): thermal and mechanical properties and biodegradation behaviour. Polymer Degradation and Stability 2004, 83, (1), 101-110.

[32] Sharma, N.; Chang, L. P.; Chu, Y. L.; Ismail, H.; Ishiaku, U. S.; Ishak, Z. A. M. A study on the effect of pro-oxidant on the thermo-oxidative degradation behaviour of sago starch filled polyethylene. Polymer Degradation and Stability 2001, 71, (3), 381-393.

[33] Albertsson, A. C.; Griffin, G. J. L.; Karlsson, S.; Nishimoto, K.; Watanabe, Y. Spectroscopic and mechanical changes in irradiated starch-filled LDPE. Polymer Degradation and Stability 1994, 45, (2), 173-178.

[34] Albertsson, A. C.; Barenstedt, C.; Karlsson, S. Degradation of enhanced environmentally degradable polyethylene in biological aqueous media: mechanisms during the first stages. Journal of Applied Polymer Science 1994, 51, (6), 1097-1105.

[35] Wiles, D. M.; Scott, G. Polyolefins with controlled environmental degradability. Polymer Degradation and Stability 2006, 91, (7), 1581-1592.

[36] Billingham, N. C.; Grigg, M. N. The kinetic order of decomposition of polymer hydroperoxides assessed by chemiluminescence. Polymer Degradation and Stability 2004, 83, (3), 441-451.

[37] Jakubowicz, I. Evaluation of degradability of biodegradable polyethylene (PE). Polymer Degradation and Stability 2003, 80, (1), 39-43.

[38] Koutny, M.; Lemaire, J.; Delort, A. M. Biodegradation of polyethylene films with prooxidant additives. Chemosphere 2006, 64, (8), 1243-1252.

[39] Albertsson, A. C.; Karlsson, S. Environment-adaptable polymers. Polymer Degradation and Stability 1993, 41, (3), 345-349.

[40] Roy, P. K.; Surekha, P.; Rajagopal, C.; Choudhary, V. Effect of cobalt carboxylates on the photo-oxidative degradation of low-density polyethylene. Part-I. Polymer Degradation and Stability 2006, 91, (9), 1980-1988.

[41] Khabbaz, F.; Albertsson, A. C.; Karlsson, S. Chemical and morphological changes of environmentally degradable polyethylene films exposed to thermo-oxidation. Polymer Degradation and Stability 1999, 63, (1), 127-138.

[42] Jones, P.; Prasad, D.; Heskins, M.; Morgan, M.; Guillet, J. Biodegradability of photodegraded polymers. I. Development of experimental procedures. Environmental Science and Technology 1974, 8, (10), 919-923.

[43] Lourdin, D.; DellaValle, G.; Colonna, P. Influence of amylose content on starch films and foams. Carbohydrate Polymers 1995, 27, (4), 261-270.

[44] Lorcks, J. Properties and applications of compostable starch-based plastic material. Polymer Degradation and Stability 1998, 59, (1-3), 245-249.

[45] Griffin, G. Synthetic resin sheet material. US4021388, May 03, 1977.

[46] Sailaja, R. R. N. Mechanical properties of esterified tapioca starch-LDPE blends using LDPE-co-glycidyl methacrylate as compatibilizer. Polymer International 2005, 54, (2), 286-296.

[47] Sailaja, R. R. N.; Reddy, A. P.; Chanda, M. Effect of epoxy functionalized compatibilizer on the mechanical properties of low-density polyethylene/plasticized tapioca starch blends. Polymer International 2001, 50, (12), 1352-1359.

[48] Sailaja, R. R. N.; Chanda, M. Use of maleic anhydride-grafted polyethylene as compatibilizer for HDPE-tapioca starch blends: Effects on mechanical properties. Journal of Applied Polymer Science 2001, 80, (6), 863-872.

[49] Sailaja, R. R. N.; Chanda, M. Use of poly(ethylene-co-vinyl alcohol) as compatibilizer in LDPE/thermoplastic tapioca starch blends. Journal of Applied Polymer Science 2002, 86, (12), 3126-3134.

[50] Jeziorska, R.; Zakowska, Z.; Stolbinska, H.; Ratajska, M.; Zielonka, M. Properties of blends of starch, polyethylene and poly(ethylene-co-acrylic acid) copolymer. Polimery 2003, 48, (3), 211-214.

[51] Wang, S.; Yu, J.; Yu, J. Preparation and Characterization of Compatible and Degradable Thermoplastic Starch/Polyethylene Film. Journal of Polymers and the Environment 2006, 14, (1), 65-70.

[52] Raghavan, D.; Emekalam, A. Characterization of starch/polyethylene and starch/polyethylene/poly(lactic acid) composites. Polymer Degradation and Stability 2001, 72, (3), 509-517.

[53] Griffin, G. Synthetic/resin based compositions. US4125495, Nov 14, 1978.

[54] Griffin, G. Degradable plastics. US4983651, Jan 08, 1991.

[55] Griffin, G. Degradable plastics. US5212219, May 18, 1993.

[56] Suominen, H. Production of biologically degradable films. US5133909, Jul 28, 1992.

[57] Suominen, H. Biologically degradable plant cover film and method of preparing same. US5118725, Jun 2, 1992.

[58] Abou-Zeid, D.-M.; Mueller, R.-J.; Deckwer, W.-D. Biodegradation of Aliphatic Homopolyesters and Aliphatic-Aromatic Copolyesters by Anaerobic Microorganisms. Biomacromolecules 2004, 5, (5), 1687-1697.

[59] Briassoulis, D. An overview on the mechanical behaviour of biodegradable agricultural films. Journal of Polymers and the Environment 2004, 12, (2), 65-81.

[60] Lenz, R. W.; Marchessault, R. H. Bacterial Polyesters: Biosynthesis, Biodegradable Plastics and Biotechnology. Biomacromolecules 2005, 6, (1), 1-8.

[61] Renstad, R.; Karlsson, S.; Albertsson, A.-C. Influence of processing parameters on the molecular weight and mechanical properties of poly(3-hydroxybutyrate-co-3-hydroxyvalerate). Polymer Degradation and Stability 1997, 57, (3), 331-338.

[62] Bucci, D. Z.; Tavares, L. B. B.; Sell, I. PHB packaging for the storage of food products. Polymer Testing 2005, 24, (5), 564-571.

[63] Eldsater, C.; Karlsson, S.; Albertsson, A.-C. Effect of abiotic factors on the degradation of poly(3-hydroxybutyrate-co-3-hydroxyvalerate) in simulated and natural composting environments. Polymer Degradation and Stability 1999, 64, (2), 177-183.

[64] Doi, Y.; Kanesawa, Y.; Kunioka, M.; Saito, T. Biodegradation of microbial copolyesters: poly(3-hydroxybutyrate-co-3-hydroxyvalerate) and poly(3-hydroxybutyrate-co-4-hydroxybutyrate). Macromolecules 1990, 23, (1), 26-31.

[65] Wang, Y.-W.; Mo, W.; Yao, H.; Wu, Q.; Chen, J.; Chen, G.-Q. Biodegradation studies of poly(3-hydroxybutyrate-co-3-hydroxyhexanoate). Polymer Degradation and Stability 2004, 85, (2), 815-821.

[66] Gunaratne, L.; Shanks, R. A. Melting and thermal history of poly(hydroxybutyrate-co-hydroxyvalerate) using step-scan DSC. Thermochimica Acta 2005, 430, (1-2), 183-190.

[67] Gunaratne, L.; Shanks, R. A.; Amarasinghe, G. Thermal history effects on crystallisation and melting of poly (3-hydroxybutyrate). Thermochimica Acta 2004, 423, (1-2), 127-135.

[68] Withey, R. E.; Hay, J. N. The effect of seeding on the crystallisation of poly(hydroxybutyrate), and co-poly(hydroxybutyrate-co-valerate). Polymer 1999, 40, (18), 5147-5152.

[69] Grassie, N.; Murray, E. J.; Holmes, P. A. The thermal degradation of poly(-(D)-b-hydroxybutyric acid). Part 2. Changes in molecular weight. Polymer Degradation and Stability 1984, 6, (2), 95-103.

[70] Janigova, I.; Lacik, I.; Chodak, I. Thermal degradation of plasticized poly(3-hydroxybutyrate) investigated by DSC. Polymer Degradation and Stability 2002, 77, (1), 35-41.

[71] Grassie, N.; Murray, E. J.; Holmes, P. A. The thermal degradation of poly(-(D)-b-hydroxybutyric acid). Part 3. The reaction mechanism. Polymer Degradation and Stability 1984, 6, (3), 127-134.

[72] Kopinke, F. D.; Remmler, M.; Mackenzie, K. Thermal decomposition of biodegradable polyesters. I: poly(b-hydroxybutyric acid). Polymer Degradation and Stability 1996, 52, (1), 25-38.

[73] Iordanskii, A. L.; Kamaev, P. P.; Ol'khov, A. A.; Wasserman, A. M. Water transport phenomena in 'green' and 'petrochemical' polymers. Differences and similarities. Desalination 1999, 126, (1-3), 139-145.

[74] Rosa, D. D.; Gaboardi, F.; Guedes, C. D. F.; Calil, M. R. Influence of oxidized polyethylene wax (OPW) on the mechanical, thermal, morphological and biodegradation properties of PHB/LDPE blends. Journal of Materials Science 2007, 42, (19), 8093-8100.

[75] Pospisil, J.; Pilar, J.; Billingham, N. C.; Marek, A.; Horak, Z.; Nespurek, S. Factors affecting accelerated testing of polymer photostability. Polymer Degradation and Stability 2006, 91, (3), 417-422.

[76] Hinsken, H.; Moss, S.; Pauquet, J. R.; Zweifel, H. Degradation of polyolefins during melt processing. Polymer Degradation and Stability 1991, 34, (1-3), 279-293.

[77] Billingham, N. C. Oxidative degradation of polymers: An introduction. Abstracts of Papers of the American Chemical Society 2001, 221, U328-U328.

[78] Moss, S.; Zweifel, H. Degradation and stabilization of high-density polyethylene during multiple extrusions. Polymer Degradation and Stability 1989, 25, (2-4), 217-245.

[79] ASTM Standard D2765-01, 2006, Standard Test Methods for Determination of Gel Content and Swell Ratio of Crosslinked Ethylene Plastics, ASTM International, West Conshohocken, PA, www.astm.org.

[80] Qualità delle acque dei corsi d'acqua dei bacini di Pisa Nord e Pisa Sud, Agenzia Regionale per la Protezione Ambientale della Toscana (ARPAT) – Dipartimento Provinciale di Pisa: Pisa - Italy, 2003.

[81] Atkins, P. W.; De Paula, J., Atkins' Physical Chemistry. 7th ed.; Oxford University Press: Oxford (UK), 2002.

[82] Kaczmarek, H.; Oldak, D. The effect of UV-irradiation on composting of polyethylene modified by cellulose. Polymer Degradation and Stability 2006, 91, (10), 2282-2291.

[83] Sturm, R. N. Biodegradability of nonionic surfactants. Screening test for predicting rate and ultimate biodegradation. Journal of the American Oil Chemists Society, 1973, 50, 159-167.

[84] ASTM Standard D 5209, 1992, Determining the Aerobic Biodegradability of Plastic Materials in the Presence of Municipal Sewage Sludge, ASTM International, West Conshohocken, PA, www.astm.org.

[85] ASTM Standard D 5338, 1998, Determining Aerobic Biodegradation of Plastic Materials Under Controlled Composting Conditios, ASTM International, West Conshohocken, PA, www.astm.org.

[86] Chiellini, E.; Corti, A.; D'Antone, S. Oxo-biodegradable full carbon backbone polymers - biodegradation behavior of thermally oxidized polyethylene in an aqueous medium. Polymer Degradation and Stability 2007, 92, (7), 1378-1383.

[87] Chiellini, E.; Corti, A. A simple method suitable to test the ultimate biodegradability of environmentally degradable polymers. Macromolecular Symposia 2003, 197, (7th World Conference on Biodegradable Polymers & Plastics, 2002), 381-395.

[88] ASTM Standard E 1720, 2001, Determining Ready, Ultimate, Biodegradability of Organic Chemicals in a Sealed Vessel $CO_2$ Production Test, ASTM International, West Conshohocken, PA, www.astm.org.

[89] OECD 301, 1992, Guideline for Testing of Chemicals - Ready Biodegradability, Organisation for Economic Co-operation and Development, www.oecd.org.

[90] EN ISO 14593, 1999, Water Quality - Evaluation of Ultimate Aerobic Biodegradability of Organic Compounds in Aqueous Medium . Method by Analysis of Inorganic Carbon in Sealled Vessels ($CO_2$ Headspace Test), CEN European Committee for Standardization, Brussels, www.cen.eu/cenorm/aboutus/index.asp.

[91] ASTM Standard D1238-04c, 2004, Standard Test Method for Melt Flow Rates of Thermoplastics by Extrusion Plastometer, ASTM International, West Conshohocken, PA, www.astm.org.

[92] Gulmine, J. V.; Janissek, P. R.; Heise, H. M.; Akcelrud, L. Degradation profile of polyethylene after artificial accelerated weathering. Polymer Degradation and Stability 2003, 79, (3), 385-397.

[93] ASTM Standard E104-02, 2002, Standard Practice for Maintaining Constant Relative Humidity by Means of Aqueous Solutions, ASTM International, West Conshohocken, PA, www.astm.org.

[94] ASTM Standard D1708-06a, 2006, Standard Test Method for Tensile Properties of Plastics by Use of Microtensile Specimens, ASTM International, West Conshohocken, PA, www.astm.org.

[95] ASTM Standard D882-02, 2002, Standard Test Method for Tensile Properties of Thin Plastic Sheeting, ASTM International, West Conshohocken, PA, www.astm.org.

[96] Zheng, Y.; Yanful, E. K.; Bassi, A. S. A review of plastic waste biodegradation. Critical Reviews in Biotechnology 2005, 25, (4), 243-250.

[97] Kim, J.; Kim, J. H.; Shin, T. K.; Choi, H. J.; Jhon, M. S. Miscibility and rheological characteristics of biodegradable aliphatic polyester and linear low density polyethylene blends. European Polymer Journal 2001, 37, (10), 2131-2139.

[98] Hay, J. N.; Sharma, L. Crystallisation of poly(3-hydroxybutyrate)/polyvinyl acetate blends. Polymer 2000, 41, (15), 5749-5757.

[99] Yoon, J. S.; Oh, S. H.; Kim, M. N. Compatibility of poly(3-hydroxybutyrate)/poly(ethylene-co-vinyl acetate) blends. Polymer 1998, 39, (12), 2479-2487.

[100] Lee, M. S.; Park, W. H. Compatibility and thermal properties of poly(3-hydroxybutyrate)/poly(glycidyl methacrylate) blends. Journal of Polymer Science Part a-Polymer Chemistry 2002, 40, (3), 351-358.

[101] An, Y.; Dong, L.; Li, G.; Mo, Z.; Feng, Z. Miscibility, crystallization kinetics, and morphology of poly(b-hydroxybutyrate) and poly(methyl acrylate) blends. Journal of Polymer Science, Part B: Polymer Physics 2000, 38, (14), 1860-1867.

[102] Hale, A.; Bair, H. E., Polymer Blends and Block Copolymers. In Thermal Characterization of Polimeric Materials, 2nd ed.; Turi, E. A., Ed. Academic Press: San Diego, 1997; Vol. I.

[103] Day, M.; Cooney, J. D.; Shaw, K.; Watts, J. Thermal analysis of some environmentally degradable polymers. Journal of Thermal Analysis and Calorimetry 1998, 52, (2), 261-274.

[104] Fernandes, E. G.; Lombardi, A.; Solaro, R.; Chiellini, E. Thermal characterization of three-component blends for hot-melt adhesives. Journal of Applied Polymer Science 2001, 80, (14), 2889-2901.

[105] Lee, S. N.; Lee, M. Y.; Park, W. H. Thermal Stabilization of Poly(3-hydroxybutyrate) by Poly(glycidyl methacrylate). Joural of Applied Polymer Science 2002, 83, 2945-2952.

[106] Huang, J. W.; Kang, C. C. Unusual thermal degradation behavior of PEGMA in air at diffeirent heating rates. Polymer Journal 2004, 36, (7), 574-576.

[107] Chiellini, E.; Fernandes, E. G.; Pietrini, M.; Solaro, R. Factorial design in optimization of PHAs processing. Macromolecular Symposia 2003, 197, (7th World Conference on Biodegradable Polymers & Plastics, 2002), 45-55.

[108] Aoyagi, Y.; Yamashita, K.; Doi, Y. Thermal degradation of poly (R)-3-hydroxybutyrate , poly epsilon-caprolactone , and poly (S)-lactide. Polymer Degradation and Stability 2002, 76, (1), 53-59.

[109] Dodson, B.; McNeill, I. Degradation of polymer mixtures. VI. Blends of poly(vinyl chloride) with polystyrene. Polymer Science, Polymer Chemistry 1976, 14, (2), 353-364.

[110] Barham, P. J.; Keller, a.; Otun, E. L.; A, H. P. Crystallization and morphology of a bacterial thermoplastic: poly-3-hydroxybutyrate. Jounal of Materials Science 1984, 19, (9), 2781-2794.

[111] Poley, L. H.; Siqueira, A. P. L.; da Silva, M. G.; Vargas, H.; Sanchez, R. Photothermal characterization of low density polyethylene food packages. Polimeros: Ciencia e Tecnologia 2004, 14, (1), 8-12.

[112] Chartoff, R. P., Thermoplastic Polymers. In Thermal Characterization of Polymeric Materials, 2nd ed.; Turi, E. A., Ed. Academic Press: San Diego, 1997; Vol. I.

[113] An, Y.; Dong, L.; Li, L.; Mo, Z.; Feng, Z. Isothermal crystallization kinetics and melting behavior of poly(B-hydroxybutyrate)/poly(vinyl acetate) blends. European Polymer Journal 1999, 35, 365-369.

[114] Na, Y. H.; He, Y.; Asakawa, N.; Yoshie, N.; Inoue, Y. Miscibility and phase structure of blends of poly(ethylene oxide) with poly(3-hydroxybutyrate), poly(3-hydroxypropionate), and their copolymers. Macromolecules 2002, 35, (3), 727-735.

[115] Xing, P. X.; Ai, X.; Dong, L. S.; Feng, Z. L. Miscibility and crystallization of poly(beta-hydroxybutyrate)/poly(vinyl acetate-co-vinyl alcohol) blends. Macromolecules 1998, 31, (20), 6898-6907.

[116] Velayudhan, S.; Ramesh, P.; Varma, H. K.; Friedrich, K. Dynamic mechanical properties of hydroxyapatite-ethylene vinyl acetate copolymer composites. Materials Chemistry and Physics 2004, 89, (2-3), 454-460.

[117] Simanke, A. G.; Galland, G. B.; Freitas, L.; Alziro, J.; Da Jornada, H.; Quijada, R.; Mauler, R. S. Influence of the comonomer content on the thermal and dynamic mechanical properties of metallocene ethylene/1-octene copolymers. Polymer 1999, 40, (20), 5489-5495.

[118] Huang, Y.; Jiang, S.; Wu, L.; Hua, Y. Characterization of LLDPE/nano-SiO2 composites by solid-state dynamic mechanical spectroscopy. Polymer Testing 2004, 23, (1), 9-15.

[119] Cimmino, S.; Iodice, P.; Silvestre, C.; Karasz, F. E. Atactic poly(methyl methacrylate) blended with poly(3-D(-)hydroxybutyrate): miscibility and mechanical properties. Journal of Applied Polymer Science 2000, 75, (6), 746-753.

[120] Popli, R.; Glotin, M.; Mandelkern, L.; Benson, R. S. Dynamic mechanical studies of a and b relaxations of polyethylenes. Journal of Polymer Science, Polymer Physics Edition 1984, 22, (3), 407-48.

[121] Gray, R. W.; McCrum, N. G. g-Relaxations in linear polyethylene and poly(tetrafluoroethylene). Journal of Polymer Science, Polymer Letters Edition 1968, 6, (10), 691-697.

[122] Rault, J. The ac transition in semicrystalline polymers: a new look at crystallization deformation and aging process. Journal of Macromolecular Science, Reviews in Macromolecular Chemistry and Physics 1997, C37, (2), 335-387.

[123] Popli, R.; Mandelkern, L. The transition in ethylene copolymers: the b-transition. Polymer Bulletin (Berlin, Germany) 1983, 9, (6-7), 260-267.

[124] Boyd, R. H. Relaxation processes in crystalline polymers: molecular interpretation - a review. Polymer 1985, 26, (8), 1123-1133.

[125] Boyd, R. H. Relaxation processes in crystalline polymers: experimental behavior. Polymer 1985, 26, (3), 323-347.

[126] Chen, D.-H.; Hong, L.; Nie, X.-W.; Wang, X.-L.; Tang, X.-Z. Study on rheological properties and relaxational behavior of poly(dianiline phosphazene)/low-density polyethylene blends. European Polymer Journal 2003, 39, (5), 871-876.

[127] Stadler, F. J.; Kaschta, J.; Muenstedt, H. Dynamic-mechanical behavior of polyethylenes and ethene-/a-olefin-copolymers. Part I. a'-Relaxation. Polymer 2005, 46, (23), 10311-10320.

[128] An, Y.; Li, L.; Dong, L.; Mo, Z.; Feng, Z. Nonisothermal Crystallization and Melting Behavior of Poly(B-Hydroxybutyrate)-Poly(vinyl-acetate) Blends. Journal of Polymer Science, Part B: Polymer Physics 1999, 37, 443-450.

[129] Zainuddin; Sudradjat, A.; Razzak, M. T.; Yoshii, F.; Makuuchi, K. Polyblend CPP and Bionolle with PP-g-MAH as compatibilizer: I. Compatibility. Journal of Applied Polymer Science 1999, 72, (10), 1277-1282.

[130] Contat-Rodrigo, L.; Ribes-Greus, A. Viscoelastic behavior of degradable polyolefins aged in soil. Journal of Applied Polymer Science 2000, 78, (10), 1707-1720.

[131] Albertsson, A.-C.; Barenstedt, C.; Karlsson, S.; Lindberg, T. Degradation product pattern and morphology changes as means to differentiate abiotically and biotically aged degradable polyethylene. Polymer 1995, 36, (16), 3075-3083.

[132] Saha, N.; , Z., M., and ; Saha, P. Modification of polymers by protein hydrolysate-a way to biodegradable materials. Polymers for Advanced Technologies 14, (2003), 854-860. 2003, 14, 854-860.

[133] Pal, J.; Singh, H.; Ghosh, A. K. Modification of LLDPE using esterified styrene maleic anhydride copolymer: Study of its properties and environmental degradability. Journal of Applied Polymer Science 2004, 92, (1), 102-108.

[134] Bonhomme, S.; Cuer, A.; Delort, A. M.; Lemaire, J.; Sancelme, M.; Scott, G. Environmental biodegradation of polyethylene. Polymer Degradation and Stability 2003, 81, (3), 441-452.

[135] Chiellini, E.; Corti, A.; Swift, G. Biodegradation of thermally-oxidized, fragmented low-density polyethylenes. Polymer Degradation and Stability 2003, 81, (2), 341-351.

[136] Drake, W. O.; Pauquet, J. R.; Todesco, R. V. a.; Zweifel, H. Processing stabilization of polyolefins. Angewandte Makromolekulare Chemie 1989, 176, (1), 215-230.

[137] Ghaneh-Fard, A. Effects of film blowing conditions on molecular orientation and mechanical properties of polyethylene films. Journal of Plastic Film & Sheeting 1999, 15, (3), 194-218.

[138] Amass, W.; Amass, A.; Tighe, B. A review of biodegradable polymers: uses, current developments in the synthesis and characterization of biodegradable polyesters, blends of biodegradable polymers and recent advances in biodegradation studies. Polymer International 1998, 47, (2), 89-144.

[139] Oldak, D.; Kaczmarek, H.; Buffeteau, T.; Sourisseau, C. Photo- and bio-degradation processes in polyethylene, cellulose and their blends studied by ATR-FTIR and Raman spectroscopies. Journal of Materials Science 2005, 40, (16), 4189-4198.

[140] Singh, A. Irradiation of polyethylene: Some aspects of crosslinking and oxidative degradation. Radiation Physic Chemistry 1999, 56, (4), 375-380.

[141] Gulmine, J. V.; Akcelrud, L. FTIR characterization of aged XLPE. Polymer Testing 2006, 25, (7), 932-942.

[142] Marcilla, A.; Ruiz-Femenia R; Hernandez, J.; Garcia-Quesada, J. C. Thermal and catalytic pyrolysis of crosslinked polyethylene. Journal of Analytical and Applied Pyrolysis 2006, 76, (2), 254-259.

[143] Craig, I. H.; White, J. R.; Kin, P. C. Crystallization and chemi-crystallization of recycled photo-degraded polypropylene. Polymer 2005, 46, (2), 505-512.

[144] Rabello, M. S.; White, J. R. The role of physical structure and morphology in the photodegradation behaviour of polypropylene. Polymer Degradation and Stability 1997, 56, (1), 55-73.

[145] Davis, G. U. Open windrow composting of polymers: An investigation into the operational issues of composting polyethylene (PE). Waste Management 2005, 25, (4), 401-407.

[146] Albertsson, A.-C.; Barenstedt, C.; Karlsson, S. Solid-phase extraction and gas chromatographic-mass spectrometric identification of degradation products from enhanced environmentally degradable polyethylene. Journal of Chromatography, A 1995, 690, (2), 207-217.

[147] Jipa, S.; Zaharescu, T.; Gigante, B.; Santos, C.; Setnescu, R.; Setnescu, T.; Dumitru, M.; Gorghiu, L. M.; Kappel, W.; Mihalcea, I. Chemiluminescence investigation of thermo-oxidative degradation of polyethylenes stabilized with fullerenes. Polymer Degradation and Stability 2003, 80, (2), 209-216.

[148] Jacobson, K.; Eriksson, P.; Reitberger, T.; Stenberg, B., Chemiluminescence as a tool for polyolefin oxidation studies. In Long-Term Properties of Polyolefins, 2004; Vol. 169, pp 151-176.

[149] Broska, R.; Rychly, J. Double stage oxidation of polyethylene as measured by chemiluminescence. Polymer Degradation and Stability 2001, 72, (2), 271-278.

[150] Broska, R.; Rychly, J.; Csomorova, K. Carboxylic acid assisted oxidation of polypropylene studied by chemiluminescence. Polymer Degradation and Stability 1999, 63, (2), 231-236.

[151] Ragnarsson, L.; Albertsson, A. C. Total luminescence intensity as a tool to classify degradable polyethylene films by early degradation detection and changes in activation energy. Biomacromolecules 2003, 4, (4), 900-907.

[152] Tavares, A. C.; Gulmine, J. V.; Lepienski, C. M.; Akcelrud, L. The effect of accelerated aging on the surface mechanical properties of polyethylene. Polymer Degradation and Stability 2003, 81, (2), 367-373.

[153] Sudhakar, M.; Trishul, A.; Doble, M.; Kumar, K. S.; Jahan, S. S.; Inbakandan, D.; Viduthalai, R. R.; Umadevi, V. R.; Murthy, P. S.; Venkatesan, R. Biofouling and biodegradation of polyolefins in ocean waters. Polymer Degradation and Stability 2007, 92, (9), 1743-1752.

[154] Singh, R. P.; Mani, R.; Sivaram, S.; Lacoste, J.; Lemaire, J. Thermooxidative Degradation of Heterophasic Ethylene-Propylene Copolymers and Their Fractions. Polymer International 1993, 32, (2), 189-196.

[155] Gugumus, F. Thermooxidative degradation of polyolefins in the solid state .1. Experimental kinetics of functional group formation. Polymer Degradation and Stability 1996, 52, (2), 131-144.

[156] Lacoste, J.; Vaillant, D.; Carlsson, D. J. Gamma-Initiated, Photo-Initiated, and Thermally-Initiated Oxidation of Isotactic Polypropylene. Journal of Polymer Science Part a-Polymer Chemistry 1993, 31, (3), 715-722.

[157] Commereuc, S.; Vaillant, D.; Philippart, J. L.; Lacoste, J.; Lemaire, J.; Carlsson, D. J. Photo and thermal decomposition of iPP hydroperoxides. Polymer Degradation and Stability 1997, 57, (2), 175-182.

[158] Lacoste, J.; Carlsson, D. J. Gamma-Initiated, Photo-Initiated, and Thermally-Initiated Oxidation of Linear Low-Density Polyethylene - a Quantitative Comparison of Oxidation-Products. Journal of Polymer Science Part a-Polymer Chemistry 1992, 30, (3), 493-500.

[159] Fernando, S. S.; Christensen, P. A.; Egerton, T. A.; White, J. R. Carbon dioxide evolution and carbonyl group development during photodegradation of polyethylene and polypropylene. Polymer Degradation and Stability 2007, 92, 2163-2172.

[160] Tudos, F.; Iring, M. Polyolefin oxidation: rates and products. Acta Polymerica 1988, 39, (1-2), 19-26.

[161] Hakkarainen, M.; Albertsson, A.-C. Environmental degradation of polyethylene. Advances in Polymer Science 2004, 169, (Long-Term Properties of Polyolefins), 177-199.

[162] Burman, L.; Albertsson, A.-C. Chromatographic fingerprinting - a tool for classification and for predicting the degradation state of degradable polyethylene. Polymer Degradation and Stability 2005, 89, (1), 50-63.

[163] White, J. R.; Shyichuk, A. V. Macromolecular scission and crosslinking rate changes during polyolefin photo-oxidation. Polymer Degradation and Stability 2007, 92, (7), 1161-1168.

[164] White, J. R.; Shyichuk, A. V. Effect of stabilizer on scission and crosslinking rate changes during photo-oxidation of polypropylene. Polymer Degradation and Stability 2007, 92, 2095-2101.

[165] Silverstein, R.; Bassler, C., Ultraviolet Spectrometry. In Spectrometric Identification of Organic Compounds Willey New York, 1981.

[166] Craig, I. H.; White, J. R.; Shyichuk, A. V.; Syrotynska, I. Photo-induced scission and crosslinking in LDPE, LLDPE, and HDPE. Polymer Engineering and Science 2005, 45, (4), 579-587.

[167] Shyichuk, A. V.; White, J. R.; Craig, I. H.; Syrotynska, I. D. Comparison of UV-degradation depth-profiles in polyethylene, polypropylene and an ethylene-propylene copolymer. Polymer Degradation and Stability 2005, 88, (3), 415-419.

[168] Girois, S.; Audouin, L.; Verdu, J.; Delprat, P.; Marot, G. Molecular weight changes during the photooxidation of isotactic polypropylene. Polymer Degradation and Stability 1996, 51, (2), 125-132.

[169] La Mantia, F. P.; Gardette, J. L. Improvement of the mechanical properties of photo-oxidized films after recycling. Polymer Degradation and Stability 2002, 75, (1), 1-7.

[170] Hamid, S. H.; Amin, M. B. Lifetime Prediction of Polymers. Journal of Applied Polymer Science 1995, 55, (10), 1385-1394.

[171] Tidjani, A.; Arnaud, R. Formation of Treeing Figures during the Photooxidation of Polyolefins. Polymer 1995, 36, (14), 2841-2844.

[172] Budrugeac, P.; Segal, E. Changes the mechanical properties and thermal behaviour of LDPE in response to accelerated thermal aging. Journal of Thermal Analysis and Calorimetry 1998, 53, (3), 801-808.

[173] Martins, T. D.; Gulmine, J. V.; Akcelrud, L.; Weiss, R. G.; Atvars, T. D. Z. Dependence of relaxation processes in a low-density polyethylene with different crosslink densities investigated by fluorescence spectroscopy. Polymer 2006, 47, (21), 7414-7424.

[174] Valadez-Gonzalez, A.; Cervantes-Uc, J. M.; Veleva, L. Mineral filler influence on the photo-oxidation of high density polyethylene: I. Accelerated UV chamber exposure test. Polymer Degradation and Stability 1999, 63, (2), 253-260.

[175] Gulmine, J. V.; Akcelrud, L. Correlations between structure and accelerated artificial ageing of XLPE. European Polymer Journal 2006, 42, (3), 553-562.

[176] Valadez-Gonzalez, A.; Veleva, L. Mineral filler influence on the photo-oxidation mechanism degradation of high density polyethylene. Part II: natural exposure test. Polymer Degradation and Stability 2004, 83, (1), 139-148.

[177] Khraishi, N.; Alrobaidi, A. Effect of Weathering on Uv-Stabilized Low-Density Polyethylene Films (Ldpe) for a Multilayer Greenhouse Cover. Polymer Degradation and Stability 1991, 32, (1), 105-114.

[178] ASTM Standard D 5510-94, 2001, Standard Practice for Heat Aging of Oxidatively Degradable Plastics, ASTM International, West Conshohocken, PA, www.astm.org.

[179] Kelly, C. T.; White, J. R. Photo-degradation of polyethylene and polypropylene at slow strain-rate. Polymer Degradation and Stability 1997, 56, (3), 367-383.

[180] Shyichuk, A. V.; Stavychna, D.; White, J. R. Effect of tensile stress on chain scission and crosslinking during photo-oxidation of polypropylene. Polymer Degradation and Stability 2001, 72, (2), 279-285.

[181] Roy, P. K.; Surekha, P.; Rajagopal, C.; Raman, R.; Choudhary, V. Study on the degradation of low-density polyethylene in the presence of cobalt stearate and benzil. Journal of Applied Polymer Science 2006, 99, (1), 236-243.

[182] Craig, I. H.; White, J. R. Mechanical properties of photo-degraded recycled photo-degraded polyolefins. Journal of Materials Science 2006, 41, (3), 993-1006.

[183] Wool, R. P., The Science and Engineering of Polymer Composite Degradation. In Degradable Polymers. Principles & Applications, Scott, G. a. G. D., Ed. Chapman & Hall: Cambridge, 1995.

[184] Itavaara, M.; Vikman, M. An overview of methods for biodegradability testing of biopolymers and packaging materials. Journal of Environmental Polymer Degradation 1996, 4, (1), 29-36.

[185] Huang, S. J.; Edelman, P. G., An Overview of Biodegradable Polymers and Biodegradation of Polymers. In Degradable Polymers. Principles & Applications, Scott, G. a. G. D., Ed. Chapman & Hall: Cambridge, 1995.

[186] Battersby, N. S.; Ciccognani, D.; Evans, M. R.; King, D.; Painter, H. A.; Peterson, D. R.; Starkey, M. An 'inherent' biodegradability test for oil products: Description and results of an international ring test. Chemosphere 1999, 38, (14), 3219-3235.

[187] Guhl, W.; Steber, J. The value of biodegradation screening test results for predicting the elimination of chemicals' organic carbon in waste water treatment plants. Chemosphere 2006, 63, (1), 9-16.

[188] Kumar, A. P.; Pandey, J. K.; Kumar, B.; Singh, R. P. Photo-bio-degradability of agro waste and ethylene-propylene copolymers composites under abiotic and biotic environments. Journal of Polymers and the Environment 2006, 14, (2), 203-212.

[189] Majid, M. I. A.; Ismail, J.; Few, L. L.; Tan, C. F. The degradation kinetics of poly(3-hydroxybutyrate) under non-aqueous and aqueous conditions. European Polymer Journal 2002, 38, (4), 837-839.

[190] Bucci, D. Z.; Tavares, L. B. B.; Sell, I. Biodegradation and physical evaluation of PHB packaging. Polymer Testing 2007, 26, 908-915.

[191] Zhao, Q.; Cheng, G. X.; Song, C. J.; Zeng, Y.; Tao, H.; Zhang, L. G. Crystallization behavior and biodegradation of poly(3-hydroxybutyrate) and poly(ethylene glycol) multiblock copolymers. Polymer Degradation and Stability 2006, 91, (6), 1240-1246.

[192] Gilan, I.; Hadar, Y.; Sivan, A. Colonization, biofilm formation and biodegradation of polyethylene by a strain of Rhodococcus ruber. Applied Microbiology and Biotechnology 2004, 65, (1), 97-104.

[193] Molitoris, H. P.; Moss, S. T.; deKoning, G. J. M.; Jendrossek, D. Scanning electron microscopy of polyhydroxyalkanoate degradation by bacteria. Applied Microbiology and Biotechnology 1996, 46, (5-6), 570-579.

[194] Koutny, M.; Sancelme, M.; Dabin, C.; Pichon, N.; Delort, A.-M.; Lemaire, J. Acquired biodegradability of polyethylenes containing pro-oxidant additives. Polymer Degradation and Stability 2006, 91, (7), 1495-1503.

[195] Albertsson, A. C.; Erlandsson, B.; Hakkarainen, M.; Karlsson, S. Molecular weight changes and polymeric matrix changes correlated with the formation of degradation products in biodegraded polyethylene. Journal of Environmental Polymer Degradation 1998, 6, (4), 187-195.

[196] Orhan, Y.; Buyukgungor, H. Enhancement of biodegradability of disposable polyethylene in controlled biological soil. International Biodeterioration & Biodegradation 2000, 45, (1-2), 49-55.

[197] Albertsson, A. C.; Karlsson, S. The Influence of Biotic and Abiotic Environments on the Degradation of Polyethylene. Progress in Polymer Science 1990, 15, (2), 177-192.

[198] Contat-Rodrigo, L.; Ribes-Greus, A.; Diaz-Calleja, R. Characterization by thermal analysis of PP with enhanced biodegradability. Journal of Applied Polymer Science 2001, 82, (9), 2174-2184.

[199] Petersen, K.; Nielsen, P. V.; Bertelsen, G.; Lawther, M.; Olsen, M. B.; Nilsson, N. H.; Mortensen, G. Potential of biobased materials for food packaging. Trends in Food Science & Technology 1999, 10, (2), 52-68.

[200] Arvanitoyannis, I.; Kolokuris, I.; Nakayama, A.; Aiba, S. I. Preparation and study of novel biodegradable blends based on gelatinized starch and 1,4-transpolyisoprene (gutta percha) for food packaging or biomedical applications. Carbohydrate Polymers 1998, 34, (4), 291-302.

[201] Averous, L. Biodegradable multiphase systems based on plasticized starch. Journal of Macromolecular Science, Polymer Reviews 2004, C44, (3), 231-274.

[202] Jane, J.; Chen, Y. Y.; Lee, L. F.; McPherson, A. E.; Wong, K. S.; Radosavljevic, M.; Kasemsuwan, T. Effects of amylopectin branch chain length and amylose content on the gelatinization and pasting properties of starch. Cereal Chemistry 1999, 76, (5), 629-637.

[203] Griffin, G. J. L. Starch Polymer Blends. Polymer Degradation and Stability 1994, 45, (2), 241-247.

[204] Mali, S.; Grossmann, M. V. E. Effects of yam starch films on storability and quality of fresh strawberries (Fragaria ananassa). Journal of Agricultural and Food Chemistry 2003, 51, (24), 7005-7011.

[205] Mali, S.; Karam, L. B.; Ramos, L. P.; Grossmann, M. V. E. Relationships among the composition and physicochemical properties of starches with the characteristics of their films. Journal of Agricultural and Food Chemistry 2004, 52, (25), 7720-7725.

[206] Mali, S.; Grossmann, M. V. E.; Garcia, M. A.; Martino, M. N.; Zaritzky, N. E. Mechanical and thermal properties of yam starch films. Food Hydrocolloids 2005, 19, (1), 157-164.

[207] Mali, S.; Sakanaka, L. S.; Yamashita, F.; Grossmann, M. V. E. Water sorption and mechanical properties of cassava starch films and their relation to plasticizing effect. Carbohydrate Polymers 2005, 60, (3), 283-289.

[208] Otey, F. H., Biodegradable starch-based blown films. US Patent 4,337,181. 1982.

[209] Lowell, P. N.; McCrum, N. G. g-Relaxation and its relation to the diffusion of n-C4H10 in polyethylene. Journal of Polymer Science, Polymer Letters Edition 1971, 9, (7), 477-482.

[210] Carvalho, A. J. F.; Job, A. E.; Alves, N.; Curvelo, A. A. S.; Gandini, A. Thermoplastic starch/natural rubber blends. Carbohydrate Polymers 2003, 53, (1), 95-99.

[211] Wang, S.; Yu, J.; Yu, J. Preparation and characterization of compatible thermoplastic starch/polyethylene blends. Polymer Degradation and Stability 2005, 87, (3), 395-401.

[212] Bikiaris, D.; Prinos, J.; Perrier, C.; Panayiotou, C. Thermoanalytical study of the effect of EAA and starch on the thermooxidative degradation of LDPE. Polymer Degradation and Stability 1997, 57, (3), 313-324.

[213] Prinos, J.; Bikiaris, D.; Theologidis, S.; Panayiotou, C. Preparation and characterization of LDPE/starch blends containing ethylene/vinyl acetate copolymer as compatibilizer. Polymer Engineering and Science 1998, 38, (6), 954-964.

[214] Kim, M. Evaluation of degradability of hydroxypropylated potato starch/polyethylene blend films. Carbohydrate Polymers 2003, 54, (2), 173-181.

[215] Bastioli, C. Properties and applications of Mater-Bi starch-based materials. Polymer Degradation and Stability 1998, 59, (1-3), 263-272.

[216] Work, W. J.; Horie, K.; Hess, M.; Stepto, R. F. T. Definitions of terms related to polymer blends, composites, and multiphase polymeric materials - (IUPAC recommendations 2004). Pure and Applied Chemistry 2004, 76, (11), 1985-2007.

[217] Bikiaris, D.; Panayiotou, C. LDPE/starch blends compatibilized with PE-g-MA copolymers. Journal of Applied Polymer Science 1998, 70, (8), 1503-1521.

[218] Matzinos, P.; Bikiaris, D.; Kokkou, S.; Panayiotou, C. Processing and characterization of LDPE/starch products. Journal of Applied Polymer Science 2001, 79, (14), 2548-2557.

[219] Pedroso, A. G.; Rosa, D. S. Effects of the compatibilizer PE-g-GMA on the mechanical, thermal and morphological properties of virgin and reprocessed LDPE/corn starch blends. Polymers for Advanced Technologies 2005, 16, (4), 310-317.

[220] Bagheri, R.; Naimian, F. Melt flow properties of starch-filled linear low density polyethylene: Effect of photoinitiators. Journal of Applied Polymer Science 2007, 104, (1), 178-182.

[221] Pedroso, A. G.; Rosa, D. S. Mechanical, thermal and morphological characterization of recycled LDPE/corn starch blends. Carbohydrate Polymers 2005, 59, (1), 1-9.